A comparison of the molecular mechanisms involved in olfactory ensheathing cell and Schwann cell interactions with astrocytes

Richard Fairless, MBioch

A thesis submitted to the Faculty of Medicine, University of Glasgow for the degree of Doctor of Philosophy

December, 2004

A doctoral study conducted at the

Department of Clinical Neuroscience

Faculty of Medicine

University of Glasgow

To my Grandad

Acknowledgements

Firstly, I would like to thank all members of N1, past and present, including Andras, Annette, Bob, Claire, Edina, Lynda, Sarah, Tom, and Una, for making the lab experience so enjoyable. I would particularly like to thank Sue Barnett, for her supervision over the years, and for giving me the opportunity to work in her lab.

In addition, I would like to thank both Margaret Frame and Val Brunton, for many informative discussions and advice, and Stephen for his help with some of the Calpain studies. I am also grateful to all of technology services for their technical support, and in particular, Tom Gilbey for his help with FACS purification of my cells.

Finally, I would like to thank both Colin and Sarah for their encouragement, and my family, in particular my Mam and Dad, for their endless support.

Table of Contents

List of Figures

CHAPTER 1

CHAPTER 3

CHAPTER 4

CHAPTER 5

List of Tables

List of Publications

Riddell JS, Enriquez-Denton M, Toft A, **Fairless R**, Barnett SC (2004)
Olfactory ensheathing cell grafts have minimal influence on regeneration at the dorsal root entry zone following rhizotomy. Glia 47:150-67

Fairless R, Frame MC, Barnett SC (2005)
N-cadherin differentially determines Schwann cell and olfactory ensheathing cell migration upon contact with astrocytes. Molecular and Cellular Neuroscience 28:253-263

Fairless R, Barnett SC (2005)
Olfactory ensheathing cells: Their role in CNS repair. International Journal of Biochemisty & Cell Biology 37:693-699

List of Abbreviations

1D	one dimensional
2D	two dimensional
A (1)	adenosine
A (2)	amps
ACM	astrocyte-conditioned media
ANOVA	analysis of variance
AraC	cytosine arabinoside
AS	astrocyte
ATP	adenosine triphosphate
BDNF	brain-derived neurotrophic factor
BrdU	5-bromo-2-deoxyuridine
BS	Bottenstein-Sato
BSA	bovine serum albumin
C	cytosine
$CaCl_2$	calcium chloride
cAMP	cyclic adenosine monophosphate
CAR	cadherin adhesion recognition

CH_3CN	acetonitrile
cGMP	cyclic guanosine monophosphate
CNS	central nervous system
CNTF	cilliary neurotrophic factor
CS-PG	chondroitin sulphate proteoglycan
CST	corticospinal tract
$CuSO_4$	copper sulphate
DAPI	4',6'-diaminidino-2-phenylindole
DEPC	diethyl pyrocarbonate
dH_2O	distilled water
DMEM	Dubco's modified eagle medium
DMSO	dimethyl sulphoxide
DNA	deoxyribonucleic acid
DNase	deoxyribonuclease
DREZ	dorsal root entry zone
DRG	dorsal root ganglion
DTT	dithiothreitol
E	embryonic
E-cadherin	epithelial cadherin

ECL	enhanced chemiluminescence
ECM	extracellular matrix
EDTA	ethylenediaminetetraacetic acid
EGF	epidermal growth factor
EGFR	epidermal growth factor receptor
EGTA	ethylene glycol bis-N,N,N',N'-tetraacetic acid
EtOH	ethanol
FACS	fluoresent activated cell sorter
FAK	focal adhesion kinase
FBS	foetal bovine serum
FGF-2	fibroblast growth factor-2
FGFR	fibroblast growth factor receptor
FITC	fluorescein
g	gram
G	guanine
GABA	gamma amino butyric acid
GAG	glycosaminoglycan
GalC	galactocerebroside
GalNAc	GlcA-N-acetyl-D-galactosamine

GalNAcPTase	N-acetylgalactosaminylphosphotransferase
GAP-43	growth associated protein 43
GDNF	glial-derived neurotrophic factor
GFAP	glial fibrillary acidic protein
GFP	green fluorescent protein
Glc A	D-glucoronic acid
GPI	glycosylphosphatdylinositol
GTPase	guanosine triphosphatase
HEPES	4-(2-hydroxyethyl)-1-piperazineethane-sulfonic acid
HGF	hepatocyte growth factor
HTK	herpes thymidine kinase
HRP	horse radish peroxidase
Ig	immunoglobulin
IGF	insulin-like growth factor
IFNγ	interferon-γ
IL-1,2,6	interleukin-1,2,6
IP	immunoprecipitation
IPG	immobilized pH gradient
IQGAP	IQ motif-containing GTPase activating protein

kb	kilobases
KCl	potassium chloride
kDa	kilodaltons
KH_2PO_4	potassium phosphate
l	litre
m	metre
M	molar
MAG	myelin associated glycoprotein
MALDI-TOF	matrix-assisted laser desorption ionisation - time of flight
MBP	myelin basic protein
MeOH	methanol
MEK	mitogen-activated/extracellular signal regulated kinase or MAP kinase kinase
$MgCl_2$	magnesium chloride
mRNA	messenger RNA
MS	multiple sclerosis
NaCl	sodium chloride
Na_2HPO4	sodium phosphate
NaOH	sodium hydroxide

Na_3VO_4	sodium orthovanadate
N-cadherin	neural cadherin
NCAM	neural cell adhesion molecule
NGF	nerve growth factor
NgR	Nogo receptor
NPY	neuropeptide Y
NH_4CO_3	ammonium carbonate
nt	nucleotide
NT-3	neurotrophin 3
O-2A	oligodendrocyte-type-2-astrocyte
OCM	OEC-conditioned media
OD	optical density
OEC	olfactory ensheathing cell
OMgp	oligodendrocyte myelin glycoprotein
OMM	OEC mitogen media
OPC	oligodendrocyte progenitor cell
ORN	olfactory receptor neuron
$P75^{NTR}$	p75 subunit of the low affinity NGF receptor
PAGE	polyacrylamide gel electrophoresis

PBS	phosphate buffered saline
P-cadherin	placental cadherin
PDGF	platelet-derived growth factor
PDGFR	platelet-derived growth factor receptor
PE	phosphate buffered saline with EDTA
PLL	poly-l-lysine
PMP22	peripheral myelin protein 22
PMSF	phenylmethylsulfonyl fluoride
PNS	peripheral nervous system
PSA	polysialic acid
PSA-NCAM	polysialic acid NCAM
PT	PBS-Tween
RIPA	radio-immuno precipitation assay
Robo	roundabout
RPE	phycoerythrin
RNA	ribonucleic acid
RNAi	RNA interference
RT	room temperature
SCM	Schwann cell-conditioned media

SC	Schwann cell
SD	soybean trypsin inhibitor-DNase
SDS	sodium dodecyl sulphate
SEM	standard error of the mean
siRNA	small inhibitory RNA
SVZ	subventricular zone
T	thymine
TCA	trichloric acetic acid
TGFα/β	transforming growth factor α/β
TNFα	tumour necrosis factor α
TRITC	tetramethylrhodamine isothiocyanate
U (1)	enzyme unit
U (2)	uracil
V	volts
X-EB	X-irradiation/ethidium bromide

Summary

The transplantation of glial cells, including olfactory ensheathing cells (OECs) and Schwann cells, for the treatment of various CNS lesions, such as demyelination and spinal cord injuries, has attracted a lot of recent focus. However, there has been much debate as to which is the superior cell for these transplantation therapies. OECs are generally considered to be superior to Schwann cells due to their greater capacity for migration and their ability to co-exist within astrocyte-rich environments. In addition, OECs induce less reactivity in host astrocytes following transplantation. However, the mechanisms which determine the differential interactions of Schwann cells and OECs with astrocytes are at present unknown. The aim of this thesis was to determine the nature of these mechanisms, with intent to further characterise these very similar glial cell types, and to highlight possible molecular targets for improving the potential of OECs and Schwann cells for transplantation.

I have addressed these issues by using *in vitro* cultures which model the interactions of OECs and Schwann cells with astrocytes, reflecting those which occur following transplantation. Initial studies confirmed that Schwann cells have a limited ability to migrate in the presence of astrocytes in comparison to OECs. However, using migration assays it was demonstrated that Schwann cells are not inferior to OECs with regard to their inherent migrational capacity, but that this inhibition only results upon contact with astrocytes. In agreement with this, Schwann cells displayed greater adhesion than OECs to astrocytes, reflecting their reduced migration upon this substrate.

To identify factors which influence the different migrational capacities of OECs and Schwann cells following astrocyte contact, I have investigated the role of the cell adhesion molecule, N-cadherin. Previous studies demonstrated that the inhibition of Schwann cell migration upon astrocyte monolayers is N-cadherin dependent, suggesting that this could be a difference between OECs and Schwann cells. I have shown here that N-cadherin is present on both OECs and Schwann cells, and is functional with regard to cell-cell interactions. However, using both N-cadherin peptide inhibitors, and siRNA to reduce N-cadherin expression, it was also demonstrated that OECs and Schwann cells have a different dependency upon N-cadherin for cell-cell interactions. Schwann cells, but not

OECs, were dependent upon N-cadherin to form strong adhesions. In addition, removal of N-cadherin overcame astrocyte-induced inhibition of migration in Schwann cells, and allowed them to intermingle with astrocytes in a manner more akin to OEC-astrocyte interactions. Thus, this demonstrates that not only do Schwann cells and OECs differ in their dependency upon N-cadherin for adhesion and migration, but also that N-cadherin is a major factor in determining the ability of Schwann cells to intermingle with astrocytes.

Due to the observation that Schwann cells induce a greater degree of astrocytosis than OECs, I have assessed some of the factors determining this astrocytic response. In order to achieve this, the role of Schwann cell-secreted factors was investigated. It is shown here that media conditioned by Schwann cells or OECs stimulated astrocytes to produce the axon-growth inhibitory molecules, chondroitin sulphate proteoglycans (CS-PGs). However, in order for astrocytes to undergo other changes characteristic of the astrocytic reactive response, such as GFAP upregulation and an increase in astrocytic area, both Schwann cell-conditioned media and an OEC-contact signal are necessary. In this way, astrocytes which are co-cultured with OECs in the presence of Schwann cell-secreted factors become reactive, but not if either OEC-contact or Schwann cell-secreted factors are absent. In addition, OECs were unable to migrate within these reactive astrocytes, but formed boundaries with astrocytes in a manner similar to Schwann cells. Thus, Schwann cell-secreted factors may be responsible for the reactive astrocytes observed in Schwann cell-astrocyte co-cultures. Since the presence of these reactive astrocytes appears to determine the ability of OECs to migrate amongst them, they may be responsible for the limited migration seen by Schwann cells in the presence of astrocytes.

In conclusion, both the function of N-cadherin and the presence of reactive astrocytes, are involved in determining the ability of Schwann cells and OECs to migrate within astrocyte-rich areas. Schwann cells differ from OECs in that they are dependent upon N-cadherin function for both adhesion and migration following interactions with astrocytes. In addition, unlike OECs, Schwann cells secrete factors which induce astrocytosis. Therefore, N-cadherin, or its various signalling components, and the putative factors secreted by Schwann cells, may now offer themselves as potential targets for intervention in order to improve the migration and integration of the cellular transplant into the host.

Declaration

I am the sole author of this thesis. All the work presented in this thesis was performed by myself unless otherwise stated.

CHAPTER 1

Introduction

1.1 Regenerative properties of the nervous system

The nervous system consists of both a central and a peripheral component. The brain and spinal cord constitute the central nervous system (CNS), whereas the peripheral nervous system (PNS) connects the rest of the body to the brain and the spinal cord. They have different regenerative responses following injury, in that the regeneration of the PNS can be successful whereas CNS regeneration typically fails. It is hoped that understanding the processes which are successful in the PNS may shed some light on why regeneration fails in the CNS, and how we may overcome this.

1.1.1 Peripheral regeneration

For over a century, the ability of the peripheral nerve to regenerate and reinnervate denervated targets has been recognised. Many factors are involved in determining the outcome of such repair, such as whether the neuron survives the injury, how supportive the growth environment is, and the ability of the nerve to reinnervate the appropriate target (Fu and Gordon, 1997).

Following injury, peripheral nerves undergo a well characterised process known as Wallerian degeneration, where axonal and myelin-derived material is removed, and the environment for regeneration is prepared. After breakdown of the distal nerve and myelin, the debris is phagocytosed by macrophages and Schwann cells. The role of Schwann cells in this process was shown when macrophages were denied access to the distal nerve stump (Beuche and Friede, 1984). In fact, during the first two days after injury, when macrophage invasion is minimal, Schwann cells are the major phagocytotic cell (Stoll et al., 1989). After this time, macrophages continue to break myelin down until approximately two weeks after injury, when they either apoptose or migrate to the lymph nodes (Kuhlmann et al, 2001).

Following axotomy, surviving neurons undergo a process known as chromatolysis. This involves morphological changes such as disintegration of the Nissl bodies, large granular condensations of rough endoplasmic reticulum, nucleolar enlargement, and cell swelling (Lieberman, 1971). The axon can then begin to regenerate, usually within a few hours of

axotomy (Fawcett and Keynes, 1990). The environment through which the axon regenerates consists of Schwann cells and their basal lamina, fibroblasts and extracellular matrix (ECM). The role of Schwann cells in this process appears to be the critical factor (see Section 1.3.1.3), whereby they produce a range of cytokines, such as interleukin 1 (IL-1; Bergensdottir et al., 1991; Skundric et al., 1997; Rutkowski et al., 1999), IL-6 (Murwani et al., 1996; Rutkowski et al., 1999) and tumour necrosis factor α (TNFα; Murwani et al., 1996; Wagner and Myers, 1996). In addition, the axon synthesises many neurotrophic factors including nerve growth factor (NGF) (Ernfors et al., 1989), brain-derived neurotrophic factor (BNDF), neurotrophin 3 (NT-3) (Ernfors & Persson, 1991) and platelet-derived growth factor (PDGF) (Yeh et al., 1991), which may help give the regenerating neuron the trophic support it needs.

1.1.2 CNS regenerative failure

The situation within the CNS is different to the PNS, since it is non-permissive to axonal regeneration. This is principally due to the inhibitory nature of the glial environment, where both the presence of myelin, and the injury response which results in a glial scar, prevent repair taking place. As a result, an injury to the CNS can result in a permanent loss of function.

Following injury, degeneration occurs in a manner similar to the PNS. Firstly, the distal part of the cut axon and associated myelin are removed, similar to Wallerian degeneration, involving both resident microglial and recruited macrophages (Kreutzberg, 1996). However, following this, cavitation around the injury site occurs due to secondary cell death of both neurons and glia (Dusart and Schwab, 1994, Fitch et al., 1999). This is induced, not by the initial injury, but rather the resulting inflammatory response. Around the injury site, a glial scar then develops, which eventually fills any vacant space (Fawcett and Asher, 1999). Before this scar appears, the surviving proximal segment of the axon may exhibit a regenerative response within 6 hours of injury (Schwab and Bartholdi, 1996) as growth cone 'clubs' develop at the severed end (Ramon y Cajal, 1928 – cited in Fry, 2001) and are directed towards the injury site. However, these sprouts can only extend for about 1mm before growth is aborted and the new sprouts are gradually retracted (Clemente, 1964). The role of the inhibitory environment in growth cone abortion was demonstrated using a PNS

tissue bridge between the adult rat medulla and spinal cord after a CNS injury. This allowed injured host axons to extend along the bridge, although they were unable to re-enter the host tissue (David and Aguayo, 1981). This was the first demonstration that CNS axons have the capacity to grow when given a permissive environment.

1.1.2.1 Myelin

Inhibitory myelin proteins, which are not normally present on the outer surface of intact myelin, become exposed following injury. This is due to both direct damage to the myelin sheath itself, and the presence of dying oligodendrocytes. These proteins are probably the main factor contributing to inhibition of axonal regeneration in the period before the glial scar has formed, and they are only removed slowly by microglia, a process which can take several weeks (Buss and Schwab, 2003). The role of myelin in inhibiting neuronal regeneration has been known for a while (Berry, 1982), and its appearance during development correlates with the loss in the ability of neurons to regenerate (Macklin and Weill, 1985; Ferretti et al., 2003).

There are three principle molecules which have been shown to inhibit neuronal outgrowth, Nogo, myelin associated glycoprotein (MAG) and oligodendrocyte myelin glycoprotein (OMgp). Nogo exists in three isoforms, -A, -B and –C, formed by differences in promoter usage and splicing. However, they all share a common carboxy terminal domain containing two transmembrane domains separated by a 66 amino acid extracellular loop (Nogo66) (GrandPre et al., 2000). Both Nogo66, and the amino terminal domain, can induce growth cone collapse in extending neurons (GrandPre et al., 2000; Prinjha et al., 2000). MAG is another inhibitory molecule (McKerracher et al., 1994), containing an extracellular domain which is inhibitory to axonal regeneration (Tang et al., 1997). Unlike Nogo, MAG is present in both the CNS and the PNS (Schachner & Bartsch, 2000), although within the PNS, its removal by phagocytosis is necessary before regeneration can occur (Fawcett and Keynes, 1990). A third, recently discovered inhibitory myelin protein is OMpg (Wang et al., 2002b). This is a glycosylphosphatidylinositol (GPI)-linked protein, expressed on the surface of oligodendrocytes and adjacent myelin layers (Mikol et al., 1988; Mikol et al., 1990), which potently inhibits neurite outgrowth in culture (Wang et al., 2002b).

Interestingly, all three molecules have been shown to bind the same receptor (Fourneir et al., 2001; Woolf and Bloechlinger, 2002; Wang et al., 2002), which is termed the Nogo receptor (NgR) due to its original demonstration to bind Nogo (Fourneir et al., 2001). This observation probably explains the redundancy observed between inhibitory myelin molecules. However, NgR has no transmembrane or cytoplasmic domains and therefore must induce inhibition through a membrane-bound co-receptor, which transduces the extracellular signals. An interesting development has been the observation that $p75^{NTR}$ is probably this co-receptor, where it is involved in both MAG signalling (Wong et al., 2002) as well as Nogo and OMgp (Wang et al., 2002a). The guanosine triphosphatase (GTPase) Rho appears to be the downstream target of such receptor complexes, since blocking Rho-GTPase activity allows neurites to grow on MAG substrates *in vitro* (Lehmann et al., 1999), as does inhibiting its downstream target, Rho-kinase. These observations lend themselves to more potent methods of blocking myelin-induced inhibition, where targeting either NgR or $p75^{NTR}$, or even Rho, may be a better strategy than targeting each of the three inhibitory molecules individually.

In contrast, a recent study demonstrated that deletion of the NgR gene failed to relieve the effect of myelin inhibition (Zheng et al., 2004). Here it was shown that neurons cultured *in vitro* were as susceptible to myelin inhibition as wild type neurons. In addition, there was little corticospinal tract (CST) regeneration following a dorsal hemisection of the spinal cord. The apparent contradiction between this study and others demonstrating that inhibitors of NgR reduced myelin inhibition (GrandPre et al., 2002; Fournier et al., 2002) may result from differences in myelin preparations. Alternatively, the possibility exists that NgR antagonists may also target other myelin receptors, for example other NgR homologues, which are not disrupted by NgR gene deletion. An additional study analysing an NgR knock out mouse confirmed that CST regeneration was minimal, but did report that regeneration was possible in alternative tracts, such as raphe spinal fibres (Kim et al., 2004).

1.1.2.2 The glial scar

The major barrier to regeneration within the CNS, is the formation of a glial scar following injury. This occurs over a period of several days and involves several different types of cells, with astrocytes playing the major role (Fawcett and Asher, 1999).

The first cells to arrive, within hours of the injury, are macrophages, recruited from the blood, and microglia, which are activated from a quiescent state within the CNS (Kreutzberg, 1996). Another cell type recruited to areas of injury are oligodendrocyte precursors, which are identified by their expression of the proteoglycan NG2, and the PDGF-alpha receptor. A proportion of these cells have been shown to respond to demyelination by differentiating into myelin-expressing mature oligodendrocytes (Gensert and Goldman, 1997), and therefore probably contribute to endogenous remyelination of axons. Although these cells, unlike mature oligodendrocytes, do not express inhibitory myelin proteins, certain proteoglycans such as NG2 are present on their surface, and are also inhibitory to axonal growth (Dou and Levine, 1994; Fiddler et al., 1999).

The major cellular component of the glial scar, however, is the astrocyte. These cells undergo several defined changes upon injury, known as astrocytosis, including morphological changes as well as changes in gene expression. This process allows the damaged area to be sealed off and will be discussed in more detail (Section 1.2.1.4). Where the surface of the brain has also been disrupted, meningeal cells can also invade, and along with the astrocytes, they participate in reforming the glia limitans (Kruger et al., 1986).

1.1.2.3 CSPGs

Another key component of the glial scar are inhibitory extracellular matrix (ECM) molecules, including the chondroitin sulphate proteoglycans (CS-PGs). These were originally believed to be only produced by astrocytes, although it is now understood that many other cell types, including oligodendrocyte precursor cells (OPCs), meningeal cells and macrophages also produce them (Jones et al., 2002; Fawcett and Asher, 1999) (see Table 1.1).

Table 1.1. Cellular sources of inhibitory chondroitin sulphate proteoglycans, produced following CNS injury.

Cell type	CS-PG	Reference
Astrocyte - unreactive	Brevican	Yamada et al., 1997
	Neurocan	Asher et al., 2000; McKeon et al., 1999
Astrocyte - reactive	Brevican	Yamada et al., 1997
	Neurocan	Asher et al., 1999; McKeon et al., 1999
	Phosphacan	McKeon et al., 1999
	CS-56	Lakatos et al., 2000; 2002, Plant et al., 2001
Oligodendrocytes	Tenascin R	Pesheva et al., 1989; Probstmeier et al., 2000
Oligodendrocyte progenitor cell	NG2	Jones et al., 2002
	Versican	Asher et al., 2002
	Phosphacan	Fawcett and Asher, 1999; Dawson et al., 2000
Meningeal cell	NG2?	McTigue et al., 2001; Levine et al., 1999
Macrophages/Microglia	NG2	McTigue et al., 2001; Levine et al., 1994

Several lines of evidence point to the inhibitory nature of the CS-PGs. It has been demonstrated that there is a correlation between the presence of CS-PGs and areas inhibitory to axonal growth. Following injury, there is a considerable increase in CS-PG expression around the injury site, and in fact these CS-PG deposits have been precisely shown to correlate with the areas where axonal regrowth stops (Davies et al., 1997). This same correlation is seen in development where axons are directed away from inhibitory glial boundaries which are rich in CS-PGs (Fitch and Silver, 1997a; Fawcett and Asher, 1999). For example, the optic axons in the retina are directed towards the centrally located optic nerve by the presence of inhibitory CS-PGs in the peripheral retina (Brittis et al., 1992). In addition, the inhibitory nature of CS-PGs has been demonstrated directly *in vitro*, where CS-PGs act to either inhibit axon growth directly (Yamada et al., 1997; Dou and Levine, 1994), or to inhibit molecular interactions that promote axon growth (Milev et al 1994; Fawcett and Asher, 1999). Furthermore, direct evidence of the role of CS-PGs in inhibiting regeneration has been demonstrated in models of injury, where digestion of CS-PGs was achieved through use of the enzyme chondroitinase ABC. Here, the removal of inhibitory CS-PGs allowed subsequent axonal regeneration (Moon et al., 2001), and even functional recovery (Bradbury et al., 2002).

The CS-PG family consists of many different members, with great structural and functional diversity. They are all highly glycosylated glycoproteins, containing glycosaminoglycan (GAG) chains linked to their core proteins. These GAG chains consist of different repeating disaccharides which can be linked at various positions, as well as being differently modified. For example, the CS-PG family, as opposed to other proteoglycans, contain D-glucoronic acid (GlcA)-N-acetly-D-galactosamine (GalNAc)-repeating GAG units, modified by sulphate additions (Prydz and Dalen, 2001). The core protein can either be linked to the cell membrane via a GPI anchor, or present as a transmembrane or ECM component. It is both the GAGs and the core protein which are believed to mediate CS-PG functions (Fawcett et al., 2001). The inhibitory nature of the GAG chains themselves has been demonstrated through their digestion using chondroitinase (Moon et al., 2001; Bradbury et al., 2002), and inhibition of their sulphation using sodium chlorate (Smith-Thomas et al., 1995), both of which led to increased axonal outgrowth.

How CS-PGs affect axonal outgrowth is still not fully understood, but various theories have been put forth, such as, they may interact with the binding properties of adhesion molecules, or alternatively mask growth-promoting ECM molecules. Several types of CS-PGs have been shown to interact directly with adhesion molecules, such as neurocan and phosphocan. Neurocan interacts with N-CAM (Friedlander et al., 1994), TAG-1/axonin-1 (Milev et al., 1996), and tenascin (Milev et al., 1997), and inhibits axon growth mediated by Ng-CAM/L1 (Friedlander et al., 1994)). It has also been shown to regulate N-cadherin and β1-integrin-mediated adhesion and neurite outgrowth via a neurocan receptor, GalNAcPTase (Li et al., 2000). Phosphacan has also been shown to block several interactions that promote axon growth through interacting with contactin (Peles et al., 1995), N-CAM, Ng-CAM/L1 (Milev et al., 1994), TAG-1/axonin-1 (Milev et al., 1996) and tenascin (Milev et al., 1997). It was demonstrated that some CS-PGs may mask other growth-promoting molecules, since digestion of CS-PGs allowed axon growth upon CNS cryostat sections, which was then inhibited by antibodies against laminin. Such a role has also been demonstrated for specific CS-PGs such as versican (Schnaelfedt et al., 2000) and brevican (Yamada et al., 1997). In contrast, the mouse form of phosphacan, DSD-1, as well as being inhibitory, can actually promote the growth of embryonic hippocampal axons (Clement et al., 1998, Faissner et al., 1997). This has also been demonstrated for the transmembrane form of phosphacan, receptor tyrosine phosphatase RPTP-β (Sakurai et al., 1997).

Very little is known about the mechanisms by which CS-PGs are regulated, although as previously mentioned, upon injury they are expressed by most of the cell types involved in the glial scar. Astrocytes upregulate expression of neurocan (McKeon et al., 1999; Asher et al., 2000), brevican (Yamada et al., 1997) and possibly phosphacan (McKeon et al., 1999), whereas OPCs upregulate NG2 (Jones et al., 2002) and versican (Asher et al., 2002). TGFβ has been implicated in the regulation of CS-PGs since TGFβ neutralising agents reduced the deposition of CS-PGs in the glial scar. In addition, TGFβ was shown to directly upregulate neurocan expression in astrocytes in culture (Asher et al., 2000). In fact, several cytokines and growth factors involved in triggering and maintaining the activated astrocyte response, such as fibroblast growth factor 2 (FGF-2, also known as basic FGF or bFGF) and IL-6, may be involved in CS-PG production due to a correlation between areas

of expression, and CS-PG deposition (Fitch and Silver, 1997b). Neurocan expression in cultured astrocytes is upregulated by epidermal growth factor (EGF), and downregulated by PDGF and IFNγ (Asher et al., 2000).

As to which CS-PGs are contributing most to the inhibitory response, CS-56 immunoreactive CS-PGs and neurocan appear to be the most abundant, and correlate closely with areas of astrocytosis, suggesting a key role in inhibition (McKeon et al., 1999; Asher et al., 2000). However, despite NG2 making up less than 1% of the total ECM in the glial scar, it has been shown to be very potent, and thus may be making a greater contribution (Fidler et al., 1999; Jones et al., 2002).

1.1.2.4 Intrinsic neuronal state

Although the environment can modulate the ability of axons to regenerate, the inherent properties of neurons can also be a factor with different classes of axons demonstrating different growth response in the same environment. For example, following a dorsal root crush, the dorsal root ganglion (DRG) neurons can regenerate back towards the spinal cord, but are blocked at the CNS interface. In contrast, if motor axons are directed to the same place, by anastomosing the ventral horn and reattaching it to the dorsal root horn, they can penetrate much further into the spinal cord (Fawcett, 1992). These differences between neurons have been shown to be dependent upon the age as well as the type of neuron (Fawcett, 1992). This may reflect the ability of neurons to reexpress genes associated with growth and development. Certainly, following CNS injury, neurons fail to reexpress at least some of the growth-associated proteins that are expressed during development (Fu and Gordon, 1997), for example, Purkinje cells in the cerebellar cortex do not upregulate growth associated protein 43 kDA (GAP-43) in response to axotomy (Vuadano et al., 1995).

The response of a neuron to inhibitory factors is also modulated by its intrinsic state. For example, during development, rather than being inhibitory, MAG actually functions as a growth-promoting molecule. However, after development there is a switch to an inhibitory function for MAG, which has been shown to be caused by a decrease in intracellular cyclic adenosine monophosphate (cAMP) concentration within the neuron (Cai et al., 2001). In the same way, the response of an axon to a guidance cue, such as BDNF or acetylcholine, is

dependent upon intracellular levels of cAMP, such that an attractive response can be switched to a repulsive response through cAMP inhibition, using either a protein kinase A inhibitor or by applying a competitive analogue of cAMP (Song et al., 1997). This same mechanism is seen for axonal repulsion of Xenopus spinal axons induced by semaphorin III (Sema3) which is reversed in the presence of an analogue for cyclic guanosine monophosphate (cGMP) (Song et al., 1998).

In order to understand how cAMP functions to modulate axon growth, the Rho family of GTPases, RhoA, B, C and G; Rac1A, 1B and C; and Cdc42; are now being investigated. These are important regulators of the actin cytoskeleton (Luo et al., 1997) and have been shown to regulate growth cone collapse and neurite retraction (Dickson et al., 2001). Their involvement in these processes was demonstrated when inhibition of Rho blocked myelin-induced growth cone collapse (Lehmann et al., 1999). In addition, Sema3A-induced growth cone collapse (see below) can be blocked by dominant negative Rac in both DRG neurons and spinal motor neurons (Jin & Strittmatter, 1997).

1.1.2.6 Inhibitory axon guidance molecules

Another set of molecules involved in the inhibitory environment of the CNS are guidance molecules, including the semaphorins, netrins, ephrins and slits. These act both as short range guidance molecules via cell to cell contact and also as long range diffusible factors (Astic et al., 2002). They have mainly repulsive effects, although can also be attractive, functioning by instructing growth cones to turn towards or away, to alter their speed and expand or collapse. This is achieved through alterations in the axonal actin cytoskeleton, probably mediated by the Rho family of GTPases (Yu & Bargmann, 2001).

The most widely studied family of guidance molecules are the glycoprotein semaphorins, of which more than 20 have currently been characterised. Semaphorins exist in either a secreted or transmembrane form, and are classified by the presence of a 500 amino acid conserved C-terminal "sema" domain (Goodman et al., 1999). They were originally called collapsins due to their induction of growth cone collapse, and function via two families of receptors, the neuropilins and the plexins (Fujisawa, 2004). The first semaphorin to be discovered and subsequently the best known, is Sema3A (formerly known as collapsin-1).

Another family of guidance molecules are a group of laminin-related proteins called netrins. So far six members have been described, netrin1-4 (Yin et al., 2000), β-netrin (Koch et al., 2000) and netrin-G1 (Nakashiba et al., 2000). These function through transmembrane receptors of the Ig superfamily, deleted in colorectal cancer (DCC or UNC-40) and UNC-5. Like the semaphorins, netrins can act as both repulsive or attractive guidance cues, where UNC-5 receptors mediate repulsive netrin signalling, and DCC are mainly required for attraction, although the interaction of DCC and UNC-5 may determine this outcome (Hong et al., 1999). The netrins are secreted molecules that play an important role in the developing nervous system. They may also be involved in the adult nervous system, particularly netrin-1 which is constitutively expressed by both neurons and oligodendrocytes in the adult spinal cord. It is particularly enriched in the periaxonal myelin at the interface between axon and myelin (Manitt et al., 2001), leading to the suggestion that netrin-1 may contribute to the inhibitory environment of the adult CNS.

The Eph receptor tyrosine kinase family and their ephrin ligands also play important roles in controlling neuronal growth cone movement through repulsive cues. Ephrin proteins fall into two classes, ephrin-A class, defined by a GPI linkage to the cell membrane, and ephrin-B class, which have a transmembrane domain and a short cytoplasmic region. The Eph receptors are likewise subclassified, where EphA receptor bind ephrin-B class, and EphB receptors bind ephrin-A class (Gale et al., 1996). Eph receptors and ephrins provide important signals during development for migrating neural crest cells. Through mainly repulsive cues, they prevent cells or axons from entering inappropriate territory, and in turn establish patterns of tissue organisation. This is achieved through the expression of complementary Eph receptors and ephrins in appropriate domains (Wilkinson, 2001). This system may be involved in restricting axonal regeneration following injury, since not only are ephrins and their ligands expressed in the adult CNS but they are also upregulated following spinal cord injury, particularly by reactive astrocytes (Miranda et al., 1999; Willson et al., 2002; Bundesen et al., 2003).

A more recently described group of axonal guidance molecules are the slit family, encoded for by three genes, slit 1, 2 and 3 (Brose & Tessier-Lavigne, 2000). These are secreted proteins which bind to the roundabout (Robo) group of receptors, also encoded for by three genes, robo1, robo2 and rig-1 (Camurri et al., 2004), although Rig-1 might not be Slit

binding. The Slit-Robo system is involved in repulsion of migratory neurons (Brose et al., 1999; Li et al., 1999), but may also promote axon branching (Brose & Tessier-Lavigne, 2000). Mediatation of repulsion appears to be via GTPase family members (Wong et al., 2001; Ghose and Vactor, 2002). A clear role, however, has not yet been shown for slit-robo in CNS regeneration failure, although it may be likely since both slit and Robo mRNAs are expressed in the adult brain (Marillat et al., 2002).

1.1.2.7 Inflammatory response

It is still a matter for debate as to whether the inflammatory response is beneficial or inhibitory for axonal regeneration following CNS injury. Microglia are known to release a range of inflammatory cytokines and other factors including IL-1 and IL-6 (Woodroofe et al., 1991), tumour necrosis factor α (TNFα) (Frei et al., 1987), TGFβ (Keifer et al., 1993), glutamate (Piani et al., 1991) and nitric oxide (Minghetti & Levi, 1998). It has been suggested that these may exacerbate damage within the system. Indeed some of these factors, such as TGFβ, have been implicated in the initiation of reactive astrocytosis (Reilly et al., 1998; Krohn et al., 1999) and the formation of the glial scar (see section 1.2.1.3). In addition, microglia, as well as probably inducing expression of CS-PGs through release of Il-6, and TGFα and β, (see section 1.1.2.3), have also been identified as a source themselves of inhibitory CS-PGs such as NG2 (Jones et al., 2002).

In contrast, evidence also exists to suggest that macrophages and microglia may actually be beneficial for regeneration. Unlike the PNS, where the macrophage response is rapid, the CNS response is a lot slower (Avellino et al., 1995). This leads to a slower removal of myelin and axonal debris. Since this debris is inhibitory to axonal growth, its persistence within the CNS is detrimental to regeneration. Support for this theory comes from studies on fish and amphibia, where microglia and macrophages respond as rapidly in the CNS as the PNS, and CNS regeneration is also observed (Avellino et al., 1995).

1.1.3 Strategies to promote CNS repair

1.1.3.1 Removal of inhibitory factors

Due to an understanding of the role inhibitory components play in preventing the regeneration of the CNS following injury, a range of procedures have been developed in order to promote regeneration by making the environment more permissive. A crude way to achieve this is to remove all inhibitory glia from the vicinity of the lesion, as has been demonstrated by ethidium bromide treatment. This resulted in a dramatic regrowth of axons for a limited time until endogenous glia surrounding the lesion were able to invade (Moon et al., 2000). This method was advantageous since it dealt with all inhibitory glia, instead of being cell-type specific. However, it is quite invasive and also abolished all beneficial properties of surrounding glia. An alternative method has been devised to remove only the reactive astrocytes by inserting the herpes thymidine kinase (HTK) gene under the glial fibrillary acidic protein (GFAP) promoter. When GFAP was upregulated by reactive astrocytes, so was HTK, which in the presence of systemic gancilovir killed the cell, leaving unreactive astrocytes in place (Delaney et al., 1996; Bush et al., 1998, Faulkner et al., 2004). This resulted in some increase of axonal growth, but also in disruption of the blood brain barrier, and a gross invasion of inflammatory cells (Bush et al., 1998).

A less invasive approach is to neutralise specific inhibitory molecules. The antibody IN-1 specifically binds the myelin protein Nogo-A, and has been successfully used both to promote regeneration of the CST (Thallmair et al., 1998), and to restore forelimb function following ischaemia induced by middle cerebral artery occlusion (Papadopulos et al., 2002). Due to the discovery that three known inhibitory myelin proteins, Nogo, MAG and Ompg, all signal via the same receptor, NgR, a more direct approach would be to block this receptor. This has been demonstrated using an antagonist peptide of NgR which allowed CST fibre re-growth following a hemisection, and again resulted in functional recovery (GrandPre et al., 2002).

Since the CS-PGs are one of the major inhibitory components of the injured CNS (see section 1.1.2.3), approaches to overcome their effects have been investigated. The enzyme chondroitinase ABC, which degrades many different CS-PG family members through

cleavage of their inhibitory GAG chains, has been used in different injury models. Application of chondroitinase ABC into lesioned dorsal columns, resulted not only in the up-regulation of GAP-43, but also the regeneration of both ascending and descending CST axons, resulting in the restoration of synaptic activity (Bradbury et al., 2002). In addition, it stimulated the long distance regeneration of axons following lesioning of the nigrostriatal tract (Moon et al., 2001).

A more general approach to reduce the inhibitory nature of the glial environment has been to prevent its activation by inflammatory factors. Since both macrophages and microglia have been shown to promote gliosis following spinal cord injury, they were depleted by an injection of liposome-encapsulated clodronate (Popovich et al., 1999). This resulted in increased axonal sprouting and an improvement in hindlimb movement. Alternatively, a blocking antibody against TGFβ2, a gliosis promoting factor, was applied following lesioning of the cerebral cortx (Logan et al., 1999). This resulted in reduced glial scarring, as well as enhanced neurite extension

1.1.3.2 Promotion of intrinsic regenerative state of neurons

Another strategy to promote regeneration is to enable axons to overcome the inhibitory nature of the CNS environment. One method for achieving this is to modulate the levels of cAMP within the neuron. As was mentioned earlier, a decrease in cAMP is associated with an increased sensitivity to inhibitory components (see section 1.1.2.4). Therefore, by increasing cAMP levels, the neuron should be rendered less susceptible to inhibition. This has been achieved both by a conditioning lesion, or by treatment with cAMP analogues. A conditioning lesion was made in a peripheral nerve 1-2 weeks before a lesion to the CNS part of a dorsal column, allowing axonal regrowth through the lesion site and beyond (Neumann and Woolf, 1999). Alternatively, addition of a cAMP analogue at both 48 hours (Neumann et al., 2002) and 1 week (Qui et al., 2002) prior to lesioning of the dorsal root resulted in the same effect.

Since CNS axons fail to up-regulate certain growth-promoting genes in response to injury, one strategy was to over express these genes prior to injury. Co-expression of GAP-43 and

CAP-23, both major growth cone components, resulted in extension of axons in adult mice following spinal cord injury (Bomze et al., 2001).

However, the translation of this kind of approach to the clinic is at present unclear since there is a need for treatment before an accident happens. Despite this, it does demonstrate a clear principle for tackling spinal cord injuries.

1.1.3.3 Application of neurotrophic factors

Neurotrophic factors have been proposed to treat CNS injury due to their role in regulating many aspects of neuronal regeneration, from survival and differentiation, to growth and plasticity. Many different strategies for delivering them to injury sites have been investigated. NGF, NT-3 and glial-derived neurotrophic factor (GDNF) treatment, when applied directly to the spinal cord following a dorsal root crush injury, resulted in nerve growth across the dorsal root entry zone (DREZ) into the spinal cord (Ramer et al., 2000). Although only small diameter non-myelinated axons responded, functional and behavioural recovery were detected. In this experiment, BDNF treatment did not promote axon growth, although recovery of synaptic activity was supported.

Fibroblasts genetically modified to express neutrorophins have been used successfully for transplantation into several models of injury. BDNF-expressing fibroblasts supported the regeneration of rubrospinal tract axons, accompanied by recovery of forelimb movement (Liu et al., 1999). NT-3-expressing fibroblasts supported regeneration of corticospinal tract axons through the grey matter for substantial distances, although these were unable to penetrate the white matter (Grill et al., 1997). In addition, GDNF-expressing fibroblasts promoted the regeneration of motor axons following transection of the hypoglossal nerve (Blesch et al., 1998)

An alternative delivery method into injury sites is the implantation of matrices infused with growth factors. Implantation of an NT-3-containing collagen matrix into a CNS lesion induced sprouting and regeneration of corticospinal fibres (Houweling et al., 1998).

Furthermore, viral vectors have been used to deliver genes of interest. Using this approach, BDNF was introduced into rubrospinal neurons, where it prevented their atrophy

following spinal cord injury (Ruitenberg et al., 2004). Additionally, NGF has been introduced in this way before a lesion, where it promoted axonal sprouting in the cortex (Ramirez et al., 2003). Gene transfer of GDNF also helped preserve neuronal fibres following a spinal cord contusion, as well as promoting hindlimb locomotor recovery (Tai et al., 2003).

1.1.3.4 Transplantation studies

Transplantation into lesion sites using a range of different cell types and tissue has been investigated, with the aim of producing a more permissive environment for axonal regeneration through either replacing lost cells, enriching the tissue with growth factors, or acting as suitable substrates for growth.

As has been mentioned in the previous section, the transplantation of fibroblasts expressing various neurotrophins has been performed with some success. In addition, transplantation of inflammatory cell types, such as microglia (Rabchevzky et al., 1997) and macrophages (Rapalino et al., 1998) has also resulted in axonal outgrowth. As discussed in Section 1.1.2.6, there is still some debate about whether inflammatory cells are beneficial or not for regeneration, nor is it clear whether resultant regeneration is due to the transplanted cells directly, or whether they recruit endogenous cells such as Schwann cells. The use of embryonic stem cells in transplant-mediated repair has also proved promising, where they have been shown to differentiate into appropriate CNS cells, such as oligodendrocytes and astrocytes (McDonald et al., 1999; Liu et al., 2000), although few neurons were generated. Studies have also been carried out with mouse embryonic stem cells restricted to a neural fate, seeded into a degradeable polymer scaffold, and transplanted into a hemi-section spinal cord injury (Teng et al., 2002) which resulted in an improvement in functional recovery. Foetal tissue transplantation is another avenue of investigation since it is rich in both ECM and trophic factors (Vaudano et al., 1995), and has been shown to promote axonal regeneration (Courmans et al., 2001; Duchossoy et al., 2001). However, such axons do not enter the host CNS (Bregman et al., 1997), although this can be partially overcome by supplementing the graft with exogenous BDNF and NT-3 (Cournans et al., 2001; Bregmann et al., 1997). Another focus of transplantation therapies is the use of glial cells, particularly OECs and Schwann cells, due to their growth-promoting properties *in situ*.

Since this is a very exciting area, which relates directly to the contents to this thesis, it will be dealt with in detail in section 1.3.1.4 and 1.4.4.

Despite the benefits of using many of the above strategies to promote regeneration of the damaged CNS, it looks like a combinatorial approach would be a more realistic way to tackle CNS injury. In this way we can take advantage of a range of different beneficial properties, where one strategy alone may favour sprouting, and another long distance growth. This has already been carried out with some success, for example, foetal grafts (Courmans et al., 2001) and Schwann cell bridges (Xu et al., 1995a) have both been supplemented with neutrotrophins, which allow the re-entry of axons into the host tissue. In addition, Schwann cell grafts have been supplemented with methods to raise the neuronal cAMP concentration, such as addition of rolipram (phosphodiesterase IV inhibitor) or dibutyryl (db)-cAMP. This resulted in an increased sparing of neurons following spinal cord contusion, and also increased myelination (Pearse et al., 2004). Best results were obtained when both rolipram and db-cAMP were used with Schwann cell grafts, resulting in significantly more nerve fibre growth beyond the grafts, and even recovery of locomotor function (Pearse et al., 2004).

1.2 Glial cells of the CNS

1.2.1 Astrocytes

The most abundant cell type within the CNS are the astrocytes, which comprise as much as 25% of the cells and 35% of the total mass of the CNS (Eng et al., 1992). They are generally stellate in shape with branching processes, which wrap around neuronal cell bodies and dendrites, and interact with the basal lamina of blood vessels and the pial surface (Goldstein, 1988; Suarez and Raff, 1989). However, the astrocyte population is a very heterogeneic one, being divided generally into protoplasmic and fibrous types, the former existing within the grey matter, and the latter in the white matter (Wilkin et al., 1990). There are also further regional variations due to differential gene expressions, for example, only cerebellar astrocytes express somatostatin mRNA whereas proenkephalin mRNA and enkephalin peptides were present in cortical, striatal and cerebellar astrocytes (Shinoda et al., 1989). Marked differences have also been observed in the levels of

glutamine synthetase and GFAP, as well as neutrotransmiatter receptors and enzymes, in astrocytes cultured from different brain regions (Shinoda et al., 1989).

1.2.1.1 Functions under normal conditions

It was originally believed that astrocytes played a merely supporting role for the 'all-important' CNS neurons, by providing only a structural scaffolding, hence they were viewed as a kind of brain 'glue', leading to the term neuroglia, meaning nerve glue (Ransom et al., 2003). As such, astrocytes form barriers around blood vessels and connections between nerve cells. However, experiments carried out in recent years have led to the understanding that astrocytes play a role in almost all of the brain's functions, both during normal and pathological conditions.

Astrocytes function primarily as the housekeeping cells of the CNS, maintaining and supporting its normal functions. In this way, they are involved in maintaining tight control of pH homeostasis and local ion concentrations, such as K^+ and Ca^{2+}, as well as regulating the extracellular volume within the CNS (Sykova et al., 1992). They also provide neurons with glucose and metabolic substrates, while removing neuronal waste such as metabolic byproducts and neurotransmitters, for example glutamate and gamma amino butyric acid (GABA), released during synaptic transmission (Schousboe et al., 1992). In addition, astrocytic processes interact with endothelial cells of capillaries to form the blood brain barrier. This protects the brain from the entry of numerous large molecules, such as proteins and toxic substances, from the blood. Other processes, known as perivascular end feet, contact the pia mater, where they seal off the CNS through tight association of these processes, forming the glia limitans.

More recently, however, it has been shown that astrocytes also function to dynamically regulate neuronal activity. Astrocytes, along with other CNS glia, are known to envelop synapses, in what was presumed to be a passive manner. However, evidence has arisen showing that in response to neurotransmitter release, the astrocytes feed back to the presynaptic neuron to either enhance or depress the signal, as well as to the postsynaptic neuron, producing either excitatory or inhibitory responses (Perea and Araque, 2002; Newman, 2003). Evidence also suggests that they may be involved in synaptogenesis,

regulating the formation, maturation and maintenance of such synapses (Slezak and Pfiegar, 2003).

1.2.1.2 Development

Astrocytes are understood to arise mainly from the neuroepithelium, via an intermediate radial glial cell. Radial glia are the first cells that can be distinguished from neuroepithelial stem cells of the embryonic ventricular zone, first appearing at the onset of neurogenesis. They serve as a scaffold for migrating neurons, which are also generated in the ventricular zone, before they terminally differentiate into astrocytes (Schmechel and Rakic, 1979; Voigt, 1989), and neurons (Tamamaki et al., 2001). However, once development is completed, multipotent progenitor cells persist in the adult brain within the subventricular zone (SVZ). These are able to form neurons (Doetsch et al., 1997), many of which migrate to the olfactory bulb in the rostral migratory stream, as well as forming astrocytes and oligodendrocytes (Levison and Goldman, 1993). In fact, these progenitor cells have been shown to be the SVZ astrocytes (Doetsch et al., 1999), which may also derive from radial glia (Taramontin et al., 2002). These cells may be a source of tissue replacement following injury, thus demonstrating that a fully differentiated glia can act as a stem cell.

An additional progenitor cell which can give rise to astrocytes is the O-2A, or oligodendrocyte-type-2-astrocyte, progenitor, so named because *in vitro* it was shown to differentiate into both oligodendrocytes, and type-2 astrocytes (Raff et al., 1983). They were was discovered in the optic nerve and were shown to develop postnatally, hence type-2 astrocytes were so named to distinguish them from type-1 astrocytes which develop within the embryo. These astrocytes also retain the oligodendrocyte-lineage marker A2B5. However, *in vivo*, the O-2A only gives rise to oligodendrocytes (Fulton et al., 1992), and was therefore renamed the oligodendrocyte progenitor cell (OPC). This may be due to environmental cues *in vivo* which either promote oligodendrocyte development, or inhibit astrocyte differentiation.

1.2.1.3 Reactive astrocytosis

Following injury, astrocytes undergo many changes becoming what is termed a reactive astrocyte (see Figure 1.1). This response occurs rapidly and can be detected within one hour of a focal mechanical trauma (Mucke et al., 1991). These astrocytes act to preserve the host tissue integrity following injury. This was clearly demonstrated in experiments where reactive astrocytes were ablated following spinal cord injury (see section 1.1.3.1). Here, the blood brain barrier was not repaired, and further damage to neurons and oligodendrocytes occurred (Faulkner et al., 2004). Reactive astrocytes also participate in the repair process by forming a scar, re-establishing a glial limiting membrane made up of compact astrocytes bound together by gap and tight junctions (Fawcett and Asher, 1999; Shearer and Fawcett, 2001). This astrocytic scar protects the CNS from exposure to the external, peripheral environment, as well as walling off areas of tissue necrosis and filling space resulting from neuronal loss.

Reactive astrocytes are characterised by many defined changes such as hypertrophy and in some cases, proliferation (Eng and Ghirniker, 1994). In addition, they undergo changes in gene expression, many of which are used to identify the reactive form, which lead to a complex and varied response to injury (Eddleston and Mucke, 1993). The hallmark change involved in astrocytosis is a morphological one, with an increase in multi-branched processes and astrocyte swelling (hypertrophy), and the upregulation of GFAP expression. GFAP is the principle intermediate filament of mature astrocytes, and has been shown to be necessary for the formation of astrocytic processes in response to neuronal signals (Weinstein et al., 1991). The precise functions of GFAP are not fully understood as yet, although experiments on GFAP knock out mice have suggested important roles in normal astrocyte function, such as mediating astrocyte-neuronal interactions and modulation of synaptic efficacy in the CNS (McCall et al., 1996). Other protein changes occurring during astrocytosis may have obvious biological roles in regulating the environment of the injured CNS. These include the upregulation of proteases and protease inhibitors, which may help remodel the ECM or clear up debris; cytokine production, which could regulate the inflammatory response and the blood brain barrier; and the production of neurotrophic factors which help protect neurons and other brain cells (Eddleston and Mucke, 1993).

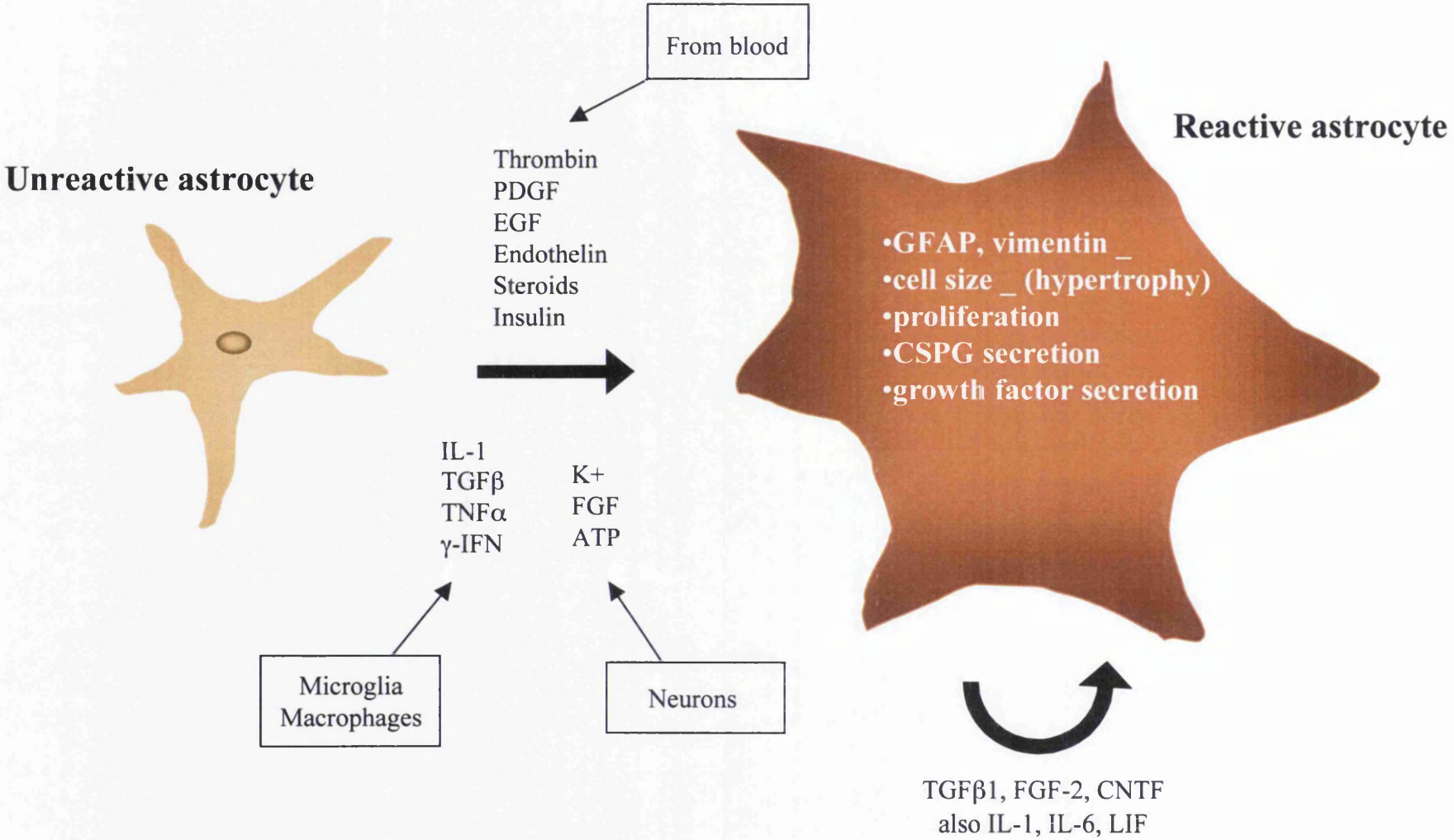

Figure 1.1 Schematic showing major changes occuring during astrocytosis.

Triggers during CNS injury include IL-1 and TGFβ produced by macrophages and microglia, amongst others. Reactive astrocytes then undergo several defined changes including upregulation of GFAP, increase in size (hypertrophy), proliferation, and also the production of inhibitory CS-PGs and growth factors. Many of these growth factors probably maintain the reactive response, such as TGFβ1, FGF-2 and CNTF.

However, the glial scar resulting from reactive astrocytosis also has detrimental effects on the ability of the CNS to regenerate. Firstly, this compact scar tissue acts as a mechanical barrier preventing regenerating CNS axons from penetrating it. In addition, the scar is also rich in a range of ECM components, produced by astrocytes, which are inhibitory to axonal outgrowth (Fitch and Silver, 1997a). One such group of proteins are the CS-PGs (Fawcett and Asher, 1999), as has been covered in detail (see section 1.1.2.3). GFAP itself has also been shown to be involved in axonal inhibition, since astrocytes lacking GFAP actually promoted neuronal extension *in vitro*, rather than inhibiting it (Menet et al., 2000).

The regulation of the astrocytic response is not fully understood in any detail, particularly due to the range of cell types that are involved in the post-injury response and scar formation. Within such structures, not only astrocytes, but also inflammatory cells such as microglia and macrophages, and OPCs are involved. In addition, they all release many cytokines and growth factors which may either be involved in activating the post-injury response, or in its maintenance or regulation. Upon invasion of microglia and macrophages in the early stages following injury, initial signalling between them and astrocytes probably involves IL-1 (Lee et al., 1995; Herx and Yong, 2001). They are also a source of TGFβ which has been demonstrated to induce astrocytic hypertrophy and increased GFAP expression *in vivo* (Laping et al., 1994) and *in vitro* (Reilly et al., 1998; Krohn et al., 1999). Astrocytes themselves are also a source of TGFβ1 (da Cunha et al., 1993), thus is likely to be acting as an autocrine or paracrine mechanism. In fact, astrocytes release a range of cytokines and growth factors, which have also been shown to induce astrocytic hypertrophy or proliferation in culture (Eddleston and Mucke, 1993). For example, FGF-2 (Menon and Landerholm, 1994) and ciliary neurotrophic factor (CNTF) (Rudge et al 1994), are substantially upregulated in injured tissue. FGF-2 has been shown to induce GFAP upregulation in cultured astrocytes (Reilly et al., 1998), and CNTF induces hypertrophy both *in vivo* and *in vitro* (Hudgins and Levison, 1998).

In addition, the astrocytic response is very heterogeneic, with not all astrocytes adopting the same phenotype. For example, not all reactive astrocytes are associated with increased amounts of ECM molecules, and conversely, in areas of increased ECM, not all astrocytes

have become reactive (Fitch and Silver, 1997a). Therefore, a lot of work is still required to clarify the processes involved in gliosis.

1.2.2 Oligodendrocytes

1.2.2.1 Biological function

Oligodendrocytes are the myelinating cells of the CNS, and along with the astrocytes, are the other major class of CNS glia. Due to their ability to produce multiple processes, they are able to ensheath and myelinate fifteen axons on average, as well as surround neuronal cell bodies in the grey matter. This myelin sheath allows action potentials to pass along the CNS axons by saltatory conduction, but following injury, provides one of the major sources of inhibitory molecules (see section 1.1.2).

1.2.2.2 Myelinating disease

In demyelinating diseases, such as multiple sclerosis (MS), it is this myelin sheath that is lost, although there is evidence that axonal damage also occurs (Giuliani and Yong, 2003). Spontaneous remyelination can occur, for example in experimentally-created demyelinating animal models (Blakemore et al., 1977) and in the early inflammatory phases of MS (Zamvil and Steinman, 2003). However, with the onset of chronic demyelination, new myelin is no longer produced. It is a matter for debate whether remyelination is due to mature oligodendrocytes or OPCs, and whether failure to remyelinate results from a depletion in replacement cell stocks, or differentiation and recruitment malfunction (Franklin, 2002a).

In models of experimentally-created demyelination both transplanted and endogenous mature oligodendrocytes are unable to myelinate (Keirstead and Blakemore, 1999). Furthermore, within remyelinated areas of the CNS, there was an enhanced number of mature oligodendrocytes observed (Prayoonwiwat and Rodriguez, 1993) despite their inability to proliferate (Keirstead and Blakemore, 1999). This has suggested that rather than oligodendrocytes, OPCs may be the remyelinating cell, which in turn can give rise to a mature population of oligodendrocytes, as has also been supported by lineage labelling experiments (Carroll and Jennings, 1994; Gensert and Goldman, 1997).

1.2.2.3 Repair of persistent demyelination

Several approaches have been investigated to enhance remyelination of demyelinated lesions. One suggestion has been to enhance spontaneous remyelination through delivery of growth factors, such as PDGF and FGF, which may be involved in the recruitment phase of remyelination, or insulin-like growth factor 1 (IGF-1), whose levels are enhanced during spontaneous remyelination (Hinks and Franklin, 1999, 2000). Alternatively, since MS is believed to be a chronic inflammatory disorder, modulation of the inflammatory response may prove a more effective method. This is the favoured strategy for dealing with MS at present, where the immunomodulatory drugs, interferon beta and glatiramer acetate, significantly reduce the inflammatory response and demyelination (Flachenecker and Rieckmann, 2003). An additional strategy, would be to replace myelin through transplantation of myelin producing cells. This would be beneficial in situations where remyelination has failed due to a depletion of endogenous myelinating cell stocks. However, there is ongoing debate regarding which stage in the oligodendrocyte lineage is best for tranplantation, i.e. whether OPCs, immature or mature oligodendrocytes (Targett et al., 1996; Keirstead and Blakemore, 1997; Franklin, 2002b). In addition, these cells may not be beneficial within chronic MS lesions where they may continue to be a target of the ongoing autoimmune destruction of CNS myelin (Milner et al., 1997). Alternative cells with myelinating capacity proposed for transplantation, therefore, include the OEC and the Schwann cell, which will be discussed in more detail later (section 1.3.1.4 and 1.4.4).

1.2.3 Microglia

Microglia are the resident phagocytes of the CNS. It has long been debated whether they are actually glial cells, or whether they are more related to cells of the mononuclear phagocyte lineage. However, it is generally accepted now that they are ontogenetically related to mononuclear phagocytes (Kreutzberg, 1996). Resting microglia are small cells with short, branched processes that comprise approximately 5% of the glial population of the CNS. They show a downregulated immunophenotype which is adapted to the specialised microenvironment of the CNS. However, upon injury, they become activated, and function mainly as scavenger cells, although they also play other roles involved in tissue repair and neural regeneration. Their activation is tightly controlled by the nature of

insult, such that a graded response results. As well as responding to traumatic injury, they can respond to subtle alterations in their microenvironment such as imbalances in ion homeostasis that precede pathological changes (Kreutzberg, 1996). Their role in gliosis is discussed in more detail in section 1.1.2.5.

1.3 Glial cells of the PNS

1.3.1 Schwann cells

The Schwann cell is the major glial cell of the PNS, although others do exist such as the teloglia of somatic motor terminals, satellite cells associated with neuronal cell bodies in sensory, sympathetic and parasympathetic ganglia and the enteric glia in the ganglia of the gut. In the PNS, all axons are ensheathed by Schwann cells, and these are either myelinated or not depending on the diameter of the axon. If the axon is less than 1μm in diameter, several axons, usually in bundles, are ensheathed by one non-myelinating Schwann cell, with no myelin protein present (Jessen and Mirsky, 1991). However, for larger axons, one myelinating Schwann cell forms a myelin sheath around a single axon, resulting in a signet ring appearance. The functions of the Schwann cell include 1) providing an interface between the axon and the surrounding tissue, 2) allowing increased saltatory conduction of the nerve impulse due to its myelin sheath, and 3) playing important roles in the regeneration and development of nerves, particularly after injury.

1.3.1.1 Schwann cell development

The majority of Schwann cells in adult nerves originate directly from the neural crest (Jessen and Mirsky, 1992; Le Deourain et al., 1991), along with the other main glial cells of the PNS, as well as peripheral neurons and melanocytes. It was suggested that some Schwann cells may arise from other sources, such as the ventral neural tube or from neuroepithelial cells in the spinal cord after migration of the neural crest is complete (Lunn et al., 1987; Sharma et al., 1995). However, recent experiments have demonstrated that this secondary source of Schwann cells is actually derived from boundary cap cells (Maro et al., 2004; see below), which in turn also have a neural crest origin (Niederlander and Lumsden, 1996). The generation of Schwann cells from the neural crest follows a pathway involving

two main intermediate cell types (Mirsky and Jessen, 1999). First, a Schwann cell precursor is formed, and is observed in rat peripheral nerves at embryonic day (E) 14 and 15. These cells do not express S100, and do not have a basal lamina. They are also dependent upon axonal signals for survival (Jessen et al., 1994). From these precursor cells, the immature Schwann cell is formed which can be detected from E17 until time of birth (Jessen et al., 1994; Dong et al 1995, 1999). These cells envelop unmyelinated axons and also form a basal lamina. From the time of birth, mature myelinating Schwann cells begin to form, although the non-myelinating cell appears later (Mirsky and Jessen, 2002). This last step is axon-dependent and also reversible, Schwann cells being able to interchange between myelinating and non-myelinating phenotypes. Schwann cell development is believed to be regulated in part by the neuregulins, since they influence proliferation and survival of Schwann cells (Grinspan et al., 1996; Trachtenberg and Thompson, 1996). The neuregulins have also been implicated in myelination since inactivation of the neuregulin receptor ErbB3 led to the formation of thinner myelin sheaths (Garratt et al., 2000). Reduced myelin sheath thickness also resulted from reducing neuregulin-1 expression too (Michailov et al., 2004).

The formation of the DREZ is an important aspect of development since this is a transition zone between the permissive PNS and the inhibitory CNS. It is here that Schwann cells and astrocytes contact each other, forming an interface which may resemble that which occurs following transplantation of Schwann cells into the astrocytic environment of the CNS (see Section 1.5.2). This interface arises during early development as a result of cellular interactions between the neural crest and neuroepithelial cells (Golding et al., 1997). Before these cells give rise to Schwann cells and astrocytes respectively, a population of cells, known as boundary cap cells, cluster at what will later become the axon entry and exit points to the spinal cord (Niederländer and Lumsden, 1996). These boundary caps are believed to be transient neural-crest-derived structures, which allow the entry and exit of axons before the formation of the inhibitory glia limitans. A correlation between the timing of boundary cap dispersal, and the loss of capacity for dorsal root axons to enter the spinal cord supports this proposal (Carlstedt 1988; Golding and Cohen, 1997), as does the observation that neurites can enter CNS-tissue in culture if boundary cap cells are present (Golding and Cohen, 1997). Soon after birth in the rat, these boundary cap cells decline in

number and allow astrocyte processes, which are previously hindered by the presence of boundary caps, to extend into the dorsal roots and form the DREZ (Carlstedt, 1988; Golding et al., 1997). As a result, Schwann cells and astrocytes come into contact over an extended area, and the resulting interface is inhibitory to both Schwann cell and axon migration. Thus, after the loss of boundary caps, cut axons can regrow through the peripheral dorsal root, but this growth is abruptly inhibited at the glial limitans (Liuzzi and Lasek 1987; Carlstedt, 1988). The inhibitory effect of the astrocytes can be demonstrated following experimental disruption of the spinal cord glia limitans by X-irradiation, which allows penetration of both regenerating sensory axons and Schwann cell populations which can enter the astrocyte-free DREZ (Franklin and Blakemore, 1993; Sims and Gilmore 1994).

1.3.1.2 Myelinating versus non-myelinating phenotype

Schwann cells require axonal contact to drive their differentiation from immature Schwann cells to non-myelinating or myelinating mature Schwann cells (Mirsky and Jessen, 1999). This mature phenotype, however, remains very plastic, with cells being able to return to a cell type similar to the immature phenotype (Mirsky and Jessen, 1996), before redifferentiating into either myelinating or non-myelinating cells. This can be demonstrated both in culture and after transection of a mature nerve, where developmental regression of individual Schwann cells accompanied by myelin breakdown is observed. Reestablishment of appropriate axonal contact, as seen in regenerating nerves or in myelinating co-cultures of Schwann cells and neurons, leads to redifferentiation, and myelination. It is believed that cAMP may be involved in the regulation of Schwann cell phenotype, although the exact axonal signals have not been fully determined. Schwann cells cultured in the absence of axons, which possess an antigenic and morphological phenotype similar to non-myelinating Schwann cells, can be induced by addition of cAMP promoting agents such as forskolin, to adopt a phenotype more similar to myelinating Schwann cells (Scherer et al., 1994; Morgan et al., 1991).

Mature Schwann cells are recognised by the O4 antibody (Mirsky et al., 1990), but the myelinating and non-myelinating phenotypes can easily by distinguished. Myelinating

Schwann cells express many myelin proteins such as protein zero (P0), MAG, myelin basic protein (MBP), and peripheral myelin protein 22kDa (PMP22) (Scherer, 1997). They also express the glycolipid galactocerebroside (GalC). In contrast, non-myelinating Schwann cells express a diffuse form of GFAP, N-CAM, GAP-43 and $p75^{NTR}$ (Mirsky et al., 1986; Jessen et al, 1990; Curtis et al., 1992).

1.3.1.3 Peripheral nerve repair

Following injury to the peripheral nerve, nerve fibres distal to the lesion undergo a process called Wallerian degeneration. This leads to the removal and recycling of axonal myelin-derived material, and prepares the environment for subsequent axonal growth by the regenerating nerve. After the axon and myelin degenerate the remaining Schwann cells are stimulated to proliferate within the basal lamina tube that surrounded the original nerve fibre; these columns are known as endoneurial tubes or bands of Büngner (Torigoe et al., 1996; Burnett and Zager, 2004). This tube then acts as a conduit for the re-growing axon. In this way, injuries which damage the basal lamina such as a transection, do not repair as well as when the basal lamina is left intact, such as in a crush injury. This basal lamina consists of collagen, fibronectin and laminin, produced by Schwann cells (Baron von Evercooren et al., 1986). Both fibronectin and laminin have been shown to be potent substrates for neurite outgrowth (Cohen et al., 1987; Humphries et al., 1988). The proliferation of Schwann cells within these bands are believed to be stimulated by both the axonal membrane and myelin debris (Salzer and Bunge, 1980; Salzer et al., 1980), as well as invading macrophages (Baichwal et al., 1988).

Schwann cells have been shown to be the key component of subsequent axonal regeneration in experiments where a length of peripheral nerve has been frozen, killing the Schwann cells but leaving the basal lamina intact. If this nerve is grafted on to a proximal stump in a host animal, regeneration through it is only possible if migrating Schwann cells accompany the nerve (Fawcett and Keynes, 1990).

Schwann cells in the bands of Büngner do not die since they are maintained by an autocrine mechanism. This has also been demonstrated in culture, where mature Schwann cells are

able to survive without axonal contact. The active factors involved in this aurocrine survival loop, are believed to be IGF-2, PDGF-BB and NT-3 (Meier et al., 1999).

Schwann cells are suited to promoting axonal regeneration since they produce many neurotrophins such as neuregulin (Raabe et al., 1996), BDNF and GDNF (Yamamoto et al., 1993). In addition, they also express several growth stimulatory cell adhesion molecules such as integrins, L1, NCAM (Martini et al., 1994) and N-cadherin (Bixby et al., 1988; Lakatos et al., 2000). Inhibitory antibodies to L1, beta-1 integrin and N-cadherin have highlighted a significant role for these molecules in neurite outgrowth (Bixby et al., 1988). Remyelination of regenerating axons is also possible following peripheral injury, occurring within 3 weeks (Fawcett and Keynes, 1990).

1.3.1.4 Transplantation studies

Since Schwann cells mediate the axonal-growth-promoting properties of the peripheral nervous system, it was investigated whether they could be used to provide a permissive environment for CNS regeneration after injury. Many experiments have demonstrated that Schwann cells can indeed be used to promote repair of the injured CNS. This was firstly done using peripheral nerve grafting (Tello 1911 - cited in Franklin and Barnett, 1997; Richardson et al., 1980; Benfrey and Aguayo, 1982), and later by transplantation of Schwann cells either in suspension (Rasiman et al., 1993; Brook et al., 1994, 2001) or when seeded into channels (Xu et al., 1995b, 1999; Plant et al., 2001). Such experiments have shown that the presence of Schwann cells can promote the extension of nerves into grafted channels. In addition Schwann cells can induce sprouting of axons (Li and Rasiman, 1994), as well as directing subsequent nerve growth (Brook et al., 1994).

However, for such results to be clinically beneficial, the observation of functional recovery is necessary. This has been assessed using behavioural tests or by direct measurement of electrical conductivity using electrophysical methods. Fortunately, restoration of nerve conduction have been observed following complete transection of the spinal cord (Imazuimi et al., 2000). Functional synaptic contacts were also re-established following optic nerve

transection and subsequent replacement with a segment of peripheral nerve (Vidal-Sanz et al., 1987).

Schwann cells have also been used successfully to remyelinate demyelinated axons. This has been shown in experimentally-generated demyelinating lesions, where lesions are produced by gliatoxins, such as ethidium bromide and lysolecithin, thus leaving the axons intact, and subsequent repair by endogenous glial cells prevented by X-irradiation, known as the X-EB model (Blakemore et al., 1977). Following Schwann cell transplantation, peripheral myelin was identified, as well as the characteristic one-to-one glia-axon relationship, demonstrating remyelination was attributable to the transplanted Schwann cells (Blakemore 1977; Blakemore and Crang, 1985). The clinical relevance of such cellular transplantations has been supported by the restoration of conduction through the lesions (Smith and Hall, 1980, Felts and Smith, 1992; Honmouu et al., 1996).

However, despite all this success, there are limitations to the use of Schwann cells for transplantation repair, which will be discussed later (see section 1.5.1).

1.4 The Olfactory System

The primary olfactory system comprises of both CNS and PNS tissue (see Figure 1.2). The olfactory bulb is located within the CNS part of the primary olfactory system and is a laminated structure, whereas the epithelium exists within the PNS. The outer layer of the bulb consists of olfactory receptor neuron (ORN) axons, which extend from the peripheral epithelium, and associated glial cells. This layer is known as the olfactory nerve layer. Beneath this is the glomerular layer consisting of round structures, termed glomeruli, which are collections of synapses between ORNs, interneurons and second order neurons.

The ORNs project cilia into the nasal cavity, which contain olfactory receptors, capable of binding odorant molecules. These olfactory receptors are a family of G-protein-coupled seven-helix transmembrane proteins, and were first cloned by Buck and Axel (1991). The oderant receptor family has now been found to be the largest gene family known, due to the presence of between 500-1000 genes in the mammalian genome (Buck, 1992). It is also now

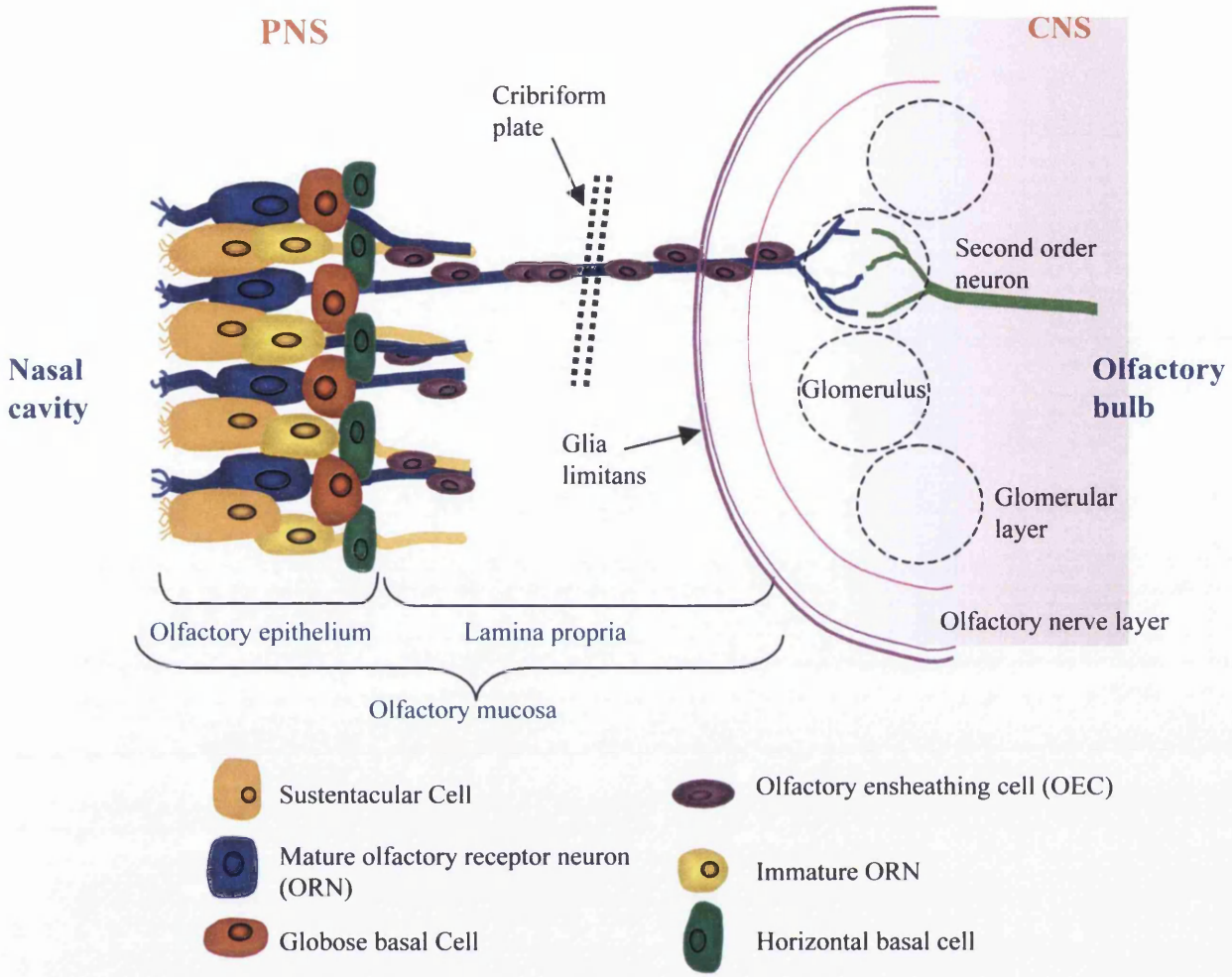

Figure 1.2 Schematic of the primary olfactory system.

The olfactory system is composed of both peripheral nervous system (PNS) and central nervous system (CNS) tissue. The PNS component contains the olfactory mucosa which is subdivided into the olfactory epithelium and lamina propria. The olfactory epithelium contains olfactory receptor neurons (ORNs; which project cilia into the nasal cavity), sustentacular cells (non-neuronal supporting cells), globose basal cells (putative stem cells for the epithelium), horizontal basal cells (putative stem cells) and Bowman's gland and ducts. The lamina propria consists of loose connective tissue and olfactory ensheathing cells (OECs), which ensheath bundles of olfactory receptor axons extending from the olfactory epithelium. The olfactory receptor axons course through the cribriform plate and enter the olfactory nerve layer of the CNS environment of the olfactory bulb, where they synapse to form glomeruli with the second order neurons in the glomerular layer.

apparent that each ORN only expresses one receptor gene (Malnic et al., 1999). Upon binding an odorant molecule, an electrical signal is generated in the ORN which is then transmitted from the PNS to the CNS, where the information is processed.

The olfactory system is unique in that, not only is it one of only a few regions of the CNS which are capable of spontaneous repair following injury, but ORNs also constantly undergo neurogenesis throughout the life of the organism (Graziadei and Graziadei, 1979). ORNs are constantly replaced from presumptive stem cells residing at the base of the olfactory epithelium, and have an average life span of between 4-8 weeks depending on the environment (MacKay-Sim and Kittel, 1990) and the species (Ramon-Cueto and Avila., 1998). These newly generated neurons then extend axons through the peripheral part of the olfactory system to the glia limitans, where they not only penetrate the CNS part of the olfactory bulb, but also form new synapses within the glomerular layers (Valverde et al., 1992; Treloar et al., 1999). This unique property has been suggested to be due to the presence of a novel glial cell within the olfactory system known as the olfactory ensheathing cell (OEC). These glial cells were first described by Golgi and Blanes (reviewed in Ramon-Cueto and Avila., 1998) at the end of the nineteenth century, when two types of macroglial cells were observed in the olfactory bulb. They described stellate cells distributed throughout the entire bulb, which are now known to be astrocytes, and fusiform cells, which were located in the first two layers of the olfactory bulb, and are now known to be OECs.

1.4.1 OEC morphology and antigenic profile

1.4.1.1 *In vivo*

In the olfactory system, OECs exist in a close relationship with axons, where OECs ensheath bundles of unmyelinated axons along the axons' length, crossing the PNS-CNS transition zone, from the epithelium to the outer layers of the olfactory bulb (Doucette, 1991, Ramon-Cueto and Valverde. 1995). The OEC has a mixture of properties in common with both Schwann cells from the PNS, and astrocytes from the CNS (Doucette, 1984;. Chuah and Au, 1991). Like the non-myelinating Schwann cell, OECs ensheath bundles of axons (Bunge et al., 1986; Jessen and Mirsky, 1991), and express $p75^{NTR}$ (Barnett et al.,

1993), laminin (Liesi et al., 1985) and L1 (Miragall et al., 1988). In common with the astrocyte, OECs express fibrous GFAP (Barbour and Dahl, 1987), whereas Schwann cells express a more diffuse form of GFAP (Jessen et al., 1990). OECs also form part of the olfactory bulb glia limitans at the PNS-CNS transition zone, in a manner resembling the glia limitans of astrocytes at other cranial and spinal nerves (Doucette, 1991). Hence, not only does the OEC span both the PNS and the CNS within the olfactory system, but it also shares properties in common with the glial cells from these two different regions.

However, despite these similarities to both Schwann cells and astrocytes, the OEC is in fact a distinct type of glial cell. It differs from the non-myelinating Schwann cell by ensheathing bundles of up to 200 axons, opposed to the 20 ensheathed by Schwann cells (Franklin and Barnett, 1997). In addition, OECs have a distinct antigenic profile (Barnett et al., 1993; Franceschini and Barnett, 1996), for example, unlike both myelinating and non-myelinating Schwann cells, they lack Gal C (Jessen and Mirsky, 1991). On the basis of this antigenic profile, they can be purified by fluorescent-activated cell sorting (FACS) for O4+/GalC- (Barnett et al., 1993). They are also distinct from astrocytes, due to their ultrastructure, OECs having an electron dense cytoplasm with fewer intermediate filaments, in contrast to astrocytes which contain bundles of intermediate filaments in an electron lucent cytoplasm (Doucette, 1984, 1990).

Within the bulb, however, OECs appear to exist as a heterogenous population, where the O4 positive olfactory nerve layer (Barnett et al., 1993) can be divided into further layers including an inner polysialylated form of NCAM (PSA-NCAM, also known as embryonic-NCAM or E-NCAM)-positive layer, surrounded by a $p75^{NTR}$-positive outer layer (Franceschini and Barnett, 1996). In the mouse, the S100-positive olfactory nerve layer was divided into a GFAP/neuropeptide Y (NPY)-positive inner layer and a $p75^{NTR}$-positive outer layer (Au et al., 2002).

1.4.1.2 *In vitro*

In accordance with the *in vivo* observations, OECs in culture also consist of a heterogeneous population. The antigenic profile of OECs in culture (purified by FACS

sorting for O4+/GalC-; Barnett et al., 1993) at first resembled those seen *in vivo*, but with time some of these markers change. In serum-containing conditions, OECs lose expression of O4 and PSA-NCAM, gaining $p75^{NTR}$ and diffuse GFAP, and attaining a flatter morphology. However, if OECs are maintained in serum-free conditions supplemented with astrocyte-conditioned media (ACM), two morphologically and antigenically distinct cell types can be identified. These consist of 1) a flat astrocyte-like/fibroblast-like cell, with high levels of PSA-NCAM and filamentous GFAP, but no $p75^{NTR}$, and 2) a non-myelinating Schwann cell-like cell, with a spindle morphology, expressing high levels of $p75^{NTR}$ but no PSA-NCAM (Franceschini and Barnet, 1996). However, some cells have been observed to have a phenotype intermediate between these two phenotypes, expressing both $p75^{NTR}$ and PSA-NCAM in culture (Franklin and Barnett, 1997).

The precise relationship between these different cell phenotypes is as yet not fully understood, although a clonal OEC cell-line was able to give rise to both astrocyte-like and Schwann cell-like OECs, demonstrating that the two cell types are indeed related and share a common lineage (Franceschini and Barnett, 1996). Thus, it appears that the OEC is a plastic cell which can, depending upon culture conditions, adopt various phenotypes. This has been demonstrated clearly in culture where OECs can rapidly adopt different morphologies depending upon the culture conditions, and also upon contact with other cell-types such as astrocytes and neurons (van den Pol and Santarelli, 2003; Vincent et al., 2003).

1.4.2 Development

A further distinction between OECs and previously characterised glia is their developmental origin. Whereas astrocytes are derived from the neuroectoderm and Schwann cells from the neural crest, OECs have been shown to originate, along with the olfactory epithelium, from the olfactory placode (Doucette, 1989; Chuah and Au, 1991). The olfactory bulb, however, along with other CNS structures, develops from the neural tube (Doucette, 1989). Therefore, as the bulb and the epithelium come together during embryonic development, primitive olfactory neurons are required to extend axons from their origin in the epithelium to where they penetrate the bulb. This is achieved since

neurons migrating forwards are accompanied by a mass of migrating placodal cells, including OEC progenitors which are distinguished by their electron-dense ultrastructure from the other migrating cells (Doucette, 1989, 1993). As these cells reach the primitive bulb, the bulb evaginates and the migrating cells cover it in a thin layer. These then penetrate the glia limitans, which at this stage comprises of ventricular layer-derived astrocytes, leading to the formation of the olfactory nerve and glomerular layers. It is within these newly formed layers, that OECs and astrocytes are then able to intermingle, forming a new glia limitans at the bulb surface. This glia limitans is different to that surrounding other areas of the CNS, since it remains penetrable to axons throughout adulthood.

1.4.3 Role of OECs in olfactory regeneration

Due to the presence of OECs in a tissue capable of constant neuronal turnover, it was proposed that the OECs may play a major role in promoting regeneration (Doucette, 1989). In fact, since the PNS-CNS entry zone of the olfactory system is continuously permissive to the entry of olfactory nerve fibres and has a glia limitans consisting of OECs as well as astrocytes, in contrast to other restrictive PNS-CNS interfaces (such as the DREZ) consisting of just astrocytes, this seemed a very plausible suggestion. Further support for a role for OECs in regeneration came from *in vitro* studies, showing OECs to be a highly conducive substrate for primary olfactory axon outgrowth (Goodman et al., 1993; Chuah and Au, 1994, Kafitz and Greer, 1998, 1999). Although the precise molecular mechanisms by which OECs are able to support axonal growth is not fully understood, they do express many molecules suitable for such a task. These include axon growth-promoting adhesion molecules such as L1 (Miragall et al., 1988) and PSA-NCAM (Franceschini and Barnett, 1996). It has been noted that the continued presence of PSA-NCAM in the adult olfactory system, indicates a retention of embryonic features, which may underlie its remarkable regenerative capacity (Miragall et al., 1988). This is supported by the presence of PSA-NCAM in other brain areas which can also generate neurons or exhibit morphological or physiological plasticity (Seki and Arai, 1993).

A large array of survival and growth factors which can influence axonal outgrowth, are produced by OECs, such as NGF, BDNF, NT-3/4 and neuregulin (Thompson et al., 1999; Boruch et al., 2001; Woodhall et al., 2001). In addition, OECs are immunoreactive for PDGF (Kott et al., 1994) and NPY (Ubink et al., 1994). They also produce ECM components, which may support axonal growth, such as laminin (Doucette, 1996; Kafotz and Greer, 1997), fibronectin and type-IV collagen (Doucette, 1996). Laminin, in particular, is seen as a preferential substrate for ORN neurite extension *in vitro* (Krafitz and Greer, 1997).

It has also been shown that in a model of olfactory system regeneration where olfactory fasicles are destroyed following zinc sulphate treatment of the olfactory system (Matulionis, 1975), OECs remain in their original position with processes that ensheath axons remaining, suggesting that they may act as a conduit for the regenerating ORN axons (Williams et al., 2004).

1.4.4 Role in Transplantation

Due to the potential regeneratory properties of the OEC, it was a logical step to see how OECs could be used to contribute to the repair of CNS pathologies. Following on from the hypothesis that it was the presence of OECs at the glia limitans of the olfactory bulb that might permit the entry of growing axons, their regeneration-promoting properties were directly demonstrated in the DREZ (Ramon-Cueteo and Nieto-Sampedro, 1994). Here, following injury, the glia limitans prevents dorsal root axons from crossing from the PNS to the CNS. However, when OECs were transplanted into the DREZ following dorsal root transection, numerous regenerating dorsal root axons could be observed re-entering the spinal cord.

This initial success has since been followed by many other examples of OECs apparent ability to support axonal regeneration in different experimental models of CNS injury. Following a complete transection of the thoracic spinal cord, Ramon-Cueto and co-workers followed up their pioneering experiment by showing that transplanted OECs could support long-distance regeneration of spinal cord axons (Ramon-Cueto et al., 1998). Likewise,

following a focal lesion of the rat corticospinal tract, OECs inhibited the profuse axonal banching ('abortive sprouts') and led to a directed elongation of regenerated corticospinal axons, both across the lesion site and back into the distal part of the white matter tract (Li et al., 1998). Many other experiments have also shown this remarkable capacity of OECs to support axonal outgrowth following injury (Smale et al., 1996; Li et al., 1997, 2003; McDonald et al., 1999; Navarro et al., 1999; Ramon-Cueto et al., 2000; Lu et al., 2002).

As with Schwann cells, for OEC transplantation to be a therapeutic strategy for treating spinal cord injuries, restoration of function needs to be observed, and indeed has been demonstrated by many researchers. Recovery of locomotor behaviour in rats following complete transection was reported when OECs were transplanted into the spinal cord (Ramon-Cueto et al., 2000), even if the transplantation occurred 4 weeks after the injury (Lu et al, 2002). In the same way, restoration of breathing and climbing was demonstrated following a hemi-transection of the spinal cord followed by immediate transplantation of an OEC-containing endogenous matrix (Li et al, 2003). The restitution of spinal reflex functions has also been reported (Navarro et al., 1999; Taylor et al., 2001), along with direct observation of impulse conductions across a transected dorsal column following OEC transplantation.

In addition to its success in spinal cord injury repair, the OEC has also shown much promise for treatment of persistent demyelinating diseases such as multiple sclerosis. *In situ*, the OEC is associated with small diameter olfactory receptor axons which are not myelinated, however, due to its many similarities to the non-myelinating Schwann cell, which is also normally engaged with small diameter axons, it was proposed that OECs might have the potential to myelinate axons if the diameter was of an appopriate size. This was confirmed *in vitro* where OECs co-cultured with dorsal root ganglions were capable of forming a myelin sheath (Devon and Ducette, 1992). In the X-EB model of demyelination (see section 1.3.14), where a chemically demyelinated lesion was formed, an OEC cell line was also capable of myelinating axons (Franklin et al., 1996). Interestingly, this myelin was of a peripheral composition and morphology, such as the expression of P0, further supporting the Schwann cell-like nature of OECs. Such models of remyelination have also been shown to restore efficient conduction along the axons (Imaizumi et al., 1998).

The clinical potential of OECs for CNS repair has become more possible due to the recent observation of a human equivalent cell (Barnett et al., 2000), which shares many properties in common with the rat OEC, such as similar growth factor requirement and expression of $p75^{NTR}$. Similar to the rat, human OECs also myelinated demyelinated CNS axons following transplantation (Barnett et al., 2000, Kato et al., 2000).

Furthermore, whereas previous OEC cultures have mainly been taken from the bulb (Barnett et al., 1993; Smale et al., 1996; Navarro et al., 1999; Plant et al., 2002; Li et al., 2003), recently OECs have been obtained from the lamina propria, beneath the olfactory epithelium (Au and Roskams, 2003). Thus, a peripheral source of OEC may be available which would make obtaining such cells for autologous repair of human pathologies much safer than the invasive procedures required to gain access to the olfactory bulb.

Whether the different OEC phenotypes (see section 1.4.1.2) fulfil different roles *in vivo* is not known at present. Following transplantation, it has been suggested that the Schwann cell-like OEC may ensheath the regenerating fibres, whilst the astrocyte-like OEC, may be forming an outer perineurial-like sheath around the regenerating axon and associated Schwann cell-like OECs (Raisman, 2001). However, the astrocyte-like OEC observed following transplantation may actually be due to contaminant fibroblasts or meningeal cells (Lakatos et al., 2003b; Li et al., 2003). However, in the majority of transplantation studies, cultures were almost homogenous for $p75^{NTR}$ positive/GFAP diffuse OECs, typical of the Schwann cell-like cell (Navarro et al., 1999; Ramon-Cueto et al., 1998, 2000; Verdu et al., 2001; Plant et al., 2002; Takami et al., 2002), and probably reflecting the popular purification technique of $p75^{NTR}$ immunopanning. However, despite the observation of a purely $p75^{NTR}$ population, Smale and colleagues (Smale et al., 1996) distinctly saw two morphologies following transplantation, one being slender or spindle shaped, and the other being large and flat. As previously mentioned, little is known about the relationship between the different OEC phenotypes, except their obvious plasticity.

1.5 Comparison of Schwann cells and OECs

It can be summarised, from the previous sections (1.3.1.4 and 1.4.4), that OECs and Schwann cells have many general properties in common. First, both OECs and Schwann cells are involved in promoting neurogenesis *in situ*. OECs support neuronal growth, both as part of the general turnover of olfactory receptor neurons, and following injury to the olfactory system. Likewise Schwann cells are involved in the development of the PNS, and facilitate regeneration of peripheral nerves following injury. In addition, they both share similar antigenic properties (see Table 1.2), where OECs, like non-myelinating Schwann cells, can adopt a spindle-like morphology, and express GFAP and $p75^{NTR}$. Furthermore, they have both been shown to promote axonal regrowth and remyelination upon transplantation into models of CNS lesions (see section 1.3.1.4 and 1.4.4). Interestingly, not only do OECs express myelin typical of the PNS following remyelination (Franklin et al., 1996; Kato et al., 2000), but this remyelination is controlled using similar signalling mechanisms as for Schwann cells. It has been shown that the transcription factors, Krox-20 and SCIP/Oct-6 are involved (Blanchard et al., 1996; Smith et al., 2001), and that desert hedgehog, which is implicated in control of peripheral nerve myelination (Bitgood and McMahon, 1995) is also expressed by OECs (Parmantier et al., 1999; Smith et al., 2001).

Schwann cells and OECs also display similar growth responses, where proliferation of both cell types is induced following an increase of intracellular cAMP (Wewetzer et al., 2002; Ramon-Cuteo et al., 1998; Yan et al., 2001). In addition, both cell types proliferate in response to a similar spectrum of growth-promoting molecules – including heregulin, GGF-2, and hepatocyte growth factor (HGF) (Krasnoselsky et al., 1994; Levi et al., 1995; Zhang et al., 1995; Pollock et al., 1999; Chuauh et al., 2000; Yan et al., 2001).

However, despite these similarities, there are some differences between OECs and Schwann cells, some of which were discussed in section 1.4.1.1. This is particularly seen in their interactions with astrocytes, for example, following transplantation.

Table 1.2. Antigenic and morphological comparison of astrocytes, Schwann cells and OECs.

		Antigenic marker						Morphology
		$p75^{NTR}$	GFAP	E-NCAM	O4	GalC	P0	
Astrocyte		-	fibrous	-/+*	-	-	-	flat
Schwann cell	Myelinating	-	diffuse	-	+	+	+	spindly
	Non-myelinating	+	diffuse	+	+	+	+	spindly
OEC	Schwann cell-like	+	diffuse	-	+	-	+**	spindly
	Astrocyte-like	-/+	fibrous	+	+	-	+**	flat

OECs have properties akin to both astrocytes and Schwann cells. The Schwann cell-like OEC most resembles the non-myelinating Schwann cell phenotype, but differs in Gal C expression. * Some reactive astrocytes are E-NCAM positive (Alonso and Privat, 1993; Nomura et al., 2000). ** P0 not seen *in situ*.

1.5.1 Transplantation studies

In order to achieve successful repair following transplantation into injury models, certain criteria must be fulfilled by the transplanted cells. Firstly, the cells must be able to survive within the host tissue for long enough to promote repair. Secondly, it is important that they are able to migrate to areas of damage, rather than remain within the graft. Thirdly, they would need to display suitable properties, which would be beneficial for promoting repair of the injury site. This could be through the promotion of neuronal regeneration, which requires subsequent formation of functional neuronal synapses, or through sparing of tissue or promotion of remyelination. In addition, the transplanted cells must not contribute to the formation of the glial scar at the injury site to a level which could inhibit regeneration.

Both OECs and Schwann cells are candidates for transplant-mediated repair of CNS lesions and in different ways meet several of these criteria. There is still debate as to which might be the superior candidate and this will be discussed.

Following transplantation into CNS tissue, regenerating nerves respond differently to Schwann cells and OECs. It was shown that whereas Schwann cells stimulated axonal sprouting at the lesion site (Li and Rasiman, 1994), axonal sprouting was reduced by OECs, which instead caused an increase in growth into the distal part of the transected spinal cord (Li et al., 1997, 1998). This ability to promote long distance axonal regeneration was also demonstrated by Ramon-Cueto et al (1998), where although axons could enter Schwann cell-filled guidance channels, they could not leave the channel and re-enter the spinal cord at the distal graft-host interface. The presence of OECs at the channel/tissue interface, however, could promote this. Further evidence that Schwann cells fail to promote the exit of axons from the graft was observed by Plant et al (2001). They speculated that this may result from the high concentration of chemoattractant growth factors within the graft, such as FGF, which prevent the axons leaving such a favourable environment. Alternatively, it could be due to an unfavourable tissue reaction at the distal interface leading to astrocytosis and the generation of inhibitory factors, such as the CS-PGs. OECs might improve this situation by producing factors favouring long-distance elongation of

axons, or through prevention of such an inhibitory response by the distal host tissue, as has been proposed by Verdu et al. (2001).

In contrast, under different experimental conditions, Schwann cells have been demonstrated to be a superior candidate for repair than the OEC, for whom limitations were observed. Following a contusion injury, Schwann cell transplantation led to an improvement of locomotor activity where OEC transplants were of no benefit (Takami et al., 2002). In addition, *in vitro* myelination assays demonstrated that under conditions where Schwann cells could form myelin, OECs failed (Plant et al., 2002). Whether this was due to the OEC preparation used remains a possibility. It has recently been shown that pure OEC preparations were less efficient at myelinating axons, following tranplantation into models of demyelination, than preparations containing contaminant meningeal cells (Lakatos et al., 2003b). Further *in vivo* studies have also failed to repeat the initial successes of OEC transplantation into experimental CNS injury models (Barnett and Riddell, 2004). For example, following dorsal root sectioning and re-anastomosis, OEC transplants did not enhance the number of fibres entering the spinal cord in comparison to control samples, nor did electrophysiology measurements demonstrate any functional reconnection between regenerating fibres and spinal cord neurons (Riddell et al., 2004). Reasons for these discrepancies between experiments may be due to any number of reasons from variations in cell preparations; such as age of donor tissue, time in culture, and culture conditions of cell transplants; to differences in transplantation sites and injury models. It therefore appears that there are many factors which determine the efficacy of glial cell transplantations, which need to be addressed in order to improve the reliability of such therapies. One such factor is their ability to integrate with the host tissue following transplantation.

1.5.2 Compatibility with host tissue

Many researchers, have reported that OECs are able to migrate and co-exist within host tissue (Li et al., 1998; Ramon-Cueto et al., 1998; Gudino-Cabrera et al., 2000), following transplantation into the injured spinal cord. In contrast, Schwann cells do not migrate as well (Baron von Evercooren et al., 1992; Franklin and Blakemore, 1993; Iwashita et al., 2000), instead being restricted to the lesion site itself (Iwashita et al., 2000; Shields et al.,

2000). In fact, Schwann cells also exhibited poor survival in these studies (Iwashita et al., 2000). Such observations are reminiscent of the Schwann cell-astrocyte interface *in situ* at the glia limitans of the DREZ, where Schwann cells and astrocytes exist either side of a defined boundary. Interestingly, if the formation of this glia limitans is impeded during development by X-irradiation of astrocytes, extensive Schwann cell myelination of CNS tracts will occur (Gilmore and Duncan, 1968 – cited by Franklin and Barnett, 1997), demonstrating the inhibitory nature of the astrocytic glia limitans for Schwann cell migration. Likewise, the ability of the OEC to integrate with astrocyte-rich tissue reflects its co-existence with astrocytes within the glia limitans of the olfactory bulb.

However, in contrast to this, there is evidence that Schwann cells can migrate within the CNS, for example, upon grafting into the hippocampus (Brook et al., 1993; Raisman et al., 1993). However, they may have travelled predominantly along blood vessels and the pia mater rather than through astrocyte-rich areas. Whether OECs are capable of migrating extensively within the CNS after transplantation also remains controversial, since some studies report extensive migration (Gudino-Cabrera and Nieto-Sampedro, 1996), whereas others show that OECs are in fact confined to the graft (Smale et al., 1996). In addition, very few direct comparisons have been made between OEC and Schwann cell migratory potentials. In one direct comparison, both Schwann cells and OECs displayed limited migration within the spinal cord, where they remained in clusters at the transplant site (Lakatos et al., 2003a). However, these cells were transplanted into non-injured tissue and migration might have been impeded by the lack of space to migrate into, in contrast to transplantation studies into experimental lesions (Gudino-Cabrera et al., 2000; Ramon-Cueto et al., 1998; Li et al., 1997, 1998). In addition, non-injured tissue may lack many of the growth factors which are present following injury, that may influence cellular migration.

In contrast to the results obtained *in vivo*, the different abilities of OECs and Schwann cells to migrate within astrocyte-rich areas *in vitro* have been clearly demonstrated. In these assays Schwann cells cultured with astrocytes formed discrete boundaries, being unable to migrate amongst them (Ghirniker and Eng, 1994; Wilby et al., 1999). OECs cultured with astrocytes, however, did not form such boundaries (Lakatos et al., 2000), but instead were able to interact much more favourably, where they intermingled and migrated extensively within astrocyte territories. An additional observation in these *in vitro* experiments was

that astrocytes in contact with Schwann cells underwent a hypertrophic response, becoming enlarged and enhancing their expression of GFAP (Ghirniker and Eng, 1994) and CS-PGs (Lakatos et al., 2000). Neither of these markers were upregulated in OEC-astrocyte co-cultures.

This also reflects studies *in vivo*, where following Schwann cell transplantation, reactive astrocytes are observed (Plant et al., 2001; Lakatos et al., 2003a). These astrocytes may restrict the efficiency of Schwann cells in subsequent regeneration, a theory supported by the observation that Schwann cell remyelination of CNS tissue only occurs in astrocyte-free areas (Woodruff and Franklin, 1999; Shields et al., 2000), and also that Schwann cells myelinate CNS axons more extensively in situations where the astrocyte-formed glia limitans was disrupted (Franklin and Blakemore, 1993). In addition, Schwann cell transplantation has led to a greater expression of CS-PGs within the host tissue (Plant et al., 2001), than that seen for OEC transplantation (Lakatos et al., 2003a). It has also been suggested that OEC transplantations following a photochemical lesion to the spinal cord may actually lead to a decrease in CS-PG expression (Verdu et al., 2001). An increase in CS-PG expression has been proposed as one of the major factors responsible for the failure of axonal regeneration (Fawcett and Asher,1999; Plant et al., 2001; see Section 1.1.2.3).

1.5.3 Molecular mechanisms determining Schwann cell and OEC interactions with astrocytes

At present, very little is understood, regarding the molecular mechanisms responsible for determining Schwann cell and OEC interactions with astrocytes. The inability of Schwann cells to migrate into astrocyte-rich areas was suggested to be mediated by contact inhibition between the astrocyte and the Schwann cell. In particular, evidence from experiments by Wilby et al (1999) suggest that N-cadherin may be involved in this process, limiting Schwann cell migration through the formation of strong adhesions with astrocytes. In these experiments, inhibitory peptides and antibodies against N-cadherin blocked the adhesion and increased the migration of Schwann cells on astrocyte monolayers. A similar mechanism has also been demonstrated for oligodendrocyte precursors (Schnaedelbach et al., 2001). Since OECs migrate more extensively within an astrocyte environment than

Schwann cells, it was originally suggested that OECs may lack N-cadherin, and thus might not be restricted by such inhibition. This, however, has been shown not to be the case since OECs express N-cadherin at similar levels to Schwann cells (Lakatos et al., 2000). It remains to be seen whether N-cadherin does indeed regulate these differences between OEC and Schwann cell interactions with astrocytes, and since it is expressed on both, why its role in the two cells should be different.

Furthermore, little is known why OECs and Schwann cells should induce different astrocytic responses upon contact with astrocytes, both as modelled *in vitro*, and following transplantation. As has been reviewed earlier, we know of several cytokines and growth factors capable of inducing an astrocytic reaction (see Section 1.2.1.3), however, this list is by no means exhaustive at present, and whether these factors act to induce or maintain such a response is still unknown, as are their precise origins. It is known that Schwann cells, under certain conditions such as Wallerian regeneration, can produce many of these astrocytosis-inducing cytokines, such as IL-1 (Bergsteinsdottir et al., 1991; Skundric et al., 1997; Rutkowski et al., 1999), IL-6 (Murwani et al., 1996; Rutkowski et al., 1999) and TNFα (Murwani et al., 1996; Wagner and Myers, 1996). Whether these factors are also produced by OECs is at present unclear, and may highlight another similarity or difference between the two glia. Any induction of astrocytosis by transplanted cells might, not only limit the ability of these cells to migrate away from the transplantation site, but also mask any benefit and hinder the regeneration of axons. It is also important to assess the degree to which Schwann cells contribute to scarring after injury since endogenous Schwann cells can penetrate the injured CNS (Bruce et al., 2000) and may contribute to the reactive response throughout the CNS.

1.6 Migration and Adhesion

Since OECs and Schwann cells have been shown to have different abilities to migrate into astrocytic areas (Gudino-Cabrera and Nieto-Sampedro, 1996; Iwashita et al., 2000; Lakatos et al., 2000;), it will be important for this thesis to review some of the processes involved in cell migration. Migration requires a coordination of many events involved in both cell propulsion, as well as cellular adhesion, both to the ECM and to other cells. Due to the

proposal that Schwann cell-inhibition upon astrocytes may be due to the function of N-cadherin, particular emphasis will be made on cadherin function and regulation.

1.6.1 Integrins

1.6.1.1 Migration

Cell migration is important for many biological and pathological processes, including embryogenesis, inflammation, tissue repair and regeneration as well as tumour invasion and metastasis. Of particular interest here, migratory processes are involved in axonal outgrowth leading to regeneration, and importantly, determine the ability of transplanted cells for CNS repair to reach appropriate targets.

Migration can be viewed as a multi-step cycle, involving the extension of a cellular protrusion, formation of stable attachments near the leading edge of the protrusion, translocation of the cell body forward, release of adhesions and retraction of the rear of the cell (Webb et al., 2002; Wehrle-Haller and Imhof, 2003). In this way, coordination of adhesion assembly and disassembly is very important, and therefore tightly regulated. The actin cytoskeleton is important for driving the initial extension of the plasma membrane at the cell front, and can connect to the ECM through a large family of transmembrane receptors, known as integrins due to their ability to integrate the extra- and intra-cellular skeletons. It is these attraction sites that are believed to function as traction points for the propulsive forces that move the cell body forward.

1.6.1.2 Focal adhesions and turnover

The integrins are receptors for ECM proteins such as fibronectin, vitronectin, laminin and collagen. They are composed of α and β families of transmembrane subunits which can heterodimerise to form more than 20 different receptors which exhibit different patterns of expression and binding specificity. At integrin adhesion sites, over 50 different proteins have been found (Zamir and Geiger, 2001). The classification of these adhesions, including, fibrillar adhesions, focal complexes, focal adhesions and podosomes, depends upon the morphology and method of formation. Fibrillar adhesions are central $\alpha5\beta1$ integrin-

containing structures, whereas focal complexes are small Rac activated adhesions at the cell front (Zamir and Geiger, 2001) which drive rapid cell migration (Beningo et al., 2001). Focal adhesions, which are relatively stable structures that may inhibit cell migration, are the best studied since they are also involved in other processes such as the formation and remodelling of extracellular matrices (Geiger et al., 2001). It has also been observed that these different adhesion structures have different molecular compositions. The formation and disassembly of adhesions are complex processes and require a coordinated interaction of actin or actin-binding proteins, signalling molecules, structural proteins, adaptor molecules and microtubules, as well as the integrins (see Figure 1.3).

It appears that adhesion formation is sequential, with recruitment of individual proteins rather than a preformed complex. Upon integrin binding and aggregation, recruitment of focal adhesion kinase (FAK) and tensin results, followed by that of the cytoskeletal proteins such as α-actinin, paxillin, vinculin and talin (Miyamoto et al., 1995; Yamada and Miyamoto, 1995). Paxillin however, seems to be recruited in a small preformed complex with signalling components such as p21-activating kinase (PAK) and PAK-interacting factor (PIX) (Matafora et al., 2001).

Dispersion of adhesion occurs both at the cell rear, where retraction of the cell tail occurs, and at the cell front, allowing formation of new protusions and adhesions, but the mechanisms at these two locations are different. At the rear, integrin remains associated with its substrate while the intracellular adhesive components, which are under tension from the cytoskeleton, slide along the actin fibres towards the cell body and eventually disperse, hence is not a simple reversal of assembly. However, at the front of the cell, turnover of components by assembly reversal does occur. This difference appears to be directed by the presence or absence of α-actinin, whose presence in the adhesions causes them to be no longer turned over but instead to slide inwards towards the cell body (Webb et al., 2002).

Adhesion turnover is regulated by many different proteins, particularly the Rho family of GTPases. Rac is required for the formation of new adhesions at the cell front, whereas Rho is required for the maturation of existing contacts, as well as promoting adhesion disassembly (Rottner et al., 1999). Other regulatory proteins include FAK. This protein

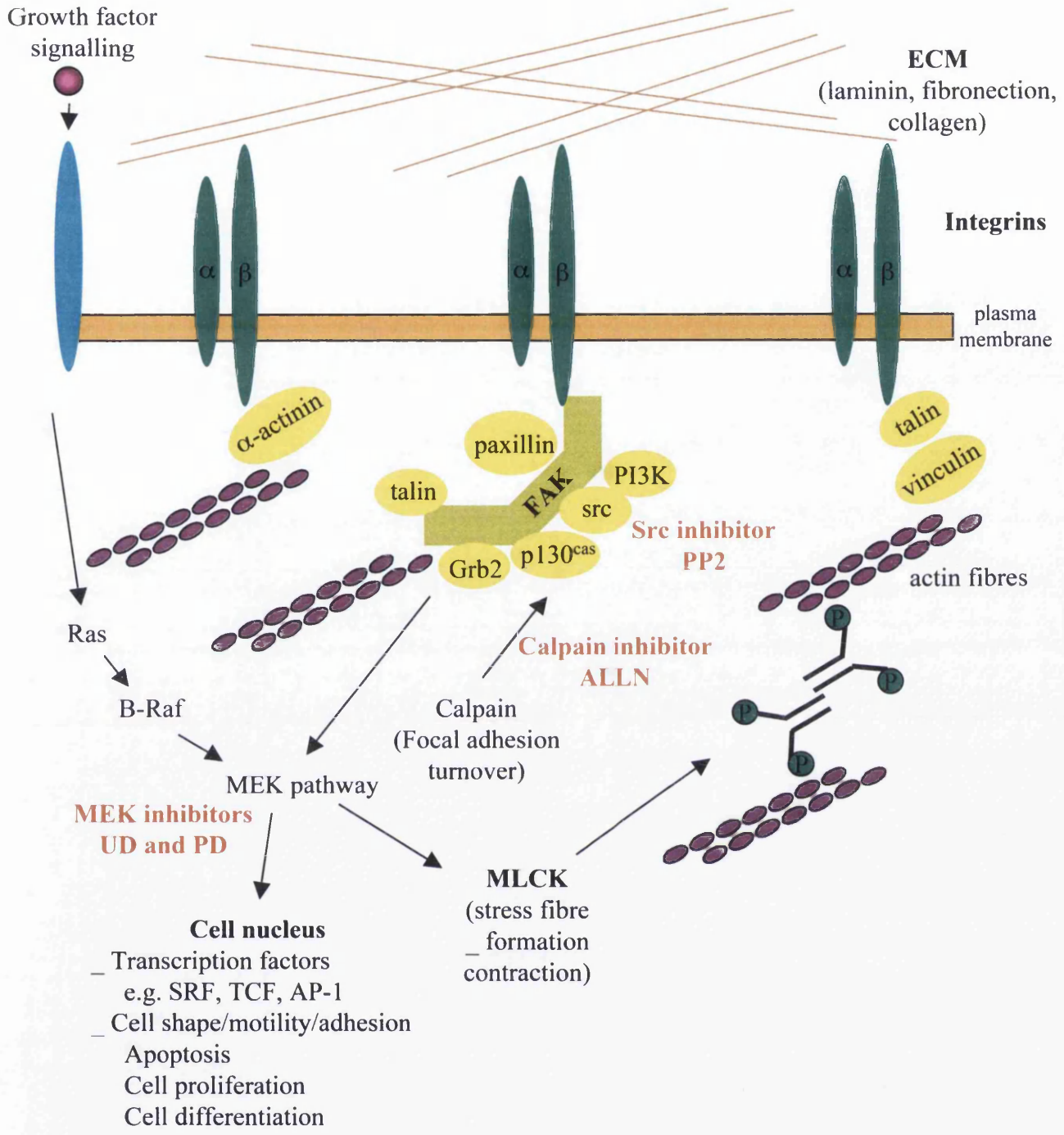

Figure 1.3 Integrin signalling and motility

A schematic showing various integrin signals to the cytoskeleton, either directly via a-actinin and talin/vinculin, or via complex focal adhesion interactions. FAK acts as a multi-protein scaffold of the focal adhesion, and regulates its turnover. Focal adhesion turnover is also regulated by calpain and src interactions. Stress fibre formation is promoted by myosin light chain kinase (MLCK) phosphorylation of myosin. The actions of various inhibitors used throughout this thesis are marked in red.

co-localises to focal adhesions, where it acts downstream of both the GTPases and integrin-mediated cell adhesion, to promote both assembly (Richardson et al., 1997) and disassembly (Fincham et al., 1995) of focal adhesions. Upon activation, it undergoes complex tyrosine phosphorylation at 6 or more sites, allowing it to interact and form a complex with src, which is also necessary for migration, and particularly focal adhesion turnover (Fincham and Frame, 1998). This FAK-src complex can promote the phosphorylation of substrates such as paxillin and Crk-associated substrate (CAS). FAK has been shown to be necessary for migration since FAK-deficient cells spread more slowly on ECM proteins, and migrate poorly in response to chemotactic signals (Parsons, 2003). In addition, overexpression of FAK in Chinese hamster ovary cells resulted in enhanced cell migration (Cary et al., 1996). The role of FAK in focal adhesion turnover has been suggested to mediate its control of migration due to the need for functional interactions between several FAK-interacting proteins, such as paxillin, Cas and src, which FAK may scaffold together (Webb et al., 2002). In addition, FAK is also involved in mediating signalling pathways necessary for migration, such as the MEK pathway (Schlaepfer and Mitra, 2004).

Calpain, a calcium-dependent protease, is also implicated in the regulation of migration, particularly through the control of focal adhesion disassembly. Several calpain isoforms exist, two of which are ubiquitous (calpain I and II), several are tissue-specific isoforms, and one is a small 28-kDA regulatory subunit (calpain 4). Its activity is tightly regulated by its endogenous inhibitor calpastatin (Wendt et al., 2004), and it differs from most proteases due to its ability for limited cleavage of its protein substrates into stable fragments rather than complete proteolytic digestion. It is this cleavage of focal adhesion components, including integrins (Du et al., 1995), FAK (Cooray et al., 1996), paxillin (Yamaguchi et al., 1994) and talin (Beckerle et al., 1997) amongst others, that promotes the disassembly of these complexes (Bhatt et al., 2002) resulting in reduced cell adhesion and increased migration (Carragher and Frame; 2002). Inhibition of calpain I function, therefore generally reduces migration (Huttenlocher et al., 1997; Carragher et al., 2001), however there are some exceptions. For example, inhibition of calpain I function in resting neutrophils actually led to an increase in random migration, and resulted in decreased directional migration towards chemotactic stimuli (Lokuta et al., 2003). Thus calpain plays a complex

role in regulation of migration, and may regulate chemotaxis in neutrophils too. The function of calpain has been linked to FAK and src regulation of migration since v-src activity induces the synthesis of calpain (Carragher et al., 2002), and also induces the cleavage of FAK by calpain (Carragher et al., 2001).

1.6.2 Cadherins

As well as integrin adhesion to the ECM, migration is also dependent upon the function of cellular adhesion molecules, including immunoglobulin cell adhesion molecules (Ig CAMs) and selectins, as well as the Ca^{2+}-dependent cell adhesion molecules, known as cadherins.

1.6.2.1 Cadherin family/structure

The cadherin family is a large superfamily consisting of five subfamilies, the classic types I and II, desmosomal cadherins, protocadherins and cadherin-related proteins. The classic cadherins include E- (epithelial), N- (neural), P – (placental), L- (liver), R- (retinal), K- (kidney), and M- (muscle) cadherin, named after the tissue in which they were first discovered, of which E- and N-cadherin are the most widely studied. The classic cadherins are transmembrane glycoproteins with an extracellular region (ectodomain) comprising five extracellular homologous domains, a single membrane-spanning region and a cytosolic domain. These cadherins have important roles in Ca^{2+}-dependent intercellular adhesion and signalling pathways. Adhesion occurs when extracellular cadherin domains from one cadherin bind to the extracellular portion of a similar cadherin on an opposing cell, these cells can be of the same type (forming homo-typic junctions) or of a different cell-type (hetero-typic junction). The role of Ca^{2+} in mediating these junctions has been studied in some detail, where calcium has been shown to bind to two Ca^{2+} binding sites between each cadherin extracellular domain, stabilising their orientation away from the cell (Nagar et al., 1996) (see Figure 1.4A). This allows cadherin-cadherin cis-dimers to form on the same cell, and facilitates interaction with cadherin dimers on opposing cells, forming a trans-dimer. Once trans-dimers are formed, the clustering of cadherin at the cell-cell interface can occur, through a combination of cis- and trans-dimerisation, resulting in an adherens junction. The specificity of classic cadherins is determined by the most N-terminal part of the

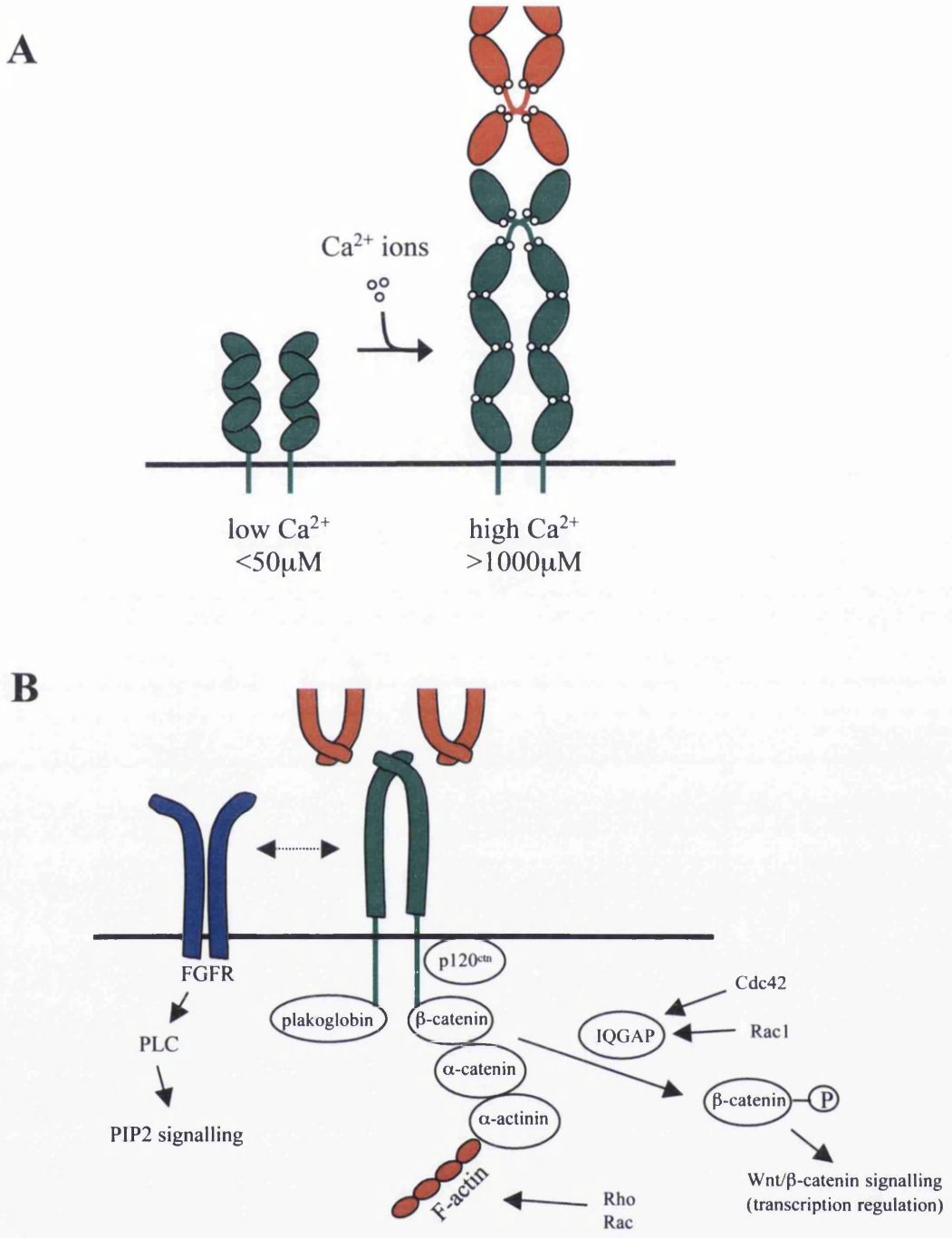

Figure 1.4 Cadherin structure and regulation.

(A) Cadherin ectoderms (5 domains) are already clustered on the cell surface due to connection to the cytoskeleton (not shown), but have a more globular shape in the absence of Ca^{2+} ions. Higher concentrations are required for cis interactions between N-terminal domain pairs (*). Only at high Ca^{2+} is cadherin fully activated and can form trans interactions with opposing cis dimers (adapted from Koch et al., 1999). (B) Summary of localisation and regulation of cadherins. Cadherins connect to the actin cytoskeleton via various proteins including β-catenin, α-catenin and α-actinin. Protein-protein interactions are regulated via several phosphorylation and dephosporylation events (adapted from Steinberg and McNuff, 1999).

ectodomain, which mediates both cis- and trans-dimerisation, as was shown by its crystal structure, leading to the proposal of a zipper-like mechanism (Shapiro et al., 1995).

1.6.2.2 Cadherin function within nervous tissue

Within the nervous system, about 80 different cadherin types have been identified, including N-, E- and R-cadherin from the classical family. N-cadherin, the major cadherin within the nervous system, has many roles in developmental processes including neurulation (Kintner, 1992), neuronal migration (Nakagawa and Takeichi, 1998) and axon growth (Bixby and Zhang 1990; Doherty et al., 1991). Recent studies suggest that cadherin expression identifies developing neuron populations into organised functional circuits (Redies, 1997). During axon growth and target selection, axons of different origins express distinct, and often multiple, cadherin types. In fact since axons can express multiple cadherins, they can bind to axons with a complementary set, thus the cadherins may provide an adhesive 'code' for directing the neuronal connections (Ranscht, 2000).

Recently, cadherin subclasses have been identified at different synapse populations on the same axon, thus specifying and maintaining specific neuronal connections (Ranscht, 2000). This has been demonstrated through the use of N-cadherin antibodies which disrupted synapse formation in specific layers of the retinorecipient tectal layers (Inoue and Sanes, 1997). The cadherins may also be important for regulating synapse function, for example, depolarisation of neuronal membranes actually increases N-cadherin stability and adhesive function, thus mediating activity-dependent stability of a synapse (Tanaka et al., 2000).

In addition, cadherins can have both stimulatory and inhibitory effects on migration. Traditionally, strong adhesion has been associated with a lack of migration. This is reflected by observations that tumour cells which progress to a metastatic phenotype are often associated with a downregulation of E-cadherin expression (Perl et al., 1998; Christofori and Semb, 1999), which presumably allows them to detach from the primary tumour mass. However, it has now been shown that N-cadherin is upregulated in invasive cancer cell lines (Tran et al., 1999; Hazan et al., 2000) and tumours (Tomita et al., 2000; Li et al., 2001). Rather than just reflecting a change in adhesive specificity, N-cadherin actually promotes this invasive phenotype, where N-cadherin-expressing breast cancer cells migrated more

efficiently, even when expression of E-cadherin is maintained (Hazan et al., 2000). This is contradictory to the role of N-cadherin in glial cells where it has been shown to restrict migration (Wilby et al., 1999; Schnaedelbach et al., 2000), but fits with data suggesting that whereas E-cadherin promotes only tight cell-cell adhesion, N-cadherin may promote both stable and labile cellular interactions that facilitate dynamic processes such as neurite outgrowth and cell migration (Bixby and Zhang, 1990; Doherty et al., 1991). Thus N-cadherin can play different roles determining migration or adhesion, which presumably reflect variability in its regulation.

1.6.2.3 Cadherin regulation

The cytosolic domain of cadherins are associated with proteins known as catenins, including β-catenin, γ-catenin/plakoglobin and α-catenin. These physically anchor the cadherins to the cytoskeleton, through interactions with actinin and then actin, as well as mediating signalling pathways (see Figure 1.4B). Other cadherin associated proteins include vinculin, the src substrate $p120^{ctn}$, IQGAP, and the tumour suppressor protein adenomatous polypous coli (APC). Cadherin-catenin interactions are essential for the establishment of functional adherens junctions, where the formation of a cadherin-catenin complex, reflects tight adhesive interactions. Due to the need for both strong, stable adhesive contacts in some situations (such as synapse stability and tissue maintenance) and also weak interactions in others (such as axonal extension and migration), the adherens junction needs to be dynamically and transiently regulated. This can be modulated through phosphorylation of the cadherin-catenin complex, particularly though tyrosine phosphorylation of β-catenin, which then is lost from the cadherin-catenin complex, thus inhibiting cell adhesion (Balsamo et al., 1996). Several tyrosine phosphatases and kinases are associated with the regulation of the phosphorylation status, including the small GTPases Rac, Rho and cdc42. IQGAP, a Rac and Cdc42 effector, displaces α-catenin from the cadherin-catenin complex, as well as interacting directly both with cadherin and β-catenin, thus disrupting the association of the complex with the cytoskeleton, and therefore inhibiting cell adhesion (Briggs and Sacks; 2003).

The cadherins and catenins, as well as having roles in cell-cell adhesions, have also been implicated in cell signalling. Upon being released from the cadherin-catenin complex, β-

catenin is able to bind the lymphoid enhancer binding factor (LEF-1) and the Xenopus homolgue XTcf-3 (Behrens et al., 1996; Molenaar et al., 1996). This complex can then translocate to the nucleus and lead to transcriptional activation. In this way, β-catenin acts downstream of the Wnt signalling pathway, which is particularly important in embryonic patterning , including dorsal-ventral axis determination in Xenopus (Itoh et al., 1998).

N-cadherin can also regulate neurite outgrowth through FGFR signalling. N-cadherin and FGFR have been shown to co-localise together, and also N-cadherin stimulation was necessary for FGFR-dependent neurite outgrowth (Utton et al., 2001). It has been suggested that, whereas catenin interaction with cadherins mediates their adhesive functions, interaction and activation of FGFR may be important for their migratory functions. This is supported by the dependency of migratory N-cadherin-expressing tumour cells upon FGF signalling, whereby N-cadherin and FGF-2 synergistically increased migration and invasion of breast tumour cells (Hazan et al., 2000)

N-cadherin function in neurite growth is also regulated by interactions with receptor tyrosine phosphatase μ (Burden-Gulley and Brady-Kalnay, 1999), although the intracellular signals elicited by this interaction are not as clear as for FGFR signalling. In addition, binding of the CS-PG neurocan to an N-cadherin-associated cell surface glycosyl transferase exerts negative regulation on N-cadherin, inhibiting both cadherin and integrin functions in neurite extenstion (Lilien et al., 1999; Li et al., 2000).

Another mechanism for N-cadherin regulation is through the repulsive guidance cue, slit (as discussed in section 1.1.2.6). Upon binding and activating its ligand, Roundabout (Robo), slit induces the inhibition of N-cadherin-mediated cell adhesion (Emerson and Vactor, 2002; Rhee et al., 2002). This presumably allows the cells to migrate away from the repulsive cue. It appears that activated Robo is able to form a complex with Abelson (Abl) kinase and N-cadherin, resulting in phosphorylation of β-catenin and its loss from the adhesive cadherin-catenin complex. However, it is still not understood how all these and additional mechanisms cooperate to achieve the concerted action on cadherin-mediated functions.

1.6.3 Communication between integrins and cadherins

Cross-talk between the cadherins and other complexes involved in adhesion and migration is a necessary property of the cell, in order to coordinate these events. Communication is evident between cadherins and integrins (Monier-Gavelle and Duband, 1997; Gimond et al., 1999), particularly through the Rho-like GTPases (see Figure 1.5). Activated Cdc42, Rac and Rho are necessary for the formation of filopodia, lamellipodia and stress fibres, respectively (Hall and Nobes, 2000), and these proteins have also been shown to regulate the activation status of each other through a cascade, for example activation of Cdc42 leads to a rapid localised activation of Rac (Nobes and Hall, 1995). As such, the balance between GTPase activity is important for determining migratory and adhesive behaviour. Since they have been shown to regulate the adhesive strength of the adherens junctions (section 1.6.1.3) as well as regulating integrin function (section 1.6.1.2), they therefore bridge adhesion and migration. This has been demonstrated in FAK and paxillin-signalling impaired cells, where siRNA-mediated knockdown of both FAK and paxillin resulted in impaired assembly of N-cadherin-containing cell-cell adhesions in both HeLa cells and human fibroblasts (Yano et al., 2004). This effect was reversed by expression of a dominant-negative Rac1 mutant, and mimicked by constitutively active Rac1, suggesting FAK and paxillin may normally function to attenuate Rac1 signalling.

In addition, integrin and cadherin function is balanced through the regulation of, amongst others, a nonreceptor tyrosine kinase called fer. This protein coordinates integrin and N-cadherin function through its ability to bind to both complexes, whereby its displacement from one results in its accumulation at the other (Arregui et al., 2000). This mechanism has been observed upon neurocan binding to its receptor GalNAcPTase, in the chick neural retina (Li et al., 2000), where fer translocates from the cadherin complex to the integrin complex, resulting in inhibition of both N-cadherin- and β1-integrin-mediated adhesion and neurite outgrowth.

1.7 Summary

It has long been known that the CNS is unable to regenerate following injury and it is now understood that this is due to the interplay between several different mechanisms. These

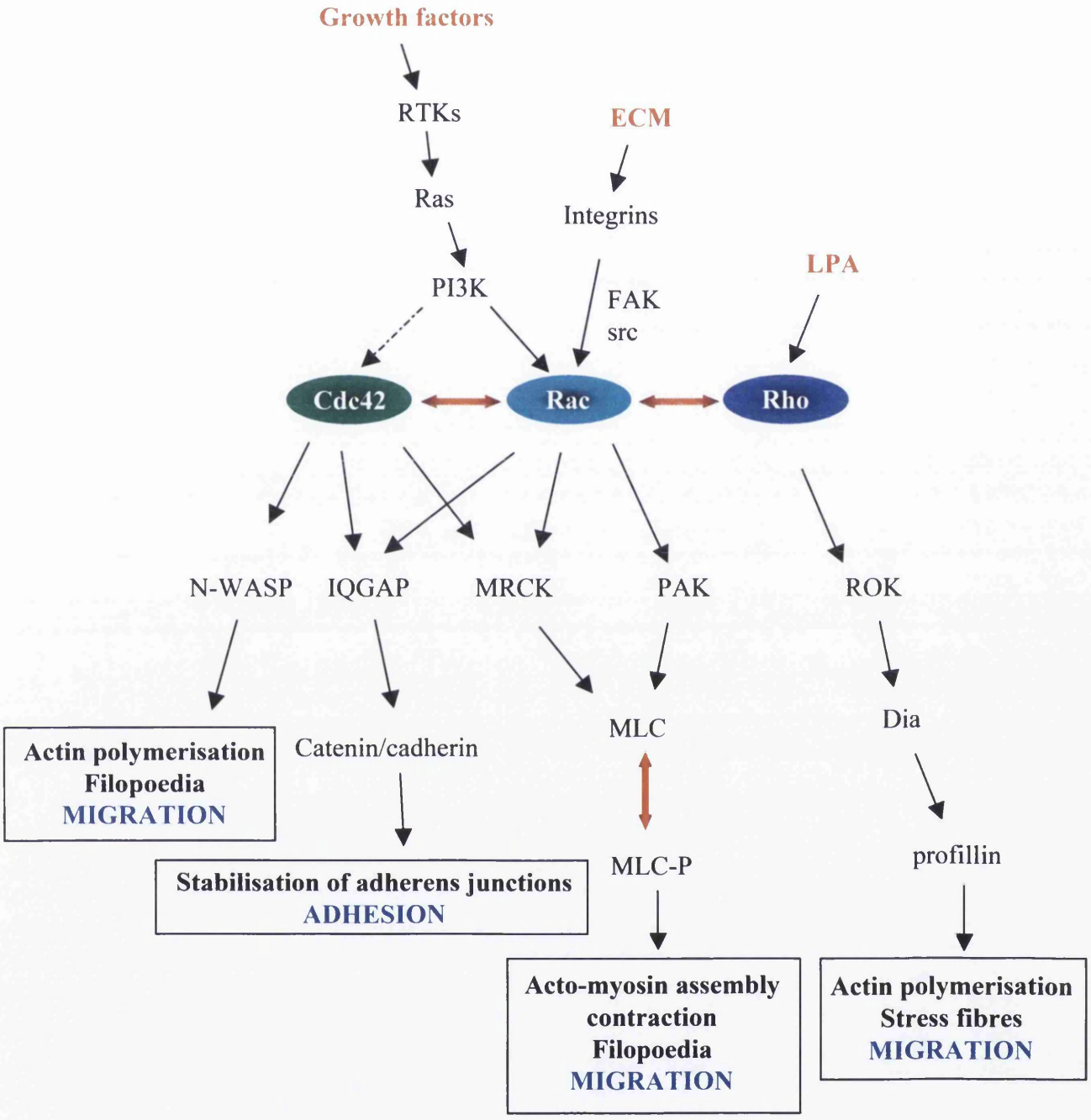

Figure 1.5 Schematic of small GTPase regulation of migration and adhesion.

Communication between the small GTPases, Cdc42, Rac and Rho, coordinately regulate migration and adhesion. Adapted from Schmitz et al., 2000.

include the innate state of CNS axons; the presence of inhibitory myelin components, which are not efficiently cleared from the injury site by the immune response; the presence of inhibitory guidance molecules and, in particular, the formation of a glial scar. This glial scar functions to inhibit regeneration in the CNS both through its formation of an impenetrable barrier to repair, and the presence of inhibitory molecules within it, namely the CS-PGs. As a result, in order to promote the regeneration of the CNS, a number of different methods of intervention are required.

One promising method is the transplantation of cells with regeneration-promoting capacities. Of these, OECs and Schwann cells are high on the list of candidates. Despite some of the more obvious similarities between OECs and Schwann cells, they also display many different properties which are important when deciding which is the superior candidate for transplantation. For example, Schwann cells appear to have a more limited ability to survive and migrate within CNS tissue, and may also induce a greater reactive response following transplantation than OECs. However, this comparison is not as clear as is sometimes reported, since in some models, OECs also show a limited ability both to migrate and to promote regeneration, and also induce a degree of reactivity in the host. For this reason, Schwann cells are still a potential candidate, and at present remain more probable for autologous transplantation due to the ease of obtaining them and culturing them in large numbers.

Thus, a comparison of OEC and Schwann cell interactions with the host CNS, and in particular astrocytes, is important in evaluating their transplantation potential. The mechanisms which determine the different cellular interactions of OECs and Schwann cells with astrocytes remain to be investigated. Such knowledge would allow both a more detailed comparison of the candidates to be made, and may also allow the possibility of manipulating these cells in order to improve their potential for repair. For example, if the more easily obtained Schwann cell could be made to integrate with astrocytes in a manner more similar to OECs, while inducing less reactivity in the host tissue, its scope for promoting repair may be enhanced.

1.8 Aims of Thesis

This thesis will address the interactions of OECs and Schwann cells with astrocytes, and will aim to highlight the mechanisms involved in regulating these interactions. Firstly, a more general comparison of OEC and Schwann cell behaviour in the presence of astrocytes will be made. This is in order to evaluate the differences between OECs and Schwann cells, to assess how reproducible the published literature is in regards to modelling their interactions *in vitro*, and to establish models by which these can be investigated in more detail. Secondly, a comparison of Schwann cell and OEC migration and adhesion capacities, both in the presence and absence of astrocytes, will be made to determine the similarities of their inherent capacities for migration and adhesion.

Due to the hypothesis that N-cadherin may be a potential candidate for limiting Schwann cell migration in the presence of astrocytes, a direct comparison will be made between the function of N-cadherin in Schwann cells and OECs, in order to determine whether this may give rise to the observed differences in Schwann cell and OEC migration and adhesion in the presence of astrocytes. siRNA will be employed to definitively address these issues.

In addition, the role that astroytosis plays in determining Schwann cell and OEC abilities to migrate within astrocytes-rich areas will also be studied. Since Schwann cells are reported to induce more astrocyte reactivity than OECs, this response could differentially determine the ability of these cells to interact with astrocytes. Both factors that determine the outcome of the astrocyte response, and the result this has on cellular migration and adhesion will be addressed.

CHAPTER 2

Materials and Methods

2.1 Tissue culture

2.1.1 General tissue culture

Primary cell cultures of astrocytes, Schwann cells and olfactory ensheathing cells (OECs) were purified as outlined as below. All cell cultures were grown in T25 (cm^3) and T75 (cm^3) culture flasks, 6-well culture plates or on polished borosilicate glass coverslips inserted into 24-well culture plates. All dishes and coverslips were coated in poly-L-lysine solution (PLL, 13.3 μg/ml in distilled water) in a volume of 2 ml, 4 ml, 1 ml or 0.5 ml respectively. PLL was left on the dishes and plates for at least 20 minutes at 37°C, washed twice in distilled water (dH_2O) and then left to air-dry in a tissue culture hood before use.

All cell cultures were maintained in DMEM-10%, with appropriate growth factors added depending on the cell type (see below). Cultures grown in T25 flasks, T75 flasks, 6-well plates, or in 24-well plates were fed with 4 ml, 12 ml, 2 ml or 0.5 ml of media respectively, and were re-fed two or three times a week, by removing half of the media, and replacing with fresh media. All fresh media and tissue culture reagents were filtered through a 0.22 μm filter.

Cell cultures were passaged when they became confluent, by removing the cells with trypsin, and splitting between two flasks (or moving up to a larger size flask). First, cells were washed in pre-warmed (37°C) phosphate-buffered saline (PBS), and then pre-warmed PBS containing 0.1% trypsin (or 0.2% for astrocytes cultures) added at either 1.5 ml for a T25 flask, or 2.5 ml for a T75 flask. Flasks were left at 37°C for 5 minutes, with frequent agitation to assist cell detachment. The PBS-trypsin containing the cell suspension was then transferred to a 15 ml Falcon tube, and trypsin activity inhibited by addition of 10ml DMEM-1%. The suspension was then spun at 1200 rpm for 6 minutes. The resulting pellet was resuspended in fresh media and re-plated onto dishes as required. All flasks and plates were then maintained at 35°C in a 7% CO_2 incubator.

In some instances, the cell suspension was counted before addition of DMEM-1%. This was done by placing 10 μl of suspension in a haemocytometer and counting the number of

cells within the grid under a light microscope, and multiplying this by 10^4 to give the total number of cells/ml.

2.1.2 Astrocyte culturing

Neonatal Sprague Dawley rat pups at age 1-2 days were killed by decapitation (Schedule 1 procedure). Instruments were sterilised using 100% ethanol, and ethanol was also applied to the skin before dissection. The skin was cut away on the head, exposing the skull. The brain was exposed by cutting away the skull over the eyes to a point above the nose. Both the olfactory bulbs and the cerebellum dissected, allowing the cortices to be removed and placed in a small petri dish (90 mm^2) containing 200-400 µl L-15 media. The cortices were separated from the midbrain, hippocampus and majority of white matter, before the meninges were carefully peeled off using micro-tweezers. The cortices were then pooled (7 animals per preparation) and stored in ice-cold L15.

Tissue was chopped with a sterile scalpel into approximately 0.25-0.5 mm pieces in order to increase the reactive surface for enzymatic digestion. The tissue was then transferred into 0.5 ml of collagenase solution and incubated for 30 minutes at 37°C. After this time the enzymatic activity was inhibited by the addition of 1ml Soybean trypsin inhibitor-DNase (SD), followed by trituration in the same solution. Trituration was done gently 5 times using a blow-out pipette, followed once with a 21G needle, and then a 23G needle. The homogenate was transferred to a 15 ml falcon tube and washed by adding 10 ml DMEM-1%, and spun at 1200 rpm for 6 minutes. Cells from the 7 cortices were then resuspended and put into two T75 flasks, containing DMEM-10% and incubated for around 1 week, after which time astrocytes became fully confluent, and neuronal debris had disappeared.

Once the cells reached confluency, they were re-fed, and the flasks gassed with 5% CO_2/21% O_2 in N_2 for 20 seconds, and the lids tightly fastened prior to incubation in a non-gassed environment. Flasks were then incubated for two days at 37°C, with gentle shaking. This brought the contaminant cells, such as oligodendrocyte progenitor cells (OPCs), to the surface of the astrocyte monolayer, and many came away into suspension. After this time, the flasks were washed in pre-warmed PBS, removing any suspended cells, and contaminant cells were selectively removed using a low concentration of trypsin

(0.05%) which left the astrocyte monolayer intact. These contaminant cells were discarded. The monolayer was washed in pre-warmed PBS, and passaged using a higher concentration of trypsin (0.2%) as outlined in the above section. An aliquot of cells were plated onto coverslips to assess astrocyte purity by immunolabelling for glial fibrillary acidic protein (GFAP; see section 2.3). Further purification steps were only performed if necessary, such as the addition of the cytotoxic agent cytosine arabinoside (Ara C, $2x10^{-5}M$). This was added to the media for two days and killed any rapidly dividing cells. It was added once the astrocytes had become confluent and were no longer proliferating, while contaminant cells above the astrocyte monolayers were able to continue dividing. After Ara C treatment, the astrocytes were washed in PBS, and then passaged as necessary. After purification, astrocytes cultures were typically greater than 95% pure (see Figure 3.1).

2.1.3 Schwann cell culturing

Sciatic nerves were dissected from 7-day-old Sprague Dawley neonatal rat pups (killed by a Schedule 1 protocol). The skin was sterilised with 100% ethanol, a dorsal incision made in the skin along the leg, and the muscles separated to reveal the sciatic nerve. This was dissected out and placed in a petri dish. Any remaining muscle tissue was removed and then the nerves were chopped finely using a sterile scalpel. As with astrocyte purification, small tissue pieces of approximately 0.25-0.5 mm were digested in 0.5 ml collagenase. After 15 minutes, 0.5 ml of trypsin was added, and incubated for a further 15 minutes. At the end of this time, the enzymes were neutralised by addition of 500 µl SD. Cells were transferred to a 15 ml Falcon, and washed with 10 ml DMEM-1%. The pelleted cells were resuspended and approximately 5 sciatic nerves were cultured in each T25 flask. The cells were cultured in DMEM-10% until purification was complete. After 24 hours, Ara C was added to the flask (at a final concentration of $2x10^{-5}$ M) in order to kill the fast proliferating fibroblasts. After a further 48 hours, the media containing Ara C was removed, and the flasks were washed twice in PBS. Flasks were left for a further 24 hours in DMEM-10% to recover before this step was repeated. Following the Ara C treatment, cells were left another 24 hours before Schwann cells were selectively removed from the flask using a low concentration of trypsin (0.02%). This left the contaminant fibroblasts behind, which were

discarded. The trypsinised cells, were washed in DMEM-1%, and the resulting pellet was purified further by complement kill using anti-Thy1.1.

The pellet was resuspended in a mixture containing 50 µl DMEM and 150 µl anti-Thy1.1. antibody, which specifically labels fibroblasts, and incubated for 15 minutes at RT, before a further 40 µl of rabbit complement was added to the cell suspension. This was then incubated for 45 minutes at 37°C, allowing complement-mediated lysis of any remaining fibroblasts. Cells were washed twice in DMEM-1%, and re-plated in T25 culture flasks. The DMEM-10% culture medium was supplemented with 2 µM forskolin and 20 ng/ml beta-1 heregulin.

Schwann cell purity was assessed by plating an aliquot of cells on to coverslips and labelling with anti-$p75^{NTR}$ (see section 2.3, and Figure 3.1). Schwann cell cultures were typically over 90% pure, any cultures not meeting this requirement were discarded and purification repeated.

2.1.4 Olfactory ensheathing cell cultures

Olfactory ensheathing cells (OECs) were purified from olfactory bulbs of 7-day-old Sprague Dawley rat pups. As with astrocyte purification, the skin was dissected away to reveal the skull, which was also removed. Meninges covering the olfactory bulbs were removed, and olfactory bulbs excised after cutting the olfactory tracts connecting them to the forebrain. Tissue was treated as outlined above in sections 2.1.2 and 2.1.3. Briefly this involved chopping into small pieces with a scalpel followed by digestion in collagenase.

The resulting tissue pellet was then purified using the fluorescence-activated cell sorter (FACS) as described by Barnett and colleagues (Barnett et al, 1993). Approximately $2x10^7$ cells were resuspended in a mixture of 1 ml O4 and 1 ml GalC hybridoma supernatants and incubated on ice for 1 hour. Cells were washed twice in 10 ml DMEM-1%, and then resuspended in 2 ml DMEM-1% containing goat anti-mouse IgM-fluorescein (FITC; 1:100) and goat anti-mouse IgG3-phycoerythrin (RPE; 1:100). This was incubated for 45 minutes on ice, and cells were then washed twice in DMEM-1%. The pellet was resuspended in 4 ml DMEM-1%, poured through a 70 µm cell strainer to ensure large

pieces of tissue did not cause blockages in the FACS machine, and then transferred to a polystyrene round bottom 5 ml tube.

Cell sorting was carried out with the attendance of Mr. Tom Gilbey.

A 'FACVantage SE' sorter was used to purify the cells according to the protocol by Barnett and colleagues (Barnett et al, 1993). Briefly, sorts were carried out by exciting the fluorophores with a 488 nm argon laser at 100-150 mW. Since our cells were dual labelled with FITC (emission 530 nm) and RPE (emision 578 nm), the compensations (FL-1 and FL-2) were set to reduce the spillover of the fluorophores into each channel. This was done by running fluorescently-labelled beads, either FITC- or RPE-labelled, through the machine prior to sorting, to set the gating. Then the sort windows were set in order to firstly separate live cells from dead cells and debris, by size (forward scattering of light) and granularity (side scatter), and then to select O4-positive (FITC) GalC-negative (RPE) cells.

Purified cells were collected in a second polystyrene round bottom 5 ml tube (containing 4 ml of DMEM-1%) and then spun at 1200 rpm. The pellet was resuspended in 20 µl, and plated as a strip within a T25 flask, and incubated until the strip became confluent. Cells were passaged into an entire T25 flask. Cells were cultured in OEC mitogen media (OMM) which has been shown to be a potent mitogen for promoting prolonged growth of $p75^{NTR}$ expressing OECs (Alexander et al., 2001). A small aliquot of each purification preparation was also plated on to coverslips in order to assess the purity of the cells. This was carried out by immunolabelling, using both O4 and GalC antibodies, immediately after sorting. However, if purity was assessed after the cells had been cultured for any length of time, they were immunolabelled for just $p75^{NTR}$, since OECs lose expression of O4 with time in culture (Franceschini and Barnett, 1996). All cultures were about 95% pure (see Figure 3.1), as before, any cultures which were not pure enough were discarded, and the process repeated.

2.1.5 Hybridoma cells and collection of antibodies

Hybridoma stocks were stored in liquid nitrogen until use. Cells in cryo-vials removed from storage were allowed to thaw rapidly in warm water before the cells were removed and

washed twice in 8 ml of DMEM-1%. This removed any residual DMSO which is toxic to the cells. After washing, the resultant pellet of cells was resuspended in 4ml of DMEM-10%-1966 and transferred to a T25 flask. The cells were grown at 37°C until confluent when they were removed from the flask (no need for trypsin, just agitation) and placed in a T75 containing 12 mls DMEM-10%-1966, and again grown until confluent.

When confluent, the cells were pelleted and resuspended in 6 ml of DMEM-10%-1966. Of this, 0.5 ml aliquots were placed into two T25 flasks, and allowed to grow to confluency, before freezing down to replace hybridoma stocks. The remaining 5 ml were put into a T125 which was topped up to 20 ml of DMEM-10%-1966. Cells were grown until 80% confluent, at which time they were ready for antibody collection.

For collection of antibody, media was removed from the T125 flask, and the cells washed in PBS. 30 mls of DMEM-BS-1966 was then added to the cells, and the flask was incubated at 37°C for 2 days. After this time, the media was collected and spun at 1200 rpm for 6 minutes to remove any cell debris. The antibody was then ready to test, and 1 ml aliquots made and stored at –20°C.

2.1.6 Collection of Astrocyte, Schwann cell and OEC conditioned media (ACM, SCM and OCM).

Conditioned media from Schwann cells and OECs were collected from confluent cultures of cells grown in T25 flasks. Flasks were washed twice in PBS and then 4 ml of DMEM-BS was added to the flask. Two days later the media was removed and centrifuged at 1200 rpm for 6 minutes to remove any cell debris. The collected media was then filtrated using a 0.22 μm filter, and was then ready for use. Exactly the same procedure was used for generating astrocyte conditioned media (ACM), apart from confluent astrocyte cultures were maintained in T75 flasks, to which 10 ml of DMEM-BS was added.

Media which was intended for concentrating and 2D electrophoresis analysis was collected in BSA-free DMEM-BS, and treated as normal (see Section 2.5).

SCM and OCM were added to cell cultures at a 1:1 ratio with DMEM-10%, except for proliferation studies, where media were titrated with DMEM-BS.

2.1.7 Digestion of SCM

SCM was digested in order to assess if its activity was proteinaceous in nature. 2 ml of SCM was placed in a falcon tube, to which 100 µl of trypsin-agarose bead suspension was added (50:50 suspension beads to PBS; 2.5 units). The beads had previously been washed of all storage solution (containing sodium azide). The SCM-trypsin-agarose suspension was then put on a rotator at 37°C and left to digest for 24 hours, after which time the suspension was spun at 1200 rpm for 6 minutes, and the supernatant collected. The beads could then stored in 10 mM acetic acid, pH 3.2 at 4°C, ready for re-use. The digested SCM was then filtered through a 0.22 µm syringe filter, and stored at 4°C.

2.1.8 Culturing cells in low Ca^{2+} media.

For some experiments, cells were cultured in low Ca^{2+}-containing media in order to assess the effect of calcium on cell-cell junctions. Cells were plated onto coverslips as outlined above and maintained in DMEM-10% (high Ca^{2+}, 1 mM) until the experiment was performed. This media was removed, and the cells washed twice in PBS. 500 µl keratinocyte growth media (low Ca^{2+}, 0.03 mM) was then added to each 24-well, and the cells maintained at 37°C for a further 4 hours before fixing and immunolabelling.

2.2 Assays

2.2.1 Co-cultures

Astrocytes:OEC and astrocyte:Schwann cell co-cultures were performed by mixing either OECs or Schwann cells with astrocytes at a ratio of 1:1 (for N-cadherin immunolabelling) or 3:1 (for assessing hypertrophy). Primary cultures were generally maintained for 2-6 weeks prior to setting up the assays. Trypsinisation, washing and counting of cells was carried out as outlined above (section 2.2.1.1). Cells were mixed in suspension at a total cell number of $4x10^3$ per well and then added to PLL coated coverslips in 24-well plates

containing 500 µl of DMEM-10%. Alternatively, for creating cell lysates, a total cell number of $1.6x10^4$ was added to each well of a 6-well plate, containing 2 ml of DMEM-10%.

These cultures were maintained for either 2 days (for N-cadherin immunolabelling, by which time cells were in contact with each other) or 14 days (for hypertrophy analysis, by which time an astrocytic response had been elicited, Lakatos et al., 2000; Eng and Ghirniker, 1994). After this time, cultures grown on coverslips in 24 wells were fixed and immunolabelled (as outlined in section 2.3), and cultures grown in 6-well plates were lysed for immunoblotting (see section 2.4).

2.2.2 Confrontation assays

In order to investigate cellular responses after contact between populations of different glial cells, a 'confrontation assay' was set up, as previously described (Wilby et al, 1999). Cells were counted as before, and each cell type resuspended to a final concentration of $1x10^6$ cells per ml. Of these suspensions, a 10 µl strip (containing 10,000 cells) of astrocytes was made at one side of a coverslip, by drawing the cell suspension out using a pipette tip. Parallel to this, a second 10 µl strip was made, containing either Schwann cells or OEC, such that a cell free area was present between the two cell populations (approximately 1mm wide). Cells were allowed to attach to the coverslip for 1 hour, before any unattached cells were carefully washed in 500 µl DMEM-1%. Cell cultures were then maintained in DMEM-10% and allowed to grow and migrate towards each other where they could 'confront' each other. Cultures were maintained for 14 days, by which time they had fully interacted with each other (Lakatos et al, 2000). After this time, coverslips were removed and immunolabelled as required.

To quantify the number and type of cells which crossed the cellular interface between OECs/Schwann cells and astrocytes, coverslips were immunolabelled for $p75^{NTR}$ and GFAP. Images were taken at random of the confrontation interaction zone using a Leica SP2 confocal microscope at 20x magnification. A boundary distance of 300 µm was calculated (using a graticule) and marked on the images, and the number of OECs or Schwann cells which had crossed from the OEC/Schwann cell zone into the astrocyte

domain within this boundary distance were counted. Measurements were carried out in triplicate for three separate experiments (n=3), and displayed as the mean number of cells crossing the boundary +/- standard error of the mean (SEM).

2.2.3 Adhesion assay

Cells were labelled for detection with Vybrant (Vybrant CFDA SE (carboxyfluorescein diacetate, succinimidyl ester) by incubating them with the dye diluted in PBS (1:500) which had been prewarmed, for 15 minutes. Cells were washed in DMEM-1% and 20,000 labelled cells (Schwann cells or OECs) plated on to coverslips covered with a confluent monolayer of either astrocytes, Schwann cells or OECs (maintained in DMEM-10%). After 30 minutes at 37°C with gentle shaking on a rotating table, coverslips were removed, washed three times in Hanks staining solution and then fixed in 3.7% formaldehyde for 15 minutes before mounting in Vectashield fluorescent mounting medium. The number of Vybrant labelled cells remaining adhered to the coverslip were counted. All experiments were carried out in triplicate, and performed three times (n=3).

2.2.4 Time-lapse migration

In order to assess the migration speeds of Schwann cells and OECs on different substrates, coverslips were coated either with PLL (as outlined above) or with confluent astrocytes. To generate astrocyte monolayers, cells were plated in suspension at a concentration of 40,000 cells in 500 μl DMEM-10% and left to adhere to PLL-coated coverslips. Cultures were maintained in DMEM-10% at 37°C (in a humidified incubator) until they reached confluency. For the assay, OECs and Schwann cells were labelled with Vybrant (see above) and seeded onto PLL-coated or astrocyte-monolayer-covered coverslips at a density of 10,000 cells per well, and left to adhere overnight. Time-lapse imaging of the cells was performed using an Axiovert S100 microscope connected to an Apple Mac Computer, using Open Lab Time Lapse Video Microscopy System. Additional media was added to a volume of 1 ml to keep the pH stable, and reduce the effect of any evaporation. A thin layer of mineral oil was placed on top of the media in order to further reduce evaporation, and the 24-well plate placed underneath the microscope on a hot plate, set at 37°C.

Fields of view were chosen (at 10x magnification), where healthy cells had adhered and spread, showing that Vybrant labelling had no adverse effect on them. Vybrant-labelled cells were also demonstrated to still be immunoreactive for $p75^{NTR}$ (data not shown). Images were then taken of the cell at intervals of 20 minutes, for a period of 3 hours. The position of the cell body was measured for each time point, and an average speed of migration for each cell calculated. At least 5 measurements were taken for each experiment, and experiments performed in triplicate (n=3).

2.2.5 Wound assay

To assess migration, a wound assay was performed where cultures of OECs or Schwann cells were maintained on PLL-coated coverslips until they reached confluency. A single scratch wound was made in the middle of the coverslip using a micropipette tip, and cultures maintained at 37°C in a humidified incubator for a further 8 hours. Digital photos were taken of the wound at time 0 (when the scratch had just been made), and at 8 and 48 hours after wounding. An inhibitor of calpain 1 (ALLN) was added to the cultures 1 hour before wounding at a concentration of 50 μM.

Wounds were analysed by projecting the outline of the average wound size at time 0 (calculated as 246.4 +/- 12.7 μm, n=3) onto all wound images (see Figure 3.9a). The number of cells which had migrated into this wound area were then counted, and presented as an average +/- SEM. Stephen Thomson, a BSc honours medical student, assisted with these assays, particularly with quantifying the resultant migration.

2.2.6 Use of Inhibitors in assays

2.2.6.1 Time-lapse inhibition

In migration assays, several different inhibitors were used to investigate the mechanism of migration (see Figure 1.3 for inhibitor sites of action). PP2 (a src inhibitor), UD and PD (MEK inhibitors), and ALLN (calpain 1 inhibitor) were applied to coverslips ready for time-lapse imaging. These were applied 1 hour before imaging began, at the relevant working concentrations (see Table 2.1). Supplementary media, added to coverslips just

Table 2.1 Inhibitor list, including working concentrations.

Target	Inhibitor Name	Stock concentration and diluent	Working concentration	Source	Experiment
Protein synthesis	Emetine	10 mM in EtOH	10 μM	Sigma,UK	Protein lifetime
Calpain 1	ALLN (MG-101)	100 mM (in DMSO or EtOH)	50 μM	Calbiochem, UK	1) Time-lapse 2) Wound Assay 3) Adhesion Assay
Src	SU6656	10 mM	10 μM	Calbiochem, UK	Confrontation
Src	PP2 (AG1879)	In DMSO	20 μM	Calbiochem, UK	Time-lapse
MEK	UO126	10 mM in DMSO	50 μM	Calbiochem, UK	Time-lapse
MEK	PD98059	In DMSO	10μM	Calbiochem, UK	Time-lapse
FGFR1	SU5402	10 mM stock in DMSO	10 μM	Calbiochem, UK	SCM experiments
EGFR	AG1478	10 mM	300 nM	Calbiochem, UK	SCM experiments
PDGFR	AG1295	10 mM stock	10 μM	Calbiochem, UK	SCM experiments

before time-lapse microscopy to protect the cells from evaporation and pH change (section 2.2.4), also contained inhibitors at the appropriate concentration.

2.2.6.2 N-cadherin peptide inhibitor

To investigate the role of N-cadherin in interactions between astrocytes, and OECs and Schwann cells, a peptide inhibitor of N-cadherin was used in adhesion assays and confrontation assays. The cyclic peptide, containing the cadherin adhesion recognition (CAR) sequence, His-Ala-Val (HAV; Williams et al., 2000), was added to the 24-wells used in adhesion assays at a final concentration of 0.3 mg/ml (from a 10 mg/ml stock), one hour before the plating of Vybrant-labelled cells. The assay was then performed as normal.

The cyclic peptide inhibitor was also used in confrontation assays. Here the peptide was added to the assay, again at a final concentration of 0.3 mg/ml, after the strips had been plated and non-adherent cells washed off. The peptide was reapplied every two days, when the assay was re-fed (by removing half of the media, and replacing with fresh DMEM-10%), keeping the final concentration constant.

2.2.6.3 N-cadherin peptide agonist

To assess the role of N-cadherin in inducing a hypertrophic response in astrocytes, a peptide agonist of N-cadherin was used. This contained a dimeric version of the stimulatory peptide sequence, His-Ala-Val-Asp-Ile (HAVDI; Williams et al., 2002), and was applied to low density astrocyte cultures maintained on coverslips, at a final concentration of 30 μg/ml (from a 20 mg/ml stock; Skapa et al., 2004) for 24 hours.

2.2.6.4 Tyrosine Kinase inhibitors

To assess if tyrosine kinases play a role in the mechanism of action of SCM, inhibitors of the tyrosine kinase receptors fibroblast growth factor receptor (FGFR), epidermal growth factor receptor (EGFR) and platelet-derived growth factor receptor (PDGFR) were used. These were applied at the appropriate working concentrations (see Table 2.1) to cultures at the time of feeding with SCM, and refreshed 24 hours later.

2.2.6.5 Protein synthesis inhibition with emetine

In order to analyse the lifetime of certain cellular proteins, cultures of OECs and Schwann cells were maintained in 6-well plates to a density of around 80% confluency. To these cultures, emetine was added at a final concentration of 10 μM. Protein lysates were generated at regular time points, as outlined in section 2.4.1, and immunoblotting performed.

2.3 Immunocytochemistry

For details of antibodies and immunocytochemistry, see Tables 2.2 and 2.3

Cells for immunolabelling were grown on coverslips (see sections 2.1.1 and 2.2). These coverslips were removed from 24-well plates and any remaining media blotted onto paper. Coverslips were washed twice in PBS. Between all steps, any excess liquid remaining on the coverslips was blotted on paper. Cells were fixed by addition of 3.7% formaldehyde before covering and incubating for 10 minutes at RT. After this time, coverslips were washed in PBS and permeablised with 0.5% Triton-X 100/1% BSA in PBS, and incubated for 15 minutes at RT in the dark. After washing, the cells were incubated in blocking solution (10% FBS in PBS) for 30 minutes at RT. For some extracellular antibodies, the coverslips were blocked straight after fixation, followed by the extracellular antibodies. Permeablisation was then performed before applying the intracellular antibodies.

Primary antibodies were diluted in blocking solution at the appropriate dilutions (Table 2.2). and added to the coverslips for 1 hour at RT. Washes were performed three times in 0.025% Tween 20 for 15 minutes. The appropriate secondary antibodies were diluted 1:100 in blocking solution, and this was then added to the coverslips for 45 minutes, before further washing. Secondary antibodies of the appropriate class specificity were either FITC- (green) or TRITC- (red) conjugated as needed. After washes, coverslips were rinsed once in distilled water (dH_2O) and mounted on slides, using Vectashield mounting medium for fluorescence, supplemented with 4',6'-diaminidino-2-phenylindole (DAPI) to aid detection of cell nuclei. Finally, the edges of the coverslips were sealed using nail varnish.

Table 2.2. Primary antibody list.

PRIMARY ANTIBODIES				
ANTIBODY	**CLASS**	**USE**	**DILUTION**	**SOURCE**
N-cadherin	IgG1	Immunolabelling Immunoblotting Immunoprecipitation	1:100 1:1000	BD Transduction laboratories, Lexington, KY, USA
β-catenin	"	Immunolabelling Immunoblotting Immunoprecipitation	1:100 1:1000	"
$p120^{ctn}$	"	Immunolabelling Immunoblotting Immunoprecipitation	1:100 1:1000	"
E-cadherin	"	Immunolabelling Immunoblotting	1:100 1:1000	"
P-cadherin	"	Immunolabelling Immunoblotting	1:100 1:1000	"
vinculin	"	Immunolabelling Immunoblotting	1:100 1:1000	"
paxillin	"	Immunolabelling Immunoblotting	1:100 1:1000	"
GFAP	anti-rabbit polyclonal	Immunolabelling	1:100	Dako, Bucks, UK
actin	IG2A	Immunoblotting	1:100	Sigma, UK
BrdU	IgG1	Immunolabelling	1:20	Dako, Bucks, UK
actin	phalloidin-conjugated to TRITC	Immunolabelling	1:200	Sigma, UK
Laminin	anti-rabbit polyclonal	Immunolabelling	1:100	Sigma, UK
Fibronectin	anti-rabbit polyclonal	Immunolabelling	1:50	Dako, Buck, UK
Neurocan (IG2)	IgG	Immunolabelling Immunoblotting	1:2 1:20	Gift from Dr Oohira, Japan
CS-56	IgM	Immunolabelling Immunoblotting	1:100	Sigma, UK
473HD	"	Immunolabelling	1:25	Gift from Dr Faissner, Germany
O4	"	Immunolabelling	1:4	Hybridoma; Sommer and Schachner, 1981
$p75^{NTR}$	IgG1	Immunoblotting FACS sorting	1:4	Hybridoma; Yan and Johnson, 1987
Gal-C	IgG3	FACS sorting	1:5	Hybridoma; Ranscht et al., 1982
Thy 1.1	IgM	Complement killing	1:4	Hybridoma; ECACC, UK

Table 2.3. Secondary antibody list.

SECONDARY ANTIBODIES				
ANTIBODY	**CLASS**	**USE**	**DILUTION**	**SOURCE**
IgG1 (anti-mouse)	Goat	Immunolabelling	1:100	Southern Biotechniques, Cambridge Bioscience, Cambridge, UK
IgG2a (anti-mouse)	"	Immunolabelling	1:100	"
IgG3 (anti-mouse)	"	Immunolabelling FACS sorting	1:100	"
IgM (anti-mouse)	"	Immunolabelling FACS sorting	1:100	Jackson Labs
Anti-rabbit	"	Immunolabelling	1:100	Southern Biotechniques, Cambridge Bioscience, Cambridge, UK
Anti-mouse HRP	-	Immunoblotting	1:7000	Jackson Labs
Anti-rabbit HRP	-	Immunblotting	1:7000	Jackson Labs

For CS-56 immunolabelling, cells were first washed in solution A (see appendix 6.3ii) and then fixed with 4% paraformaldehyde (in solution A) for 10 minutes at RT. After fixation the cells were incubated in 0.5% triton x-100 (in solution A) for 1 minute also at RT. Solution A was also used for all washing steps as a substitution for PBS.

For BrdU labelling, cells were pre-treated with 20 μM BrdU (diluted in warmed PBS) while the cells were while still in culture. BrdU, which is intercalated into synthesised DNA, was left to incorporate into the cells for 16 hours. After this time, coverslips were removed and fixed in methanol at –20°C for 20 minutes and then washed in PBS. Further fixing was performed in 0.2% paraformaldehyde diluted in Hanks staining solution, for exactly 1 minute, followed by washing. 0.07 M NaOH was added to the coverslip and incubated for 7-10 minutes at RT. After further washing, BrdU antibody (1:20) was incubated on the cells or 45 minutes at RT in the dark. As with other staining protocols, the coverslips were washed before addition of the appropriate secondary for 30 minutes, followed by mounting, as previously described.

2.3.1 Microscopy

Confocal microscopy was carried out using a Leica SP2 confocal microscope at 10, 20 and 40x magnification. Other fluorescent microscopy was carried out using Axioshop and Axioplan microscopes, at 10 and 20x magnification.

For measurements of astrocytic area, images were taken at 10x magnification. These images were visualised using NIH Image software, and direct measurements were taken of the astrocyte area, and calibrated using a graticule. At least 5 cells were measured per image, and 3 images taken per experiment. Experiments were performed in triplicate (n=3).

BrdU immunolabelling was performed (as outlined above in section 2.2.3) to quantify the number of proliferating cells in culture. The BrdU positive cells were identified using indirect fluorescent microscopy. Briefly, random areas containing at least 200 cells per view were chosen, and the number of BrdU positive cells counted and displayed as a percentage of total cells in view. At least 5 fields of view were counted per experiment, and experiments performed in triplicate (n=3).

2.4 Immunoblotting

2.4.1 Preparation of protein extracts

Whole cell lysates were prepared using ice-cold lysis buffer. Confluent flasks or dishes were rinsed twice with ice-cold PBS. The culture vessels were inclined and allowed to drain to minimise the amount of residual PBS on the cells. Ice-cold lysis buffer was added to the cells (100 µl for a T25 flask, or 25 µl per 6 well) and lysis occurred over 10 minutes on ice, after which time lysates were collected, using a disposable cell scraper, into micro-centrifuge tubes. Typically, lysates from at least 2 wells of a 6-well plate were pooled.

The lysates were sonicated, using a Soniprep 150 sonicator, and cleared of insoluble cell debris by centrifugation at 12,000 rpm at 4°C for 10 minutes. The total protein concentration of the lysates was estimated by adding 200 µl of 2% $CuSO_4$ in Bicinchoninic acid to 10µl of protein sample (at various dilutions) in a 96 well. This was incubated for 30 minutes at 37°C before measuring the absorbance of the samples at 562 nm using a microplate reader. Experimental values were compared to a standard curve (obtained using BSA, from a 2 mg/ml stock) and the total protein concentration in each sample calculated.

Protein extracts for immunoblotting with antibodies against the chondroitin sulphate proteoglycans (CS-PGs), were pretreated with chondroitinase, in order to remove GAG chains which can give a smeary blotting profile (McKeon et al., 1999; Asher et al., 2000). 0.2 U chondrotinase was diluted 1:10 with chondroitinase activating buffer. Of this, 0.02 U/ml was added to protein extract, before incubation at 37°C for 3 hours.

2.4.2 Protein electrophoresis

Lysates were standardised for total protein content (maximum 15 µg protein per sample) before adding 4X sample buffer containing 4% β-mercaptoethanol. The lysates were boiled for 10 minutes, spun at 12,000 rpm for 30 seconds, and allowed to cool before loading onto SDS-polyacylamide gel electrophoresis (PAGE) gels for electrophoresis. Protein samples were separated on NuPAGE Bis-Tris 4-12% gels in NuPAGE MOPS buffer. Gels were run at 150V and 200mA for approximately 1 hour until the dye-front had reached the

bottom of the gel. All gels were run with SeeBlue molecular weight markers, and either stained directly (2.4.7) or the protein blotted on to nitrocellulose for immuno-probing (2.4.3).

2.4.3 Immunoblotting

After electrophoresis, proteins were transferred onto a 0.45 mm pore-size nitrocellulose membrane by electrophoretic semi-dry blotting. Briefly, the nitrocellulose membrane was soaked in methanol followed by dry blot buffer, and 12 pieces of 3MM paper were soaked in dry blot buffer alone. The SDS-PAGE gel and nitrocellulose membrane was sandwiched with 6 sheets of 3MM paper on each side, such that the membrane was on the cathode side of the gel. After gently excluding air bubbles from the paper/gel/membrane stack, by rolling a 1 ml pipette over the top, the proteins were transferred for 1 hour at a maximum current of 200 mA and a maximum voltage of 20 V for a gel of 140 cm^2.

2.4.4 Antibody incubation and detection by ECL

Following the transfer, the nitrocellulose membrane was blocked in the appropriate blocking solution (PBS containing 0.2% Tween-20 (PBS/Tween) supplemented with either 5% (w/v) milk powder or 3% (w/v) bovine serum albumin (BSA)) for 1 hour at RT on a shaker. After blocking, the blots were probed with primary antibody (1:1000 see Table 2.2) diluted in blocking solution for either 3 hours at RT or overnight at 4°C. After this, the blots were washed 3 times in PBS/Tween (15 minutes per wash) and were incubated in horseradish peroxidase (HRP)-conjugated secondary antibody (1:7000; anti-mouse IgG) for 30 minutes at RT. After further washing in PBS/Tween, the blots were drained and incubated in ECL reagent for 1 minute with gentle agitation and wrapped in Saran-wrap. The blots were placed in contact with X-ray film, in an x-ray film holder in a dark room, for a period of time sufficient for a signal from the enhanced chemiluminescence (ECL) to be detected and the film then processed in a Kodak automated processor.

2.4.5 Removing bound anti-sera from immunoblots

It was necessary to remove bound anti-sera from blots prior to reprobing with a different antibody. First, the blot was washed in PBS/Tween to remove spent ECL reagent, and then

incubated in stripping buffer (Reblot, 1:10 dilution) for 15 minutes at RT with shaking. At the end of this incubation, the blot was washed again and blocked as above, prior to incubation with the appropriate antibodies.

2.4.6 Immunoprecipitation of extracted proteins

Lysates for immunoprecipitation were prepared in RIPA buffer. These lysates were then standardised for total protein content (ideally 1.0 mg per sample). Antibody against the protein of interest was then incubated with the lysate (2 μg Ab to >0.5 ml protein) overnight at 4°C to form IgG complexes. These complexes were then collected by incubation for 1 hour at 4°C with 50 μl of a 50% slurry of protein-A sepharose beads against rabbit antibodies, or a slurry of IgG- or IgM-agarose beads against mouse antibodies. The collected immuno-complexes were washed 3 times in RIPA lysis buffer before resuspending in 20 μl of 4X sample buffer and boiling for 10 minutes at RT. Electrophoresis and blotting was performed as outlined in section 2.4.2.

2.4.7 Labelling of protein within the gel

Several staining methods were used to visualise the proteins in the gel depending on the sensitivity required.

If only a general view of protein components was required, following electrophoresis, the gel was stained in coomassie blue solution. Coomassie blue was added to the gel and shaken gently at RT for 30 minutes, before destaining in 7% acetic acid/5% methanol solution over night. The gel was then scanned.

Alternatively, when a more sensitive method was required, the gel was stained with Brilliant Blue Colloidal. Following electrophoresis, the gel was fixed by incubating in 7% acetic acid/40% methanol for 30 minutes. Brilliant blue stock solution (produced by adding 800 ml deionised water to the bottle, mixing by inversion, and storage at 4°C) was then mixed 4:1 with methanol. This solution was incubated with the gel for 2 hours. After this time, the solution was removed and the gel destained in 10% acetic acid/25% methanol for

60 seconds, followed by a wash with water for 1 hour. The gel was then scanned at 600 nm.

For staining of two dimensional (2D) gels (Section 2.2.5) Sypro Orange was used. This was diluted 1:5000 in PBS and the gel was incubated for 30 minutes in the solution in the fridge. The fluorescent stain could then be detected at 580 nm using Typhoon software on a Typhoon 9400 transilluminator.

2.4.8 Densitometry reading of protein bands

To assess relative densities of immunoblotting bands, images were measured using QuantiOne Software by Biorad. Readings were normalised to the background, and also to the densities of a loading control (actin or vinculin).

2.5 2D protein electrophoresis

2.5.1 Sample collection

SCM and OCM intended for 2D electrophoresis were collected as outlined in section 2.2.1.6 but using DMEM-BS lacking BSA, in order to reduce contaminant protein levels. All media were concentrated using Centricon Plus-20 (centrifugal filter devices) tubes with a cut off of 5,000 kDa, by centrifugation at 4,000 rpm for approximately 10 minutes. The filtrate was then discarded, and the concentrated sample was collected. This was carried out by inserting a collection tube, inverting the centricon tube, and spinning at 1,000 rpm for 1 minute. The final solution was approximately 20 times more concentrated than the original solution.

2.5.2 Sample preparation

1/100 volume of 2% Na-deoxycholate was added to 100μg of protein and left on ice for 30 minutes. To this, 1/10 volume of trichloric acetic acid (TCA) was added and left on ice for 1-2 hours, after which the precipitated protein was collected by centrifugation for 15 min at 15,000 rpm at 4°C, before washing in –20°C acetone, and incubating on ice for a further 30 minutes. The wash was repeated and the sample left on ice for 20 minutes. The sample

was then centrifuged for 15 minutes at 15,000 rpm at 4°C, left to air dry and resuspended in 125 µl of 2D gel sample buffer 1.

2.5.3 First dimension

Firstly, the IPGphor unit strip holders were placed on top of the IPGphor unit. The protein sample was then added dropwise along the groove in the strip holder (avoiding bubbles) and the immobilise dry strip placed on top of the sample. The pointed end (or marked '+') of the dry strip was pushed to the top of the groove. The sample and dry strip were then covered with 1 ml Dry Strip Cover Fluid.

The lid of the IPGphor unit was closed and the programme started, using a 12 hour rehydration step of the IPG strip, followed by 6-8 hours polarisation of the sample at 5000 V.

2.5.4 Second dimension

The strip was removed from the electrode and rinsed in dH_20, followed by a 15 minute incubation in 1 ml 2D gel sample buffer 2, with shaking. The strip was rinsed again, and then incubated for 15 minutes in 1ml 2D gel sample buffer 3, while shaking. After a further rinse, the strip was loaded onto a pre-cast gel (containing an IPG loading well). The gel was run as for 1D gels at 150 V and 200 mA for about 1 hour until the dye-front had reached the bottom of the gel, with SeeBlue molecular weight markers in parallel.

2.5.5 Fixation and staining

Following electrophoresis, the gel was fixed overnight at RT in 30% ethanol/5% acetic acid, followed by 30 minutes in 0.05% SDS in PBS. Staining was performed using either Brilliant Blue Colloidal or Sypro Orange protein gel stain (Section 2.2.4.7).

2.6 Mass Spectrometry

2.6.1 Sample preparation – with assistance from Chris Ward (proteomics manager, Beatson Institute)

Bands or spots of interest in the gels were carefully excised using a scalpel on a clean glass plate, carried out in a fume cupboard, while wearing gloves, to minimise keratin contamination. Care was taken to minimise the gel size, avoiding excess gel. The gel piece was then cut into small pieces and placed in a sterile 1.5 ml microcentrifuge tube. The pieces were washed in 300 µl Milli-Q water for 15 minutes and the supernatant removed.

The gel pieces were then washed with 300 µl 100 mM NH_4HCO_3/CH_3CN (50:50 v/v) for 15 minutes and the supernatant removed, followed by a 15 minute wash with 300 µl 100 mM NH_4CO_3 for 15 minutes, and removal of supernatant. If the gel pieces were still blue, these steps were repeated once or twice to remove the stain. After a final wash in NH_4HCO_3/CH_3CN, 100 µl CH_3CN was added for 10 minutes to dehydrate the gel. The supernatant was removed, and the pieces dried in a Speedvac for 5 minutes, before storing at –20°C.

Trypsin digestion of the protein sample was performed by addition of 10 µl of digestion buffer (25 µg/ml of modified trypsin in 20 mM NH_4HCO_3) per band. This was left for 20-30 minutes to rehydrate the gel pieces. If necessary, more 20 mM NH_4HCO_3 (without trypsin) was added to cover the pieces (although keeping the volume to a minimum). The sample was then incubated at 30°C for a minimum of 4 hours, before storage at –20°C until needed.

Samples were analysed (by Chris Ward) by mass spectrometry. Briefly, 1D gel samples were ionised by electrospray ionisation (ESI) and then analysed by Q-star. 2D samples were ionised using matrix-assisted laser desorption ionisation (MALDI) and analysed by time-of-flight analysers (MALDI-TOF). These allow the production of trypsin digest spectras giving a peptide mass fingerprint which were then compared to University databases for identification

2.7 RNAi

2.7.1 Design of nucleotides

Twenty-one nucleotide double-stranded RNA sequences were designed against N-cadherin mRNA as recommended (ref:

http://www.mpibpc.gwdg.de/abteilungen/100/105/sirna.html).

The following rules were applied:

1. Sequences were chosen in the coding region of the mRNA with a GC ratio as close to 50% as possible
2. Regions within 50-100 nt of the AUG start codon or 50-100 nt of the termination codon were avoided
3. Poly G sequences (more than 3 guanisines in a row) were avoided
4. Target sequences were chosen which started with two adenosines
5. Target sequences underwent a BLAST search to ensure that no unwanted genes with similar sequences were silenced
6. dTdT overhangs were used instead of UU since they were easier and cheaper to synthesise, as well as being more protected from nucleases

Sequences were ordered from Dharmacon Research in a ready annealed form. These were diluted in diethyl pyrocarbonate (DEPC; 0.1%) treated water to a concentration of 20 μM. Successful sequences used were:

sense siRNA: 5' AAGAUGUUUACAGCGCGCGGU
anti-sense siRNA: 5'ACCGCGCGCUGUAAACAUCdTdT

Scrambled RNAi were also designed for control experiments and subjected to a BLAST search to check that they did not correspond to any known RNA sequences. Sequences used were:

sense siRNA 5' AAGCUAUCGCUACGUGCACGU

anti sense siRNA 5' ACGUGCACGUAGCGAUAGCdTdT

2.7.2 RNAi Transfection

Cells were set up for transfection by trypsinizing cells and then plating them on PLL-coated 6 wells at a density of 40-60% confluency 24 hours before transfection.

Transfection was performed using both FuGENE and oligofectamine transfection protocols (according to manufacturers instructions). A transfection mixture containing 3 μl siRNA and 8 μl FuGENE was made in 200 μl DMEM-BS and added to each 6 well, already containing 2 ml of culture medium.

Alternatively, a mixture containing 12 μl siRNA and 12 μl Oligofectamine was made in 400μl serum-reduced OPTIMEM, before adding to 6 wells containing only cells and no media. Cells were incubated for 4 hours at 37°C before adjusting the final culture volume with DMEM-10% to 2 ml. For both protocols, cells were left for 48 hours before making lysates, or being used in experiments.

2.8 Statistics

Statistical analyses were performed using either a 2-tailed t-test, where 2 samples were compared and assuming unequal variance, or using the one-way ANOVA test with Tukey's *post hoc* analysis, where more than 1 group was being compared.

Data was expressed as the mean +/- SEM, and p-values were rounded to 3 digits. P-values below 0.05 were considered significant, and all experiments were performed at least in triplicate.

CHAPTER 3

Characterisation and comparison of Schwann cell and OEC migratory and adhesive properties

3.1 Introduction

In recent years olfactory ensheathing cells (OECs) and Schwann cells have both been proposed as candidates for transplant-mediated repair of central nervous system (CNS) lesions (Franklin and Barnett, 2000; Raisman, 2001; Wewetzer et al., 2002). Both cells have a similar repair repertoire, being able to remyelinate experimentally demyelinated lesions (Franklin et al., 1996; Barnett et al., 2000; Imaizuimi et al., 2000), and permit rapid saltatory conduction to take place (Imaizumi et al., 1998; Honmou et al., 1996) using similar transcriptional mechanisms (Smith et al., 2001). In addition, both OECs and Schwann cells can support axonal outgrowth, in experimental models of spinal cord injury (Ramon Cueto et al., 1994, 2000; Li et al., 1997, 2003a, 2003b).

Despite these similarities, there are significant differences between the two cell-types which may affect their candidature for transplant-mediated repair. For example, Schwann cells may have a limited potential to repair CNS damage due to their inability to migrate and survive within the CNS environment after transplantation (Baron von Evercooren et al., 1992; Franklin and Blakemore, 1993; Iwashita et al., 2000). This inhibitory environment is characterised by the presence of reactive astrocytes (Norenberg, 1994; Eng and Ghirnikar, 1994), which may be a restrictive component of CNS tissue since remyelination by Schwann cells is only observed in astrocyte-free areas (Woodruff and Franklin 1999; Shields et al., 2000). This propensity of Schwann cells to avoid astrocyte-rich areas was also demonstrated *in vitro* where Schwann cells cultured with astrocytes formed discrete boundaries being unable to migrate amongst them (Ghirniker and Eng, 1994; Wilby et al., 1999). In contrast to Schwann cells, OECs interact much more favourably with astrocytes and are able to intermingle and migrate amongst co-cultured astrocytes (Lakatos et al 2000), perhaps due to their inherent ability to exist *in situ* alongside astrocytes within the olfactory system (Doucette, 1991, 1993).

Another difference between Schwann cells and OECs is seen in the reactive response elicited when either cell-type is co-cultured with astrocytes (Lakatoes et al., 2000). When in contact with Schwann cells, but not OECs, astrocytes became enlarged and enhanced expression of the hypertrophic marker glial fibrillary acidic protein (GFAP), and

chondroitin sulphate proteoglycans (CS-PGs), an inhibitory component of the glial scar (Norenberg, 1994). This may be an important consideration when trying to minimise glial scarring, as supported by *in vivo* studies demonstrating that transplanted Schwann cells within the CNS induced a greater host tissue inhibitory response to axon regeneration by upregulating expression of CS-PGs and astrocytic GFAP compared to that associated with OEC transplantation (Plant et al., 2001; Lakatos et al., 2003).

It has been reported in the literature that there are migrational differences between OECs and Schwann cells when they come into contact with astrocytes *in vitro*. For instance, in co-cultures with astrocytes OECs can migrate into astrocytic areas, but Schwann cells cannot (Lakatos et al., 2000). At present, it is not known whether these migrational differences are intrinsic to the glial cells, such as relating to their inherent motility and their regulatory mechanisms of migration, or whether they are a result of differential interactions with astrocytes, such as their adherence. The aim of this chapter, is to investigate some of the mechanisms which may explain how Schwann cells and OECs differ in their migration and adhesion. In order to achieve this, the adhesive and migratory properties of OECs and Schwann cells will be characterised on various substrates. In addition, the expression and localisation of molecular components associated with adhesion and migration will be investigated to assess if there are any substantial differences between how the cell types organise the machinery necessary for these processes. Since migration and adhesion are related phenomena (see Introduction, section 1.6.1.1), it is hoped that these functions can be dissected in order to assess the contribution of each to the resultant behaviour of OECs and Schwann cells in the presence of astrocytes.

As previously described in the introduction (section 1.4.1.2), OECs can exist as a heterogenous population, consisting of a Schwann cell-like and an astrocyte-like phenotype. In order to simplify the comparison between OECs and Schwann cells in this thesis, OECs were cultured in conditions (Alexander et al., 2004) which favoured the Schwann cell-like phenotype (see Figure 3.1Aii). This preparation also reflects the cells used in the majority of reported transplantation experiments which were $p75^{NTR}$-positive (Ramon-Cueto et al., 1998, 2000; Navarro et al., 1999; Plant et al., 2002).

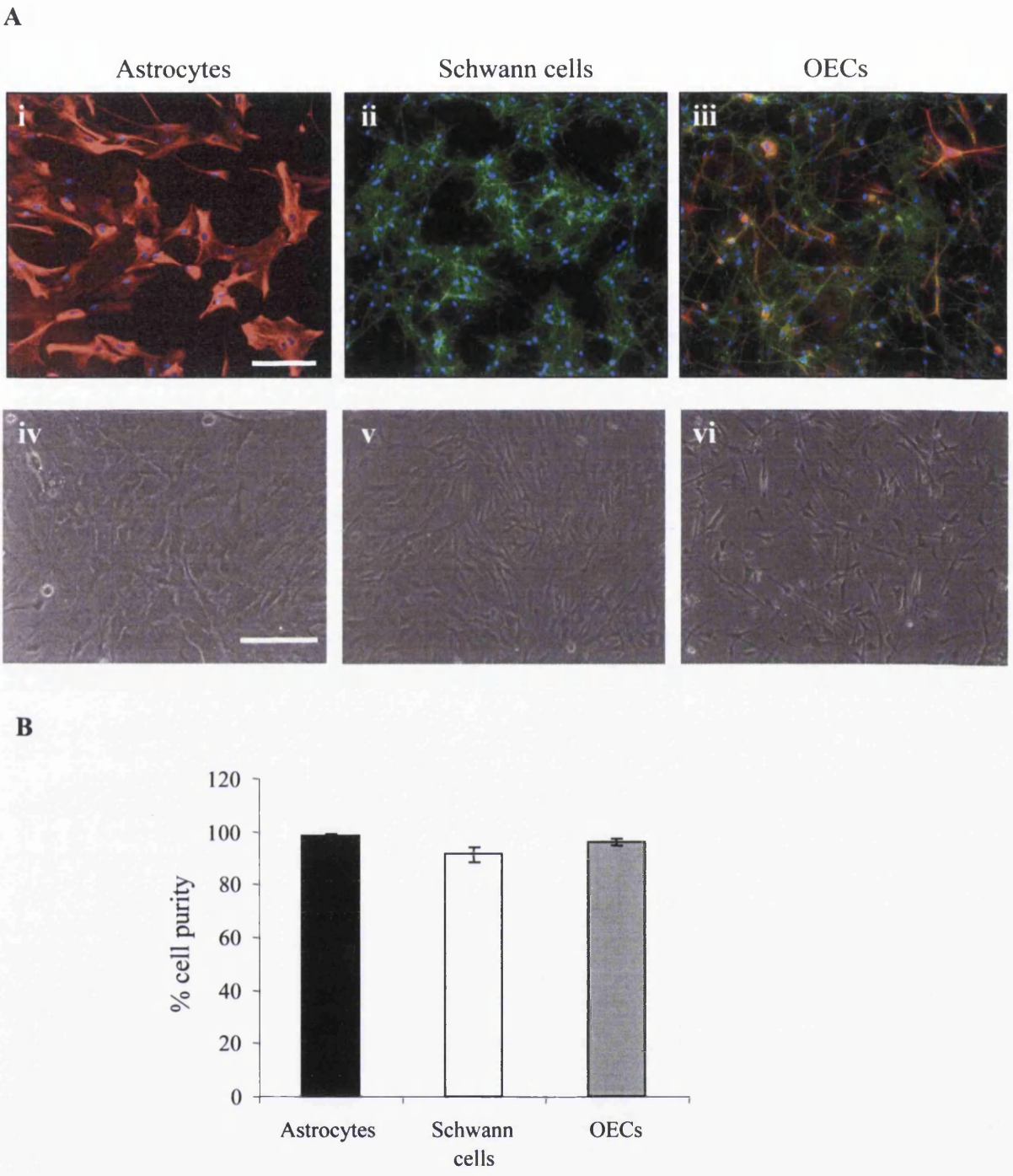

Figure 3.1. Cell purity of different cultures.

(A) Immunocytochemistry (i, ii, iii; co-labelled for GFAP-TRITC, $p75^{NTR}$-FITC and DAPI) and phase (iv, v, vi; different fields of view) of astrocytes (i, iv) cultured in DMEM-10%, Schwann cells (ii, v) cultured in DMEM-10% supplemented with heregulin and forskolin, and OECs (iii, iv) cultured in OEC mitogen media (OMM). Scale bar = 100 μm. (B) Average purity of cultures used in experiments (percentage of GFAP-positive cells (astrocytes) or $p75^{NTR}$-positive cells (Schwann cells and OECs), total cell number was indicated by DAPI-labelling). n=6.

3.2 Results

3.2.1 The Confrontation assay models in vivo observations

To examine the ability of Schwann cells and OECs to intermingle with astrocytes, we have used a previously demonstrated *in vitro* assay, termed the confrontation assay, and have confirmed its reproducibility (Wilby et al., 1999; Lakatos et al., 2000). The assay consisted of strips of OECs or Schwann cells which were plated on a coverslip opposing a strip of astrocytes. These were then maintained in culture for up to 14 days and the resulting cellular interactions analysed by immunocytochemistry. The cultures were immuno-labelled for $p75^{NTR}$, to identify both OECs and Schwann cells, and GFAP, to distinguish astrocytes by their strong and fibrous GFAP expression from the weak and diffusely-expressing Schwann cells and OECs. The purity of the cells used in these experiments was also confirmed using these markers (Figure 3.1A), and was above 90% for all cell types used (Figure 3.1B).

The confrontation assay demonstrated that Schwann cells were less able than OECs to mingle with astrocytes (Figure 3.2). Schwann cells typically formed discrete boundaries against the astrocytes (Figure 3.2B and 3.2D), and in addition, induced the astrocytes to become enlarged (see asterisk), a morphology characteristic of hypertrophy. It could also be seen that Schwann cells possessed an ordered alignment amongst themselves which was absent amongst the OECs. This may be suggestive of strong adhesions between Schwann cells. These phenomena reflect the *in vivo* observations following transplantation of OECs and Schwann cells into astrocyte-rich areas (Plant et al., 2001; Lakatos et al., 2003) and therefore allowed the use of a simplified, *in vitro* approach to elucidate any molecular differences between the two glial cells in their ability to interact with astrocytes.

3.2.2 OECs and Schwann cells similarly express and localise components associated with migration and adhesion

Immunocytochemistry using antibodies against proteins typically associated with both migration and adhesion was performed in order to investigate their expression and

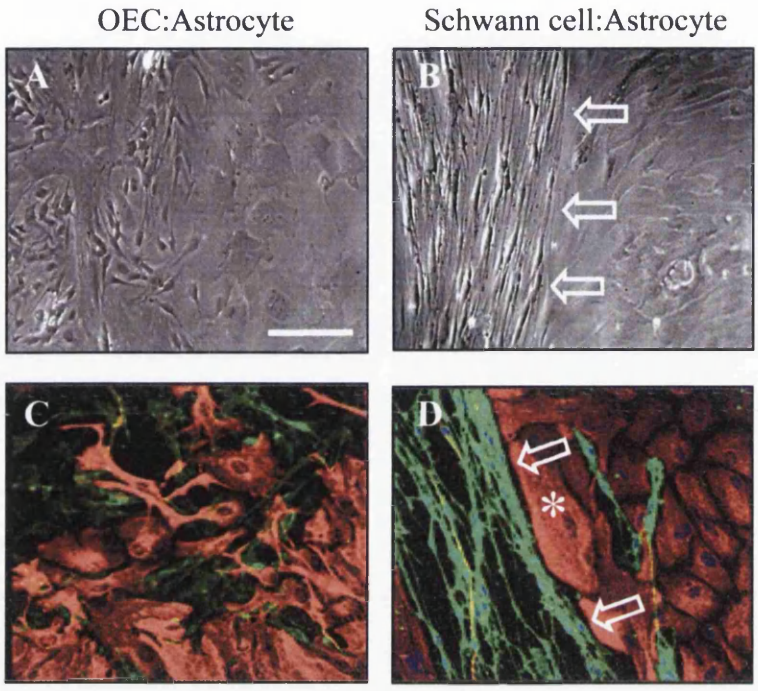

Figure 3.2. Schwann cells, but not OECs, form a boundary upon interacting with astrocytes.

A confrontation assay was set up between OECs and astrocytes (A, C) and between Schwann cells and OECs (B, D). Cells were immunolabelled after 10 days, and phase microscopy (A, B) and confocal microscopy (C, D) was performed. OECs and Schwann cells were labelled in green ($p75^{NTR}$-FITC), and astrocytes in red (GFAP-TRITC). Schwann cells formed a clear boundary against the astrocyte domain (arrows), whereas OECs have intermingled with astrocytes. An enlarged hypertrophic astrocyte can be seen, marked with an asterisk. Scale bar = 100 μm.

localisation in Schwann cells, OECs and astrocytes (Figures 3.3 and 3.4). The intention was to characterise the arrangement of these in order to highlight any gross differences between the different glia, such as the absence or inappropriate positioning of known proteins necessary for adhesion and migration. Structures investigated were focal adhesions (paxillin and vinculin), adherens junctions (N-cadherin, vinculin and β-catenin), the cytoskeleton (actin) and the extracellular matrix (ECM; fibronectin and laminin).

Paxillin and vinculin were located as expected at focal adhesions, clearly seen at the tips of cellular processes. N-cadherin and β-catenin were both associated with the cell-cell junctions where they are likely to mediate adhesion between cells. Astrocytes had more distinct junctions, compared to Schwann cells and OECs, which occurred on all surfaces, reflecting the astrocytes ability to form monolayers and syncytium (Shearer and Fawcett, 2001), whereas OECs and Schwann cells were similar in that they had only short, often patchy, contact areas. For all glial cells, clear actin stress fibres were observed. In addition, both fibronectin and laminin were detected on all cells, with a particularly diffuse pattern around astrocytes, reflecting where they were secreted.

In summary, OECs, Schwann cells and astrocytes all contain the appropriate protein structures associated with migration (focal adhesions) and adhesion (adherens junctions), and at correct cellular locations for them to function appropriately. In addition, they all expressed distinct actin stress fibres. OECs and Schwann cells both appeared to have a similar ability to secrete ECM. However, it is also noteworthy that Schwann cells displayed a more polarised morphology than both OECs and astrocytes, suggestive of greater motility.

3.2.3 Migration

3.2.3.1 Schwann cell migration is impeded on astrocytes

To compare the abilities of Schwann cells and OECs to migrate, migration assays were performed on both PLL and astrocyte substrates, using time-lapse microscopy, where the distance moved by Schwann cell and OEC cell bodies at regular time intervals was measured. On PLL, OECs and Schwann cells migrated at similar speeds (18.16 +/- 2.81

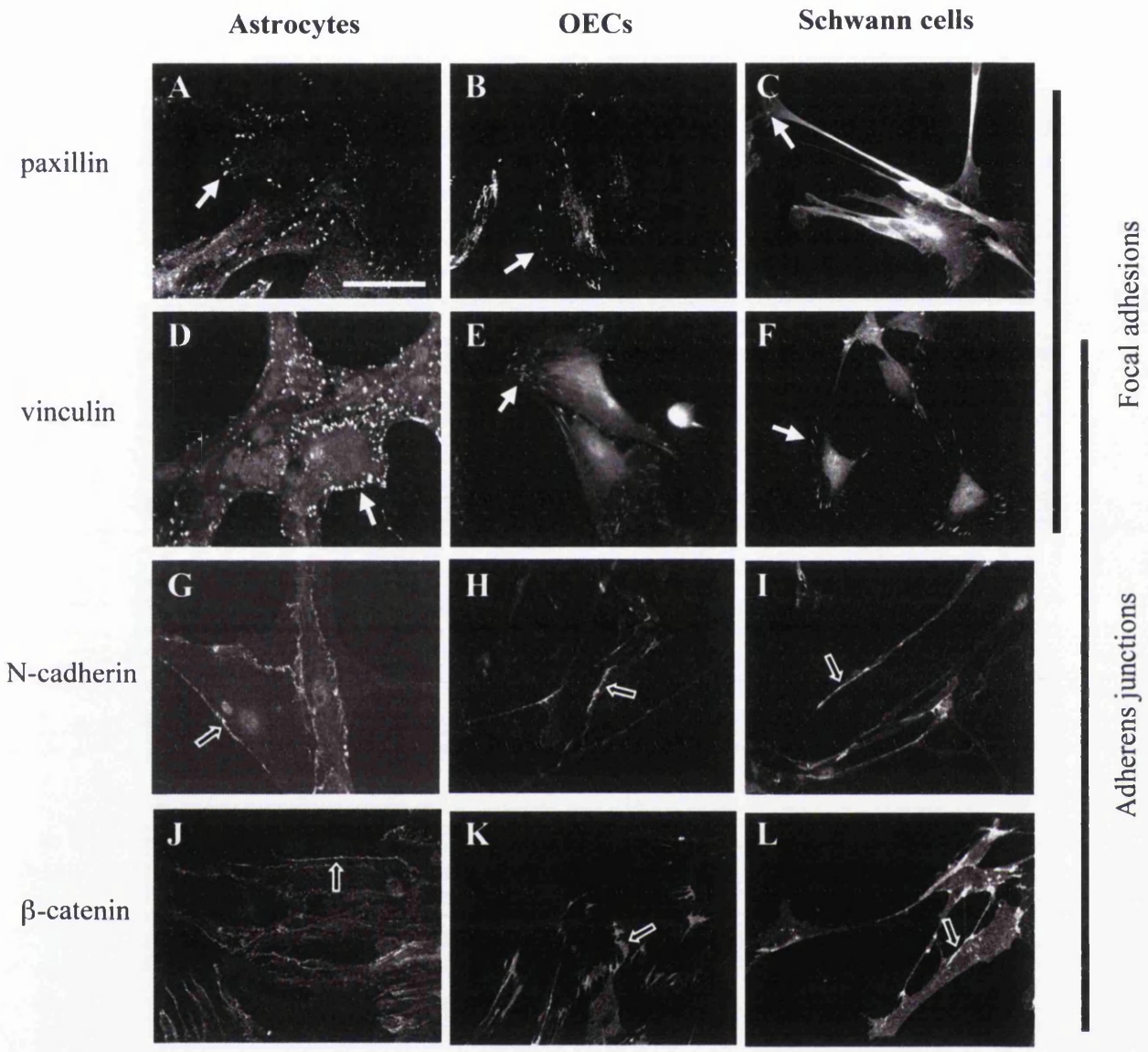

Figure 3.3. Astrocytes, OECs and Schwann cells form normal focal adhesions and adherens junctions.

Immunocytochemistry of astrocytes (A, D, G, J), OECs (B, E, H, K) and Schwann cells (C, F, I, L) showing molecular localisation of components associated with migration and adhesion, such as focal adhesions (paxillin (A, B, C) and vinculin (D, E, F), solid arrows) and adherens junctions (vinculin, N-cadherin (G, H, I) and β-catenin (J, K, L), open arrows). Scale bar = 50 μm.

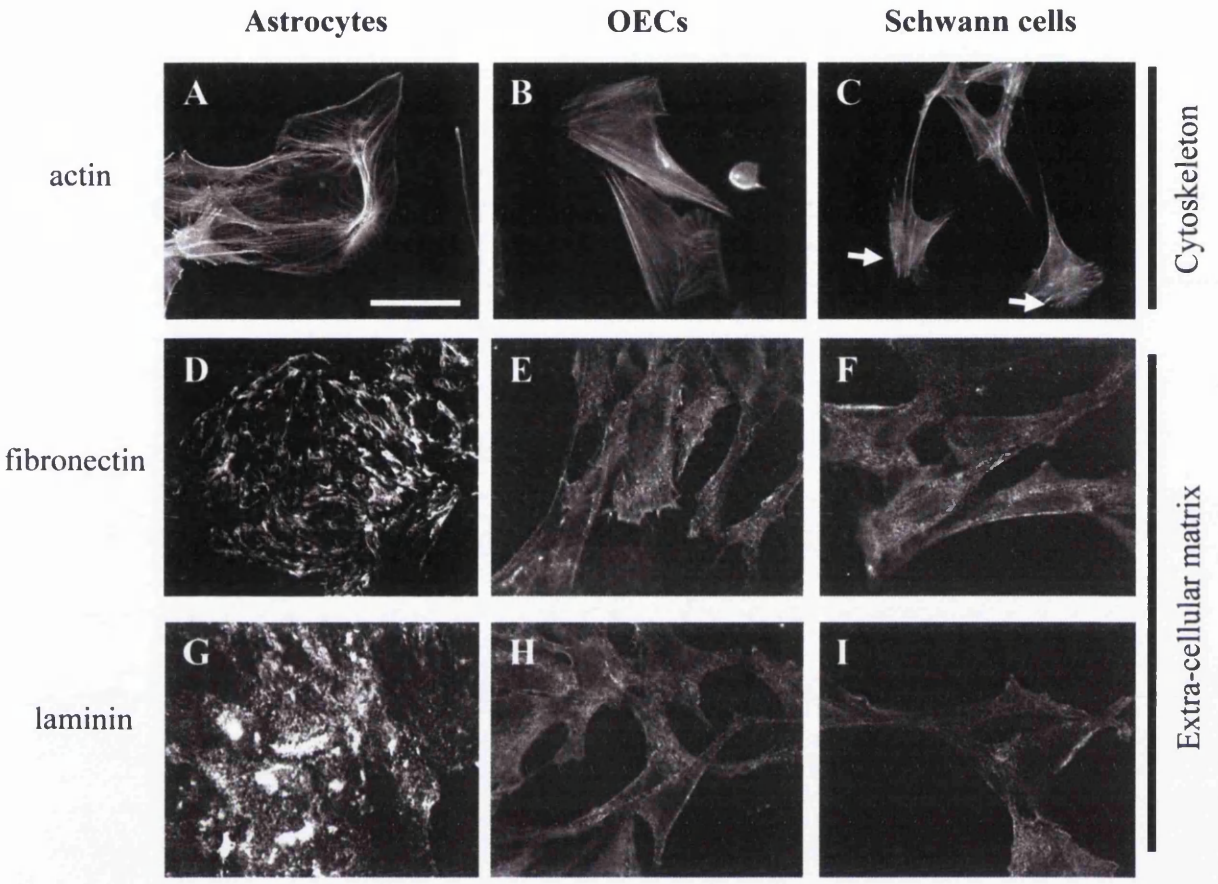

Figure 3.4. Astrocytes, OECs and Schwann cells have distinct actin stress fibres, and secrete fibronectin and laminin.

Immunocytochemistry of astrocytes (A, D, G), OECs (B, E, H) and Schwann cells (C, F, I) showing molecular localisation of components associated with migration and adhesion, including components of the cytoskeleton (actin; A, B, C) and the extracellular matrix (fibronectin (D, E, F) and laminin (G, H, I)). Arrows indicate leading edge of polarised Schwann cells. Scale bar = 50 μm.

μm/hour and 19.57 +/- 3.08 μm/hour, respectively; Figure 3.5). However, upon astrocyte monolayers (AS), OEC migration was equivalent to that assessed upon PLL (21 +/- 2 μm/hour) whereas Schwann cell migration was significantly reduced by approximately 40% (to 11.47 +/- 0.87 μm/hour, $p<0.01$). Thus, Schwann cell migration, although comparable to

OEC migration upon PLL, is inhibited when cultured upon astrocytes. This inhibition is not seen for OECs. Therefore, Schwann cell migration is comparable to OEC migration, unless astrocyte-mediated inhibition is occurring. This suggests that an inhibitory factor from astrocytes is acting upon Schwann cell migration.

3.2.3.2 OECs and Schwann cells are dependent upon similar signalling pathways to regulate migration

In order to compare and contrast the mechanisms controlling migration of OECs and Schwann cells, a number of components of signalling pathways associated with migration were inhibited (see Figure 1.3 in Introduction), and the resulting effects on migration measured. MEK and src signalling pathways were targeted since they have been shown to be important for the regulation of migration (Klemke et al., 1997; Fincham and Frame, 1998). Cells were incubated in MEK inhibitors (UD and PD), and a src inhibitor (PP2), and migration was assessed by time-lapse microscopy. All inhibitors, reduced migration significantly in both Schwann cells and OECs (Figure 3.6; $p<0.001$). Thus both Schwann cells and OECs use similar MEK and src signalling pathways to regulate migration.

3.2.4 OEC and Schwann cell focal adhesion turnover is not regulated by astrocyte contact

A reduction in cell migration can be associated with a reduced turnover of focal adhesions (see Introduction, section 1.6.1.2). This can be identified by an enlargement of the focal adhesions, resulting from the build-up of proteins at these sites which are no longer being disengaged and disassembled, and in particular, the formation of exaggerated rod-like adhesions due to the contraction of the associated actin-cables (Raghavan et al., 2003). To investigate whether such a mechanism results from the contact-mediated inhibition of Schwann cell migration, following interaction with astrocytes, any change in focal adhesion

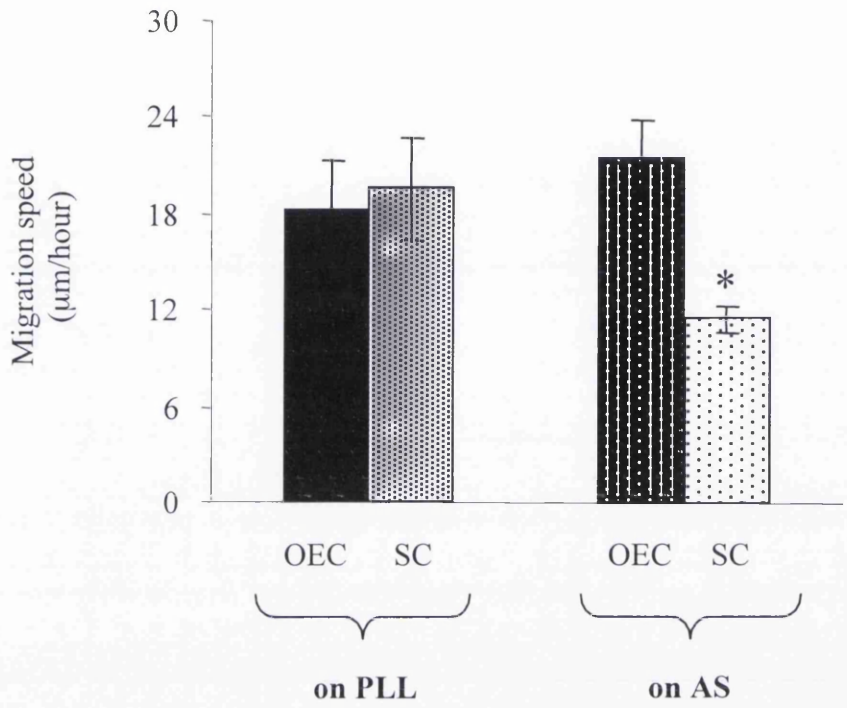

Figure 3.5. Schwann cell migration is inhibited upon astrocyte monolayers.

OEC and Schwann cell migration rates upon poly-l-lysine (PLL) and astrocyte monolayers were measured using time-lapse microscopy. The migration speeds of OECs on both PLL and astrocytes monolayers were similar, whereas Schwann cell migration was significantly decreased upon an astrocyte monolayer (*$p<0.01$, $n=15$).

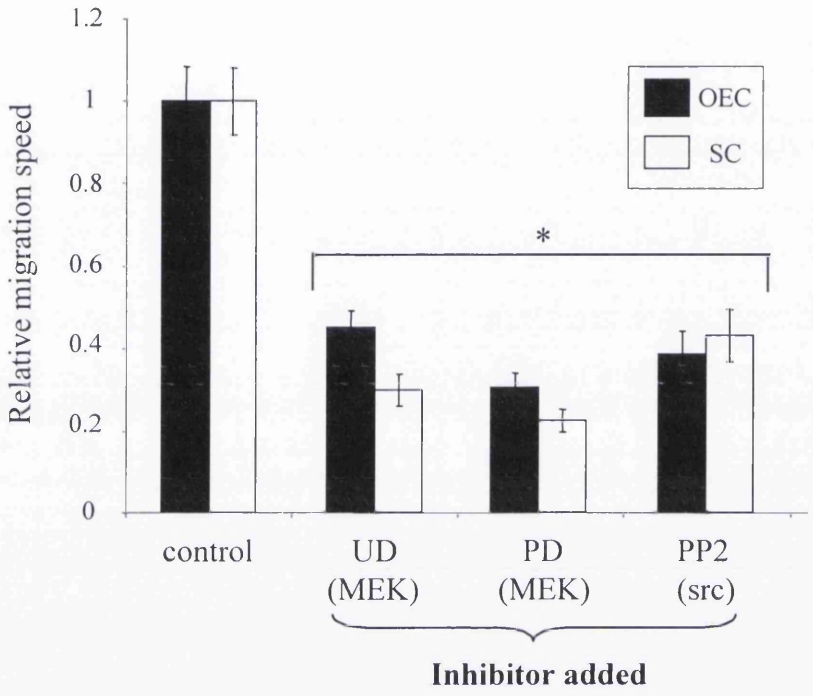

Figure 3.6. Both Schwann cells and OECs require MEK and src signalling pathways for migration.

Relative migration speeds of OECs and Schwann cells were measured using time-lapse microscopy after addition of MEK (UD and PD) and src (PP2) inhibitors. Migration was reduced in both OECs and Schwann cells by the presence of all these inhibitors. * $p<0.001$, $n=15$.

size was analysed following co-culture of Schwann cells and OECs with astrocytes. Double immunolabelling with an antibody against paxillin was used to label focal adhesions, together with anti-GFAP to identify astrocytes. All cells (astrocytes and either Schwann cells or OECs) were identified by DAPI-staining of cell nuclei. Immunofluorescence demonstrated that focal adhesion size was not significantly changed between cells in mono- and co-cultures, when assessed qualitatively by eye (Figure 3.7), suggesting that focal adhesion turnover as unaffected by astrocyte contact and was therefore not a mechanism through which Schwann cell migration was decreased.

3.2.5 Schwann cells have stronger adhesions than OECs

An adhesion assay was employed to compare the relative adhesive strengths of Schwann cells and OECs to both monolayers of themselves (homo-typic adhesion) and to astrocyte monolayers (hetero-typic adhesion). In this manner, Schwann cell inhibition (as demonstrated in the confrontation assay, Figure 3.2) could be explained either as a result of enhanced adhesion to astrocytes, preventing Schwann cells from migrating further into astrocytic areas, or due to strong mutual adhesion to themselves, which in turn prevents them from migrating away from Schwann cell areas. The adhesion assay was performed by counting the number of Schwann cells and OECs (labelled with Vybrant to aid detection) which had adhered to a monolayer of Schwann cells or OECs (respectively), or to an astrocyte monolayer.

Schwann cells displayed a greater adhesion than OECs to astrocytes (Figure 3.8; $p<0.001$), where 1197 +/- 75 Schwann cells adhered to astrocyte monolayers, compared to 469 +/- 38 OECs. Schwann cells also had greater adhesion to themselves (681 +/- 46 Schwann cells to Schwann cell monolayers), than OECs (114 +/- 9.9 OECs to OEC monolayers; $p<0.001$). This shows that Schwann cell adhesion is greater than OEC adhesion, both homo- and hetero-typically. Additionally, despite OEC adhesion being less strong than Schwann cells to either substrate, both Schwann cells and OECs adhered more strongly to astrocytes than to monolayers of themselves ($p<0.001$).

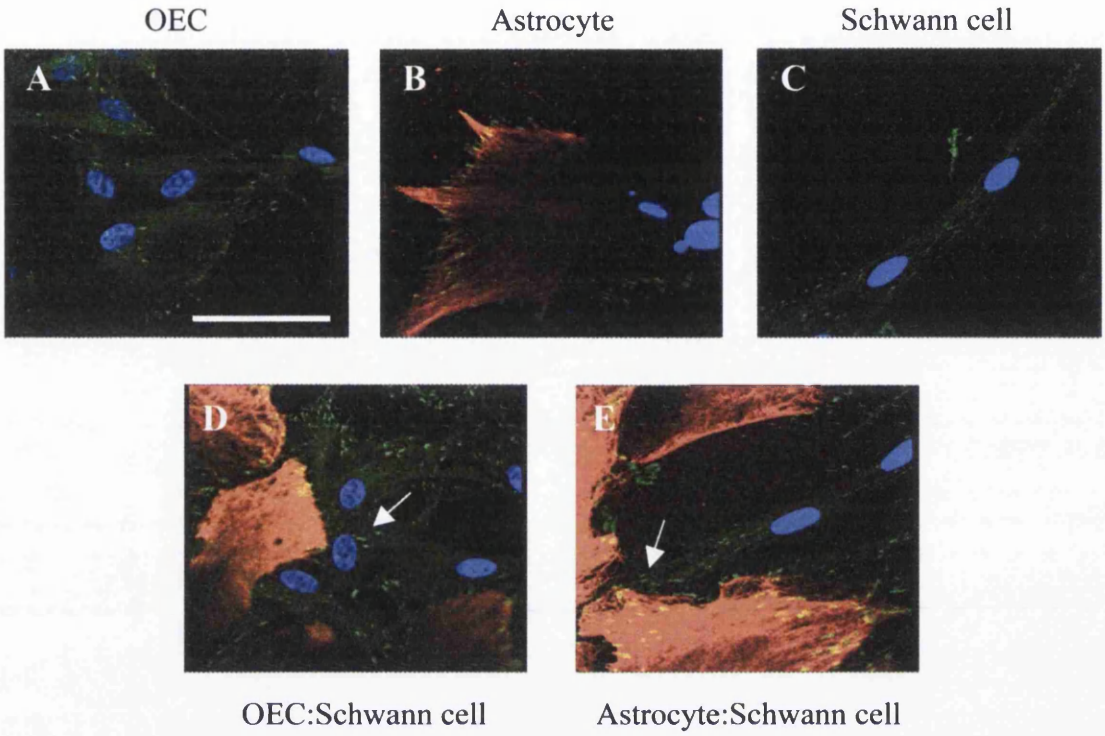

Figure 3.7. Focal adhesion size is unchanged in OECs and Schwann cells co-cultured with astrocytes.

Immunocytochemistry of paxillin (FITC) in cells both in mono-culture (OECs, A; astrocytes, B; Schwann cells, C) and co-cultured with astrocytes (astrocyte:OEC, D; astrocyte:Schwann cell, E), showing that OEC and Schwann cell focal adhesion sizes are unchanged when in contact with astrocytes, as assessed qualitatively by eye. Cell nuclei are labelled with DAPI, and astrocytes for GFAP (TRITC). Scale bar = 100 μm.

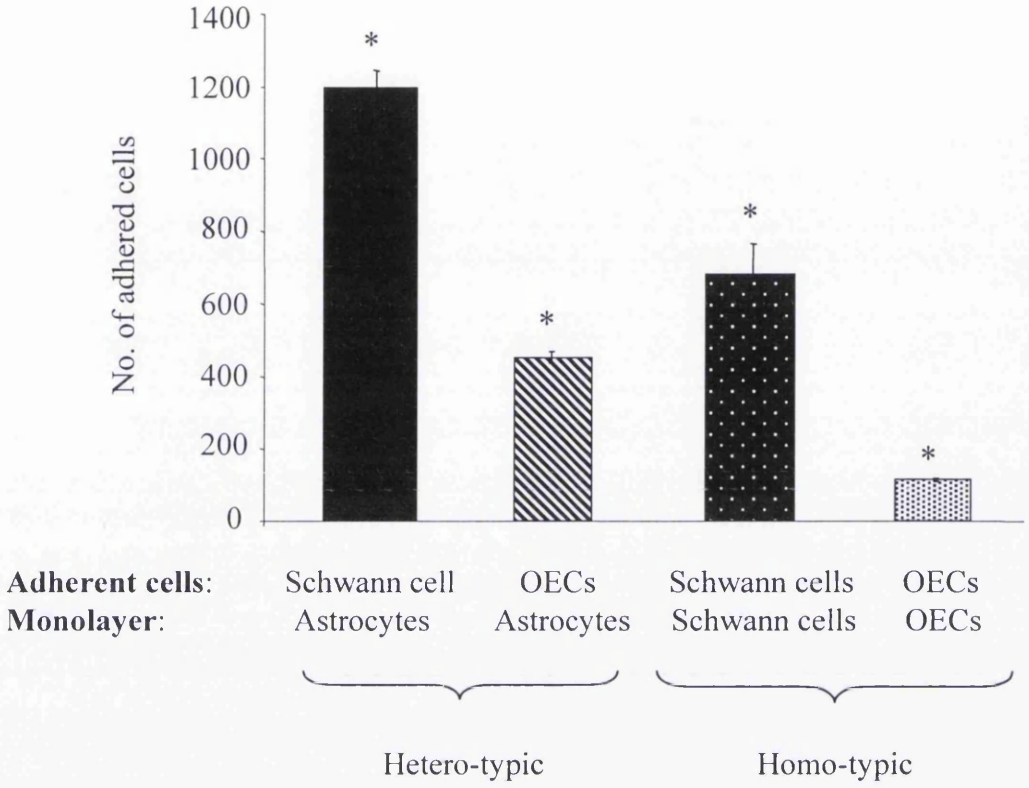

Figure 3.8. Schwann cells form stronger adhesions than OECs.

Schwann cells are capable of stronger adhesions than OECs, to both themselves (homo-typic) and astrocytes (hetero-typic). To assess adhesion, Vybrant-labelled cells were plated onto a confluent cell monolayer and left to adhere for 30 minutes with shaking at 37°C. The number of adherent cells that remained attached were then counted. * p values between every pair <0.001, n=6.

3.2.6 Role of calpain in migration and adhesion

Calpain is a protease involved in the regulation and degradation of components associated with migration and adhesion (see Introduction, section 1.6.1.2; Figure 1.3). It has been demonstrated to play different roles in various cell types, and therefore may be a determinant of the different migratory and adhesive behaviour observed in Schwann cells and OECs. In most cell types it functions to enhance migration, thus its inhibition reduces the motility of a cell (Huttenlocher et al., 1997; Carragher et al., 2001). In neutrophils, however, its inhibition actually led to a more migratory phenotype (Lokuta et al., 2003). The role of calpain in Schwann cell and OEC migration and adhesion was therefore investigated, to see how it affected the two glial cells. Cell viability was assessed for the calpain inhibitor (ALLN) before selecting the optimal concentration for experiments. This was performed, following cell-treatment with a range of inhibitor concentrations for 24 hours, by both propidium iodide labelling (50 μg/ml in PBS) and qualitatively assessing the cellular appearance by phase microscopy (data not shown). Stephen Thomson assisted with some of the optimisation. A working concentration of 50 μM was chosen since this was the highest concentration where cell viability appeared unaffected by treatment, and within the suggested effective concentration range.

3.2.6.1 Both Schwann cells and OECs are dependent upon calpain for migration

Migration assays were set up, and speeds of cells plated upon PLL and astrocyte monolayers were measured both in the presence and absence of an inhibitor of type-1 calpain, ALLN. In all experiments, in which Schwann cells and OECs were pre-incubated for 1 hour with ALLN, migration was reduced (Figure 3.9; OECs $p<0.05$, Schwann cells $p<0.01$). Therefore, no differences were seen in the dependency of Schwann cells and OECs upon calpain for efficient migration. This similar dependency upon calpain was also demonstrated using an additional assay for assessing migration, the wound assay, where confluent cultures were scraped with a pipette tip to create a 'wound'. Again, ALLN was pre-incubated for 1 hour with confluent OEC and Schwann cell cultures, prior to wounding the cultures with a micropipette. Images were taken of the cultures at 0, 8 and 48 hours after wounding (Figure 3.10). After 8 hours, cells could be seen migrating into the wound in

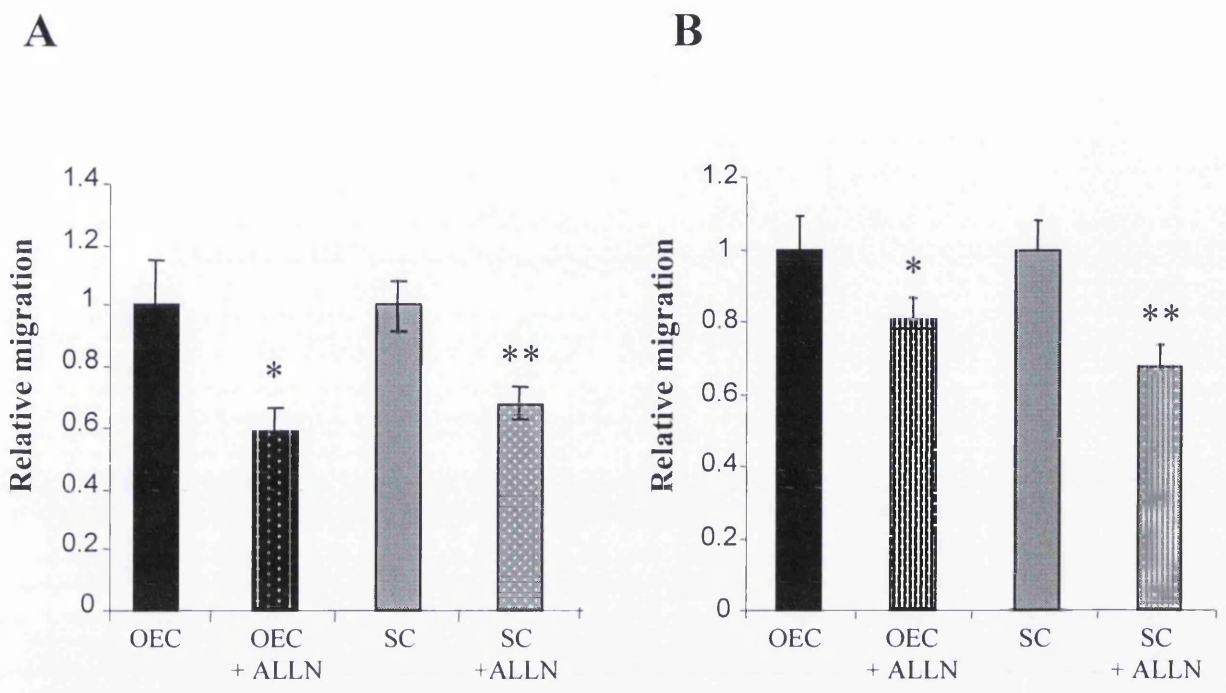

Figure 3.9. Schwann cells and OECs both require calpain function for migration.

Relative migration rates, as measured by time-lapse microscopy, were calculated for OECs and Schwann cells (SC) plated on PLL (A) and on astrocyte monolayers (B), both with and without treatment with the calpain 1 inhibitor (ALLN) (n = 10; *$p<0.05$, **$p<0.01$).

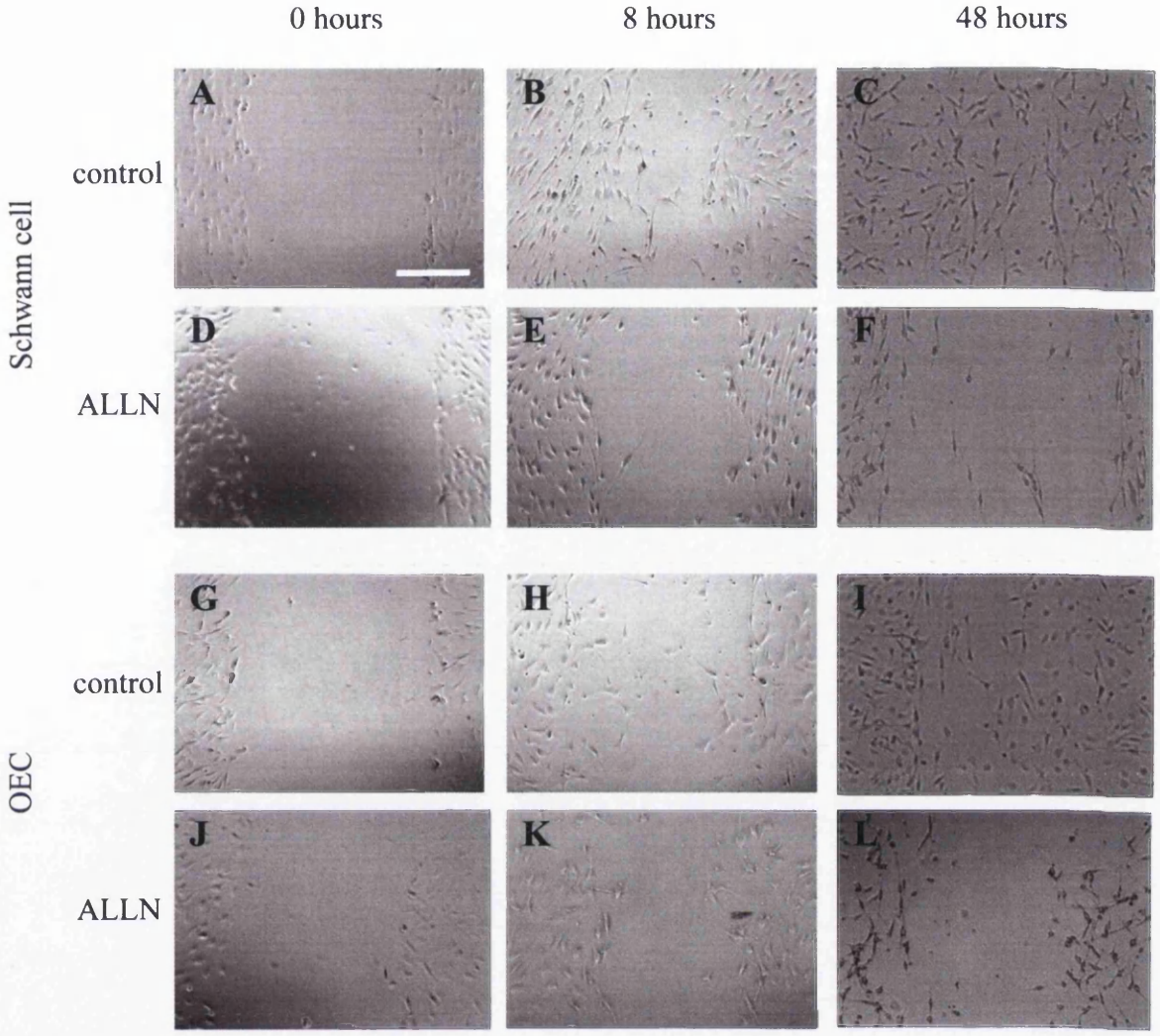

Figure 3.10. OEC and Schwann cell wound healing requires calpain activity.

Phase contrast images of wound assays were taken using confluent OEC (A to F) and Schwann cell (G to L) monolayers on PLL. Inhibition of migration is seen after treatment with the calpain 1 inhibitor (ALLN) by 8 hours (B, E, H, K) and which still occurs at 48 hours (C, F, I, L), compared to controls (A, D, G, J). Scale bar = 100 μm.

untreated cultures (Figure 3.10B and 3.10H), whereas both Schwann cell and OEC migration was prevented in the treated experiment (Figure 3.10E and 3.10K). This inhibition was seen further at 48 hours, where untreated Schwann cell and OEC cultures had almost reached confluency again (Figure 3.10C and 3.10I), whereas the wound was still clearly observable in the treated set (Figure 3.10F and 3.10L). These differences were quantified by taking images of the wounds at the various time-points following wounding. The number of cells migrating into the wound area (as designated by projecting an outline of the average wound size onto images) were counted and presented in a graphical form (Figure 3.11). Schwann cell migration into the wound following ALLN treatment was significantly reduced at 48 hours following wounding (257.6 +/- 42.4 cells per wound (untreated) to 74 +/- 16.7 cells per wound (ALLN-treated); $p<0.01$), as was OEC migration (238.75 +/- 24.1 cells per wound (untreated) to 101.5 +/- 23.4 cells per wound (ALLN-treated); $p<0.01$). It can therefore be concluded that Schwann cells and OECs are both dependent upon calpain activity for migration, and dependency is to a similar level.

3.2.6.2 OEC and Schwann cell adhesion are not dependent upon calpain activity

An adhesion assay was performed to measure the adhesion of Vybrant-labelled OECs and Schwann cells to astrocyte monolayers with and without the preincubation of ALLN for 1 hour (Figure 3.12). OEC adhesion appeared to increase upon inhibition of calpain, but this difference was not significant. Schwann cell adhesion was unaffected by the presence of ALLN.

3.3 Discussion

3.3.1 General comparison of Schwann cells and OECs

Many similarities between the cellular and molecular properties of Schwann cells and OECs were observed in the experiments performed in this chapter. These included the localisation of complexes associated with migration and adhesion, and the ability of Schwann cells and OECs to migrate upon PLL. These similarities therefore add to the

A

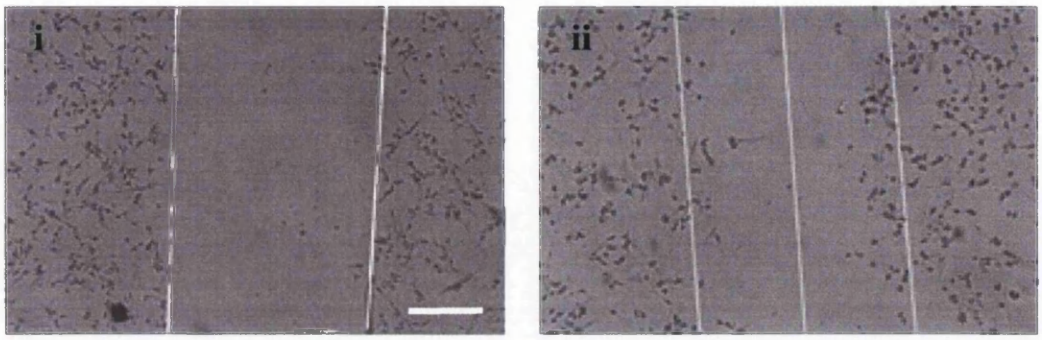

B

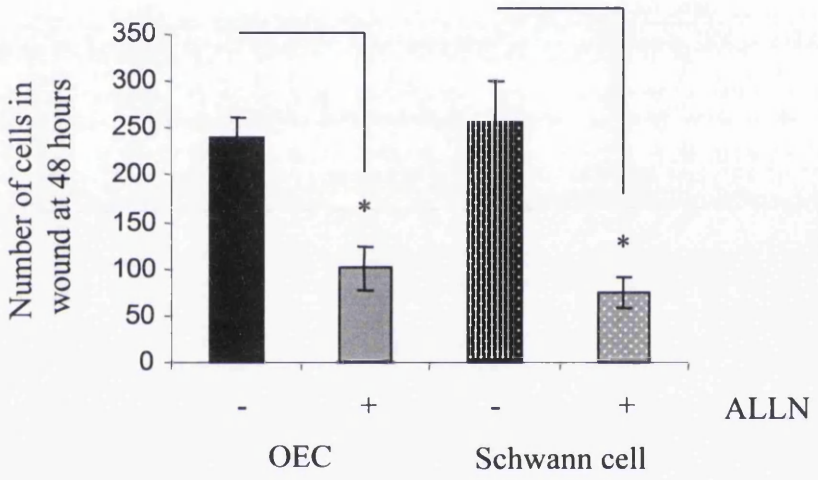

Figure 3.11. ALLN treatment significantly decreases the number of OECs and Schwann cells migrating into a wound.

(A) Phase contrast images demonstrating the projection of wound divisions to allow quantification of cells migrating into the wound space. Defined boundary edges (based on average wound size of 246.4 +/- 12.7 μm, n=6) were overlaid onto images, and the numbers of cells which migrated into this space were counted. (i) OECs immediately after wounding, and (ii) OECs 4 hours after wounding demonstrating migrating cells into wound area. Scale bar = 100 μm. (B) Quantification of number of cells migrating into scratch wound. A significant decrease in OECs and Schwann cells migrating into the wound was seen after ALLN treatment (48 hours). *$p<0.01$, n=6.

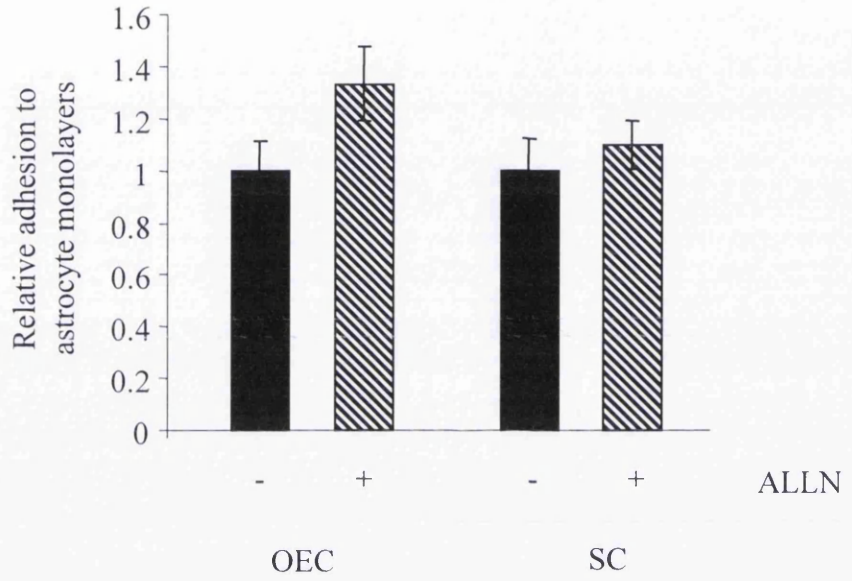

Figure 3.12. Calpain inhibition does not significantly affect OEC or Schwann cell adhesion to astrocytes.

Relative adhesion of OECs and Schwann cells (SC) to astrocyte monolayers, both with and without treatment with a calpain inhibitor (ALLN). Adhesion was measured using the adhesion assay, whereby the number of Vybrant-labelled cells adhering to an astrocyte monolayer after 30 minutes were counted. n=6.

plethora of evidence that Schwann cells and OECs share many properties in common, despite being derived from developmentally distinct regions, the neural crest and olfactory placode respectively.

However, significant differences are also seen between the two cell-types when it comes to the nature of their interactions with astrocytes, as has been highlighted both *in vitro* and *in vivo*. Thus, the data showing that Schwann cells form distinct boundaries upon interaction with astrocytes, and induce characteristics typical of hypertrophy in astrocytes, whereas OECs intermingle freely with astrocytes, confirms the published literature (Lakatos et al., 2000, 2003; Plant et al, 2002). This boundary formation property of Schwann cells may well influence their ability to integrate within the astrocyte-rich CNS tissue after transplantation.

As previously mentioned at the beginning of this chapter (Section 3.1), OECs for these experiments were cultured in conditions favouring the spindle-shaped, Schwann cell-like phenotype rather than the flatter, astrocyte-like phenotype. Despite the fact that these OECs adopted a morphology very similar to the Schwann cell, which may suggest similar

migratory behaviour between them due to their shared polarity, they were still very different in function. This suggests that the cellular behaviour of the cells are probably not determined by their morphology alone, but may reflect more fundamental biological differences between them. However, how the astrocyte-like OEC behaves under the conditions of these assays still remains an interesting question.

3.3.2 Expression and localisation of proteins associated with migration and adhesion

These data indicate that there are no inherent structural problems with the abilities of OECs and Schwann cells to migrate and adhere since there were no obvious differences detected in the expression and localisation of proteins associated with focal adhesions, adherens junctions and the cytoskeleton. The deposition of ECM was also investigated, as this has been shown to promote integrin-mediated adhesion and subsequent integrin-dependent migration. These data suggest that Schwann cells do not have any inherent

defects to explain a lack of migration. In agreement with these results, it was found by time-lapse microscopy that Schwann cells could migrate as efficiently as OECs on PLL. This is also supported by the observation that Schwann cells are very polarised with respect to their direction of movement indicative of a motile phenotype. In contrast, the presence of distinct actin stress fibres might suggest a less migratory phenotype, resulting from stable adhesion to the substratum, where focal adhesions associated with these fibres are involved in long term anchorage rather than dynamic protrusion and traction processes at the cell front (Kaverina et al., 2002). Despite this, all three glial cells had similar fibres and suggest that these are unlikely to be mediating a functional difference between the cell types. Indeed, OECs and Schwann cells appeared more alike when compared to astrocytes, since they both had short, patchy adherens junctions, reflecting their polar morphologies. In addition, OECs and Schwann cells appeared to have secreted similar amounts of ECM, which was less than that produced by astrocytes. Cultured astrocytes have been previously described as sources of fibronectin and laminin (van der Laan et al., 1997), which may reflect a role for astrocytes in maintaining the cytoarchitecture of the CNS (Rutka et al., 1988). This further highlights the Schwann cell-like properties of the OECs used in these assays.

3.3.3 Regulatory pathways of migration and adhesion

Taken together, the migration data show that Schwann cell and OEC migration is regulated in a similar manner, requiring the efficient functioning of both MEK- and src-dependent pathways, as well as calpain regulation. This calpain dependency may reflect the similar dependency upon src, in that calpain and src may be acting on similar pathways, Indeed, calpain and src are both required for focal adhesion regulation, where src activity is necessary for calpain-mediated cleavage of focal adhesion components such as FAK (Carragher et al., 2001), leading to their disassembly. Differences were, however, observed in calpain-dependency for adhesion, although these were not statistically significant. The lack of effect of calpain inhibition, which would act to reduce adhesion turnover, was probably due to the higher degree of adhesion observed in Schwann cells, compared to OECs, to astrocytes. Since adhesion was already so high, and thus turnover probably very low, inhibition of calpain had no extra effect. OECs, however, exhibited a lower cellular adhesion capacity which might reflect a more dynamically regulated adhesion process.

Calpain inhibition, and therefore an increased stability of adhesion complexes, could therefore exert an effect. The low statistical significance in these experiments may be increased by using a higher concentration of inhibitor, or increased incubation time, although the parameters used were suitable for migration inhibition. Why would these be different in migration and adhesion? A key difference between migration and adhesion could be due to the dual role of calpain as a regulator of both integrin- and cadherin-mediated adhesion. Migration on PLL would require only integrin-mediated adhesion to ECM laid down by the cells, whereas adhesion to astrocytes would also involve both integrin and cadherin complexes. Both complexes are substrates for calpain (Covault et al., 1991; Bhatt et al., 2002; Rios-Doria et al., 2003) although they may be regulated differently.

3.3.4 Migration versus Adhesion

Despite the many similarities between OECs and Schwann cells, differences were apparent in their migration capacity, as assessed by time-lapse microscopy. Although OEC and Schwann cell migration is indistinguishable upon PLL, they demonstrate very different abilities upon astrocyte monolayers, where Schwann cells have greater adhesion than OECs and display less migration. The slower migration of Schwann cells on an astrocyte monolayer may reflect their strong adhesion to astrocytes. Cell migration is the result of many coordinated events involving changes in the actin cytoskeleton, as well as the controlled formation and dispersal of adhesion sites between cells and their substrates. Thus, since OECs adhere less strongly to astrocytes, this may be why they are able to migrate more freely upon astrocyte monolayers. Conversely, Schwann cells adhere much more strongly to astrocytes, providing an explanation of why they are more restricted in their ability to migrate on this substrate.

However, it can not be determined at present whether it is Schwann cell adhesion to themselves or to astrocytes which might be playing a greater role in restricting Schwann cell migration, as seen in the confrontation assay. Schwann cell:Schwann cell adhesions were greater than OEC:OEC adhesions, and may suggest that Schwann cells were not able to migrate away and be released from contact with other Schwann cells in order to enter astrocyte-rich areas. Conversely, Schwann cell:astrocyte adhesions were also greater than OEC:astrocyte adhesion, possibly implying that Schwann cells formed strong contacts

with the first astrocytes they encountered, impeding further migration. Since adhesion to astrocytes was greater than adhesion to other Schwann cells, the latter is probably playing a more inhibitory function.

Different conclusions from mine have been drawn from time-lapse studies of Schwann cell migration upon astrocyte monolayers when the total distance moved was measured, rather than speed (Lakatos et al., 2000). Here Schwann cells and OECs had similar migration profiles. Other researchers have also reported an ability of Schwann cells to migrate over the surface of astrocytes (Franklin and Blakemore, 1995; Baron von Evercooren et al, 1996), although not through them (Xu et al., 1996; Iwashita et al., 2000). This supports the idea that migration upon astrocytes is fundamentally different from migration through astrocyte-rich areas.

One possible explanation for this is that although Schwann cell migration may be slowed down significantly upon astrocyte monolayers, with enough time they are still able to travel some distance. In contrast, migration through an astrocytic environment also requires the space to move into. Alternatively, if repulsive cues are presented by astrocytes, then cells in a confrontation assay would be restricted from entering the astrocyte domain. However, cells plated upon an astrocyte monolayer could respond by migrating away from this astrocyte contact, only to form new contacts with astrocytes, eventually reaching an astrocyte patch that may be expressing fewer of these signals. In addition, the reactive response of astrocytes to Schwann cells may provide a greater physical barrier to their migration, an effect not apparent when Schwann cells migrate upon a monolayers. This is supported by the lack of migration observed by both OECs and Schwann cells when transplanted into intact and uninjured tissue (Iwashita et al., 2000; Lakatos et al., 2003a), where they both may not have had any room to move. In contrast, cells injected into injured tissue were able to migrate further (Li and Raisman, 1994; Ramon-Cueto et al., 1998). For this reason, although the migration assay can give a lot of information regarding adhesion and migration, the confrontation assay was felt to be a better assay for modelling interactions with astrocytes in a way that best reflected the transplantation scenario.

3.3.5 Schwann cell invasion versus migration

The degree to which Schwann cells can actually migrate within the CNS is still an area of controversy. Many researchers have reported an inability of Schwann cells to migrate within astrocyte-rich areas, both *in vitro* (Wilby et al., 1999; Lakatos et al., 2000) and *in vivo* (Ramon-Cueto et al., 1998; Iwashita et al., 2000; Plant et al., 2001). However, upon disruption to the glia limitans, Schwann cells from the peripheral nerves beyond the dorsal root entry zone can invade the CNS environment of the spinal cord very easily (Bruce et al., 2000), although this tissue is typically damaged. Transplanted Schwann cells have also been shown to migrate within the CNS in some experiments (Brook et al., 1993; Li and Raisman, 1994), although due to the identification of these cells by expression of $p75^{NTR}$, it was not possible to confirm that these cells were all of transplant origin. In addition, upon transplantation of peripherally derived OECs into the injured CNS, endogenous Schwann cells were recruited to the site of injury by the transplanted cells (Ramer et al., 2004a). It is for these reasons that better labelling techniques are being developed to distinguish the repair attributed to the transplanted cells themselves, and that resulting from endogenous glia (Lee et al., 2004). Why in some instances Schwann cells can migrate within the CNS, and in others they can not is not fully understood. Since the migration observed for transplanted Schwann cells occurred predominately along blood vessels, epydyma and meninges (Brook et al., 1993; Baron van Evercooren et al., 1994, 1996; Li and Raisman, 1994), it has been speculated that endogenous Schwann cells which invade the CNS may also be migrating along these pathways, thus actually avoiding direct contact with astrocytes.

Despite the controversy, when comparing Schwann cell and OEC compatibilities with astrocytes, using both *in vitro* confrontation assays (which test the ability of cells to migrate through astrocytes) and migration assays (which test the ability of cells to migrate upon astrocytes), clear differences are apparent. These suggest fundamental differences in the biology of these glia which are of interest, both in improving our understanding of these cells and determining which might be the superior candidate for transplantation, but also in understanding possible regulatory mechanisms involved in the inhibition of transplant cell migration.

3.3.6 Conclusions

It remains to be seen what the molecular mechanisms are that govern the different OEC and Schwann cell migratory and adhesive potentials when in contact with astrocytes. Adhesion strength appears to be a key process, as demonstrated by the adhesion assay, where migratory differences may result from the greater Schwann cell adhesion to astrocytes. This appears to be supported by the lack of migratory defects seen on PLL, where Schwann cells possessed a motile phenotype and were capable of migration speeds equivalent to OECs.

In addition, the mechanism by which Schwann cells induce hypertrophy in astrocytes may also be important. Reactive astrocytes were observed only in Schwann cell:astrocyte confrontation assays and not in OEC:astrocyte cultures, also confirming the published literature (Ghirniker and Eng, 1994; Lakatos et al., 2000; Plant et al., 2001). What causes this differential reactivity, and also the degree to which it influences subsequent Schwann cell-astrocyte interactions, remains unanswered. It could be that enlarged astrocytes, resulting from initial Schwann cell-astrocyte interactions, provide a greater adhesive substrate for Schwann cells, thus restricting their migration away from this junction.

In order to answer these questions, Chapter 4 will focus more on the role of adhesion molecules in Schwann cells and OECs, with particular emphasis on their interactions with astrocytes. In particular, the role of the adhesion molecule N-cadherin will be assessed. In Chapter 5, I will investigate in more detail the astrocytic response, and how this contributes to the varying abilities of OECs and Schwann cells to migrate within astrocytic areas.

CHAPTER 4

N-cadherin differentially determines Schwann cell and OEC interactions upon contact with astrocytes

4.1 Introduction

It was shown in the previous chapter that Schwann cells and OECs are similar in their ability to migrate upon PLL-coated substrates, and in their expression of molecules associated with the processes of migration and adhesion. However, they differ in the way they interact with astrocytes, where Schwann cell, but not OEC, migration was reduced upon astrocytes. In addition, Schwann cells were shown to have stronger adhesions than OECs to both astrocytes and to themselves.

It has been previously suggested that the restriction of Schwann cell migration into astrocyte-rich regions may be mediated by contact inhibition, perhaps via N-cadherin. This was borne out by the experiments of Wilby et al (1999), where an N-cadherin inhibitory peptide blocked the adhesion and increased the migration of Schwann cells on astrocyte monolayers. Since OECs migrate more extensively within an astrocyte environment than Schwann cells, it was originally suggested that OECs may lack N-cadherin, although this has been proved not to be true, by both immunocytochemistry and immunoblotting (Figure 3.3 and 4.1; also Lakatos et al., 2000).

Thus the role of N-cadherin in both Schwann cell and OEC migration and adhesion requires further investigation. Specifically, I have addressed by precise molecular intervention whether i) N-cadherin is present and similarly functional in both OECs and Schwann cells and ii) if silencing N-cadherin using RNA interference (RNAi) has similar, or distinct, biological effects on the interactions of the two glial cells with astrocytes *in vitro*.

4.2 Results

4.2.1 N-cadherin is the major cadherin molecule for Schwann cells, OECs and astrocytes

To confirm previous data that N-cadherin was present on OECs and Schwann cells, immunoblotting was performed using lysates from astrocytes, OECs and Schwann cells. N-cadherin levels were similar for all three cell types, compared to total protein concentration (Figure 4.1A). To assess whether N-cadherin was forming functional adherens junctions,

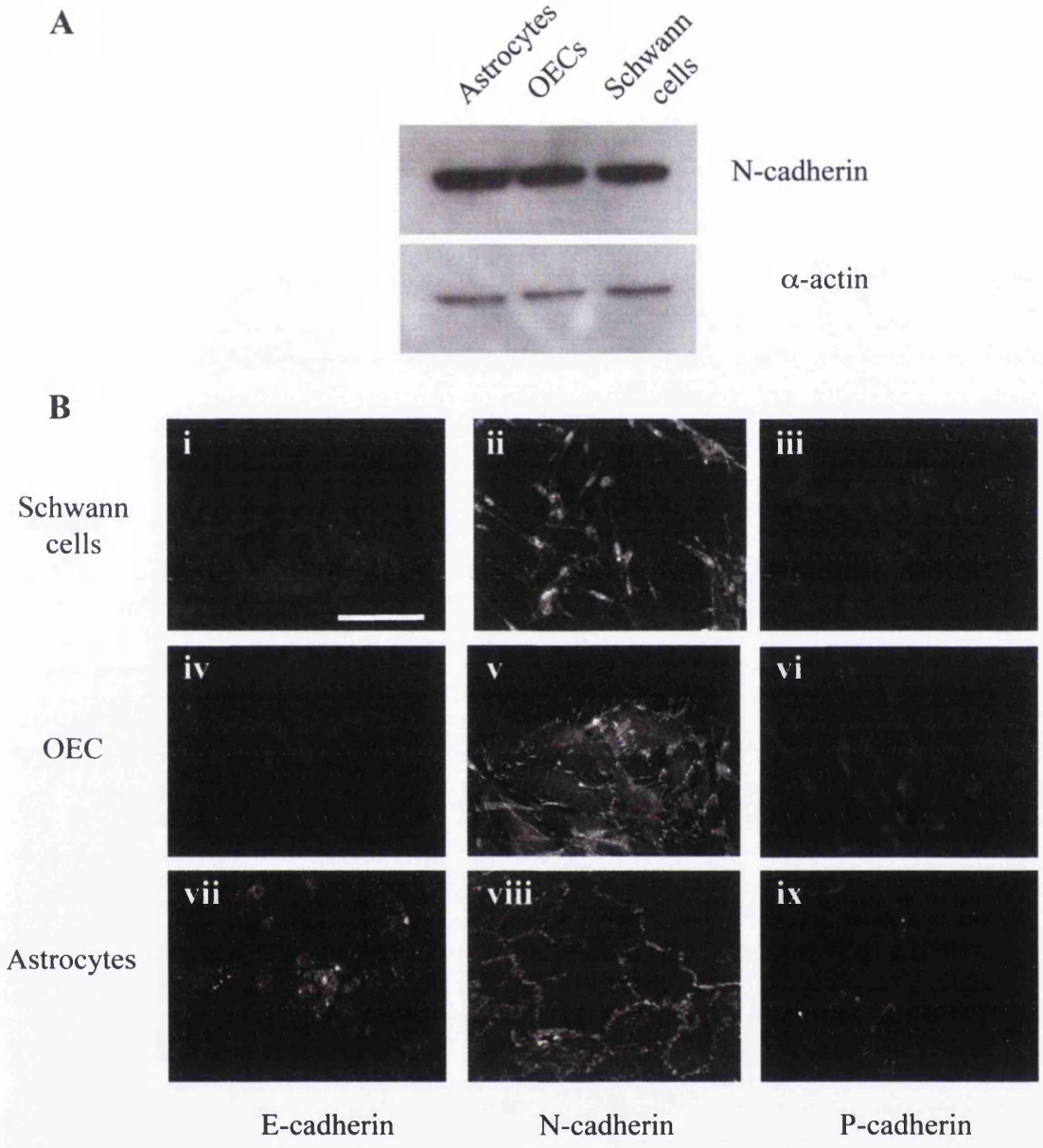

Figure 4.1. Astrocytes, OECs and Schwann cells all express N-cadherin to similar levels

(A) Immunoblot showing N-cadherin levels in the different glial cells, with α-actin loading control. (B) Immunocytochemsitry showing no redundancy in expression of the classical cadherins, since they all express N-cadherin (ii, v, viii) but not E- (i, iv, vii) or P-cadherin (iii, vi, ix). Scale bar = 100 μm.

cellular localisation and Ca^{2+} dependency was monitored by immunofluoresence. Ca^{2+} is necessary for the rigidification of N-cadherin ectoderms, which promote stable interactions between both trans and cis N-cadherin molecules (Figure 1.4), and thus modulation of Ca^{2+} concentration can be used to monitor if cadherins are functional with regards to cell-cell contacts (Nagar et al., 1996; Steinberg and McNutt, 1999). In all three glial cell types, cell-cell junctions were seen, and N-cadherin was clustered between opposing cells (Figure 4.2). Upon reducing Ca^{2+} from 1 mM (high Ca^{2+}, Figure 4.2A, C and E) to 0.03 mM (low Ca^{2+}, (Figure 4.2B, D and F) for 4 hours, the junctions disassembled and N-cadherin was no longer visible at regions of contact. Schwann cells in low Ca^{2+} appeared to have dispersed N-cadherin on the cell surface and the cells lost their highly polar alignment, becoming disorganised in appearance.

Immunocytochemistry against E-cadherin and P-cadherin demonstrated that all three glial cell types did not express either of these cadherin family members, indicating that these cadherins could not provide similar functions with regard to contact formation between glial cell-types (Figure 4.1).

Since N-cadherin junctions between both Schwann cells and OECs, were not typical in morphology of classic cadherin junctions, being only visible on small localised areas of cell surface where contact was visible (Figure 4.1; see also Figure 3.3), immunocytochemistry was performed on cells which had been plated down on PLL for only 1 hour. The reason for this was that these cells retained a morphology which was very similar to epithelial and Madin-Darby Canine Kidney (MDCK) cells, in whom cadherin function (E-cadherin) has been well characterised (Price et al., 2004; Boucher et al., 2005). At this time point, Schwann cells and OECs were still very rounded and had just begun to adhere to the substrate, thus resembling epithelial cells. N-cadherin immunolabelling of these cells showed cell-cell junctions (Figure 4.3; arrows) which were shorter and rounder, and therefore resembled classic epithelial E-cadherin junctions, indicating that they may be similarly functional.

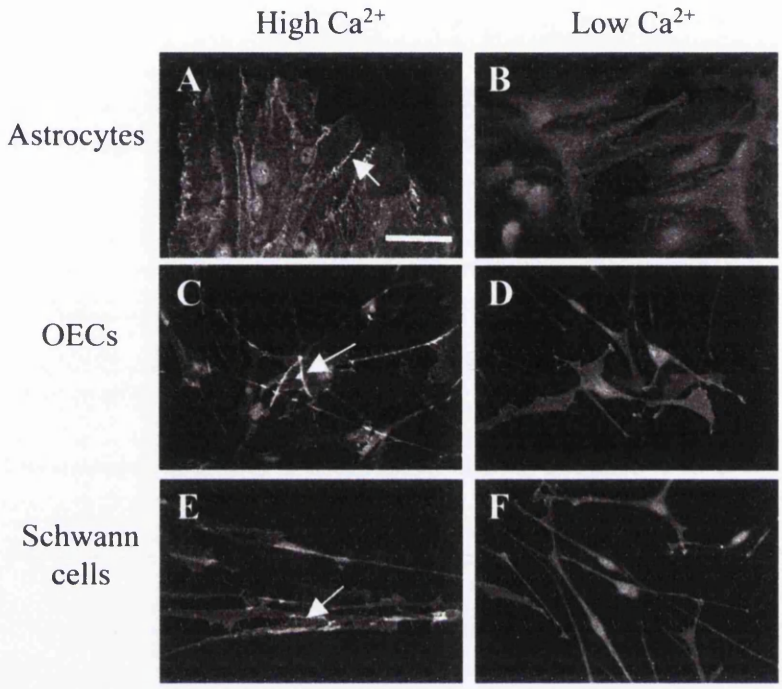

Figure 4.2. Astrocytes, OECs and Schwann cells form Ca^{2+} dependent N-cadherin junctions.

Astrocytes (A, B), OECs (C, D) and Schwann cell (E, F) in the presence of high (1 mM; A, C, E) and low (0.03 mM; B, D, F) Ca^{2+} were immunolabelled for N-cadherin. In high Ca^{2+}, these junctions were clearly formed (arrows), but upon reducing the level of Ca^{2+} the junctions began to breakdown, with an apparent loss of Schwann cell alignment. Scale bar = 100 μm.

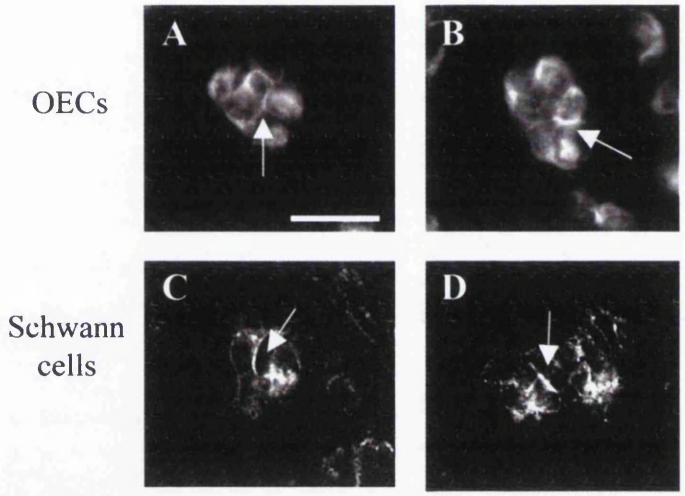

Figure 4.3. OECs and Schwann cells can form cadherin junctions with typical morphologies.

N-cadherin junctions in OECs (A, B) and Schwann cells (C, D) were analysed by immunolabelling 1 hour after initial plating on laminin (A, C) and fibronectin (B, D). At this time point, when they had just started to sit down their adherens junctions had morphologies typical of the classical E-cadherin junctions of epithelial cells. Scale bar = 50 μm.

4.2.2 N-cadherin turnover is similar in OECs and Schwann cells

Since the N-cadherin present on Schwann cells and OECs was indistinguishable in terms of its localisation and Ca^{2+} dependency, a potential difference could be its turnover within the cell. In order to measure the lifetime of N-cadherin from protein synthesis until it was degraded, emetine, a protein synthesis inhibitor, was added to Schwann cell and OEC cultures, and lysates made at regular time intervals. As for the calpain inhibitor, the optimal working concentration was chosen following titration and cell viability assessment (see Section 3.2.6). Based on this, a working concentration of 10 μM was selected. Emetine treatment allowed the persistence of N-cadherin following a block in its production to be measured and compared. For both Schwann cells and OECs, N-cadherin persisted in cells for almost 24 hours following protein synthesis inhibition, before levels began to decrease (Figure 4.4). This was in contrast to the lifetime of actin, which had started to decrease in Schwann cells and OECs at 4 hours, and was almost completely degraded by 8 hours. This data suggests N-cadherin turnover occurs at a similar rate in both Schwann cells and OECs.

4.2.3 N-cadherin is localised to heterotypic junctions

To determine if N-cadherin is involved in the interaction of Schwann cells or OECs with astrocytes, the localisation of N-cadherin was examined in junctions between the different glial cell types. Using immunocytochemistry, where all cells are identified by nuclear DAPI staining and astrocytes were identified by their intense fibrous glial fibrillary acidid protein (GFAP) immunoreactivity, the localisation of N-cadherin was examined (Figure 4.5). N-cadherin-associated junctions were visible between cells of the same type (homo-typic junctions, Figure 4.5A, B and C, broken arrows), and between different cell types (hetero-typic junctions, Figure 4.5D and 4.5E, unbroken arrows). These data suggest that both Schwann cells and OECs are capable of forming cadherin-associated inter-cellular contacts at their interface with astrocytes.

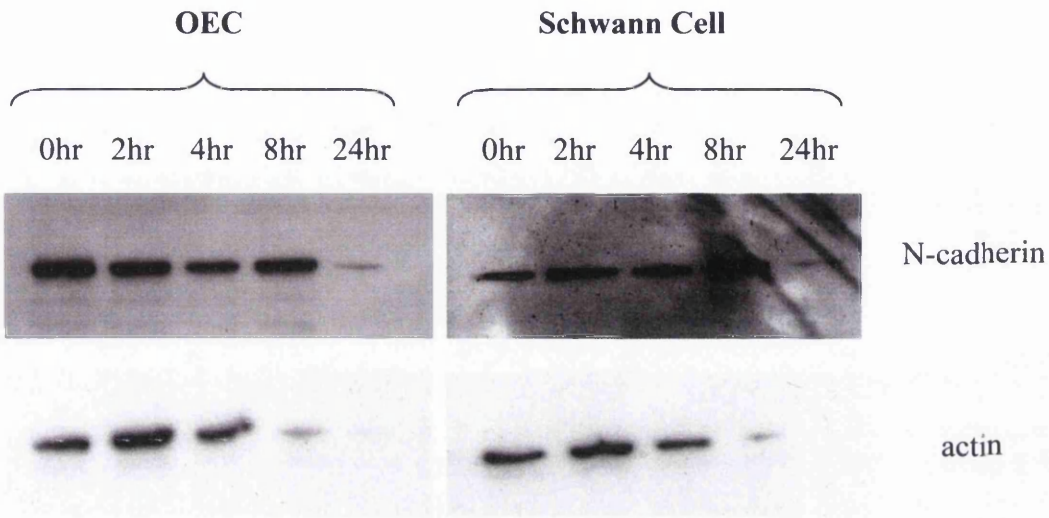

Figure 4.4. N-cadherin protein turnover is equivalent in both OECs and Schwann cells.

Western blot of N-cadherin and actin protein levels at 0, 2, 4, 8, and 24 hour time intervals following emetine (protein synthesis inhibitor) treatment.

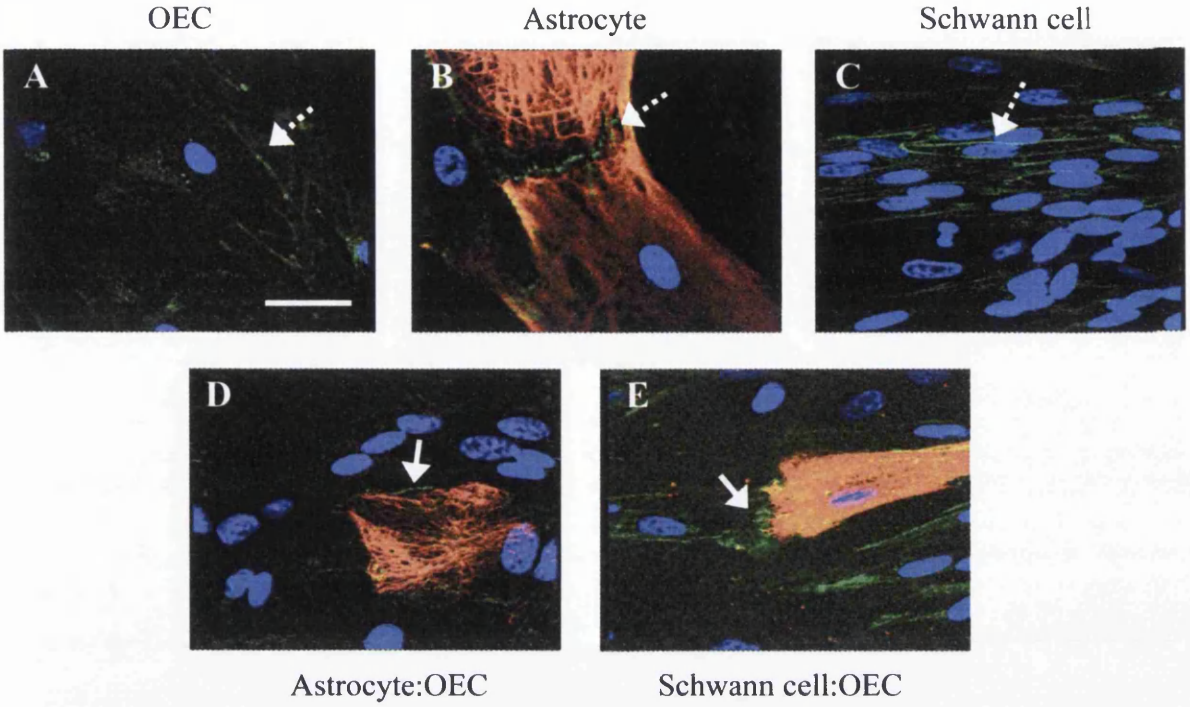

Figure 4.5. Both OECs and Schwann cells can form hetero-typic N-cadherin junctions to astrocytes, as well as homo-typic junctions.

OECs and Schwann cells were co-cultured for several days with astrocytes and then immunolabelled for GFAP (TRITC) denoting astrocytes, and N-cadherin (FITC). Nuclei were visualised with DAPI (blue). Distinct junctions were visualised between cells of the same type (OECs, A; astrocytes, B; Schwann cells, C; broken arrows), and also between different types (astrocyte:OEC, D; astrocyte:Schwann cell, E; unbroken arrows). Scale bar = 50 μm.

4.2.4 Cyclic peptide inhibition of N-cadherin

4.2.4.1 A cyclic peptide inhibitor of N-cadherin reduced Schwann cell, but not OEC adhesion

In order to assess the function of N-cadherin in Schwann cell and OEC interactions with astrocytes, a cyclic peptide inhibitor of N-cadherin was initially used. This contains the common cadherin cell adhesion recognition sequence motif, His-Ala-Val (HAV; Williams et al., 1999). An adhesion assay was performed where Vybrant-labelled OECs and Schwann cells were incubated on confluent glial monolayers, and cells that adhered were counted, in the presence and absence of the peptide inhibitor. Addition of the inhibitor reduced Schwann cell adhesion to both astrocytes (1222 +/- 145 to 864 +/- 56, $p>0.04$; Figure 4.6A) and to a confluent monolayer of Schwann cells (881.5 +/- 73 to 445 +/- 22, $p>0.05$). This effect, though modest, was statistically significant. However, the peptide had no significant effect on OEC adhesion to either astrocytes or to confluent monolayers of OECs. As was seen in the previous chapter (Figure 3.7), Schwann cells had stronger adhesions than OECs to both themselves and astrocytes (homo- and hetero-typic), and both Schwann cells and OECs adhered more strongly to astrocytes (hetero-typic) than themselves (homo-typic). These data imply that N-cadherin mediates the adhesion of Schwann cells, but not OECs, to themselves and to astrocytes.

4.2.4.2 A cyclic peptide inhibitor did not affect boundary formation

The role N-cadherin played in the development of boundaries was assessed using the confrontation assay (see Section 3.2.1), in which parallel strips of either OECs or Schwann cells were plated facing astrocytes. These were allowed to proliferate and migrate towards each other, both with and without the N-cadherin peptide inhibitor, and their resulting interactions visualised. The peptide inhibitor was added to the cultures at 2 day intervals over the 10 day period of the assay. The addition of the peptide inhibitor had no effect on either Schwann cell or OEC interactions with astrocytes (Figure 4.6C and 4.6E).

The difference in peptide inhibition seen between the adhesion assay and the confrontation assay may reflect the peptide's mode of action and also differences in the time course or

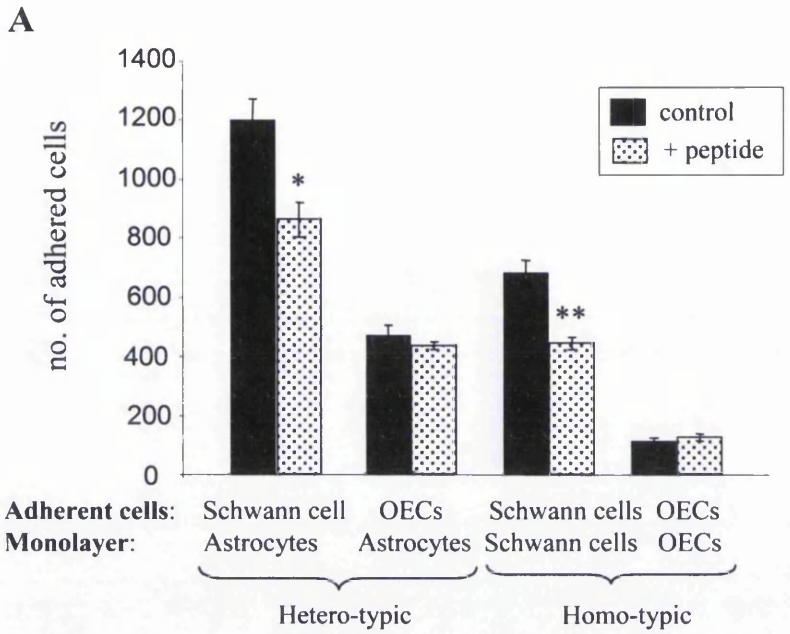

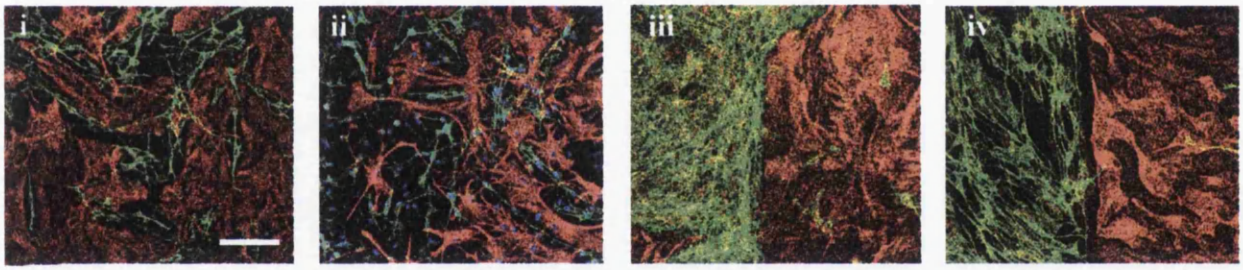

Figure 4.6. Cyclic peptide inhibitor of N-cadherin reduces Schwann cell adhesion to astrocytes, but did not affect boundary formation.

(A) An adhesion assay was performed using Vybrant labelled cells to aid detection, and were left to adhere to confluent monolayers of either astrocytes or OECs/Schwann cells for 30 minutes. Schwann cell adhesion was reduced to both astrocytes (*$p<0.05$) and Schwann cells (**$p<0.02$), n=6. OEC adhesion was unaffected by the presence of the peptide inhibitor. (B) Confrontation assays, where a strip of either OECs (i, ii) or Schwann cells (iii, iv) were allowed to grow towards a strip of astrocytes and the resulting interactions analysed by immunocytochemistry. The peptide inhibitor was added (ii, iv) at a concentration of 10 μg/ml and supplemented every two days over the duration of the assay. After addition of the peptide, a boundary still formed between Schwann cells and astrocytes, whereas OECs migrated amongst the astrocyte domain. Astrocytes are immunolabelled for GFAP (TRITC), and Schwann cells and OECs for $p75^{NTR}$ (FITC). Scale bar = 100 μm.

duration of the assays. The adhesion assay is a short term assay lasting only 30 minutes, whereas the confrontation assay takes longer, occurring over several days. Although the peptide can reversibly inhibit dynamic N-cadherin junctions during their formation, as measured in the adhesion assay, it might not be able to actively disrupt stable junctions after they have formed. Thus over the time scale of the confrontation assay, these more stable adhesions might still accumulate. For this reason, a more precise method of N-cadherin inhibition by preventing protein synthesis using RNAi technology was used.

4.2.5 RNA interference

4.2.5.1 RNAi reduced N-cadherin expression in Schwann cells and OECs

To clearly define the role of N-cadherin in these cellular interactions, the expression of N-cadherin in Schwann cells and OECs was reduced using linear, double-stranded small inhibitory RNA (siRNA). siRNA transfection leads to the degradation of RNA with complementary coding sequences. In this way, sequence-specific gene silencing can be performed (Elbashir et al., 2001a, 2001b). Introduction of siRNA against N-cadherin (Ncad siRNA) and a scrambled sequence (scramble siRNA) was carried out using two different protocols (FuGENE and Oligofectamine) to test efficiency. Forty-eight hours after transfection with siRNA, protein lysates were made and immunoblotting performed to assess the reduction in steady-state levels of N-cadherin. For both transfection protocols, N-cadherin was reduced by Ncad siRNA, but was unaffected by scramble siRNA (Figure 4.7A). However, a complete reduction in N-cadherin protein levels was not always achieved, presumably reflecting the variable transfection efficiency.

Immunocytochemistry was performed to visualise N-cadherin expression after siRNA transfection (Figure. 4.7B). Due to the nature of Schwann cell and OEC junctions, which are only visible on small, localised areas of cell-cell contact (Figure 3.3), it was difficult to quantitatively judge the absence of junctions, although disruption was clearly seen (Figure 4.7Biv and v). However, in astrocytes, Ncad siRNA-induced disruption of N-cadherin junctions in large areas of the culture was clearly visible (Figure 4.7Bvi). This is because astrocytes have a larger contact area with which N-cadherin junctions can form with other astrocytes (Figure 3.3). Junctions were not absent on all astrocytes, reflecting the

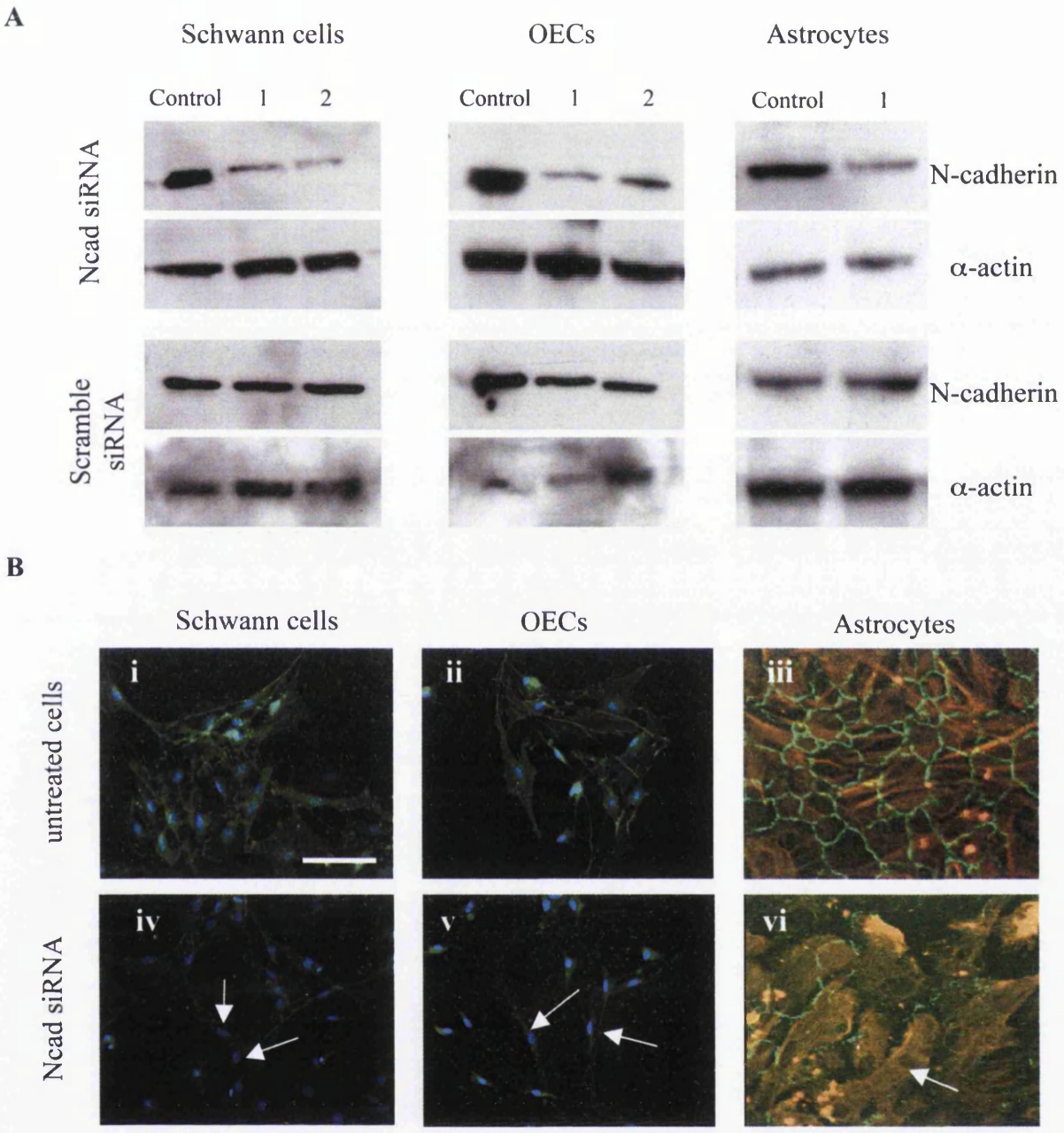

Figure 4.7. Ncad siRNA reduces N-cadherin expression in glial cells.

(A) Western blot demonstrates a reduction in N-cadherin expression following transfection with N-cadherin specific siRNA (Ncad siRNA) using both oligofectamine (lane 1), and FuGENE (lane 2). Control (untreated) cells and cells transfected with scrambled siRNA expressed similar levels of N-cadherin. (B) Immunocytochemistry for N-cadherin on Ncad siRNA-treated Schwann cells (iv), OECs (v) and astrocytes (vi) illustrated the reduction of N-cadherin on the cell surface in a proportion of cells, compared to untreated Schwann cells (i), OECs (ii) and astrocytes (iii). Cells were co-labelled with DAPI (Schwann cells and OECs) and GFAP (astrocytes). Scale bar = 100 μm.

transfection efficiency of the siRNA and the immunoblotting results. However, it was not independently confirmed which cells were transfected. One method to achieve this would be to transfect cells with vector-based siRNA. Thus, a vector encoding both siRNA and a reporter gene such as GFP, could simultaneously reduce protein expression and give information as to which cells were successfully transfected (Yoon et al., 2004, Kojima et al., 2004).

4.2.5.2 Effect of Ncad siRNA treatment on Schwann cell and OEC proliferation and migration

To assess if Ncad siRNA had any adverse biological effects on Schwann cells and OECs which could influence boundary formation and adhesion, their proliferation capacity was assessed using bromodeoxyuridine (BrdU) uptake. There was no significant change in the BrdU uptake of either OECs or Schwann cells after siRNA treatment (Figure 4.8). This data demonstrated that changes in cell proliferation could not explain any observed differences in cellular migration.As was noted in Chapter 3, Schwann migration was impeded upon astrocyte monolayers, when compared to migration upon PLL, whereas OEC migration was equivalent on both substrates (Figure 3.4). To investigate whether N-cadherin mediates these differences, OECs and Schwann cells were treated with Ncad siRNA and migration speeds on PLL and astrocyte monolayers were calculated. (Figure 4.9A and B). siRNA treatment had no significant effect on either OEC or Schwann cell migration upon PLL (OEC = 18.16 +/- 2.81 μm/hour, OEC siRNA = 19.23 +/- 2.52 μm/hour, SC = 19.56 +/- 3.08 μm/hour, SC siRNA = 20.78 +/- 7.86 μm/hour). However, differences were seen in migration speeds of cells plated on astrocyte monolayers. As shown in Figure 3.4, untreated Schwann cell migration was slower on astrocytes, when compared to untreated OECs migration on astrocytes (Figure 4.9B). Treatment with siRNA did not have a significant effect on OEC migration speeds (OEC = 21.6 +/- 2.17 μm/hour, OEC siRNA = 19.44 +/- 1.49 μm/hour), but there was an increase in Schwann cell migration on astrocyte monolayers (SC = 11.47 +/- 0.87 μm/hour, SC siRNA = 18.56 +/- 1.42 μm/hour). This difference may have been greater were it not for the case that not all cells take up siRNA after transfection, as seen in Figure 4.7. Therefore the average may under-represent the effect of Ncad siRNA. This is demonstrated in Figure 4.9B where the migration speeds of individual cells are plotted, showing a greater spread of migration speed

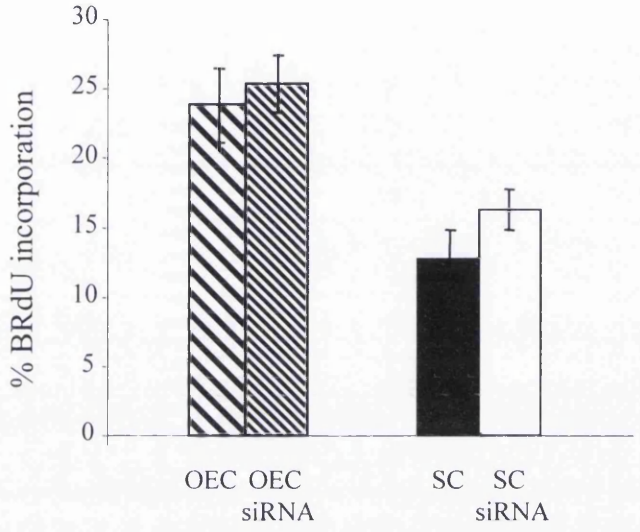

Figure 4.8. Ncad siRNA treatment does not affect OEC and Schwann cell proliferation.

BrdU incorporation into OECs and Schwann cells cultured in FCS, with and without Ncad siRNA treatment, was assessed using indirect immunoflourescence. siRNA treatment had no significant effect on proliferation as assessed by BrdU. n=6.

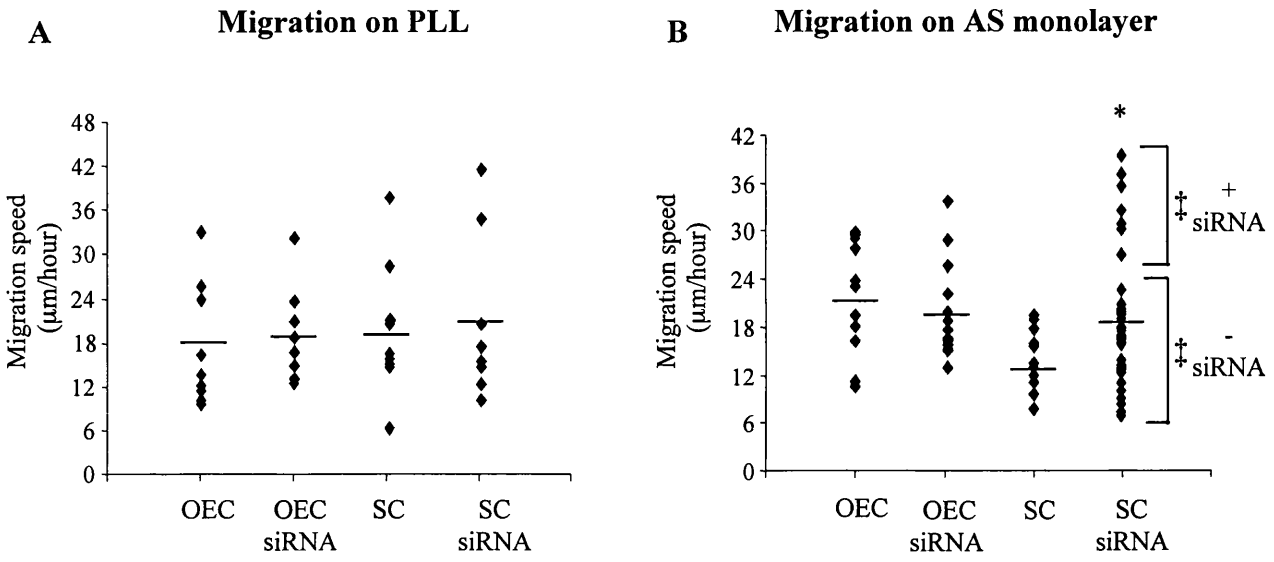

Figure 4.9. Ncad siRNA treatment increases Schwann cell migration upon astrocyte monolayers.

Migration on PLL (A) and on astrocyte (AS) monolayers (B) were measured by time-lapse microscopy, both with and without Ncad siRNA treatment. The individual migration speeds were plotted, along with the median for each set. Following siRNA treatment, there was no change in the observed migration speeds of either OECs or Schwann cells on poly-l-lysine. OEC migration upon an astrocyte monolayer was unaffected by siRNA treatment, but for Schwann cells, a proportion of the population of treated cells were able to migrate much faster (*$p<0.01$). This proportion reflects the transfection efficiency seen in Fig. 4.7.

‡ - possible population clustering

compared to the untreated set. This spread appears to reflect the transfection efficiency with siRNA (Figure 4.7) where a proportion of successfully transfected cells may be exhibiting the more migratory phenotype. This, however, could not be confirmed due to the lack of direct detection of which cells had successfully incorporated siRNA. However, even when the 2 populations are averaged, the difference in mean migration speeds between the untreated and the siRNA-transfected sets is significant, $p<0.01$. Thus, N-cadherin may mediate the slower migration speeds of Schwann cell on astrocytes, compared to OECs or to their migration on PLL.

4.2.5.3 Ncad siRNA treated Schwann cells, but not OECs, have reduced adhesion

To assess if N-cadherin mediates heterotypic adhesion (to astrocytes) and homotypic adhesion (to themselves) using an adhesion assay (Figure 4.10), Schwann cells and OECs were transfected with Ncad siRNA. Untreated cells and cells transfected with a scrambled siRNA sequence were used as controls, and yielded similar results to each other. OECs treated with Ncad siRNA adhered to astrocytes and OECs to a similar extent as controls. Thus, reducing expression of N-cadherin in OECs did not alter either hetero-typic or homo-typic adhesion. In contrast, adhesion of Schwann cells to both monolayers of astrocytes (4 fold decrease, $p<0.001$) and Schwann cells (5.5 fold decrease, $p<0.002$) was significantly reduced by N-cadherin siRNA treatment. These data indicate that Schwann cells but not OECs were dependent upon N-cadherin for homotypic and heterotypic cell-cell adhesion, in agreement with the N-cadherin peptide inhibitor results (Figure 4.6A). These data support N-cadherin mediation of cellular adhesion for Schwann cells, but not OECs, despite the latter expressing similar levels of N-cadherin, and suggest that the function of N-cadherin is different between the two cell types.

4.2.5.4 Ncad siRNA treated Schwann cells no longer form boundaries when in contact with astrocytes

To determine if N-cadherin plays a role in the formation of a cellular boundary between astrocytes and Schwann cells or OECs in confrontation assays, Ncad siRNA was used to transfect OECs and Schwann cells, and the subsequent boundary formation assessed.

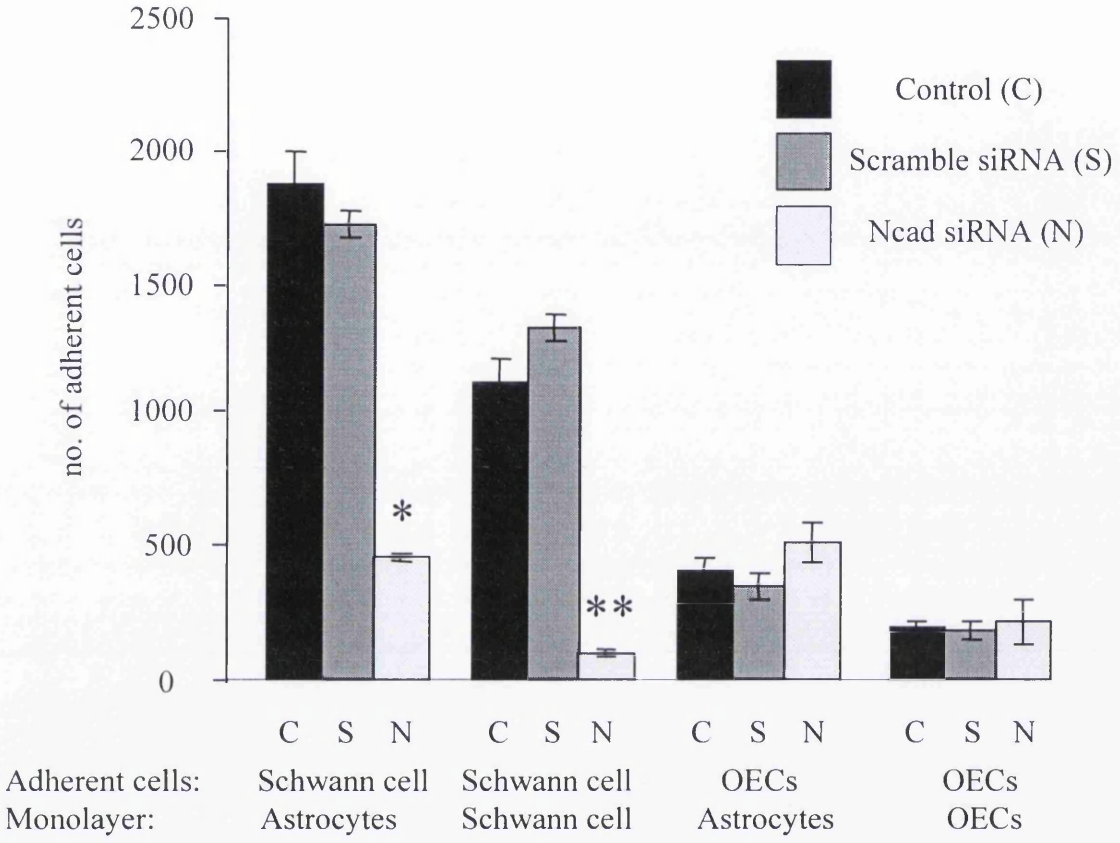

Figure 4.10. siRNA treatment reduces Schwann cell, but not OEC, adhesion.

An adhesion assay was performed using untreated, scramble RNAi-transfected and N-cadherin RNAi-transfected OECs and Schwann cells. These cells were Vybrant labelled to aid detection and left to adhere to a confluent monolayer of either astrocytes or OECs/Schwann cells. N-cadherin siRNA reduced Schwann cell adhesion to both astrocytes (*$p<0.001$) and Schwann cells (**$p<0.002$), whereas adhesion of OEC to both astrocytes or OECs was unaffected. n=6.

Confrontation assays were also performed using untreated and scramble siRNA-treated Schwann cells and OECs as controls (Figure 4.11A). Treatment with scramble siRNA did not affect the intrinsic properties of the glial cells, where Schwann cells, but not OECs, still formed boundaries against astrocytes. In contrast, Schwann cells treated with Ncad siRNA no longer formed these boundaries (Figure 4.11Aix and x), and instead intermingled with astrocytes in a similar manner to OECs. This was quantified by counting the number of Schwann cells crossing the astrocyte-Schwann cell boundary into the astrocyte domain (Figure 4.11B). For Schwann cell/astrocyte cultures there was an increase in the number of cells after Ncad siRNA treatment (22 +/- 1.75; $p<0.01$), compared to control levels (untreated = 4.33 +/- 0.76 cells, scramble siRNA treated = 5.33 +/- 0.76 per 300 μm boundary). Ncad siRNA-treated OECs, behaved as untreated OECs, migrating amongst astrocytes. These data demonstrate a role for N-cadherin in the formation of a cellular boundary between Schwann cell and astrocytes.

4.2.5.5 Ncad siRNA treatment of Schwann cells or OECs does not alter their hypertrophy-inducing properties, as measured by astrocyte area

Initial studies using co-cultures demonstrated that astrocyte area increases on contact with Schwann cells (Ghirniker and Eng, 1994; Lakatos et al., 2000). To assess if N-cadherin mediated this measurement of hypertrophy, the average area of astrocytes in contact with Schwann cells treated with siRNA (Figure 4.12) was calculated using NIH Image. The area of astrocytes in contact with Schwann cells, whether untreated or siRNA-treated, was increased two-fold, compared to astrocytes cultured in monolayers. This suggested that the treatment of Schwann cells with Ncad siRNA did not influence hypertrophy in these cultures as measured by astrocyte area, implying that regulation of these two glial properties may not be linked.

4.2.6 Downstream signalling from N-cadherin is unchanged between Schwann cells and OECs

Since N-cadherin functionality appears to be different between Schwann cells and OECs, as demonstrated by their different dependency upon N-cadherin for normal adhesion and migration (Figures 4.9 and 4.10), the next step was to investigate the regulation of N-

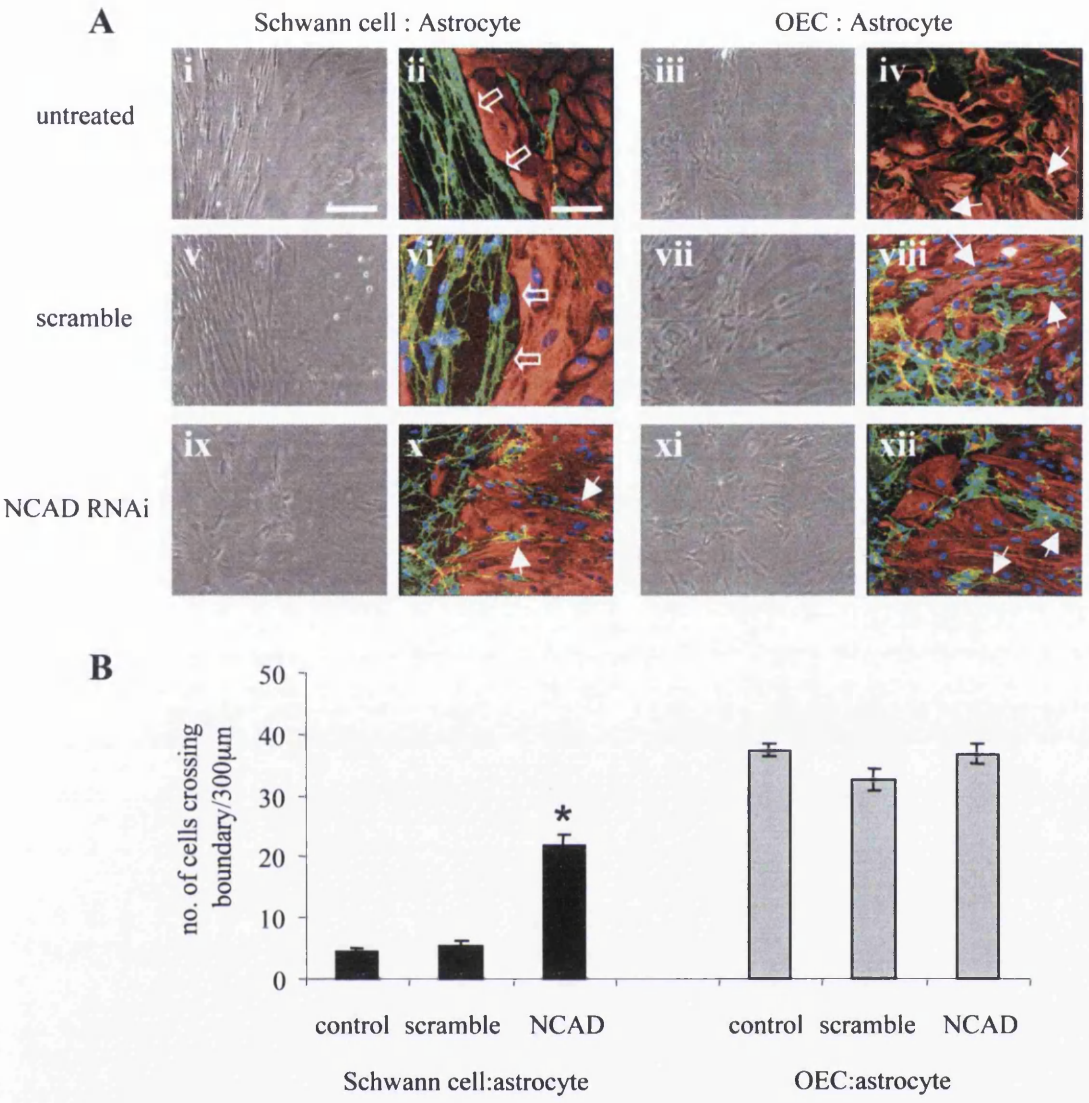

Figure 4.11. N-cadherin is required for Schwann cell/astrocyte boundary formation.

(A) Confrontation assays were performed with untreated (i to iv), scramble siRNA-treated (v to viii) and N-cadherin siRNA-treated (ix to xii) Schwann cells (i, ii, v, vi, ix, x) and OECs (iii, iv, vii, viii, xi,xii). Phase and confocal images (OECs and Schwann cells, $p75^{NTR}$-FITC; astrocytes, GFAP-TRITC) are of different fields of view. Schwann cells formed distinct boundaries against astrocytes in both untreated and scramble siRNA-treated cells (open arrows). However, N-cadherin siRNA-treated Schwann cells no longer formed boundaries but were able to intermingle with astrocytes, in a manner similar to OECs. OECs intermingled with astrocytes, whether untreated, scramble siRNA-treated, or N-cadherin siRNA-treated. Migrating cells indicated with solid arrows. Scale bar = 100 µm. (B) Quantification of the confrontation assays. The number of cells that crossed the boundary was significantly higher in Schwann cell/astrocyte confrontation assays when the Schwann cells were treated with the siRNA to N-cadherin (*$p<0.01$) but not scramble siRNA. n=6.

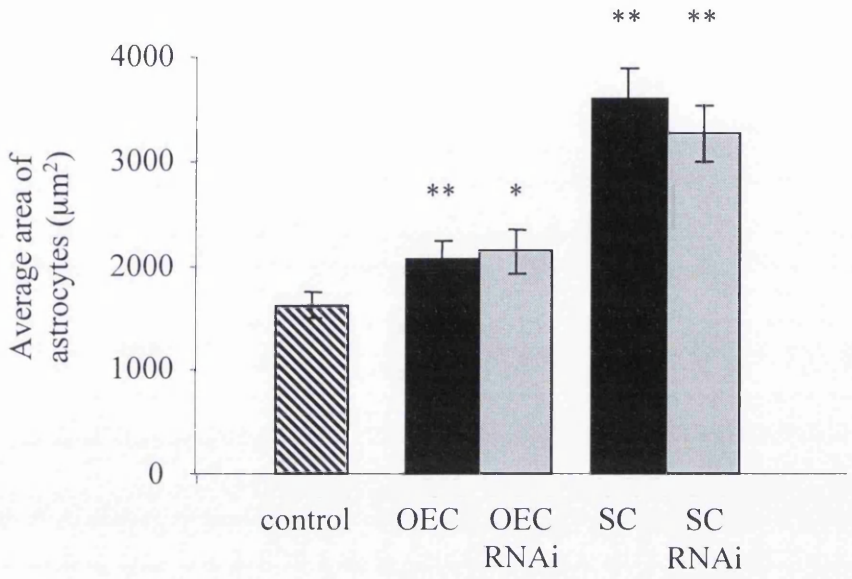

Figure 4.12. Ncad siRNA treatment does not affect astrocytic hypertrophy.

Astrocyte area was measured using NIH Image from astrocytes cultured alone (control), or co-cultured for 7 days with either OECs, OECs treated with N-cadherin siRNA, Schwann cells (SC), or Schwann cells treated with N-cadherin siRNA. Astrocyte area is increased a small amount upon co-culturing with OECs but is increased significantly when co-cultured with Schwann cells (two-fold increase; * $p<0.05$, ** $p<0.001$ compared to control). Treatment of cells with N-cadherin siRNA had no effect on this assessment of astrocyte hypertrophy (n=30).

cadherin by downstream regulators, with particular emphasis on members of the catenin family, β-catenin and $p120^{ctn}$. The catenins are immediate downstream regulators which connect N-cadherin to the actin cytoskeleton, and are therefore are suited to regulating N-cadherin-dependent migration and adhesion (see Introduction 1.6.2.3).

To assess if these downsteam candidate effectors were interacting with N-cadherin differently, immunoprecipitations were performed to measure the relative amounts of catenin bound to N-cadherin in Schwann cells and OECs, both when in mono-cultures and after co-culturing with astrocytes (Figure 4.13A). Co-cultured OECs and Schwann cells were removed from astrocyte monolayers with low levels of trypsin before making lysates to avoid astrocyte contamination. No visible difference in β-catenin or $p120^{ctn}$ co-precipitation with N-cadherin in Schwann cells and OECs was found, whether in cultures alone, or with astrocytes (Figure 4.13A). This, therefore, indicates no difference in catenin association with N-cadherin in either cell type. We also looked at the phosphorylation status of β-catenin in both mono- and co-cultures. Again, β-catenin was similarly phosphorylated in both Schwann cell and OEC cultures (Figure 4.13B). This reflects the lack of difference seen for catenin association, since phosphorylation is a mechanism for regulating cadherin-catenin interactions. Thus, at the immediate downstream level of N-cadherin regulation, there were no obvious differences which would readily explain the differences in N-cadherin functionality observed in earlier experiments.

4.2.7 Identification of N-cadherin interacting proteins

Since there was no apparent difference in catenin regulation of N-cadherin, a more general approach was taken to identify any possible candidates which may be differentially interacting with or regulating N-cadherin function. This was carried out by immunoprecipitating Schwann cell and OEC lysates with an anti-N-cadherin antibody, and staining all the co-precipitated proteins, after electrophoresis, with Brilliant Blue G-Colloidal (Figure 4.14A). N-cadherin is denoted with an asterisk. One major protein difference was apparent, marked with an arrow. In OEC cultures, both in mono- and co-culture with astrocytes, a protein with an approximate molecular weight of 54kDa was present. The band was excised from the gel and underwent Mass Spectrometry, identifying it as vimentin. Western blot analysis showed that vimentin was indeed present in OEC IPs

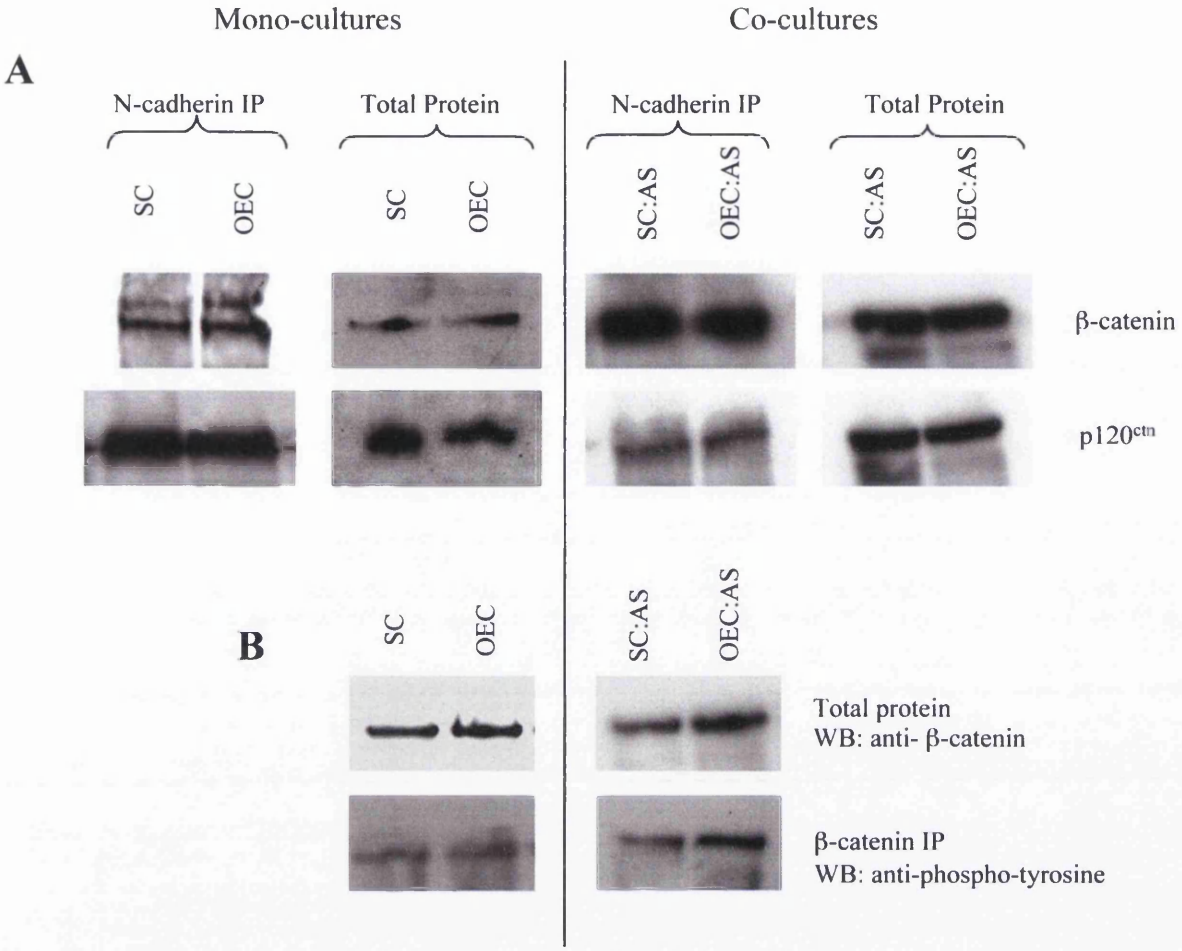

Figure 4.13. Catenin signalling is unchanged in OECs and Schwann cells following contact with astrocytes.

(A) Immunoprecipitation and Western blotting were performed to show β-catenin and p120^{ctn} levels (Total Protein) and their co-precipitation with N-cadherin (N-cadherin IP). This was carried out using Schwann cell (SC) and OEC lysates, as well as lysates made from cells which had been allowed to adhere to astrocytes for 30 minutes before trypsin treatment and generation of lysates (SC:AS and OEC:AS). (B) Phosphorylation of β-catenin was unchanged following adhesion to astrocytes.

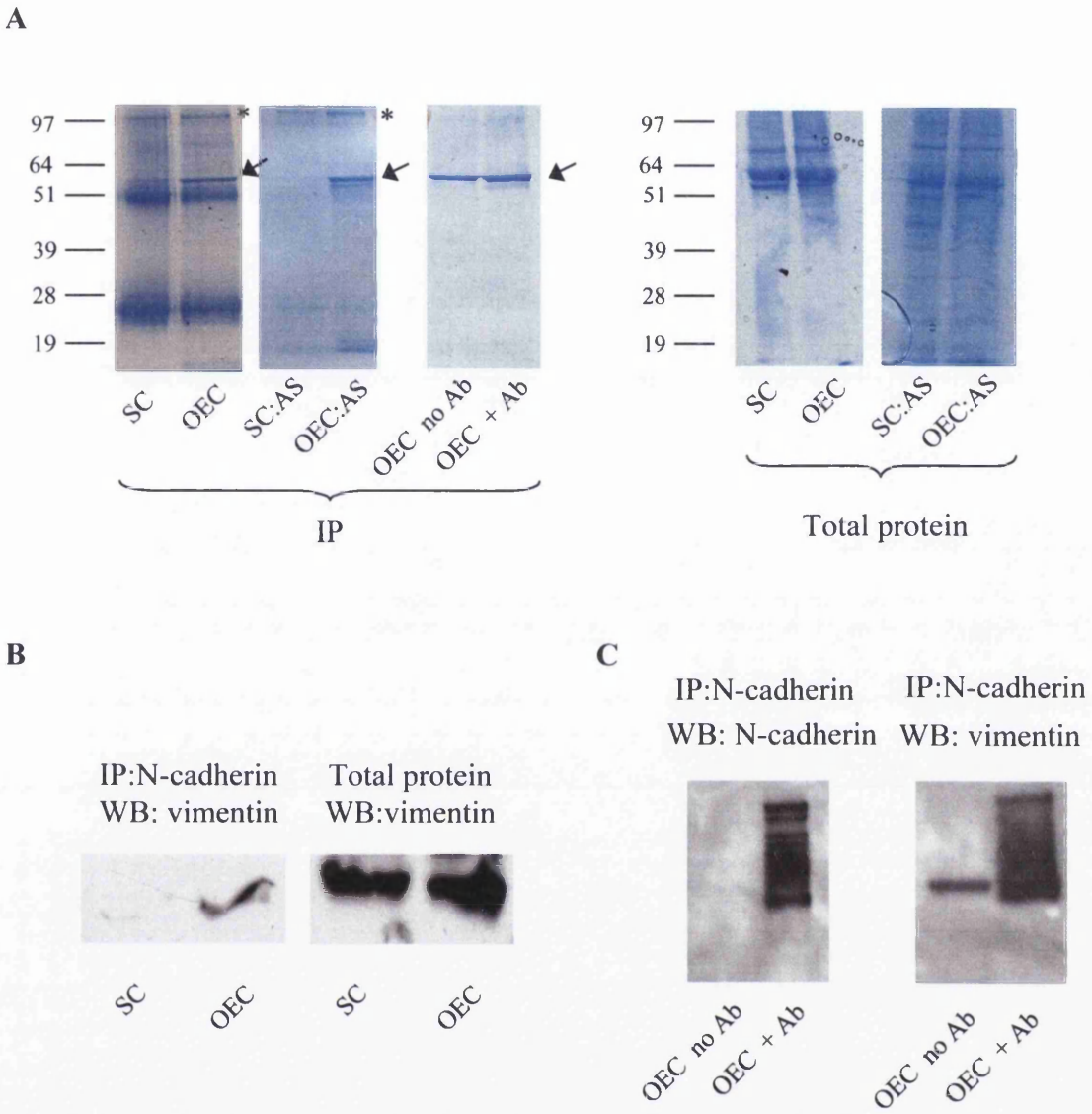

Figure 4.14. Vimentin is non-specifically 'pulled down' in OEC immunoprecipitations.

(A) N-cadherin IPs were stained with Brilliant Blue G-colloidal, of OEC and Schwann cell lysates, and also OEC:AS and SC:AS lysates. A control was performed with no anti-N-cadherin antibody, which pulled down the band (indicated by arrows) non-specifically in OEC lysate. Mass spectrometry of the band identified the protein as vimentin. N-cadherin protein is denoted by *. (B) Immuno blot of IP confirming vimentin being pulled down in OEC, but not Schwann cell lysates. (C) Immuno blot showing vimentin is pulled down non-specifically in OEC lysates.

and not in Schwann cell IPs, despite being present equally in the total lysate before immunoprecipitation (Figure 4.14B). However, both Western blotting (Figure 4.14C) and whole gel stain (Figure 4.14A) of OEC lysates without N-cadherin antibody showed that vimentin was being non-specifically pulled down in these IPs and did not reflect a preferential association with N-cadherin in OECs rather than Schwann cells. However, vimentin is present in both Schwann cell and OEC lysates, so why it should be 'stickier' in OECs than Schwann cells remains a question. No other candidates for differential N-cadherin interactions, and thus regulation, were apparent at this level of investigation.

4.3 Discussion

This study illustrates that OECs and Schwann cells both express functional N-cadherin, as demonstrated by its presence at cell-cell junctions and Ca^{2+} dependency, yet N-cadherin is apparently functioning differently in the two glial cells. For example, Schwann cells adhered more strongly to an astrocyte monolayer and migrated more slowly on astrocyte but not PLL substrates when compared to OECs. Using siRNA to reduce N-cadherin expression, the inhibition of Schwann cell migration on astrocytes was removed and their adhesion to astrocytes was reduced. On the other hand, Ncad siRNA transfection into OECs had little effect on their migration and adhesion when cultured with astrocytes. Taking the migration and the adhesion data together, these results show that the OECs and Schwann cells differ in how they use N-cadherin for adhesion and migration, highlighting a further distinction between the two cell types (Ramon-Cueto and Avila, 1998; Wewetzer et al., 2002; Barnett and Riddell, 2004).

4.3.1 Inhibition of N-cadherin

In previous studies, a role for N-cadherin was proposed for Schwann cell migration and adhesion based on competitive inhibition by the classical cadherin cell adhesion recognition sequence His-Ala-Val (HAV; Wilby et al., 1999), but no direct evidence was available for a role for N-cadherin in OEC migration (Lakatos et al, 2000). In this study the cyclic peptide was initially used, which is probably less resistant to degradation than the linear peptide (Williams et al., 2000), to demonstrate differences in the adhesive characteristics of OECs and Schwann cells. However, as there is no way of confirming its mechanism of action, and

due to its limited effect on the confrontation assay which may arise from different N-cadherin junction dynamics in short term (adhesion) and long term (confrontation) assays, it was decided to use the more precise method of N-cadherin inhibition by preventing protein synthesis with siRNA.

In this way, N-cadherin expression was successfully reduced in both Schwann cells and OECs. This resulted in the ability of Schwann cells to overcome the astrocyte-induced inhibition, as measured by adhesion, migration and confrontation assays, while not affecting OEC behaviour. As has been discussed earlier (Section 3.2.4), adhesion and migration are related processes, and therefore the slow migration of Schwann cells upon astrocyte monolayers may result from their strong adhesion to astrocytes. Likewise, the N-cadherin dependency of Schwann cell migration upon astrocytes may result from the N-cadherin-dependent adhesion of Schwann cells to astrocytes.

4.3 N-cadherin and hypertrophy

Reducing N-cadherin expression with Ncad siRNA also allowed the perturbation of the boundary formed in confrontation assays between Schwann cells and astrocytes. A predominant feature of the inhibitory astrocyte domain is the presence of greatly enlarged astrocytes (Eddleston and Mucke, 1993; Ghirnikar and Eng, 1994; Lakatos et al., 2000). These hypertrophic astrocytes are seen only in Schwann cell/astrocyte cultures, where Schwann cell migration is impeded, and not in OEC/astrocyte cultures. This leads to the speculation that the inhibition of Schwann cell migration amongst astrocytes could be determined by either the increase in astrocyte size, which would act as a physical barrier, changes in Schwann cell proliferation or by the strength of adhesion mediated by N-cadherin upon cellular contact. The reduction of N-cadherin by siRNA allowed more Schwann cells to successfully overcome this contact-induced inhibition, and penetrate the astrocyte domains but did not affect proliferation as assessed by BrdU uptake. Therefore, using Ncad siRNA, it was assessed if removal of N-cadherin reduced the increase in astrocyte area. These studies demonstrated that Ncad siRNA treatment of Schwann cells and OECs did not affect astrocyte area, and thus N-cadherin was not required for the induction of hypertrophy. Although a caveat for this result may be that a proportion of Schwann cells still express N-cadherin, due to incomplete transfection (Figure 4.7), and

thus may be able to induce astrocytic hypertrophy. However, the strong correlation of N-cadherin reduction and disruption of astrocyte/Schwann cell boundary formation suggests that strong Schwann cell adhesion to astrocytes is more likely to prevent their migration amongst astrocytes and not astrocytic hypertrophy.

4.3.4 Possible N-cadherin mechanisms

The question remains why do OECs express N-cadherin if it is not used in their adhesion to astrocytes? It may be that OECs require N-cadherin for interactions with other cell types. For example, N-cadherin is necessary for the adherence and alignment of Schwann cells to axons (Wanner and Wood, 2002) and is necessary for the initiation of myelination as has been demonstrated for oligodendrocytes (Schnadelbach et al., 2001).

Furthermore, simple adhesion models cannot readily explain the diverse functions of cadherins, and some cadherin functions might be better explained by their ability to activate signal transduction cascades rather than adhesion per se (Skaper et al., 2004). For example, N-cadherin is able to activate a fibroblast growth factor receptor (FGFR) signalling cascade (Williams et al., 1994) and an interaction between N-cadherin and the FGFR has been implicated in both developmental and pathological processes. In addition, neurite outgrowth stimulated by N-cadherin is inhibited by a wide variety of agents that inhibit FGFR function in neurons (Williams et al., 1994), including expression of a dominant-negative FGFR (Utton et al., 2001; Williams et al., 2002). More recently, N-cadherin has been reported to promote the motility of cancer cells, with evidence that FGFR might be involved (Nieman, et al., 1999; Hazan et al., 2000).

In the immunoprecipitation experiments presented in this study, no differences between N-cadherin interacting proteins were seen in Schwann cells and OECs (Figure 4.14A). However, the sensitivity of this approach may be questionable. This is highlighted by the only faint detection of the well characterised N-cadherin-interacting protein, β-catenin (Figure 4.14), which we know was successfully co-precipitated with N-cadherin due to its clear detection using immunoblotting (Figure 4.13). Therefore a more sensitive approach, such as silver staining or using more protein, might be more suitable.

N-cadherin may have different functions depending upon how it is presented, for example it may function differently when expressed in different cell types. This is demonstrated where Schwann cells presented with N-cadherin on a neurite do not have impaired migration, in contrast to when they are presented with N-cadherin on an astrocyte (Bixby et al., 1988; Wilby et al., 1999). This demonstrates that N-cadherin alone might not determine the migratory outcome, but rather that it is in conjunction with other signals or N-cadherin-interacting molecules that the decision to form either stable or dynamic junctions is made. For example, the association of N-cadherin with the catenins mediates their adhesive functions, whereas interaction with FGFR can promote migration (see Introduction 1.6.2.3). It would therefore be important to investigate both upstream and downsteam signals from N-cadherin to see how they compare between the two cell types. An initial investigation of downstream catenin signalling pathways from N-cadherin did not highlight any differences which readily explain the different N-cadherin functions observed between OECs and Schwann cells. It still remains to be investigated how upstream signals influence N-cadherin function in these assays. Since N-cadherin presentation or accompanying signals might vary between cellular targets, such as between neurites and astrocytes, differences may also arise depending upon the reactive status of the astrocyte. In other words, the astrocytic N-cadherin encountered by an OEC might actually be biochemically different in some way from the astrocytic N-cadherin encountered by a Schwann cell, due to the varying effects of Schwann cells and OECs on astrocytosis (Figure 4.12; Lakatos et al., 2000). Many potential N-cadherin-interacting candidates exist, and some are induced in reactive astrocytes, such as neurocan, (McKeon et al., 1999; Asher et al., 2000), which interacts with N-cadherin via its receptor, GalNAcPTase (Li et al., 2000).

4.3.5 Vimentin

One potential N-cadherin interacting protein identified in this study, which was present in OEC cultures but not in Schwann cell cultures, was vimentin. Under normal conditions, vimentin expression is associated with the developing CNS (Bignami et al., 1982), whereby astrocytes switch from a vimentin-based cytoskeleton to a GFAP-orientated one upon maturation. This process occurs alongside the transformation of astrocytes as a permissive environment to one that restricts axonal growth (Smith et al., 1990). In the OEC, however, vimentin remains as a major intermediate filament constituent in the adult (Franceschini and

Barnett, 1996; Ramon-Cueto and Avila, 1998), providing evidence that OECs retain an 'immature' phenotype, and may confer the cell's axonal growth-promoting properties. Schwann cells have also been reported to express vimentin (Jessen and Mirsky, 1983), as was confirmed here by both immunoblotting and immunocytochemistry. Vimentin has also been associated with motile cells, particularly due to its upregulation in the epidermal-mesenchymal transition associated with the metastatic progression of tumourous skin cells (Kirschmann et al., 1999; Avizienyte et al., 2004). This might explain a role for vimentin in the motile, or even 'invasive' OECs. However, due to the lack of specificity in vimentin precipitation, this may not be a significant observation. Why it should be pulled down in OECs but not Schwann cells is still unexplainable, but may involve different vimentin interactions with the cell.

4.3.6 Conclusions

In summary, in this chapter it has been demonstrated that silencing N-cadherin using siRNA had distinct biological effects on the interactions of OECs and Schwann cells with astrocytes. This suggests that N-cadherin functions differently in these cells and may have dual functionality, promoting either adhesion or migration. In this way, N-cadherin may be a potential target for pharmacological intervention in order to make Schwann cells behave more like OECs upon transplantation. However, due to the role of N-cadherin in mediating Schwann cell adhesion to neurons, it would not be advantageous to prevent Schwann cells from actually binding to their therapeutic targets. An understanding of N-cadherin regulatory pathways in Schwann cells, particularly upon astrocyte-interaction, might highlight appropriate specific targets for modulation which would not disrupt the essential functions of N-cadherin necessary for axonal regeneration or myelination.

CHAPTER 5

Effect of Schwann cell-conditioned media on astrocytes, and olfactory ensheathing cell/astrocyte interactions

5.1 Introduction

In the previous chapters it has been established that the inhibition of Schwann cell migration within astrocytic areas can in part result from the ability of Schwann cells to form strong cellular adhesions. This has been demonstrated by comparison of Schwann cell and olfactory ensheathing cell (OEC) adhesion and migration when interacting with astrocytes, and also from a detailed investigation of the role of N-cadherin in these processes. In addition, it has been hypothesised that Schwann cell migration may also be impeded by the inhibitory astrocytic environment, as indicated by the presence of enlarged hypertrophic astrocytes, which may occur as a result of Schwann cell interactions with astrocytes.

However, the influence of hypertrophic astrocytes upon cellular migration has not been thoroughly investigated. It has been previously established in the published literature that both Schwann cells and OECs elicit an astrocytic response *in vivo* (Plant et al., 2001; Takami et al., 2002; Lakatos et al., 2003a) as indicated by an increase in the expression of both glial fibrillary acidic protein (GFAP) and the chondoitin sulphate proteoglycans (CS-PGs). However, the astrocytic response to OECs appears to be much less than that to Schwann cells (Verdu et al., 2001; Takami et al., 2002; Lakatos et al., 2003a). This may correlate with the enhanced inherent ability of OECs to migrate within the astrocyte environment of the CNS compared to Schwann cells (Guidino-Cabrera and Nieto-Sampedro, 1996, Iwashita et al., 2000). *In vitro* studies have also confirmed these *in vivo* results where astrocytes co-cultured with Schwann cells became enlarged and hypertrophic (Ghirniker and Eng, 1994; Lakatos et al., 2000), but again the astrocytic response to co-cultured OECs was much less (see Chapter 4, Figure 4.12)

However, it remains to be determined what the specific role this astrocytic response plays in determining the different migration patterns seen between OECs and Schwann cells upon interacting with astrocytes, particularly following transplantation. In addition, a rather limited understanding of what factors might be inducing this hypertrophy exists at present. If it is possible to increase our knowledge of these processes, it might enable us to advance transplantation therapies. Generally, this might allow us to reduce the glial scarring that results following spinal cord injury, but more specifically, we may be able to enhance the

ability of transplanted cells to reach appropriate targets of repair, while keeping the host response to these cells to a minimum.

In this chapter, the approach will be taken to examine the effect of factors secreted by OECs and Schwann cells on astrocytes, in order to determine some of the signals involved in the induction of astrocytosis. In addition, the role that the resulting astrocytic reactivity plays in determining Schwann cell and OEC abilities to migrate within astrocytic areas will be addressed.

5.2 Results

5.2.1 Schwann cell-conditioned media (SCM) induces boundary formation in OEC/astrocyte confrontation cultures

Since downstream N-cadherin signalling was unchanged between OEC and Schwann cells (Chapter 4), it was hypothesised that signalling upstream from N-cadherin may differ between the cell types, for example, variations in cell-secreted factors which may regulate N-cadherin differently. Therefore, the effect of Schwann cell-conditioned media (SCM) on OEC/astrocyte interactions was investigated using the confrontation assay. SCM was collected from confluent Schwann cell cultures in DMEM-BS after 2 days incubation. This was then applied, as a 50% SCM/50% DMEM-10% solution (SCM-50%), to OEC:astrocyte confrontation cultures which had been cultured in DMEM-10% for 10 days. After 2 days in the presence of SCM, distinct boundaries began to form at the interface between OECs and astrocytes, in a similar manner detected for Schwann cell/astrocyte interactions (Figure 5.1A and B). It could also be seen that expression of glial fibrillary acidic protein (GFAP) was higher in astrocytes at the SCM-induced boundary interface than in astrocytes which were further away from OEC contact. An upregulation of GFAP expression in astrocytes contacting OECs was not observed in OEC:astrocyte confrontations maintained in only DMEM-10%.

It could also be seen in these cultures that following SCM treatment, OECs became much more aligned with each other. In this way, their alignment resembled that seen in Schwann

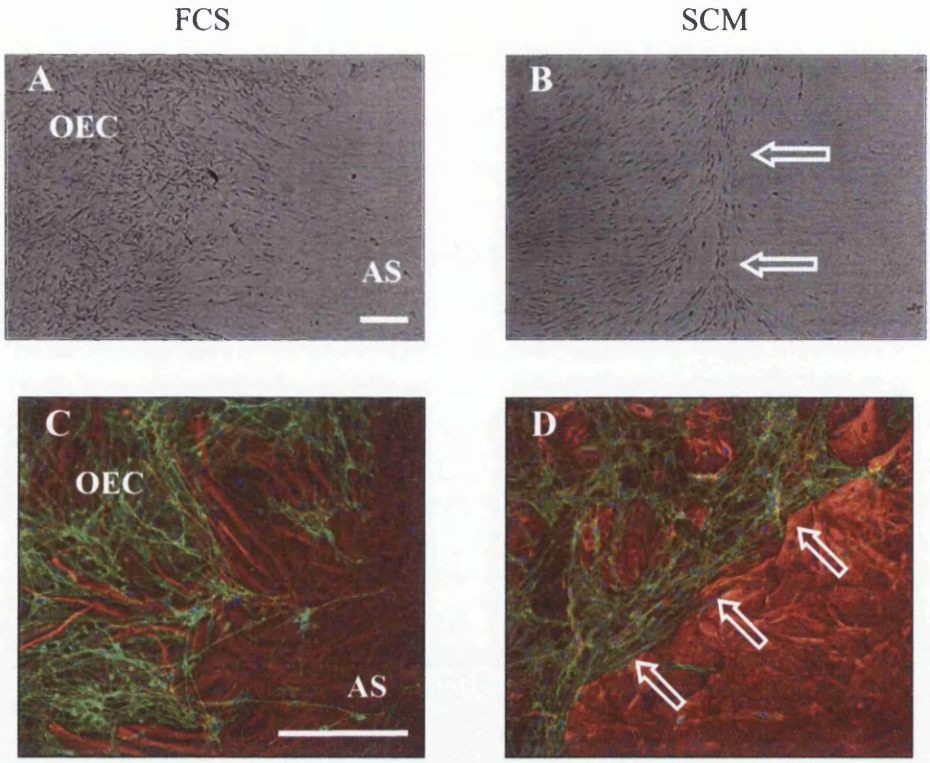

Figure 5.1. SCM induces boundary formation in OEC/astrocyte confrontation assays.

Confrontation assays were cultured in either DMEM-10% (FCS; A, C), or switched after 10 days culturing in FCS to 50% SCM/50% DMEM-10% (SCM; B, D) for 2 days, after which time clear boundaries (open arrows) were formed. Images were taken using either light microscopy (A, B) or immunocytochemistry (C, D) with $p75^{NTR}$ (OECs, FITC) and GFAP (astrocytes, TRITC). Images are of different fields of view. Scale bar = 200 μm.

cell cultures (Figure 3.2; Wanner et al., 2002). However, this response was very variable following SCM treatment, being apparent in some cultures but not all.

5.2.2 Fibroblast growth factor receptor inhibition disrupts SCM-induced boundary formation in OEC/astrocyte cultures

5.2.2.1 Inhibitors used

Inhibitors of various tyrosine receptor kinases were added to the confrontation assays in order to try and elucidate which signalling pathways were activated by addition of SCM. These inhibitors included epidermal growth factor receptor (EGFR; AG1478), platelet-derived growth factor receptor (PDGFR; AG1295), and fibroblast growth factor receptor (FGFR; SU5402). In addition, an inhibitor of the non-receptor tyrosine kinase src (SU6656) was also included. Concentrations were selected based upon the published literature for SU6656 (Src inhibitor; Bowmann et al., 2001; Blake et al., 2000), PP2 (Src inhibitor; Blake et al., 2000; Nam et al., 2002), U0126 (Zheng et al., 2003; Jadeski et al., 2003, PD98059 (MEK inhibitor; Reiling et al., 2001), SU5402 (FGFR inhibitor; Skaper et al., 2000; Mahommadi et al., 1997), AG1478 (EGFR inhibitor; Shushan et al., 2004; Zhao et al., 2003) and AG1295 (PDGFR inhibitor; Banai et al., 1998; Zhao et al., 2003). However, it does remain a possibility that the concentrations used for the different inhibitors may be at different positions on the dose-response curve, thus inhibiting targets with different efficiencies.

A degree of cross-reactivity is detectable with some of these inhibitors, where AG1295, in addition to inhibiting PDGFR (IC_{50} = 500 nM), also weakly inibits EGFR (IC_{50} = 2.5 mM). AG1295 inhibits PDGFR at high doses (IC_{50} > 100 mM) as well as the intended target EGFR (IC_{50} = 3 nM). SU6656 inhibits several closely related kinases such as Fyn (IC_{50} = 170 nM), Yes (IC_{50} = 20 nM) and Lyn (IC_{50} = 130 nM) in addition to Src (IC_{50} = 28 nM), and SU5402 only weakly inhibits PDGFR but not EGFR, in addition to its intended target FGFR (IC_{50} = 10 mM). However, for the screening purposes here, the inhibitors selected are suitable. By using the above combination of inhibitors, the functional target can be deduced, i.e. the PDGFR inhibitor can identify whether FGFR-mediated inhibition is actually due to residual PDGFR inhibition.

5.2.2.2 Effects of inhibitors

Control cultures consisted of both DMEM-10% (FCS) alone or SCM-50% without the addition of inhibitors (SCM). Inhibitors were added to OEC:astrocyte confrontation cultures at the same time that SCM was applied, which, as before, was added to cultures which had been maintained for 10 days. After 2 days, cultures were immunolabelled for GFAP (astrocytes) and $p75^{NTR}$ (OECs; Figure 5.2).

As demonstrated in Figure 5.1, it was seen that OEC:astrocyte confrontations maintained in DMEM-10% were able to intemingle with each other, whereas upon addition of SCM a clear boundary was formed (Figure 5.2Aii). The presence of hypertrophic astrocytes, identified by their enlarged appearance, could also be seen along the boundary in SCM-treated cultures. In the presence of EGFR and PDGFR inhibitors (Figures 5.2Aiii and 5.2Aiv), no differences were seen in comparison to cultures in SCM-alone, since boundaries and hypertrophic astrocytes were present in all cultures. However, inhibition of src caused a morphological change in both OECs and astrocytes (Figure 5.2Av). Here, the cells became elongated, presumably due to a decrease in focal adhesion turnover in the lagging portion of the migrating cells such that as they moved they could not detach the rear of the cell and thus became stretched. However, despite their interdigitated appearance, OECs did not cross into astrocyte domains, suggesting that despite a change in the alignment of the cellular boundary, OECs did not regain the ability to invade and migrate within the astrocytic domains.

In the presence of an FGFR inhibitor (Figure 5.2Avi), this SCM-induced boundary was again not as defined as in SCM alone, where astrocytic processes appeared to stretch into the OEC domain and interact with OECs. Enlarged astrocytes were also not as apparent.

Some OECs were observed entering into the astrocyte domain itself (arrows), although not as many as in FCS treated cultures, suggesting that FGFR inhibition did not abrogate all effects of addition of SCM, but may have prevented any morphological changes in the astrocytes cultures, such as hypertrophy. The confrontation assays were quantified by counting the number of cells which crossed the astrocyte-OEC boundary into the astrocyte

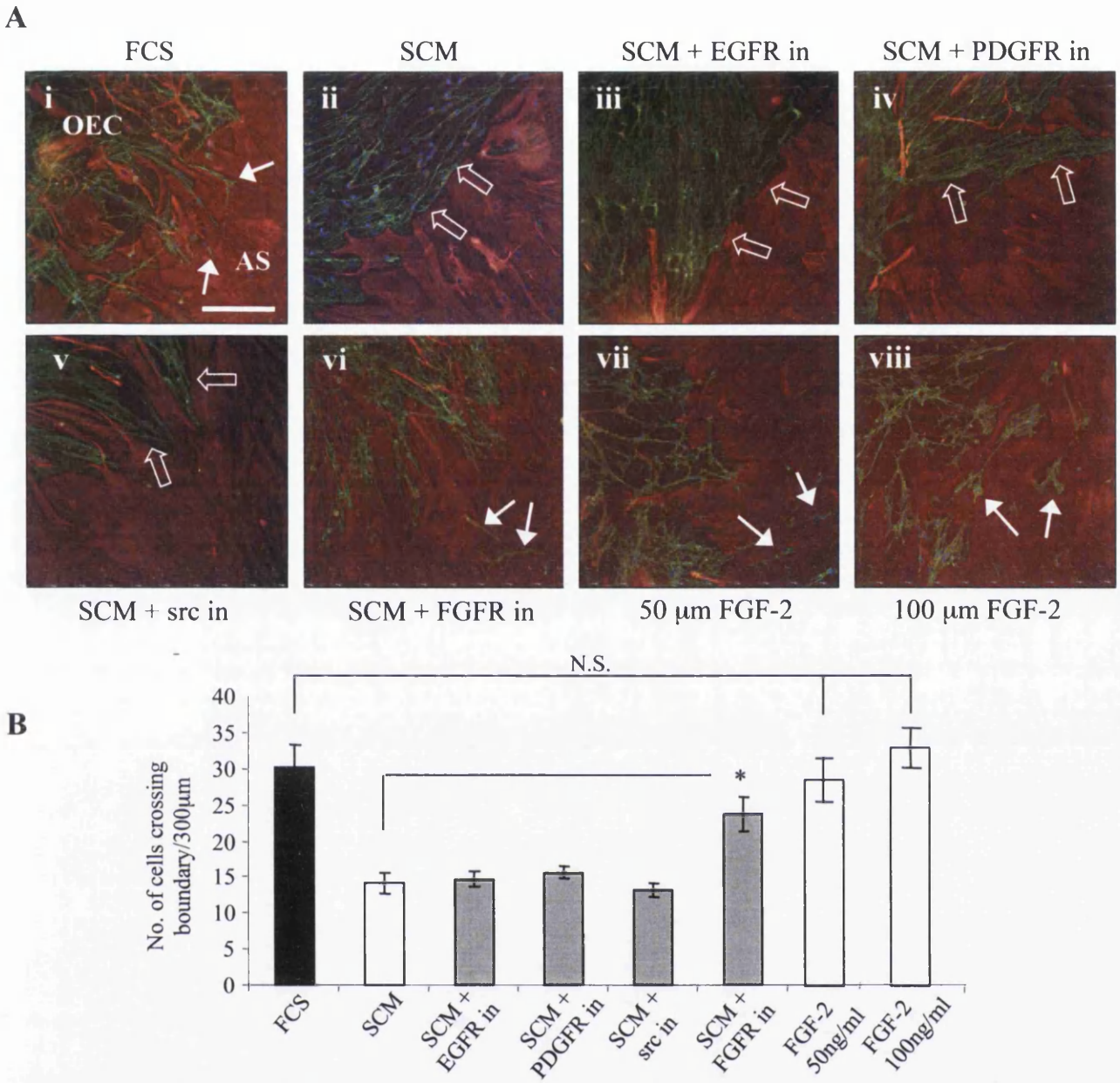

Figure 5.2. FGFR inhibition prevents OEC/astrocyte boundary formation, following SCM treatment.

(A) Tyrosine kinase inhibitors were applied to OEC:astrocyte confrontation assays to examine their effects on SCM-induced boundary formation. Astrocytes were cultured with FCS (i), SCM (ii) and SCM supplemented with inhibitors of EGFR (iii), PDGFR (iv), src (v) and FGFR (vi). In addition, FGF-2 was added to cultures at a concentration of 50 μM (vii) and 100 μM (viii). Boundaries were not disrupted by the presence of EGFR and PDGFR inhibitors (in), although astrocytes became very elongated in the presence of the src inhibitor. In the presence of an FGFR inhibitor, OECs and astrocytes formed a weaving interlay, with some intermingling. Migrating cells are indicated with a white arrow. Scale bar = 200 μm. (B) Quantification of confrontation assays, the number of cells which had crossed into astrocyte territories were counted over an astrocyte/OEC boundary distance of 300 μm. FGFR inhibition increases the number of cells migrating into astrocytic territories significantly compared to SCM treated. However, FGF-2 treatment did not mimic SCM (N.S. = not significant). n=6; *$p<0.01$.

territory (Figure 5.2B). FGFR inhibition of the SCM-treated OEC/astrocyte confrontations significantly increased the number of cells crossing this boundary from 14.2 +/- 1.47 cells per 300 μm boundary to 23.7 +/- 2.36 ($p<0.01$). This was no longer significantly different from the untreated OEC/astrocytes boundary with 30.2 +/- 3.24 cells crossing per 300 μm boundary. However, application of FGF-2 to OEC/astrocyte confrontation assays, at both 50 ng/ml and 100 ng/ml, did not induce a similar effect to SCM, with OECs being able to migrate efficiently into astrocyte-rich areas. This suggests that FGF-2 might not be responsible for the effect of SCM.

5.2.3 SCM treatment of astrocyte monolayers does not affect OEC or Schwann cell migration and adhesion upon them

Confluent astroycte cultures were maintained in DMEM-10%, and then switched to SCM-50% for 2 days. These were then used to perform both migration and adhesion assays. Vybrant-labelled OECs and Schwann cells were allowed to adhere to control and SCM-treated astrocyte monolayers overnight and then their migration speeds measured using time-lapse microscopy. As has been seen earlier (Figure 3.5. and 4.9), Schwann cells migrated at slower speeds than OECs on astrocyte monolayers (Figure 5.3A), demonstrating astrocyte-induced inhibition of Schwann cell migration, but not that of OECs. The treatment of astrocyte monolayers with SCM did not affect the ability of either Schwann cells or OECs to migrate upon them.

Adhesion assays were also performed, in which Vybrant-labelled cells were allowed to adhere to astrocyte monolayers for 30 minutes while on a shaking platform. The monolayers had been previously treated for 2 days with DMEM-10%, SCM-50% or OEC-conditioned media (OCM), again in a 50% dilution with DMEM-10% (OCM-50%). The number of cells which adhered after 30 minutes to the astrocyte monolayers were then quantified. As seen previously, the addition of SCM and OCM to astrocyte monolayers did not significantly affect the ability of either OECs or Schwann cells to adhere to astrocytes.5.2.4 SCM-treatment increases astrocyte proliferation

To assess if SCM treatment affected astrocyte proliferation, the uptake of BrdU was measured by BrdU immunofluorescence. The number of astrocytes which took up BrdU

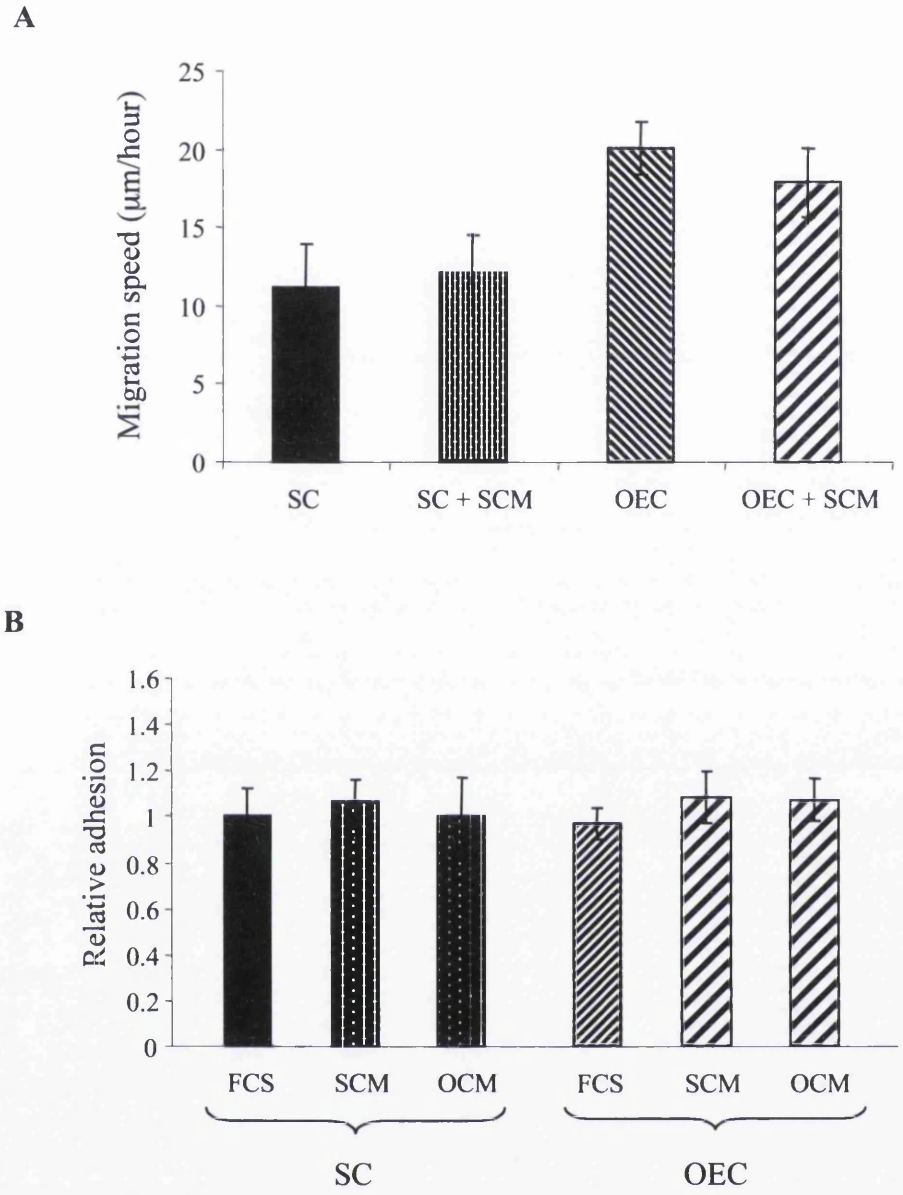

Figure 5.3. SCM treatment of astrocyte monolayers does not affect Schwann cell (SC) or OEC migration and adhesion.

(A) Schwann cell and OEC migration upon astrocyte monolayers, as assessed by time-lapse microscopy, are not significantly affected by SCM treatment. n=15. (B) SCM and OCM does not significantly affect SC or OEC adhesion to astrocytes. Adhesion assays were performed where the number of Vybrant-labelled Schwann cells and OECs adhering to an astrocyte monolayer after 30 minutes were counted. n=6.

over 16 hours following treatment were counted. Astrocytes were treated for 12 hours before addition of BrdU, with either serum-free media (DMEM-BS supplemented with heregulin and forskolin; DMEM-BS H/F), or with SCM or OCM which were diluted 1:1 with DMEM-BS. Serum-free DMEM-BS H/F was used as control media since this is the media used to collect the conditioned media, and allowed proliferation changes to be measured without being masked by the overriding effect of serum. Under these conditions, astrocyte proliferation was unaffected by addition of OCM, but was increased 2.5 fold by SCM ($p<0.001$), and the percentage of cells taking up BrdU increased from 10.2 +/- 0.8% to 24.9 +/- 3.1% (Figure 5.4A). Treatment with tyrosine receptor kinase inhibitors (EGFR, PDGFR and FGFR) did not significantly reduce SCM-induced proliferation, suggesting that the proliferative response was not induced via signalling dependent upon these receptors (Figure 5.4B). Likewise, application of EGF and FGF (at 10ng/ml, based on Bansal et al., 2003; Asher et al., 2000; Williams et al., 1994; Araujo and Cotman, 1992), did not increase astrocyte proliferation significantly, again suggesting that they were not responsible for the increase in proliferation observed following SCM treatment. In addition, the astrocytic proliferation response to SCM was concentration-dependent as demonstrated by a concentration-response assay in which SCM was titrated from 1:50 to 1:1 SCM:DMEM-BS H/F (Figure 5.4C). A significant proliferative response could be detected when SCM was diluted at 1:10, and had reached a plateau by 1:5.

5.2.5 Both OEC contact and Schwann cell-secreted factors are necessary for induction of astrocytic hypertrophy and upregulation of GFAP expression

In order to assess the effect of SCM on astrocytic hypertrophy (indicated by an increase in astrocyte area), low density astrocyte cultures were set up as mono-cultures or co-cultured with OECs or Schwann cells. These were maintained in either DMEM-10% or SCM-50%

for 2 days prior to immunolabelling for GFAP (astrocytes) or $p75^{NTR}$ (OECs or Schwann cells; Figure 5.5A). Astrocyte area was measured using NIH Image programme and the mean values calculated (Figure 5.5B). Astrocytes cultured in DMEM-10% with Schwann cells were greatly enlarged in comparison to astrocytes cultured alone (increasing from 2495 +/- 218 μm^2 to 5438 +/- 615 μm^2, $p<0.001$), in agreement with Figure 4.12. Astrocytes

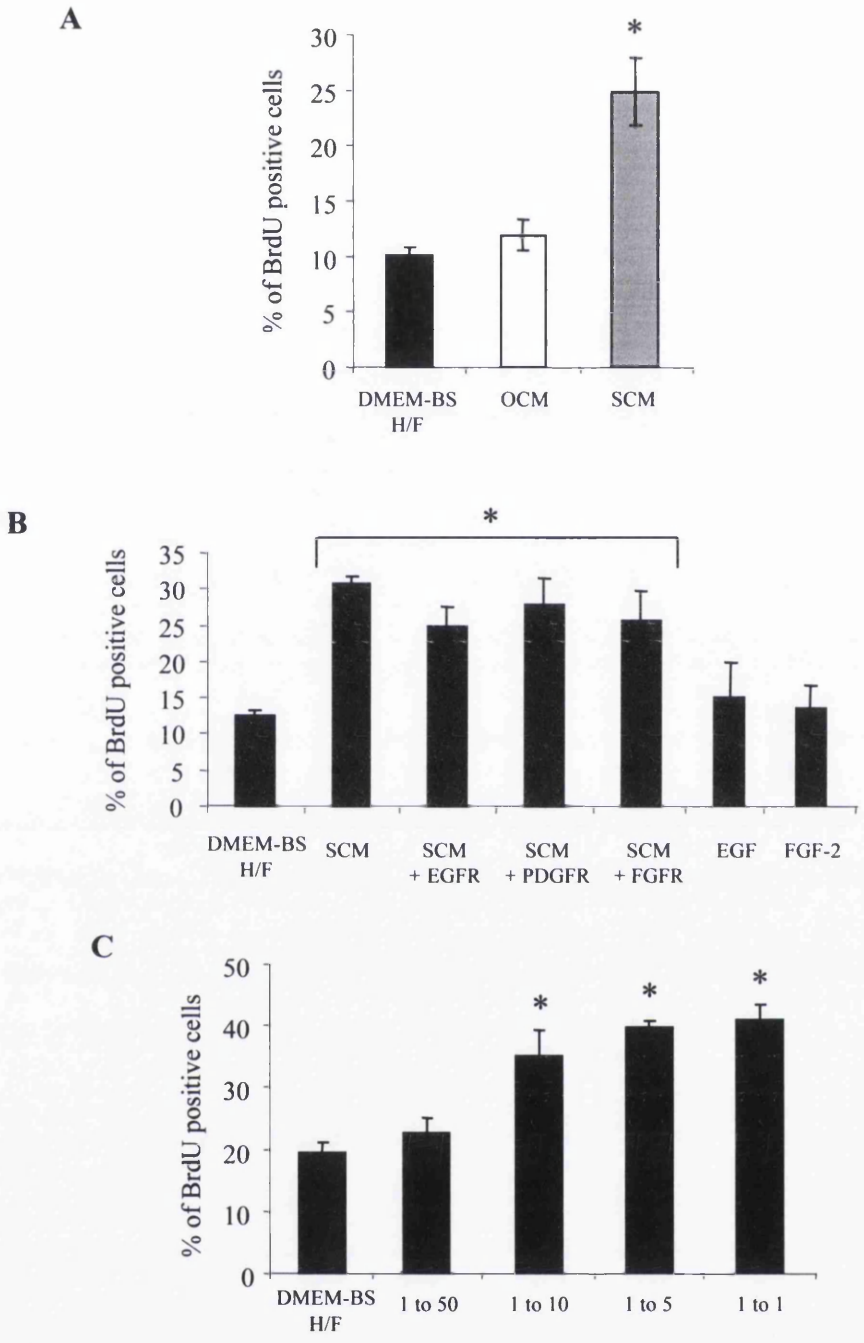

Figure 5.4. SCM induces astrocyte proliferation.

(A) Astrocytes were treated with DMEM-BS H/F, OCM and SCM, and incubated with BrdU overnight, before staining. The percentage of BrdU positive cells after 16 hours were estimated. (B) Astrocytes were incubated with SCM in the presence or absence of receptor tyrosine kinase (EGFR, PDGR, FGFR) inhibitors. In addition, EGF (10 ng/ml) and FGF-2 (10 ng/ml) were added, but did not mimic SCM addition. (C Different titrations of SCM in SATO H/F (1:50, 1:10, 1:5 and 1:1). n=6, *p>0.001.

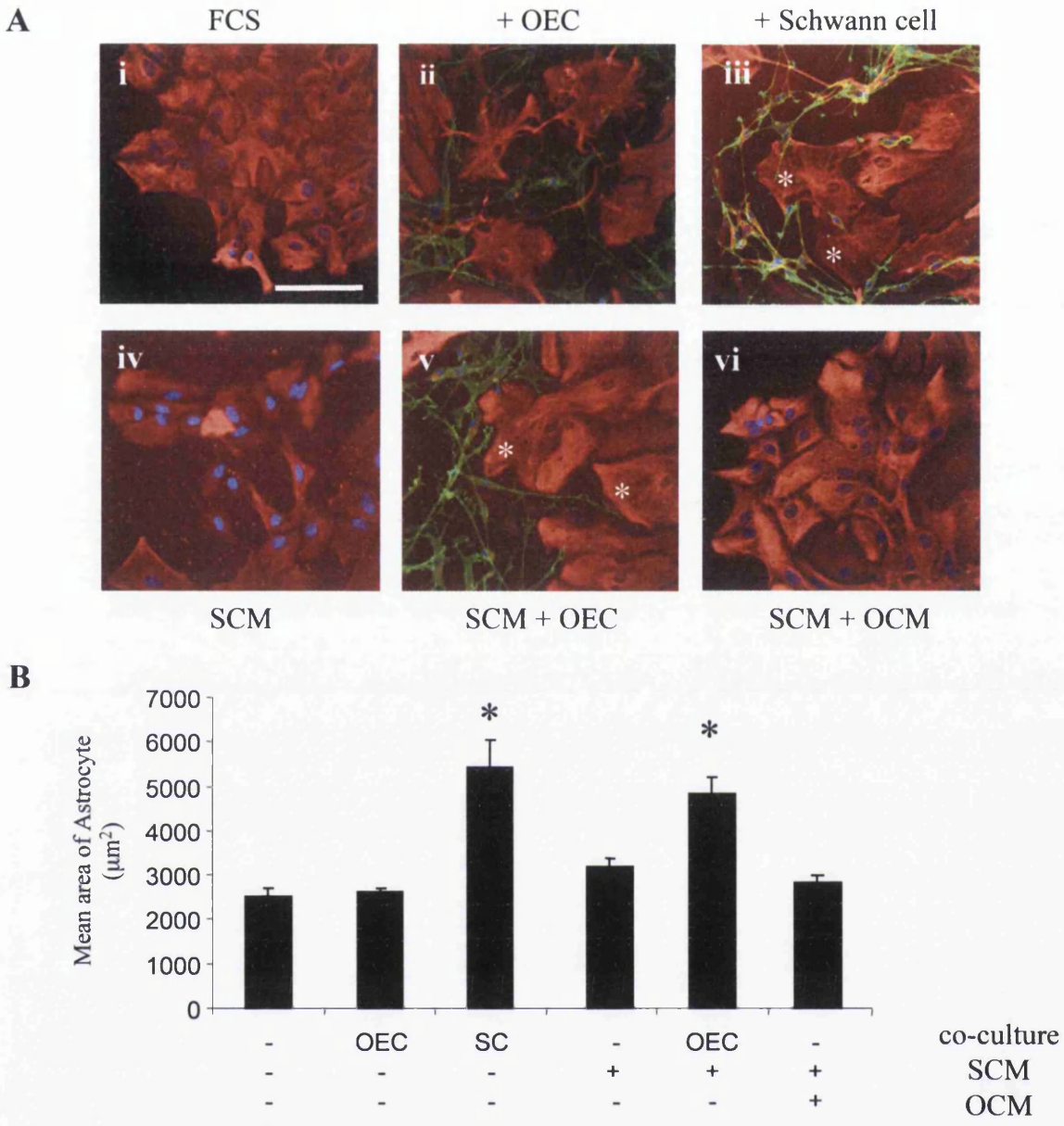

Figure 5.5. Both SCM and OEC contact are required for astrocytic hypertrophy.

(A) The effect of culture conditions upon astrocytic area was assessed by immunocytochemistry (astrocytes, GFAP-TRITC; OECs or Schwann cells, $p75^{NTR}$-FITC). Conditions included culturing astrocytes for 2 days in FCS (i), co-culture with OECs (ii) or Schwann cells (iii), SCM-treatment (iv) co-culture with OECs and SCM-treatment (v), and treatment with both SCM and OCM (vi). Hypertrophic astrocytes are marked with a white asterisk. Scale bar = 100 μm.(B) Quantification of astrocytic area using NIH Image analysis. * $p<0.001$, n=25.

cultured with OECs and mono-culture astrocytes treated with SCM did not increase in area. In contrast, astrocytes cultured with OECs with concomitant SCM treatment became enlarged (4872 +/- 413 μm^2, $p<0.001$), to a similar degree as Schwann cell:astrocyte co-cultures. To assess whether this increase in astrocyte area was a result of synergy between Schwann cell-secreted factors, present in SCM, and OEC-secreted factors, produced by the OECs in culture, astrocyte mono-cultures were treated with both SCM and OCM. This did not result in hypertrophy, suggesting that both SCM and an OEC-contact mediated signal, as opposed to an OEC-secreted signal, are necessary for the induction of hypertrophy.

A similar result was seen when expression of GFAP was assessed (Figure 5.6). After mono- and co-cultures had been treated with SCM-50% for 2 days, lysates were made and subjected to immunoblotting for GFAP, using vinculin as a control. GFAP expression was significantly upregulated in Schwann cell/astrocyte co-cultures, and in astrocytes cultured with OECs when treated with SCM, but not when cultured with OECs in the absence of SCM, or when treated with SCM alone. Once more, this demonstrates that both OEC contact and SCM are necessary for the hypertrophic response as assessed by GFAP upregulation.

To assess if FGFR signalling was involved in the induction of hypertrophy in these models, an inhibitor of FGFR was employed. This was added to cultures over the same time course, either at the time of SCM treatment, or two days before immunolabelling in non-SCM-treated cultures, and reapplied every day for two days. Coverslips were then immunolabelled for GFAP and $p75^{NTR}$ (Figure 5.7A), and astrocyte areas were measured and quantified (Figure 5.7B). As before, both astrocytes in co-culture with Schwann cells alone, and those cultured with OECs and treated with SCM, were enlarged (from 1939 +/- 150 μm2 (control) to 5286 +/- 302 μm2 (Schwann cell co-culture) and 5524 +/- 377 μm2 (OEC co-culture with SCM)). Inhibition of FGFR significantly reduced this effect, although not to control levels (OEC co-culture with SCM plus FGFR inhibitor, 2468 +/-

396 μm2; Schwann cell co-culture plus FGFR inhibitor, 3632 +/- 499 μm2). This suggests that both Schwann cell-induced and OEC/SCM-induced hypertrophy requires the function of FGFR.

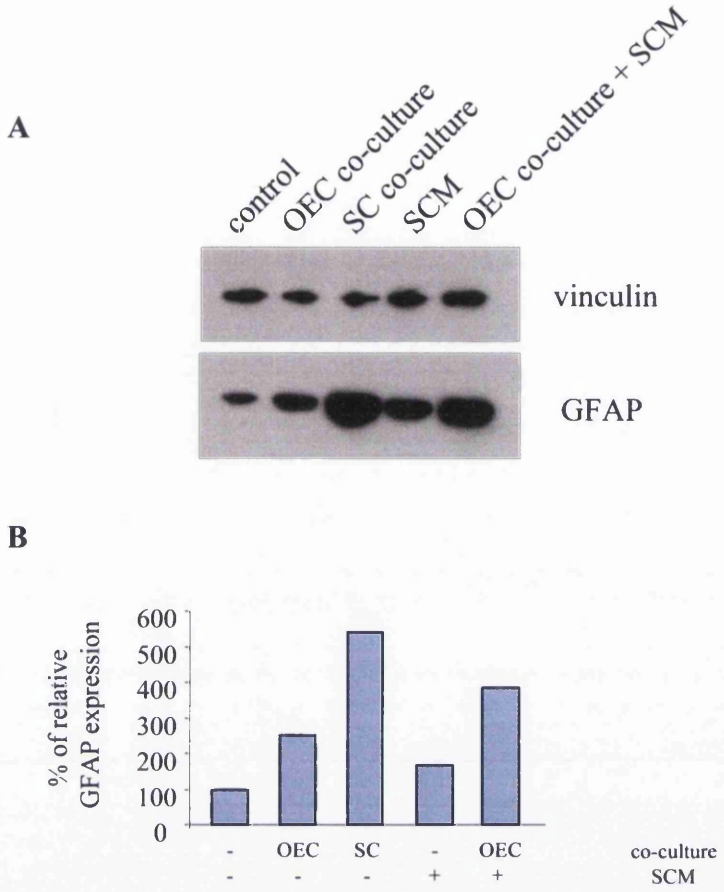

Figure 5.6. Both SCM and OEC contact are necessary for GFAP upregulation.

(A) Western blot showing GFAP expression after treatment of astrocytes. Treatments included astrocytes cultured in FCS (control), co-cultured with OECs and Schwann cells (SC), 50% SCM, and co-cultured with OECs with 50% SCM treatment. Vinculin was used as a protein loading control. (B) Densitometry of GFAP expression, relative to vinculin. GFAP was up-regulated in Schwann cell:astrocyte co-cultures, and OEC:astrocyte co-cultures only following treatment with SCM.

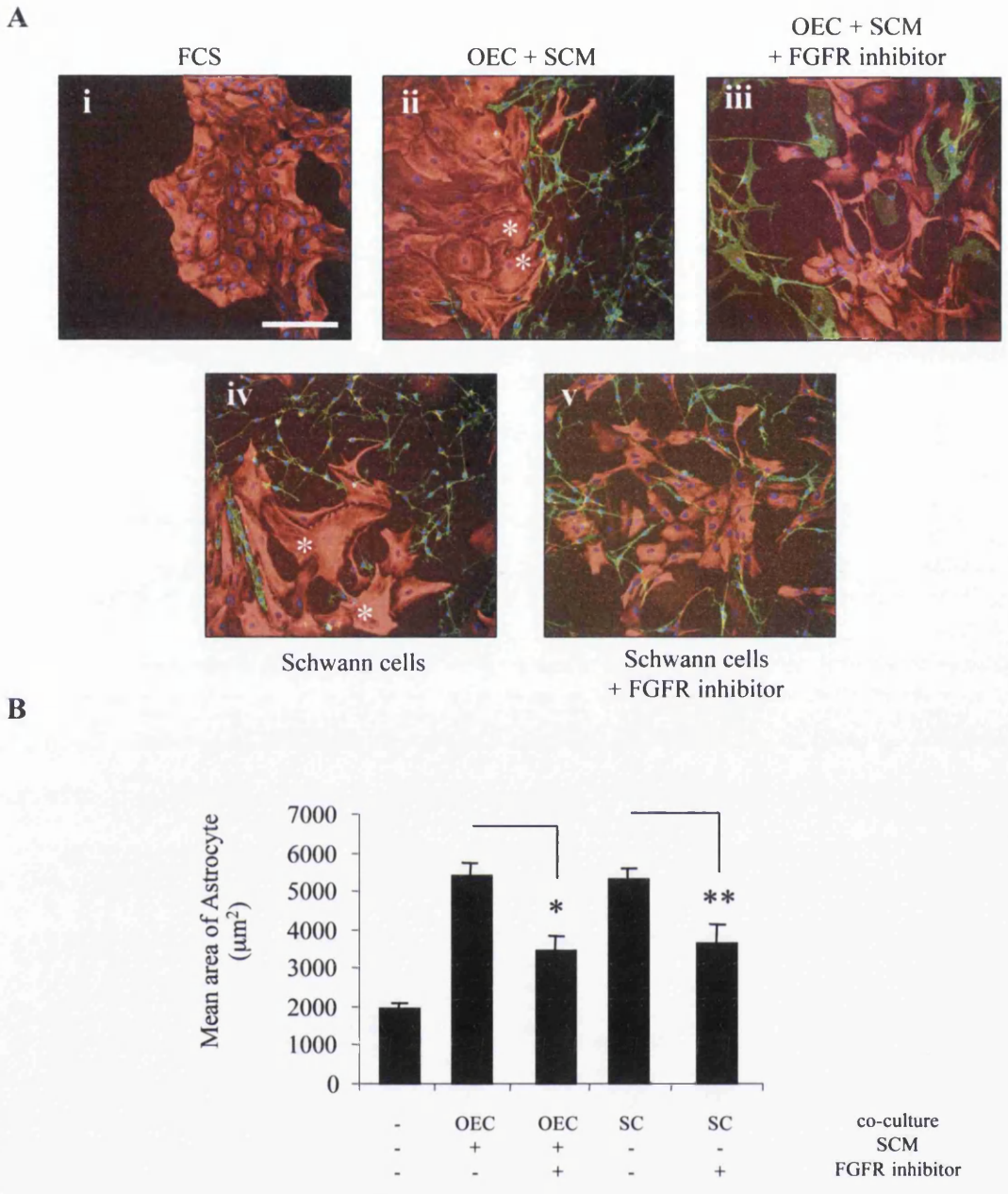

Figure 5.7. FGFR inhibitor treatment reduces Schwann cell- and OEC with SCM-induced hypertrophy.

(A) Astrocyte cultures were treated for 2 days by culturing in FCS (i), co-culturing with OECs and SCM treatment (ii), co-culturing with OECs and SCM treatment with FGFR inhibition (iii), co-culturing with Schwann cells (iv), and co-culturing with Schwann cells with FGFR inhibition (v). Cultures were immunolabelled for GFAP (astrocytes, TRITC) and $p75^{NTR}$ (OECs and Schwann cells, FITC), with nuclear staining (DAPI). Hypertrophic astrocytes are marked with a white asterisk. Scale bar = 200 μm. (B) Quantification of astrocyte area using NIH Image analysis. * $p<0.001$, ** $p<0.02$, $n=22$.

To test whether OECs were inducing astrocytic hypertrophy through N-cadherin stimulation, a cyclic N-cadherin agonist peptide was added to astrocyte cultures which were also treated with SCM (Figure 5.8). Addition of the agonist peptide did not compensate for the presence of co-cultured OECs since astrocytes did not become enlarged (astrocytes with SCM and peptide, 1199 +/- 30; astrocytes co-cultured with OECs and SCM treatment, 2565 +/- 185; $p<0.001$), but remained with a similar area as astrocytes treated with FCS or SCM alone (1284 +/- 76 and 1263 +/- 30 respectively). As a positive control, agonist peptide from the same batch was used in neurite outgrowth assays (Skaper et al., 2003) in Professor Doherty's laboratory.

5.2.6 SCM and OCM increase astrocyte chondroitin sulphate proteoglycan expression, particularly neurocan

In order to assess the effect of SCM and OCM on other markers of astrocytic reactivity, the expression of the inhibitory molecules chondroitin sulphate proteoglycan (CS-PGs) was investigated. Astrocyte cultures were maintained as mono-cultures in DMEM-10% (FCS), SCM-50% (SCM) or OCM-50% (OCM), or co-cultured with Schwann cells. As a positive control for astrocyte reactivity, astrocyte monolayers in DMEM-10% were wounded with a pipette tip and either immunolabelled immediately or left for 24 hours before immunolabelling. All cultures were immunolabelled for GFAP and also CS-PGs using either a pan-CS-PG antibody (CS-56 and 473HD) or a neurocan-specific antibody (Figure 5.9). CS-56 staining was enhanced in SCM-treated cultures (Figure 5.9C), and possibly in OCM-treated cultures (Figure 5.9D) although this was difficult to judge subjectively by eye. It was clearly upregulated in the positive controls, both immediately after wounding where cells adjacent to the wound edge wound were immunoreactive (Figure 5.9E), and also 24 hours after wounding in which strongly immunoreactive astrocyte processes could be seen throughout the cultures (Figure 5.9F). However, immunoreactivity of control (FCS) cultures was much higher than expected (Lakatos et al., 2000) and did not appear to differ significantly with astrocytes co-cultured with Schwann cells, as has been

reported previously. A similar immunoreactivity pattern was observed with the 473HD antibody. Similar to the CS-56 antibody, 473HD also labels many different types of CS-PGs, although it recognises a different epitope. An increase in CS-PG expression was

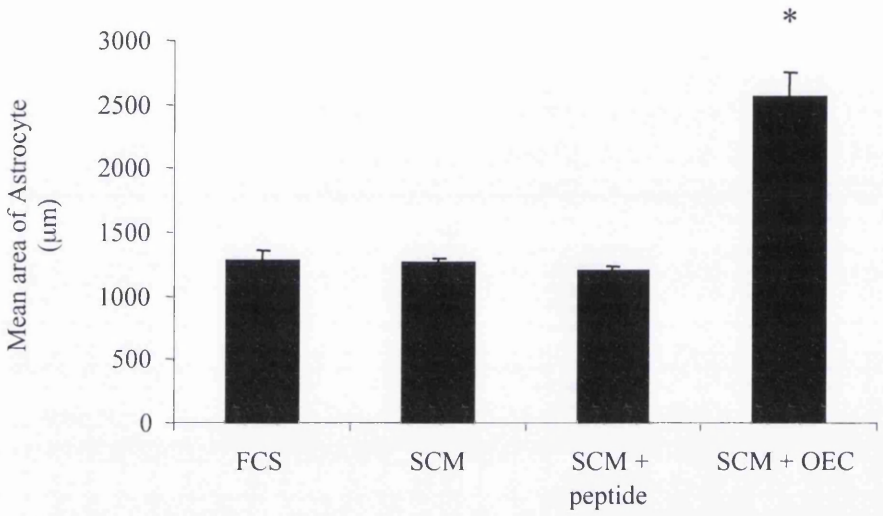

Figure 5.8. N-cadherin stimulation does not compensate for OEC contact on astrocytic area.

Low density astrocyte cultures were treated for 2 days with SCM, SCM and N-cadherin agonist peptide, and OEC co-culture with SCM treatment. The bar chart illustrates the average area of astrocyte size as quantified using NIH Image. *$p<0.001$, $n=18$.

Figure 5.9. CS-PG expression is upregulated in astrocytes following SCM treatment.

Immunocytochemistry of astrocytes after various treatments was performed for different CS-PG epitopes. Treatments included FCS (A, G, M), co-culture with Schwann cells (SC; B, H, N), treatment with SCM (C, I, O) or OCM (D, J, P), or wounding astrocytes by scratching confluent monolayers and then fixing coverslips either immediately (E, K, Q) or after 24 hours (F, L, R). Astrocytes were labelled for GFAP (TRITC) and CS-PG (CS-56 (A-F), 473HD (G-L) and neurocan (M-R) antibodies; TRITC). CS-PG expression was enhanced following SCM treatment, as detected by each antibody used. White arrows indicate areas of upregulated CS-PG expression. Scale bar = 200μm.

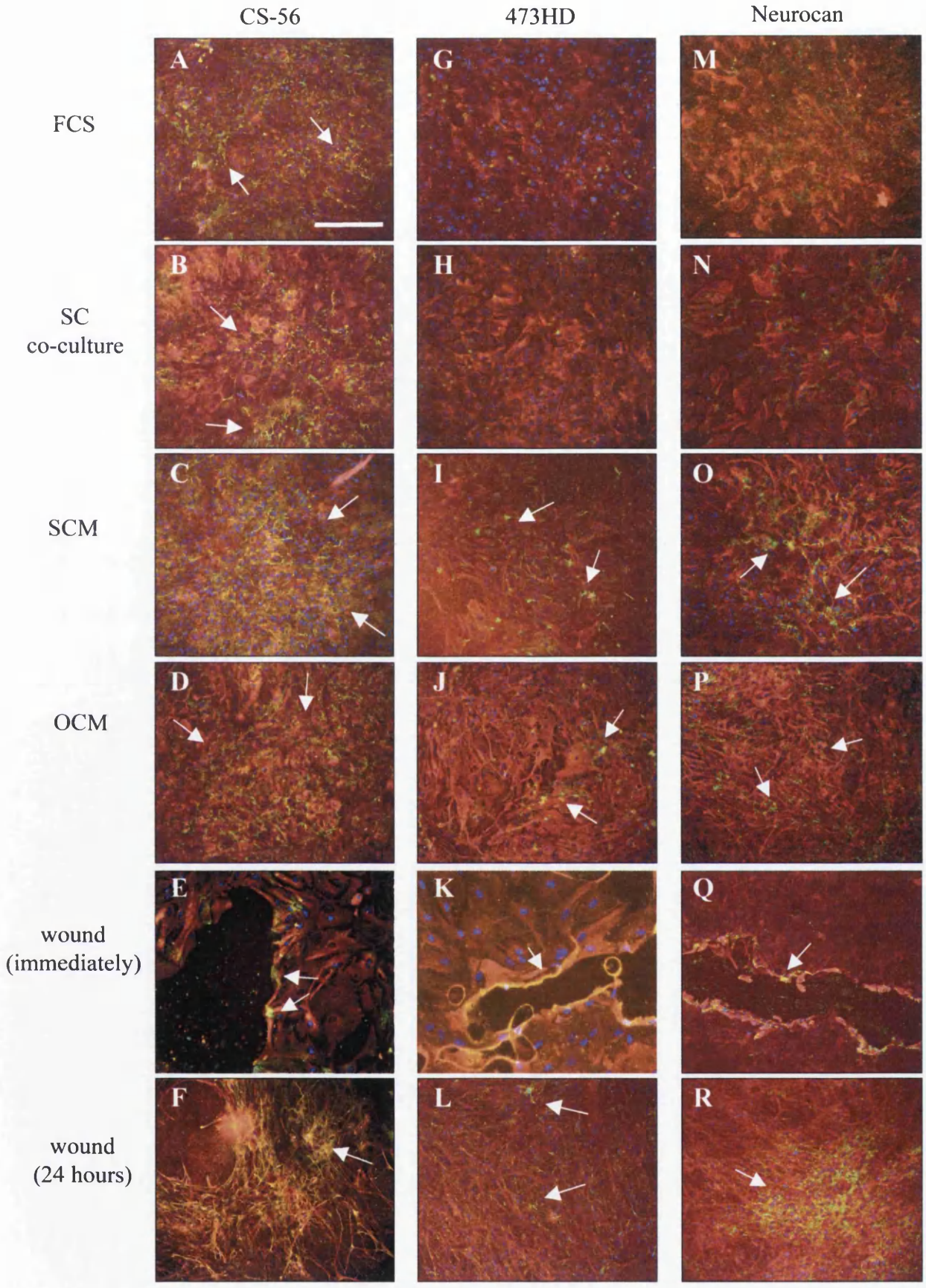

Figure 5.9. CS-PG expression is upregulated in astrocytes following SCM treatment.

particularly obvious with 473HD in the wound controls, again with immuno-reactive cells present at the wound edge immediately (Figure 5.9K), and along astrocytic processes after 24 hours (Figure 5.9L). An increase was also apparent in SCM-treated cultures (Figure 5.9I), although as with the CS-56 antibody Schwann cell-co-cultured and mono-cultured astrocytes were unchanged. An antibody against the CS-PG, neurocan, was also used and showed the most dramatic upregulation following SCM treatment (Figure 5.9O). In addition, neurocan levels were increased following OCM treatment (Figure 5.9P). The negative control (FCS) for this antibody was much lower than for both CS-56 and 473HD, but, as before, positive scratch controls were highly immunoreactive (Figures 5.9Q and 5.9R).

To measure the effect of SCM treatment on CS-PG expression in more detail, lysates of treated cultures (24 hours after scratching, 2 days after SCM or OCM treatment, or 10 days after co-culturing) were made and subjected to immunoblotting. Vinculin was used as a loading control, and both pan-CS-PG antibodies (CS-56 and 473HD) and the neurocan antibody were used to measure CS-PG levels (Figure 5.10). Before probing with anti-neurocan, lysates were digested with chondrotinase (see Materials and Methods, section 2.4.1), in order to resolve neurocan into discrete bands for identification and quantification (McKeon et al., 1999; Asher et al., 2000). Both the CS-56 and 473HD antibodies did not give a clear immunoblotting profile, producing bands with varying apparent molecular weights (data not shown), preventing a comparative analysis. However, using the neurocan antibody, full length neurocan (275 kDa) was identified. Quantification clearly showed an increase in neurocan expression following SCM treatment (12 fold), and also following OCM treatment (10.5 fold). Levels were also elevated in the wound control (10.7 fold). Interestingly, unlike the immunocytochemistry study, neurocan levels were upregulated following astrocyte co-culture with Schwann cells (6.3 fold). In conclusion, SCM and OCM treatment causes astrocytes to upregulate expression of CS-PGs, and in particular neurocan.

To determine which signalling pathways were required for the upregulation of CS-PG expression, tyrosine receptor kinase inhibitors were added to SCM-treated cultures at the time of treatment and reapplied every day for two days before cultures were immunolabelled. The addition of the FGFR inhibitor had no effect on SCM-induced

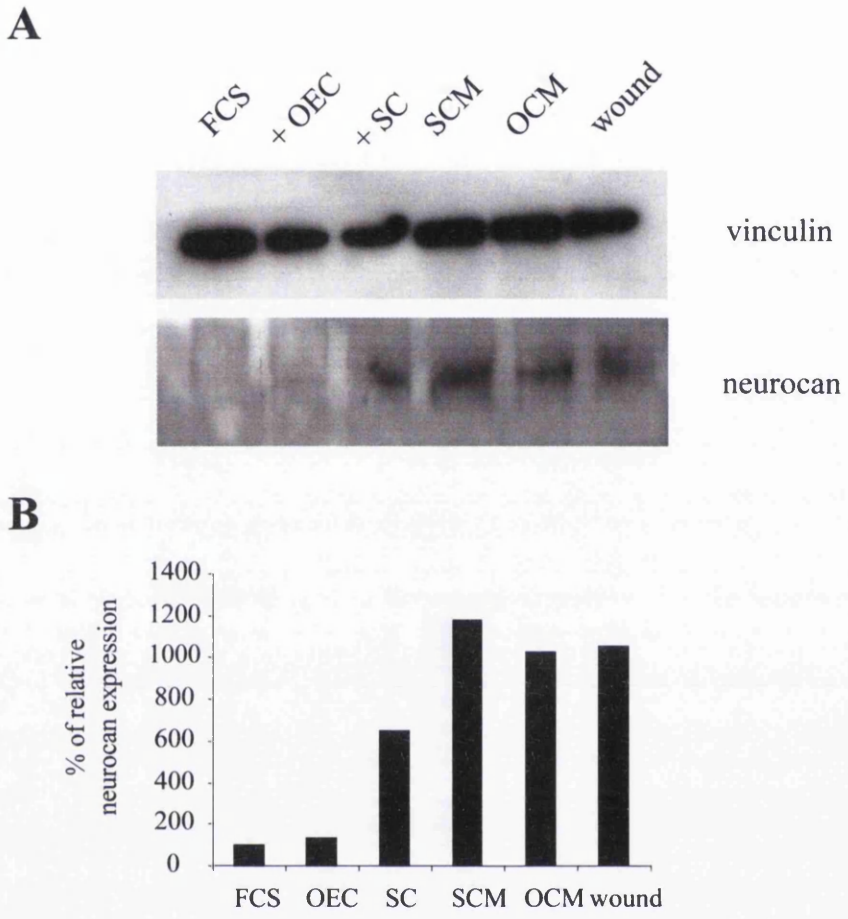

Figure 5.10. Neurocan expression increases in astrocytes after SCM and OCM treatment

(A) Immunoblotting showing effect of astrocyte treatment on expression of neurocan. Astrocyte treatments include FCS (control), co-culturing with OECs (+ OEC) and Schwann cells (+ SC), 50% SCM, 50% OCM, and wounding astrocyte monolayers as a positive control (lysates made 24 hours later). Vinculin was used as a protein loading control. (B) Quantification of neurocan expression, relative to vinculin. Neurocan expression is raised in Schwann cell/astrocyte co-cultures, and after SCM and OCM treatment.

expression of either the CS-56 epitope or neurocan (Figure 5.11). Similarly, addition of EGFR and PDGFR inhibitors had no effect on CS-PG expression in these cultures (data not shown). This suggests that SCM does not activate essential FGFR, EGFR or PDGFR-dependent signals necessary for upregulation of CS-PGs.

5.2.7 N-cadherin expression is upregulated by SCM

Lysates were made from astrocytes, cultured in DMEM-10% (FCS), SCM-50% (SCM) or OCM-50% (OCM) for 2 days, or co-cultured for 10 days with OECs or Schwann cells. Positive controls were made by wounding astrocyte monolayers with a pipette tip and leaving for 24 hours. N-cadherin levels were examined by immunoblotting, and compared to vinculin as a loading control (Figure 5.12). The levels were highly upregulated in SCM-treated cultures (17.4 fold), but only slightly increased in Schwann cell co-cultures, OCM-treated and scratched cultures (3.8, 3 and 5 fold respectively).

5.2.8 SCM-treatment does not alter other astrocyte markers, nestin, vimentin and PSA-NCAM

To assess if other markers of hypertrophy are increased in astrocytes following treatment, the upregulation of vimentin, another hallmark of astrocytosis (Dahl et al., 1981a), was examined (Figure 5.14). Nestin expression has also been reported in reactive astrocytes (Clarke et al., 1994; Frisen et al., 1995), as has PSA-NCAM (Alonso and Privat, 1993; Nomura et al., 2000), and therefore the expression of these markers was investigated on astrocytes in mono- and co-culture with Schwann cells and OECs, with or without SCM treatment (Figure 5.13; Figure 5.14). The number of cells expressing nestin was not significantly altered in any of the conditions, being approximately 50% in every case (Figure 5.13B). Both OECs and Schwann cells, as identified by their diffuse GFAP expression, were all nestin positive (white arrows). Astrocytes under these culture conditions all expressed vimentin (Figure 5.14A) but not PSA-NCAM (Figure 5.14B),

demonstrating that these markers were not significantly altered by any of the culture conditions. As detected for nestin, both Schwann cells and OECs expressed vimentin (white arrows), although only a proportion of OECs expressed PSA-NCAM (reflecting a

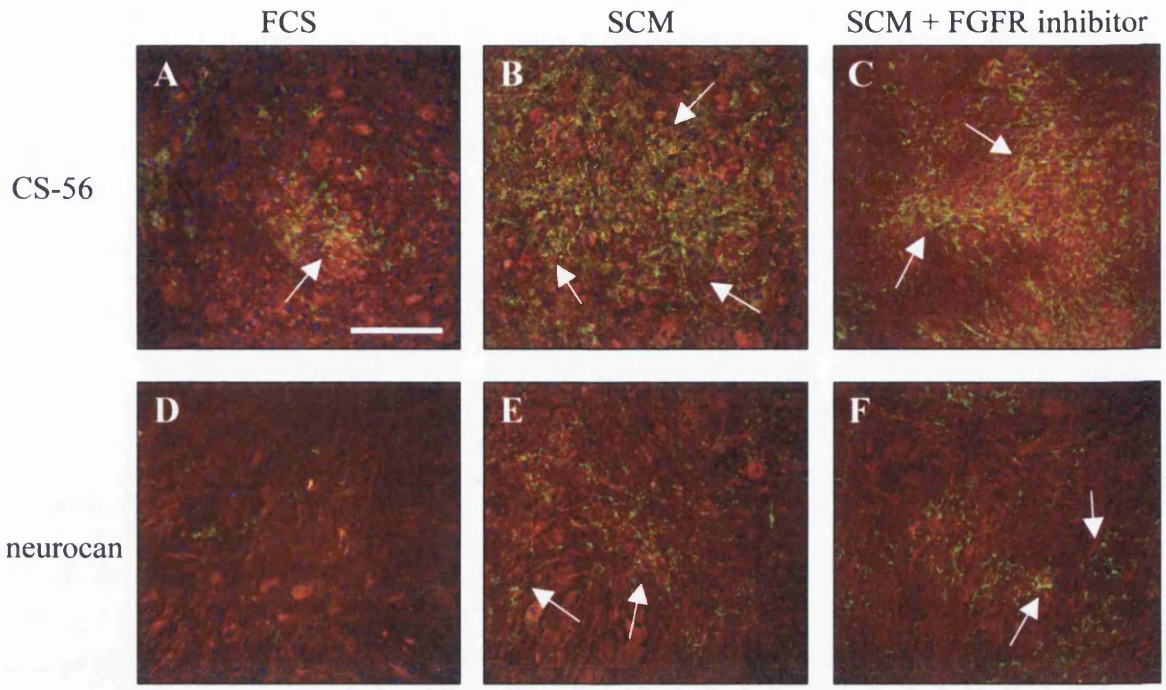

Figure 5.11. FGFR inhibitor treatment had no effect on SCM-induced CS-PG expression.

Astrocytes were treated with FCS, SCM and SCM with FGFR inhibitor for two days before immunocytochemistry (GFAP-TRITC; CS-56/neurocan-FITC). White arrows indicate strong areas of CS-PG expression. Scale bar = 200 μm.

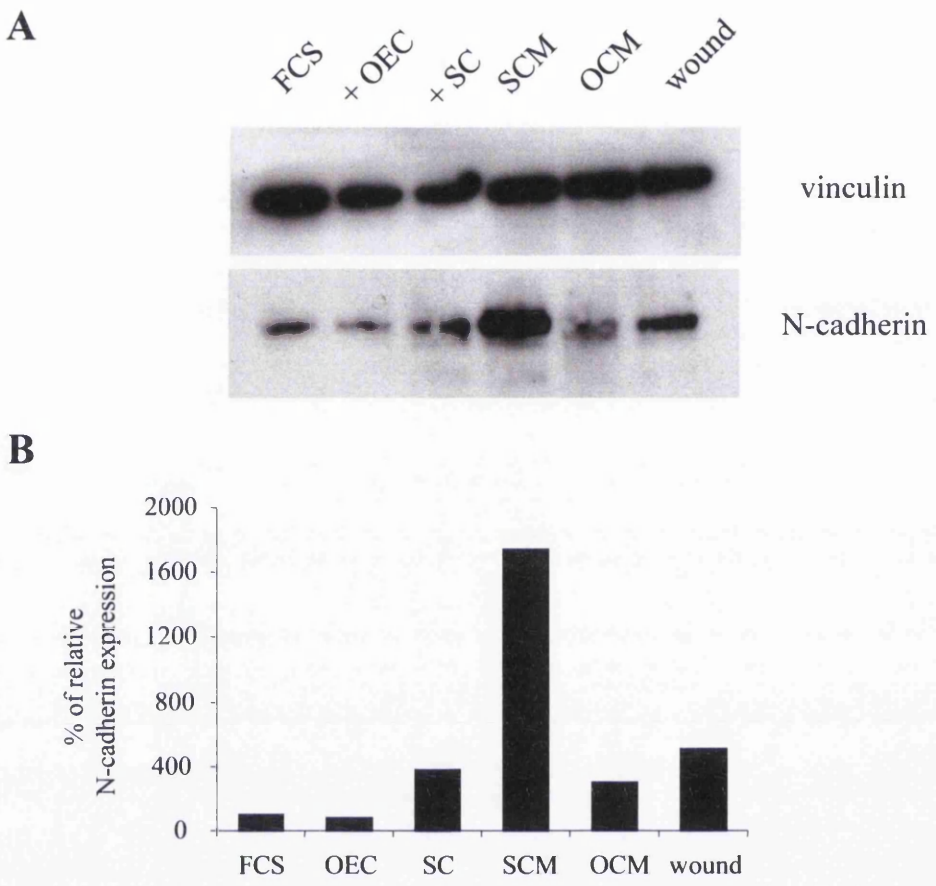

Figure 5.12. N-cadherin expression is elevated in astrocytes treated with SCM.

(A) Astrocytes were treated in various culture conditions, such as FCS or SCM treatment, co-culturing with OECs or Schwann cells (SC), or wounding the astrocyte monolayer by scratching. Lysates were made 24 hours later, and immunoblotting performed with an N-cadherin antibody. (B) Densitometry of N-cadherin expression relative to vinculin.

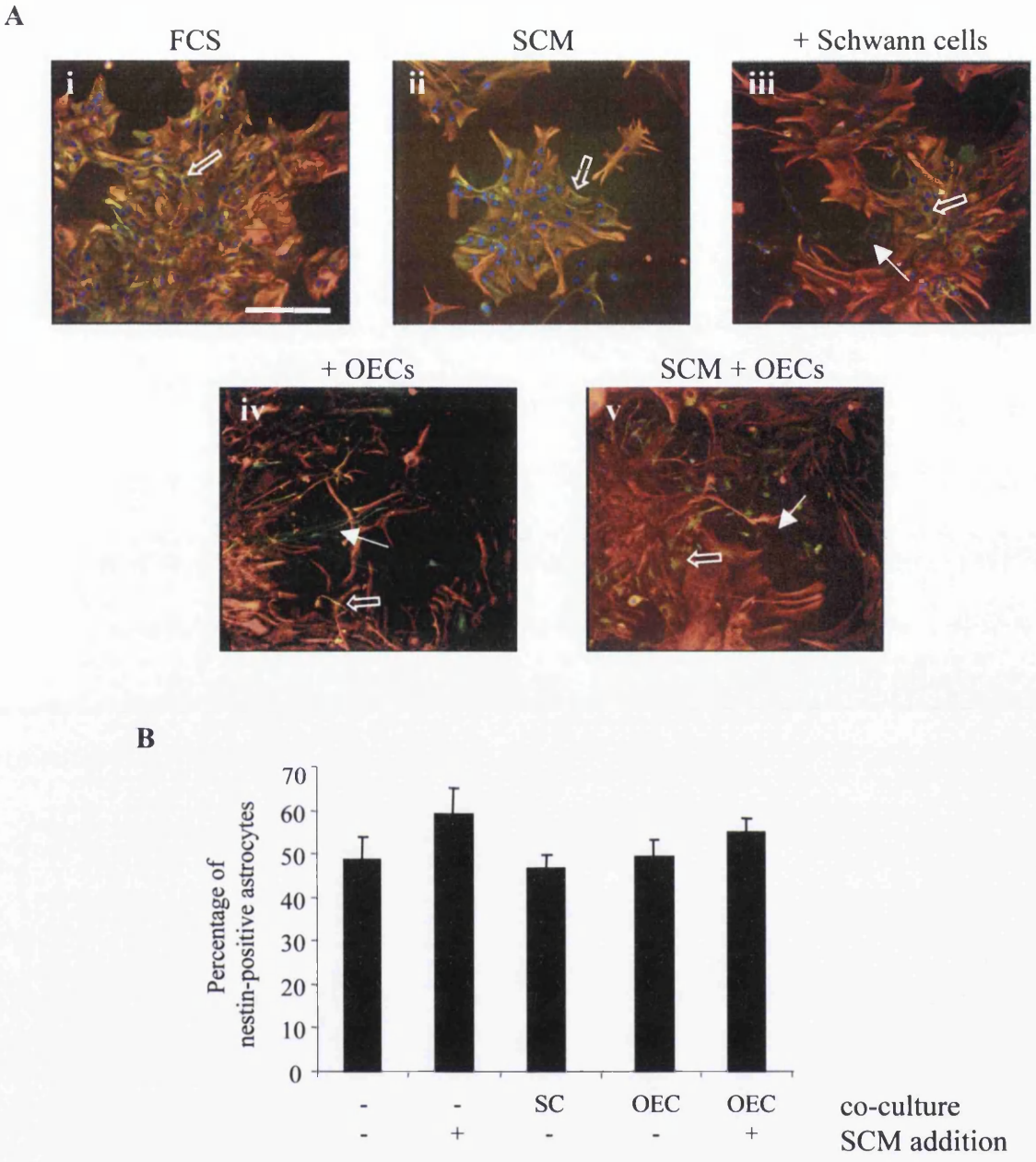

Figure 5.13. Nestin expression is unaltered by SCM treatment.

(A) Immunocytochemistry (GFAP-TRITC and nestin-FITC) and (B) quantification of nestin-positive astrocytes. Astrocytes were cultured alone in FCS (i) or SCM (ii), and in co-culture with Schwann cells (iii) or OECs (iv) in FCS, and also co-culture with OECs with SCM treatment (vi). (A) Nestin-positive astrocytes are indicated with an open arrow, and OECs and Schwann cells are indicated with a solid arrow. Scale bar = 200 μm. (B) The number of nestin-positive astrocytes did not vary significantly with treatment.

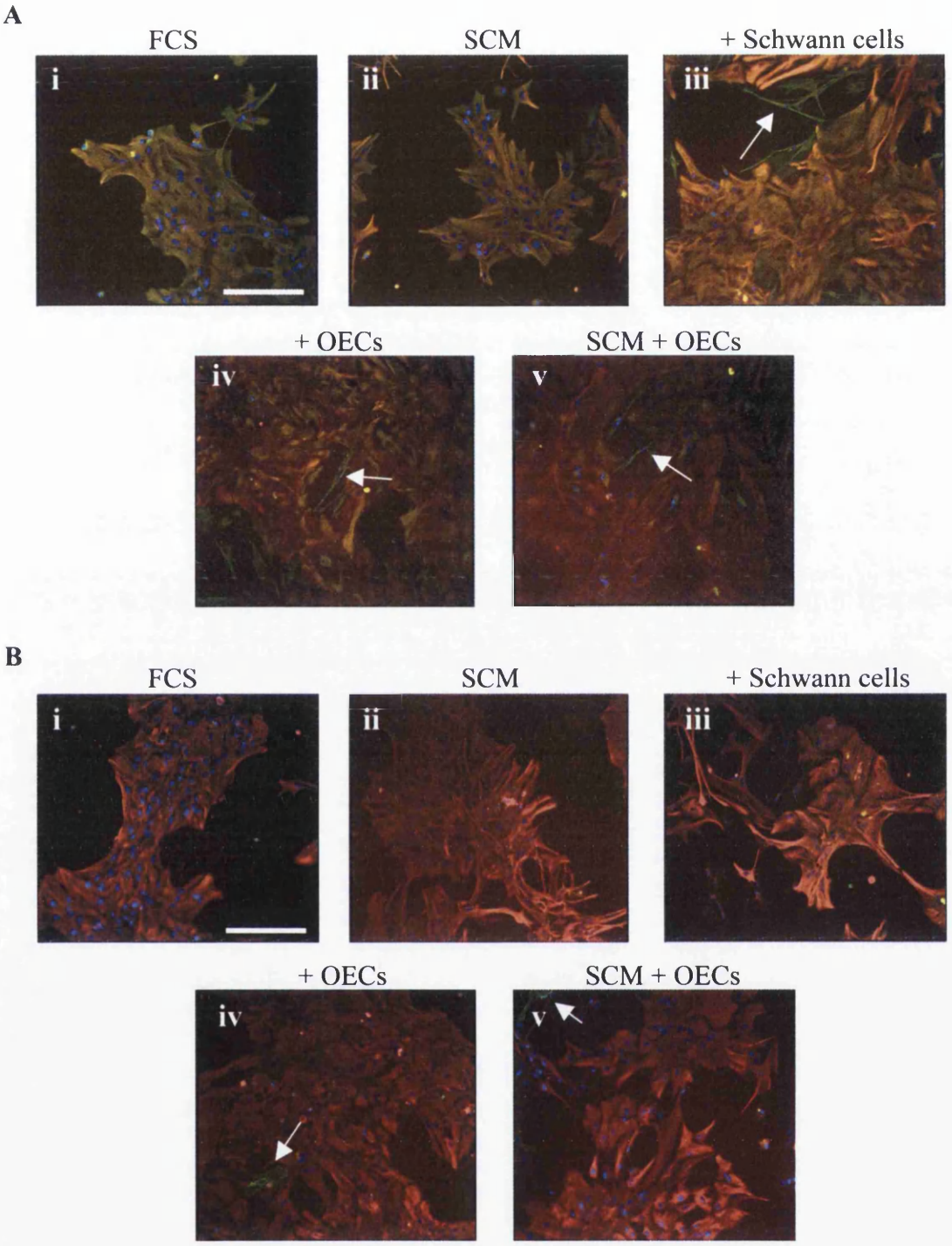

Figure 5.14. Vimentin and PSA-NCAM expression is unaffected by SCM treatment.

(A) Vimentin and (B) PSA-NCAM immunocytochemistry (FITC), with GFAP (TRITC). Astrocytes in all conditions tested (in FCS (i) or SCM (ii), and in co-culture with Schwann cells (iii), OECs (iv) and OECs with SCM (v)) were 100% vimentin positive, but lacked PSA-NCAM expression. Vimentin-positive Schwann cells and OECs, and PSA-NCAM-positive OECs, are indicated with white arrows. Scale bar = 200 μm.

subset of OECs with astroyte-like morphology; Franceschini and Barnett, 1996). These data suggest that nestin, vimentin and PSA-NCAM are not suitable markers for monitoring the astrocytic response of astrocytes in these assays.

5.2.9 Active component of SCM is trypsin-sensitive

In order to assess if the active factor within SCM is a protein, SCM was digested by the protease trypsin bound to agarose beads, as described in the Materials and Methods (section 2.1.7). The extent of proteolysis was assessed by SDS-PAGE (Figure 5.15A). The major band that could be seen in the SCM lane was transferrin (confirmed by mass spectrometry), which was succesfully reduced following trypsin digestion, producing a fragment of a lower molecular weight. The digested SCM was then used in both the astrocyte proliferation assay (Figure 5.15B) and OEC:astrocyte confrontations (Figure 5.15C) to assess function. In both assays, trypsin digestion of SCM reduced its activity. Astrocyte proliferation was reduced significantly from 24.9 +/- 3.1% after SCM stimulation, to 13.1 +/- 1.4% ($p<0.05$), although it was not decreased to levels seen with the control, DMEM-BS H/F, remaining significantly higher ($p<0.05$), presumably reflecting the incomplete digestion as seen in Figure 5.15A. Trypsinised SCM also failed to induce boundary formation in OEC:astrocyte confrontations. This confirms that a trypsin-sensitive component of SCM is responsible for the effect of SCM as seen in these assays. It cannot be excluded that residual trypsin, which could have come off the beads, may have influenced these results. However, due to the lack of effect of trypsin on cell adherence to the coverslips, this is probably unlikely.

5.2.10 Identification of protein components of SCM and OCM

In order to investigate the possible active components present in SCM, a proteomics approach was taken using both DMEM-BS H/F and OCM as controls. To achieve this, DMEM-BS H/F, SCM and OCM, collected from confluent Schwann cell and OEC cultures respectively, were concentrated by centrifugation using centricon filters to approximately

4X the initial concentration. Protein was precipitated from these media and cleaned using acetone prior to subjection to 2-dimensional gel electrophoresis (2D PAGE). The protein

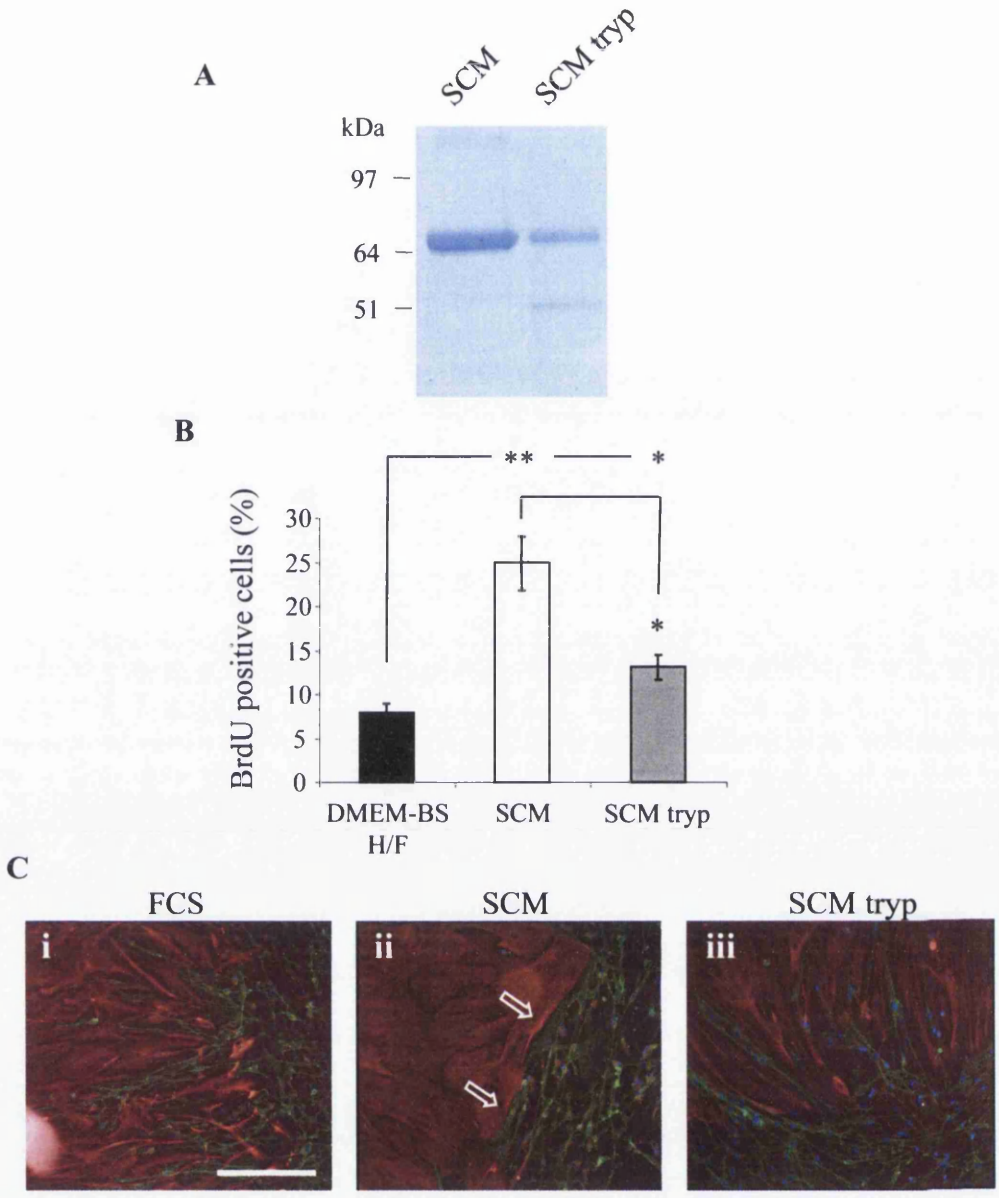

Figure 5.15. The active component of SCM is trypsin sensitive, suggesting it is a protein.

(A) SDS-PAGE gel stained with brilliant blue G-colloidal, showing breakdown of major protein bands following digestion with trypsin-agarose beads.
(B) Effect of digested SCM (SCM tryp) on BrdU assay (percentage of astrocytes taking up BrdU in 16 hours following treatment). Both SCM- and SCM tryp-treated sets have significantly greater proliferation compared to DMEM-BS H/H, but this is significantly different between SCM and SCM-tryp (*$p<0.05$, **$p<0.001$, $n=6$). (C) OEC/astrocyte confrontation assays treated with DMEM-10% (FCS, i), SCM-50% (SCM, ii) and digested SCM-50% (SCM tryp, iii; astrocyte (GFAP-TRITC), OEC ($p75^{NTR}$-FITC)). Digested SCM no longer induces boundary formation (boundaries indicated by open arrows) Scale bar = 200 μm.

content within the gel was assessed using a mass spectrometry-compatible fluoresent Supro orange dye (Figure 5.16). Several candidate proteins were present in SCM (all arrow heads, Figure 5.16B) but absent from both DMEM-BS H/F and OCM. These were excised from the gel, digested with trypsin, and identified by mass spectrometry (performed by Chris Ward). Problems arose from keratin contamination (black arrow heads), but possible candidates were identified as collagen alpha 1, in several locations (white arrow heads). Despite removal of BSA from the DMEM-BS media, an overloading protein band was present in the middle of each gel. This was identified as transferrin, a component of the DMEM-BS media.

5.3 Discussion

It has previously been shown using *in vitro* assays similar to those employed here that OECs and Schwann cells induce different responses in astrocytes (Lakatos et al., 2000), for example, astrocytes co-cultured with Schwann cells, but not OECs, were greatly enlarged. It was also seen that the expression of CS-PGs by astrocytes was enhanced significantly in Schwann cell/astrocyte cultures, but not in OEC/astrocyte cultures. My data confirmed that astrocytes become hypertrophic in the presence of Schwann cells and not OECs. However, CS-PG expression was not dramatically increased by the presence of Schwann cells. This may reflect a level of innate reactivity in the astrocytes used here, since CS-PG expression was already elevated in the control cultures compared to those documented in other studies (Lakatos et al., 2000). It has been remarked that astrocytes in culture tend to have a more reactive phenotype than their *in vivo* counterparts, as measured by expression of reactive markers such as vimentin (Bignami and Dahl, 1989). This was also confirmed by my data where all astrocytes were vimentin positive, irrespective of cellular treatment. Despite this, *in vitro* assays remain useful for measuring degrees of astrocytosis since many markers of reactivity, including CS-PG expression, were elevated significantly in the treated sets above those of control cultures. This has also been found in many other *in vitro* culture models of astrocytosis where expression patterns visibly alter following the induction of reactivity (Eddleston and Mucke, 1993; Wu et al., 1998).

Despite the relative clarity of *in vitro* studies, there is still some debate as to what degree these differences seen in OEC and Schwann cell interactions with astrocytes reflect the *in*

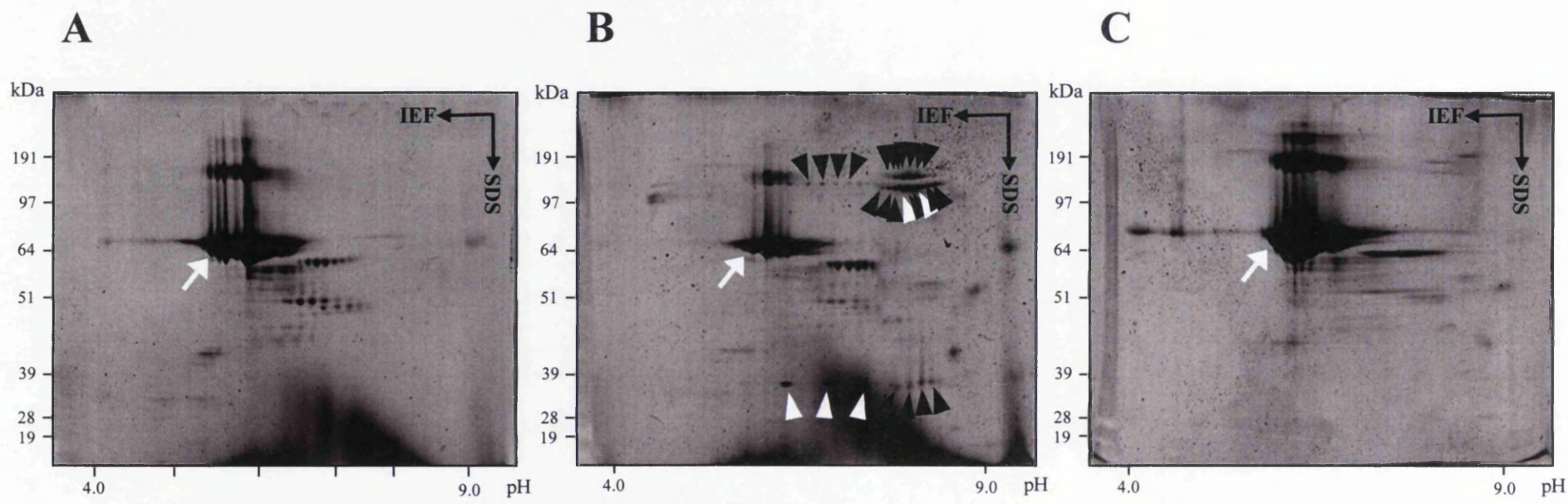

Figure 5.16. 2D gel showing protein content of DMEM-BS H/F, SCM and OCM.

DMEM-BS H/F (A), SCM (B) and OCM (C) were concentrated and subjected to 2D gel electrophoresis. Spots appearing in SCM but absent in both SATO H/F and OCM (all arrow heads) were sent off for identification by mass spectrometry. Some spots were identified as collagen alpha 1 (white arrow heads), others were contaminated with keratin (black arrow heads). Transferrin is indicated with a white arrow.

vivo environment following transplantation. Many studies have documented that following transplantation of Schwann cells, local astrocytes become reactive, upregulating both GFAP and CS-PGs (Plant et al., 2001, Takami et al., 2002; Lakatos et al., 2003a), and also that this response is greater than that induced by OECs (Verdu et al., 2001; Takami et al., 2002; Lakatos et al., 2003a). However, OECs induce more astrocytosis *in vivo* than *in vitro* (Lakatos et al., 2003a). Explanations for this discrepancy include damage caused during the actual transplantation procedure such as that caused by the needle tract or a response to the presence of injected matter within the CNS. In addition, other cells which regulate astrocytosis, such as macrophages or microglia, are noticeably absent from *in vitro* assays. These assays therefore measure the response of astrocytes purely to a controlled stimulus, rather than modelling the complex cellular interactions which occur *in vivo*. Furthermore, the injured CNS may have a greater reactivity to stimuli, due to a 'priming' mechanism such that following an injury, astrocytes are more sensitive to any further insult. This is supported by observations that following stab wound injuries, astrocytes located in distant regions from the lesion site, do display an enhanced level of reactivity (Mathewson and Berry, 1985; Moumdjian et al., 1991). Thus these astrocytes may be become more sensitive to further stimulation, such as transplantation.

Despite these drawbacks, *in vitro* models of astrocytosis still have the benefit of allowing us to dissect the various signalling events involved in this process using a well controlled and minimalist environment. In addition, the role astrocytosis plays in determining the ability of cells to migrate within astrocyte-rich areas can be directly addressed.

5.3.1 CS-PG expression

Despite the high expression of CS-56-immunoreactive CS-PGs in control astrocyte cultures (as mentioned above), a clear increase in CS-PG expression was still detectable following the addition of SCM. This media, obtained from confluent cultures of Schwann cells, might be more concentrated than that produced by the Schwann cells in co-culture, and therefore may reflect a concentration dependency upon the factors secreted by Schwann cells. In addition, this assay demonstrates that the reported increase in CS-PG expression in Schwann cell/astrocyte co-cultures (Lakatos et al., 2000), is not mediated by contact-dependent signals, but that secreted factors are sufficient.

In order to quantify the changes in CS-PG expression in these cultures, immunoblotting was used. However, limitations arose when using the CS-56 antibody since it binds to many different CS-PGs, resulting in a complex immunoblot profile which was difficult to interpret. It is for this reason, that the CS-56 antibody is generally considered poorly compatible with immunoblotting (Fidler et al., 1999; Moon et al., 2003), which lead me to use the neurocan antibody instead. This was more successful and gave a profile which correlated with the immunocytochemistry results, demonstrating that neurocan expression was elevated following treatment with both SCM and OCM.

In vivo studies have shown that CS-56 immunoreactive CS-PG expression is regulated differently in response to transplantation of either OECs or Schwann cells, being lower around OEC grafts than around Schwann cell grafts (Lakatos et al., 2003a). In contrast, the same study demonstrated that neurocan is upregulated to a similar level in response to both Schwann cells and OECs. This data is in agreement with my results presented in this chapter suggesting that Schwann cell-secreted and OEC-secreted factors are equally potent at stimulating neurocan expression. However, other studies reported no change in neurocan expression in response to Schwann cell grafting, despite noticeable changes in CS-56 (Plant et al., 2001). It remains to be addressed whether CS-56 immunoreactivity is increased in response to both OCM and SCM equally, as suggested by the immunocytochemical analysis here, or differently, as suggested by other Schwann cell and OEC co-culture experiments (Lakatos et al., 2000). This could be achieved using a clearer method than immunoblotting for quantification, such as pixel quantification of immunoreactivity images.

Previous experiments have shown that astrocytes express neurocan (Oohira et al., 1994: McKeon et al., 1999; Asher et al., 2000), and that the level of neurocan expression is regulated by soluble cytokines. They demonstrated that EGF and TGFβ caused an increase, whereas PDGF and IFNγ reduced neurocan expression (Asher et al., 2000). Using receptor tyrosine kinase inhibitors, I have shown that EGFR and PDGFR do not regulate neurocan expression in these assays. It remains to be seen whether other cytokines, such as TGFβ, are responsible for the stimulation caused by SCM and OCM. In support of this hypothesis, TGFβ expression was shown to be increased following a stab wound of the rat

spinal cord, with expression peaks correlating closely with expression of various CS-PGs, including neurocan (Tang et al., 2003).

5.3.2 Hypertrophic markers

Both the upregulation of GFAP and an increase in astrocytic area were seen in Schwann cell/astrocyte co-cultures and OEC/astrocyte co-cultures treated with SCM, thus these two markers of hypertrophy correlate. Support that these markers are dependent upon both the addition of SCM and OEC contact, as demonstrated in the co-cultures, comes from analysis of the astrocyte-OEC boundary in confrontation assays. Upon adding SCM to these cultures, GFAP expression was increased, and enlarged astrocytes were present, along the boundary where OECs contact the astrocytes. Likewise, evidence that Schwann cell/astrocyte confrontations may be providing both SCM and a necessary contact-mediated signal is provided by the fact that reactive astrocytes were mainly seen along the contact-boundary between Schwann cells and astrocytes (Figure 3.2). However, it can not be ruled out that Schwann cell contact alone may be sufficient to induce astrocytosis and therefore may be biochemically different to OEC contact which requires the addition of SCM.

The markers nestin and vimentin were also investigated since they have been shown to be additional markers of hypertrophy. Vimentin is developmentally regulated, being predominately expressed in immature astrocytes and progressively replaced by GFAP during differentiation (Dahl et al., 1981b). It remains, however, along with GFAP, as a hallmark of reactive gliosis (Dahl et al, 1981a). In addition, nestin, another intermediate filament protein which is mainly expressed by CNS progenitor cells (Lendahl et al., 1990; Dahlstrand et al., 1995), is also re-expressed in reactive astrocytes (Clarke et al., 1994; Frisen et al., 1995). However, these markers were not altered in the treated sets of astrocytes. One explanation for why vimentin was still expressed in all astrocytes is that the GFAP-vimentin transition has been reported to be incomplete in primary cultures (Bignami and Dahl, 1989). Additionally, it might reflect the purity of cultures where low levels of contaminating microglia, which produce many types of cytokines, could alter the astrocytic status, or may even be due to the presence of blood-derived factors present in

serum, from which astrocytes are usually shielded by the blood brain barrier (Eddleston and Mucke, 1993).

PSA-NCAM expression was investigated since it has been reported to be upregulated in some reactive astrocytes *in vivo* (Alonso and Privat, 1993; Nomura et al., 2000). However, in these cases, expression was localised to a subset of astrocytes from specific regions (Nomura et al., 2000) or following different types of injury (Alonso and Privat, 1993), and therefore it is not a generic marker for astrocytosis. Hence, its lack of expression in the cultures used here is not necessarily surprising, but instead may reflect the cortical source of these astrocytes, or the type of stimulation.

5.3.3 Induction of reactivity

It can be concluded from the data presented here that different signals are required for different aspects of the reactive response, i.e. they are independently regulated (see Table 5.1). Upregulation of CS-PG expression and an increase in astrocyte proliferation was dependent upon SCM alone, whereas hypertrophy and GFAP upregulation required OEC contact as well as SCM. Since Schwann cells alone can induce these responses in astrocytes, it can be speculated that Schwann cells not only provide the factors present in SCM, but also are the source of a contact-mediated signal which may or may not be fundamentally different from that provided by the OEC (see Figure 5.17A). This would help explain why previous SCM investigations reported no change in astrocyte morphology or GFAP expression following addition of SCM alone (Ghirniker and Eng ,1994). In these experiments, contact-mediated signals were absent, whether from Schwann cells or OECs.

In addition, my results may shed some light on the observed heterogeneity of astrocyte reactivity seen *in vivo* following injury, where not all astrocytes in a given area undergo a reactive response (Fitch and Silver, 1997). Despite the possibility of secreted factors being evenly distributed throughout a locality within the CNS, there may be variations in additional signals through contact with particular cells, or even ECM components.

Table 5.1. Markers of astrocytosis and their stimuli.

Marker of Astrocytosis	Stimulus					FGFR dependency
	SC	OEC	SCM	OCM	OEC + SCM	
Astrocyte size	↑	-	-	-	↑	√
GFAP expression	↑	-	-	-*	↑	N
CS-PG expression	↑	-	↑	↑	↑	-
proliferation	N	N	↑	-	↑	-

This table shows the specific astrocytic responses induced by different stimuli, and whether these astrocytic markers are dependent upon FGFR function. N = not addressed. (* as seen by immunocytochemistry).

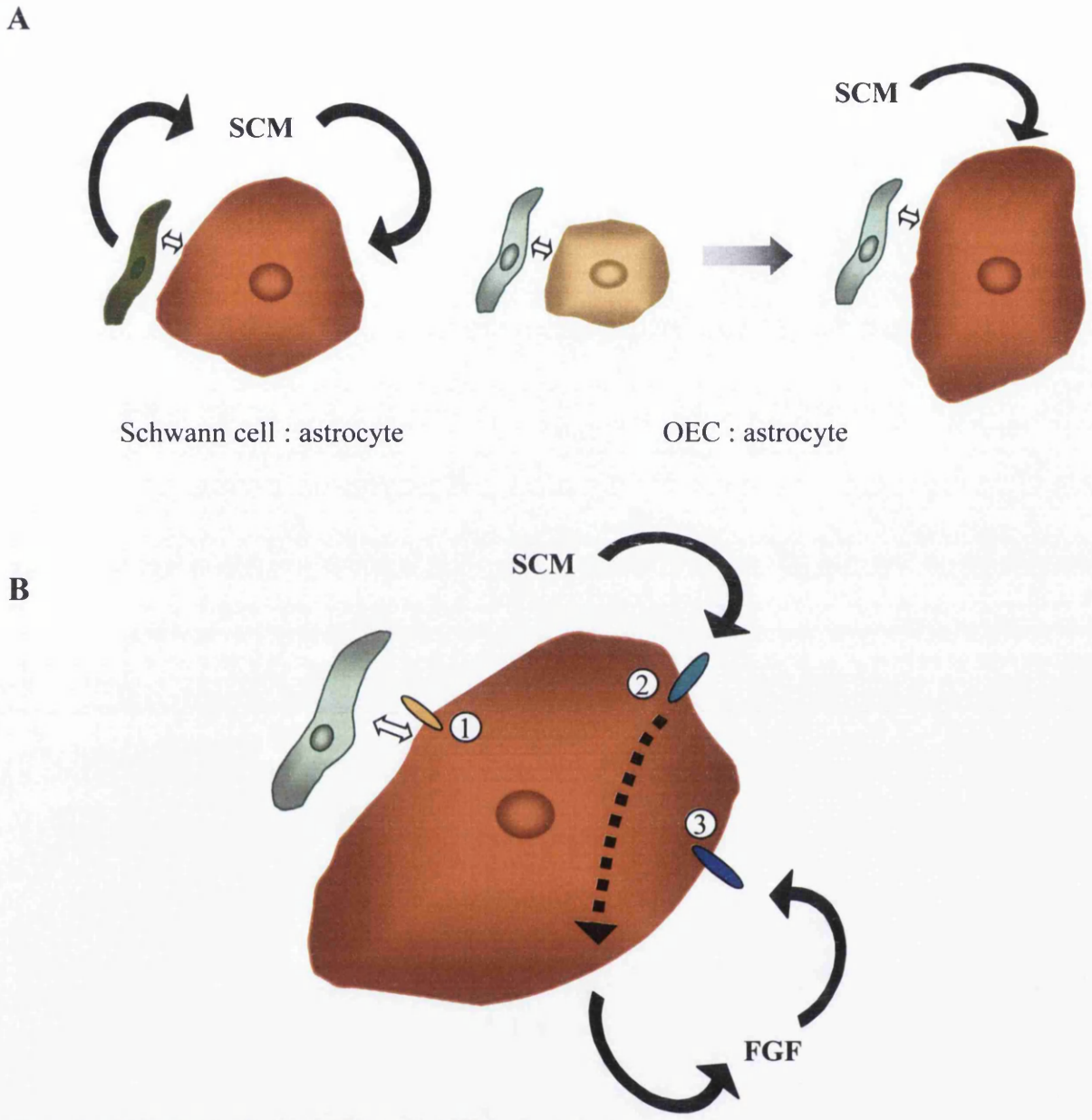

Figure 5.17 Hypothesis of SCM and FGFR function

(A) Schwann cells produce SCM and may provide a contact signal (since SCM alone is not sufficient for increase in GFAP or astrocyte size); OECs provide contact signal (which may or may not be the same as the Schwann cell contact signal), but require additional SCM for astrocyte response.

(B) Role of FGFR. 1, FGFR may interact with Schwann cell/OEC contact signal. FGFR may also interact with N-cadherin, mediating inhibition of migration, as well as induction of hypertrophy. 2, FGFR is involved in mediation SCM signalling to astrocytes. 3, FGFR may be involved in signalling downstream from SCM signal, such as an FGF autocrine loop, resulting in hypertrophic response.

⟺ Contact signal

⬭ FGFR

5.3.4 Identity of SCM factor

The active factor present in SCM, whether absent from OECs or merely expressed at lower levels, may be an example of a further difference between OECs and Schwann cells, providing more evidence that they are distinct types of glia.

Mass spectrometry was employed in an attempt to determine the identity of this factor. Analysis of differential protein spots, as identified by 2D PAGE, highlighted the presence of collagen alpha 1 in various positions. Due to its occurance in protein spots of very different molecular weights, it remains to be seen whether these spots correlate to different breakdown products or alternative splicing. It may in fact be a contaminant, although this could be ascertained by immunoblotting. As it was a rat protein, rather than human like the common contaminant keratin, this is unlikely. In addition, collagen is not reported to be a usual contaminant of 2D PAGE gels. Type IV collagen, which contains collagen alpha 1 fibrils, is produced by Schwann cells (Carey et al., 1983), however it is unclear whether OECs also produce it. Unlike Schwann cells, OECs have been reported to lack a basal lamina and collagen fibrils (Wozniak, 1993), although collagen IV is expressed along the olfactory nerve pathway (Doucette, 1996). Whether collagen alpha 1 would explain some of the observed effects of SCM remains to be tested. Collagen has been implicated in the regulation of cellular migration since type IV collagen inhibits migration of MCF-7 and in MDA-MB-231 breast cancer cell lines (Sisci et al., 2004). In addition, type I collagen has been shown to differentially regulate cell migration in neutrophils, where migration was promoted, and in macrophages, whose migration was inhibited (Kozlov et al., 1999). Thus collagen may pay a role in determining the ability of Schwann cells to migrate, particularly when in contact with astrocytes.

Other possible candidates for mediating the effects of SCM are the various cytokines which have been shown to induce astrocytes to become reactive (Eddleston and Mucke, 1993). Many of these factors have been reported to be produced by Schwann cells under certain conditions, such as Wallerian degeneration, for example, IL-1 (Bergsteinsdottir et al., 1991; Skundric et al., 1997; Rutkowski et al., 1999), IL-6 (Murwani et al., 1996; Rutkowski et al., 1999) and TNFα (Murwani et al., 1996; Wagner and Myers, 1996). Whether these factors are also produced by OECs is at present unknown, and may

highlight another similarity or difference between the two glia. Due to the high potency of these molecules, very low concentrations would be necessary to mediate these effects, and thus they might not be present at levels high enough for detection using 2D electrophoresis, as performed here.

5.3.5 Role of N-cadherin

The nature of the contact-mediated signal between OECs and astrocytes is also unknown. Based on previous investigation of the role of N-cadherin in glial cell interactions, it was postulated that the differential function of N-cadherin detected between Schwann cells and OECs make it a possible candidate. It is possible that the variability in N-cadherin function depends upon the presence of soluble factors in SCM, which may bind to N-cadherin-interacting receptors, or even regulate N-cadherin directly. It is therefore important to assess if the role of N-cadherin is involved in simple adhesion, or whether it also functions to induce astrocytosis. Based on the evidence provided here, it appears that N-cadherin is unlikely to be the contact-mediated signal necessary for induction of hypertrophy since removal of N-cadherin using siRNA did not reduce the average astrocyte area in Schwann cell co-cultures (Figure 4.13), nor did stimulation of astrocyte N-cadherin using stimulatory peptides in the presence of SCM compensate for OEC contact.

It remains to be seen if, and how, astrocytosis and adhesion are related. It can be seen that the disruption of N-cadherin-mediated adhesion prevents boundary formation in confrontation assays (see Chapter 4), and that such boundary formation is promoted by inducing astrocytosis. Two possibilities could therefore exist. Firstly, astrocytic hypertrophy may prevent other cells from entering astrocyte areas due to the formation of a physical barrier through which these cells can not penetrate. That N-cadherin expression is upregulated in reactive astrocytes (Vazquez-Chona and Geisert, 1999; Figure 5.12), may suggest that such a barrier is N-cadherin rich and that cells may form strong adhesions to this barrier, preventing further migration. Secondly, evidence that the role of N-cadherin is more important than merely creating a physical barrier is provided by the observation that siRNA-treated Schwann cells are able to penetrate the astrocyte domains even when enlarged astrocytes are present. Therefore it appears that the presence of N-cadherin on Schwann cells is a more important determinant of boundary formation than the presence of

hypertrophic astrocytes. It may be that hypertrophy functions only to enhance the likelihood that cells will adhere strongly to astrocytes in an N-cadherin-dependent manner, through a greater binding site area (hypertrophy) and more binding substrate (N-cadherin upregulation) (see Discussion, Figure 6.1). However, since N-cadherin functionality is different between OECs and Schwann cells, it remains a possibility that SCM factors, normally present in Schwann cell cultures, could be modulating N-cadherin function. This was ruled out since addition of SCM to OEC cultures, despite inducing boundary formation in confrontation assays, did not affect N-cadherin function as assessed by migration and adhesion assays. However, since confrontation assays test the ability of glial cells to migrate through an astrocytic territory, whereas migration assays test the ability of cells to migrate upon astrocytes (discussed in Section 3.3.4 and 3.3.5), these assays may be measuring different effects and therefore not be comparable.

Neurocan has been shown to regulate N-cadherin function through the neurocan receptor, GlcNAcPTase (Li et al., 2000). Thus, an upregulation of both neurocan and N-cadherin in SCM-treated astrocytes could promote neurocan-N-cadherin interactions when OECs contact astrocytes in the presence of SCM. However, neurocan stimulation of N-cadherin has been shown to promote rather than inhibit migration and thus is not likely to be the mechanism at work here (Li et al., 2000).

5.3.6 Role of FGFR

Inhibition of FGFR was shown to be involved in the induction of hypertrophy in OEC/astrocyte co-cultures, since inhibition significantly reduced the increase in astrocytic area in response to SCM. FGFR inhibition also prevented the formation of a distinct boundary in OEC/astrocyte confrontation assays when SCM was added. These two phenomena may be reflecting the same response, since the astrocytes in the confrontation assay would also have reduced hypertrophy following FGFR inhibition. Therefore, reduced hypertrophy could prevent the astrocytes from forming an impenetrable barrier to OEC invasion, allowing OECs to interdigitate with astrocytic processes. However, the reduced numbers of OECs able to penetrate the astrocyte domains compared to control (FCS-treated) cultures might reflect the effect of SCM on other aspects of astrocytosis, such as CS-PG, or even N-cadherin, upregulation.

It appeared from the immunocytochemistry study, however, that CS-PG expression was not regulated by FGFR. Therefore, the CS-PG expression resulting from SCM treatment is unlikely to be changed in the inhibitory and permissive (FGFR-inhibited) confrontation assays. This demonstrates that CS-PG expression probably does not regulate the ability of OECs to enter astrocyte domains, or it is at least not a major determinant, with hypertrophy playing a more significant role. However, in contrast, a recent paper reported that CS-PGs do play a critical role in determining the ability of Schwann cells to enter astrocytic areas, using confrontation assays similar to those employed here (Grimpe et al., 2002). Whether this highlights another difference between Schwann cells and OECs, in that Schwann cell migration may be more susceptible than OEC migration to CS-PG inhibition, or whether CS-PGs do play a significant role in OEC/astrocyte interactions, but less than that played by hypertrophy, remains to be determined.

The exact mechanism by which FGFR mediates SCM-induced effects in confrontation assays needs further investigation. FGFR can regulate the adhesive nature of adhesion molecules, such as NCAM and N-cadherin (Williams et al., 1995; Utton et al., 2001; Suyama et al., 2002), and thus may be influencing the adhesion of OECs to astrocytes. However, SCM treatment had no significant effect on OEC adhesion to astrocytes as assessed by the adhesion assay. In contrast, the evidence does suggests that FGFR is involved in the induction of astrocytic hypertrophy. Whether FGF-2 is responsible for the FGFR-dependent induction of astrocytosis remains to be seen. It is supported by the observation that injecting FGF-2 into cerebrospinal fluid induces astrocytosis (Goddard et al., 2002), and that Schwann cells have been reported to express FGF-2 in culture (Meisinger et al., 1996). However, preliminary studies suggested that addition of FGF-2 to OEC/astrocyte confrontations did not induce boundary formation, and therefore did not compensate for SCM, perhaps by requiring other factors (Figure 5.2Avii and viii). Whether FGFR function is involved in mediating direct SCM-stimulation itself, or whether SCM stimulates astrocytes, which as a result require downstream FGFR-dependent autocrine mechanisms, remains to be determined (see Figure 5.17B).

5.3.7 Summary

In conclusion, Schwann cells secrete factors which determine the astrocyte response, and in turn may inhibit the migration of Schwann cells into astrocytic areas. This is demonstrated by the ability of Schwann cell-secreted factors, present in SCM, to regulate the entry of OECs into astrocytic areas, and thus suggesting that they may be responsible for the lack of migration seen in Schwann cell/astrocyte confrontation assays. Since SCM affected astroctic hypertrophy, but did not significantly modulate OEC adhesion or migration upon astrocytes, this supports a role for astrocytic reactivity in determining the ability of glial cells to penetrate astrocyte-rich areas. It cannot be ruled out, however, that hypertrophy may be providing more than just a physical barrier to OEC migration, and that astrocytes may also be producing factors in response to SCM which regulate cellular migration. In addition, GFAP has been shown to regulate the ability of neurons to migrate upon astrocytes, despite it being an intracellular component, suggesting that astrocyte inhibition may function by a mechanism other than just adhesion (Menet et al., 2000).

The influence of SCM upon astrocytosis obviously has implications upon the use of Schwann cells in transplantation, where astrocyte responses may influence the ability of Schwann cells to coexist alongside them. Once the nature of these factors is determined, they may prove to be potential targets to improve Schwann cell/astrocyte interactions following transplantation. In addition, the presence of Schwann cells which can invade the injured CNS, known as Schwannosis (Franklin and Bakemore, 1993; Bruce et al., 2000; King et al., 2003; Ramer et al., 2004a), may add to the reactive environment of the CNS. Understanding the processes involved in inducing and maintaining astrocytosis in more detail may allow us to manage Schwannosis more effectively, and prevent an inhibitory environment to regeneration from developing.

CHAPTER 6

General Discussion

Central nervous system (CNS) pathologies are often very debilitating due to the inability of the CNS to undergo repair following damage. One such pathology is spinal cord injury (SCI) which affects almost a thousand new sufferers in the UK every year (data from the International Campaign for Cures of Spinal Cord Paralysis). The severity of SCI is very variable, depending on the type and location of the injury. Spinal cord injuries are classified as paraplegic and tetraplegic, paraplegia typically resulting from thoracic injuries, and tetraplegia from cervical injuries. Furthermore, SCI can be further classified as either complete or incomplete, which may affect the degree of recovery. CNS function can also be affected by demyelination, classically seen in diseases such as multiple sclerosis.

Many different potential therapies are being investigated at present to promote repair of the damaged CNS, ranging from growth factor delivery to improve survival rates of neurons and promote axonal outgrowth, to antibodies and pharmacological agents against inhibitory factors. However, one approach which has attracted a lot of attention over recent years is the use of cellular transplantation to mediate repair.

Although a range of cells have been studied for cellular transplantation, including oligodendrocyte progenitor cells (OPCs) and neural stem cells, this thesis has been concerned with two possible candidates, Schwann cells and olfactory ensheathing cells (OECs). Both Schwann cells and OECs have been put forward as potential candidates for transplant-mediated repair of both demyelinating diseases and SCI (Franklin and Barnett, 1997; Raisman, 2001; Wewetzer et al., 2002). Schwann cells and OECs share many properties in common, but there is still an open debate as to which is the superior cell type for transplantation therapies. One of the major differences between Schwann cells and OECs, which may be the critical test of which is the better cell, is the difference in their abilities to interact with astrocytes. This has been seen in both *in vitro* and *in vivo* injury models, where Schwann cells have been shown to exhibit two major properties which affect their candidature: (1) poor survival and migration within astrocytic environments (Ramon-Cueto et al., 1998; Iwashita et al., 2000); and (2) the ability to induce reactive astrocytosis (Ghirniker and Eng, 1994; Lakatos et al., 2000; Plant et al., 2001; Takami et al., 2002). This lack of migration and survival would seriously diminish the potential of Schwann cells to reach an appropriate site for repair, and remain there long enough to mediate either axonal regeneration or to remyelinate demyelinated axons. In addition, astrocytic reactivity

induced by Schwann cells could limit the ability of the host environment to support regeneration, since astrocytosis and the subsequent formation of a glial scar is inhibitory to repair (Clemente, 1964; Fawcett and Asher, 1999). Thus, a balance must be maintained after cellular transplantation between the repair-promoting properties of the transplant and the inhibitory environment of the host response.

In contrast to Schwann cells, OECs have been demonstrated to co-exist with astrocytes following transplantation in a more favourable manner, being able to migrate within astrocyte-rich areas (Ramon-Cueto et al., 1998; Li et al., 1998; Gudino-Cabrera et al., 2000; Lakatos et al., 2000), whilst inducing a less reactive astrocytic response (Lakatos et al., 2000, 2003a; Verdu et al., 2001). However, in some studies, OECs were not able to migrate extensively but were instead confined to the site of injection (Smale et al., 1996; Lakatos et al., 2003a). In the same way, Schwann cells can sometimes migrate within the CNS, but only following injury (Franklin and Blakemore, 1993; Bruce et al., 2000; Ramer et al., 2004a). Reasons for these discrepancies may be due to the integrity of the host tissue, whereby both OECs and Schwann cells can migrate only if there are appropriate pathways for migration such as along blood vessels, or through perivascular space (Franklin and Blakemore, 1993). However, OECs do appear to be a better candidate than Schwann cells as assessed by their inherent migratory capacities through astrocytes when compared side-by-side (Franklin and Barnett, 1997; Ramon-Cueto et al., 1998; Lakatos et al., 2000).

In order to maximise the use of cells for transplantation therapies, it would therefore be beneficial to promote their migration. This is important since the site of injection is not necessarily the best place for the cells to exert their capacity for repair, but if they can migrate away they may be able to provide continuous support for a regrowing axon across the injury site to its potential target. In addition, demyelination in MS occurs at multiple plaques, which could be treated with a single transplant if these cells could successfully migrate. A need for efficient migration was demonstrated from a study using Schwann cell-seeded grafts transplanted into a transected spinal cord, where the Schwann cells were unable to leave the graft. Although they promoted the regeneration of axons into the graft, these axons could not subsequently leave the graft to re-enter the host tissue (Ramon-Cueto et al., 1998). This lack of axonal outgrowth may have resulted from the level of growth factors being higher and more favourable within the graft, and also due to the

occurrence of glial scarring at the graft edges. For these reasons, if the Schwann cells could be encouraged to migrate away from the graft, perhaps even forming a trajectory from the graft to the axon target, then they may be able to promote repair and regeneration through either the secretion of growth factors beyond the graft, or by providing a permissive substrate or environment. Interestingly, the limitation of axons to exit the graft was overcome by the transplantation of OECs at the graft-host interface which allowed axons to re-enter the host, perhaps by the mechanisms mentioned above. It would therefore be advantageous to improve the migratory capacity of transplanted cells in order to enhance their regenerative properties.

For optimal repair, another consideration would be to keep the reactivity of the host in response to the transplant to a minimum, in order to maintain a permissive astrocytic environment for regeneration. For this reason, it is crucial to have an understanding of factors which trigger the reactive response, and how this may differ between Schwann cells and OECs. Furthermore, an increased knowledge of these processes may allow us to manage the reactive environment effectively, and therefore promote the migration of transplanted cells within the host (in the absence of a scar), in addition to enhancing the supportiveness of the host environment to repair.

From many studies in the literature, OECs appear to be the stronger candidate for transplantation based on the above criteria of migration and astrocyte reactivity (Franklin and Barnett, 1997; Lakatos et al., 2000; Wewetzer et al., 2002). This support for OECs, however, has not proved to be grounds on which to abandon the idea of using Schwann cells for transplantation.

In order that transplantation therapies can be translated to the clinic, it would be helpful to have an autologous supply of cells. This would avoid complications arising from xenotransplantation, including both the need to immunosuppress the patient in order to avoid rejection of the graft, and also the potential for zoonoses. Schwann cells are more easily accessible from peripheral nerve sources than OECs, which would require a highly invasive procedure to gain access to the olfactory bulb. This picture is beginning to change, however, due to the newly emerging peripheral sources of OECs from the olfactory mucosa (Au and Roskams, 2003). In addition, culture conditions at present may limit the number

of autologous OECs which can be cultured from the patient before transplantation of sufficient numbers (Barnett et al., 2000), although it may be possible to overcome this by finding appropriate growth factors. This is not so much of a problem for Schwann cells, where high numbers can easily be grown (Rutkowski et al., 1995).

In addition, Schwann cells have proved to be superior to OECs in some models of repair such as remyelination of dorsal root ganglion neurons under certain culture conditions (Plant et al., 2002) and in promoting locomotor recovery following a contusion injury (Takami et al., 2002). OECs and Schwann cells may also be able to compliment each other as a therapy, as in the study using both Schwann cells and OECs to promote axonal outgrowth discussed above (Ramon-Cueto et al., 1998). For these reasons, it may be beneficial to modify Schwann cell behaviour to function more like OECs in terms of migration and induction of reactivity. This would also allow us to make full use of the more accessible source of cells for transplantation (Franklin and Barnett, 2000).

In order (1) to assess the differences between Schwann cells and OECs in more detail regarding their potential as transplantation candidates, and (2) to identify mechanistic differences between them which may be a basis for improving Schwann cell transplantation therapies, I have investigated some of the molecular mechanisms which determine why OECs and Schwann cells interact differently with astrocytes.

My study has demonstrated that N-cadherin function is significant in determining the abilities of Schwann cells and OECs to migrate and adhere in the presence of astrocytes (Chapter 4). In particular, removal of N-cadherin allowed Schwann cells, which are normally inhibited, to successfully penetrate astrocyte areas in confrontation assays. Interestingly, despite N-cadherin being similarly expressed and associated with cell-cell contacts in both OECs and Schwann cells, it functions differently in these cells. It remains to be definitively determined whether N-cadherin function is regulated differently within the two cell types or whether extracellular factors, such as the status of the astrocyte to which they are binding, or the presence of extracellular modulators, may determine this outcome. However, it is likely to be a functional inherent difference between the cell types since homotypic adhesion varied in terms of both adhesion strength and N-cadherin dependency.

Furthermore, an investigation of factors involved in determining the astrocytic response to OECs and Schwann cells highlighted the role of Schwann cell-secreted factors (Chapter 5). It was also seen that the various aspects of astrocytosis, such as an increase in astrocytic area, and glial fibrillary acidic protein (GFAP) and chondroitin sulphate proteoglycan (CS-PG) upregulation, are regulated by different signals, whether by Schwann cell-conditioned media (SCM) alone, or also requiring contact-mediated signals. Thus, astrocytic reactivity is not an all or nothing response, but can be broken down into several measurable events that are regulated differently (see Table 5.1). It was also concluded that this astrocytic response was, in addition to N-cadherin function, another determining factor of the ability of co-cultured cells to migrate within astrocyte territories (see Figure 6.1). This was demonstrated in two ways: (1) by induction of hypertrophy in OEC/astrocyte confrontation assays which prevented OEC infiltration, and (2) by reducing this hypertrophy using an FGFR inhibitor, allowing more OECs to migrate through astrocytic areas.

A connection between N-cadherin function and the astrocytic response, if there is one, has not yet been determined. N-cadherin did not appear to be necessary for the initiation of astrocytosis itself. However, the ability of glial cells to successfully penetrate astrocytic areas was dependent upon both N-cadherin adhesion and the astrocytic response. In addition, astrocyte levels of N-cadherin were upregulated in response to SCM treatment, in agreement with studies that showed its upregulation in hypertrophic astrocytes following injury (Vazques-Chona and Geisert, 1999). This may facilitate the astrocytes ability to reform a syncitium between tightly bound astrocytes, which can effectively seal off the injury site and become impermeable to cellular invasion (Fawcett and Asher, 1999; Shearer and Fawcett, 2001). In this way, it remains possible that SCM treatment of confrontation assays results in increasing the effect of reactive astrocytes acting as a physical barrier to penetration. Thus, both their increased size and their expression of N-cadherin synergise in preventing Schwann cells from entering astrocyte territories. Alternatively, it is a possibility that SCM factors could regulate N-cadherin function, either directly, or indirectly via other upregulated molecules (possibly CS-PGs). In conclusion, both N-cadherin, or its various signalling components, and the putative factors secreted by

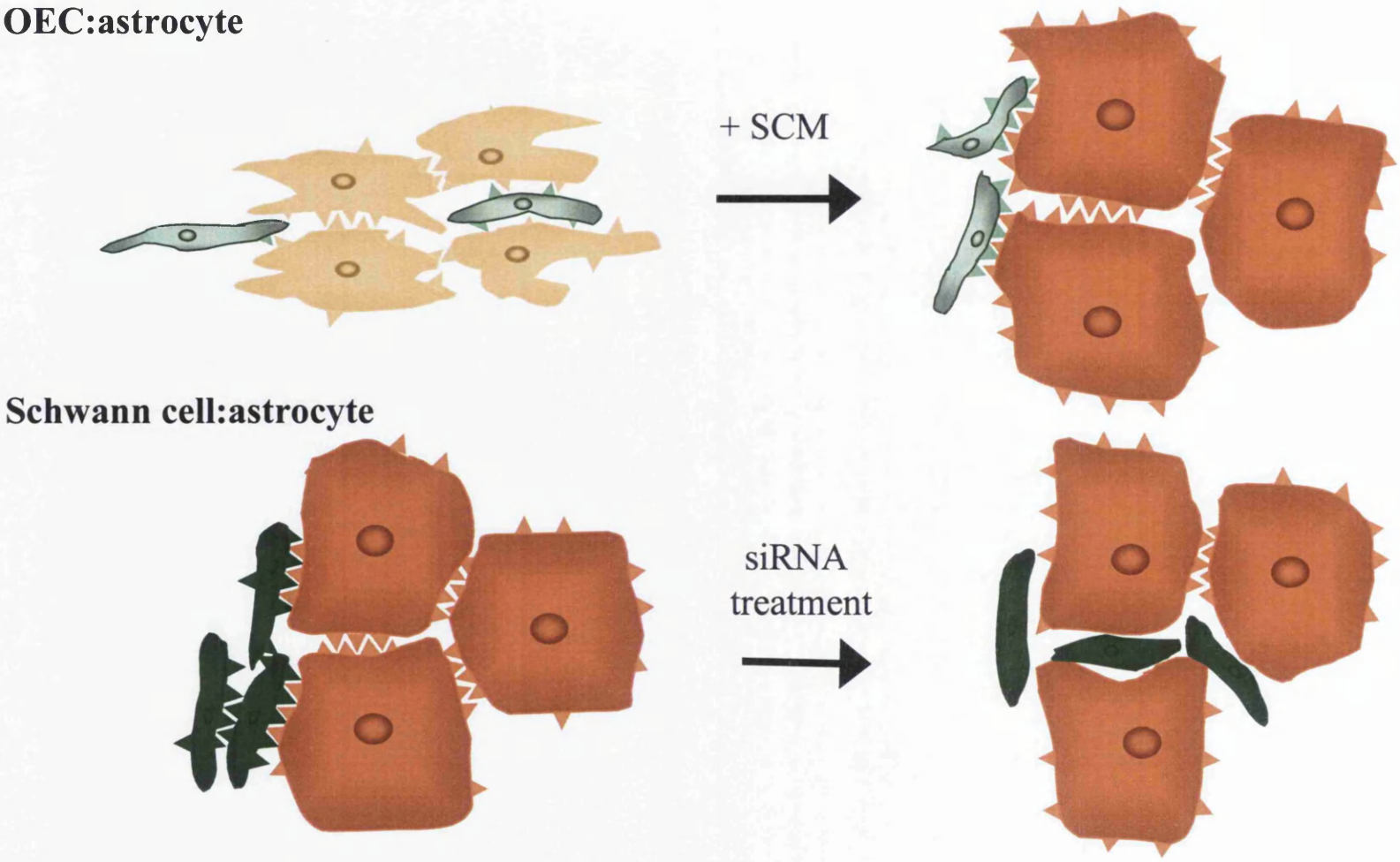

Figure 6.1 Schematic of confrontation assay interactions

Addition of SCM to OEC:astrocyte confrontations induces astrocytic hypertrophy, preventing migration of OECs into astrocyte domains due to barrier effect of large, N-cadherin-expressing astrocytes.
Removal of N-cadherin in Schwann cell:astrocyte confrontations, allows migration of Schwann cells into hypertrophic astrocyte-rich territory, despite presence of enlarged astrocytes.
N-cadherin represented by triangles (colour reflecting corresponding cell).

Schwann cells, now offer themselves as potential targets for intervention in order to improve the efficacy of transplant-mediated repair.

An understanding of how Schwann cells can induce astrocytosis would not only benefit success of repair following transplantation, but may also allow management of the reactive injury site by reducing the effects of endogenous Schwann cells which can infiltrate the injured spinal cord. It has been well documented that following disruption of the glia limitans, Schwann cells from the dorsal root are able to invade the CNS environment of the spinal cord (Schwannosis). This has been shown in both patients (Bruce et al., 2000), and in experimental models of CNS injury (Franklin and Blakemore et al., 1993; Ramer et al., 2004a). In addition, following transplantation of fibronectin mats into a spinal cord lesion, they were also shown to be subsequently infiltrated by endogenous Schwann cells (King et al., 2002). Not only does the presence of these Schwann cells potentially add to the induction of astrocytosis within the injured CNS, but also complicates the interpretation of experimental models. Resultant regeneration following transplantation experiments might not be attributable to just the transplant itself, but may result from the presence of these often unidentifiable invading cells. These cells may also be recruited in greater numbers as a response to the presence of the transplant, as has been demonstrated in a crush injury of the spinal cord, where the transplantation of OECs enhanced the number of Schwann cells invading the lesion site (Takami et al., 2002; Ramer et al., 2004a). This presence of both Schwann cells and OECs within the CNS may increase the likelihood that both the OEC-contact signal and Schwann cell-secreted factors, as has been shown in this thesis to induce astrocytosis, will be present together.

Due to the presence of recruited endogenous cells, and to determine the precise mechanisms by which transplants promote regeneration, there is, therefore, a need for better labelling techniques of transplanted cells. It is important that this label persists within subsequent cellular generations in order to successfully monitor the fate of transplant-derived cells. Previous studies identified transplanted OECs by $p75^{NTR}$ immunolabelling, sometimes with GFAP and S100 (Li et al., 1997, 1998; Takami et al., 2002; Plant et al., 2003), but this did not allow for reliable assessments to be made about OEC survival. For example there is the possibility of losing these markers due to differentiation, as occurs to $p75^{NTR}$ which is downregulated upon myelination. It was also not possible to distinguish the transplant

from endogenous Schwann cells present in the spinal cord (Plant et al., 2003). Similar results were also found following Schwann cell transplantation studies (Li and Raisman, 1997; Takami et al., 2002). Recently, many groups have tried to overcome these limitations by labelling cells with cell tracer agents such as cell tracker green (Nash et al., 2002), CFDA (Imaizumi et al., 2000), or Hoechst (Ramon-Cueto et al., 1998, 2000). These labels are good for short term studies, but with cell divisions they are diluted to undetectable levels, and there is also a possibility that they can leak and be actively taken up by phagocytotic cells, or absorbed passively by other surrounding cells. In order to allow long term detection of the fate of transplanted cells, viruses have been successfully used to label cells before transplantation, allowing detection for over 4 weeks following transplantation. Methods used include adenovirus transfection of cells with green fluorescent protein (Li et al., 2003) and retrovirus transfection of cells with β-galactosidase (Lakatos et al., 2003a; Riddell et al., 2004). In addition, it has recently been demonstrated that labelling of OECs with superparamagnetic iron oxide (SPIO) permits tracing with magnetic resonance imaging for at least 2 months following transplantation into spinal cord (Lee et al., 2004).

The potential use of OECs for repair has been supported by successful transplantation experiments demonstrating their benefit for promoting both axonal regeneration (Ramon-Cueto et al., 1994, 2000; Smale et al., 1996; Li et al., 1997, 1998, 2003; Lu et al., 2002; McDonald et al., 1999; Navarro et al., 1999) and subsequent functional recovery (Navarro et al., 1999; Ramon-Cueto et al., 2000; Taylor et al., 2001; Lu et al., 2002; Li et al., 2003). However, despite the case for OECs being superior to Schwann cells due to their better compatibility with astrocytes, there may still be limitations to the use of OECs. Not all studies confirmed the successful benefits of OEC transplantation for promoting regeneration (Ramer et al., 2004b; Riddell et al., 2004), with several studies suggesting that OECs were actually inferior to Schwann cells (Plant et al., 2002; Takami et al., 2002). It is likely that the high variability in results may reflect the equally variable OEC preparations and injury models being used to test this principle. As a result, there is a need for clarity in defining which injury model OEC transplantation better suits, and what kind of OEC preparation is most successful.

For example, the tissue source from which OECs are derived often varies. Most studies have used OECs obtained from adult animals and purified by immunopanning with $p75^{NTR}$

(Ramon-Cueto and Nieto-Sampedro, 1994; Navarro et al., 1999); whereas others have used postnatal animals which were purified by fluorescent-activated cell sorting (FACS) using the O4 antibody (Lakatos et al., 2003a; Riddell et al 2004), or have even used OECs from embryonic tissue (Smale et al., 1996). Furthermore, the tissue source of OECs can vary. Most studies have used OECs obtained from the olfactory bulb (Smale et al., 1996; Ramon-Cueto et al., 1998; Navarro et al., 1999; Plant et al., 2002, 2003; Li et al., 2003; Riddell et al., 2004). In recent years, however, a more peripheral source has been found in the lamina propria (Au and Roskams, 2003), which has been used successfully to promote regeneration (Ramer et al., 2004a).

Another variation which could arise between studies is the phenotypic heterogeneity of the OEC population transplanted. The OEC population is not homogenous, but instead has been shown to consist of several different phenotypes both *in vivo* and *in vitro*, which have been defined both morphologically and antigenically (Barnett et al., 1993; Franchescini and Barnett, 1996). Whether OECs obtained from different parts of the peripheral olfactory system possess characteristics of different OEC phenotypes remains to be seen. Studies have reported that OECs from the lamina propria consisted of two phenotypes similar to the two phenotypes found for olfactory bulb OECs, although they also expressed a novel combination of cellular markers (Au and Roskams, 2003). In addition, purification techniques may select for more of one phenotype than the other, for example FACS purification using O4 antibody led to a population consisting of both $p75^{NTR}$-positive and PSA-NCAM-positive OECs (Franceschini and Barnett, 1996), whereas immunopanning with $p75^{NTR}$ might result in a purely $p75^{NTR}$-positive population. However, due to the great plasticity of OECs (Franceschini and Barnett, 1996; van den Pol and Santarelli; 2003; Vincent et al., 2003), it may be that the final OEC population would more likely reflect the culture conditions in which they were grown rather than their position *in situ* or even the method of purification. This is supported by the observation of both spindle-shaped and flat-shaped OECs following $p75^{NTR}$ immunopanning (Smale et al., 1996; Lakatos et al., 2003b). However, the question remains as to which OEC phenotype best supports axonal repair.

There is also debate over the best cellular composition which facilitates regeneration following transplantation. Pure OEC populations have been used in most studies (Ramon-

Cueto and Nieto Sampedro, 1994; Li et al., 1998; Navarro et al. 1999; Ramon-Cueto et al., 1998), but unpurified olfactory tissue has also been used successfully to promote axonal regeneration (Lu et al., 2001). In addition, it has also been shown that supplementing a pure OEC population with meningeal cells significantly enhances their potential for myelination (Lakatos et al., 2003b). It has been suggested that meningeal cells may be a common contaminant of OECs purified from the olfactory bulb. In fact, the 'fibroblast-like' OEC reported by Raisman and colleagues to form a perineural layer around the more 'Schwann cell-like' OEC may actually be a meningeal contaminant of the preparation (Li et al., 1998; Lakatos et al., 2003b). However, a recent study proposes that this 'fibroblast-like' OEC may actually be an olfactory nerve fibroblast (Li et al., 2003).

The effect the different preparations and purities of OECs have on their eventual success is not yet fully resolved. It could be concluded that unpurified OEC populations have resulted in an improvement in functional recovery over purified preparations (Li et al., 1997, 1998; Imaizumi 2002a; Lu et al., 2002). In contrast, contaminating fibroblasts reduced the efficiency of Schwann cell remyelination of demyelinated axons (Brierley et al., 2001), and may have similar effects in OEC preparations. Unpurified lamina propria has been used successfully to promote regeneration in paraplegic rats, with similar results to purified OECs (Lu et al., 2001). However, it is not clear what additional cells were present within this lamina propria, but it is likely to be mainly fibroblasts and endothelial cells. Despite showing the lack of neurons, a possibility remains that the preparation contained neuronal progenitors. Using tissue may also have benefits beyond just providing a source of cells, since they might prevent cavitation, and also provide a structure rich in ECM for axonal outgrowth. However, it has been suggested that modulation of OEC preparations might just help to optimise the effectiveness of the OEC transplant rather than being critical to its success (Riddell et al., 2004).

Another remaining question is which type of lesion or injury model would be best suited to study transplantation therapies. OECs have been used in a variety of injury models, including dorsal root rhizotomy (Ramon-Cueto & Nieto-Sampedro, 1994; Navarro et al. 1999) where functional recovery was reported in some studies (Navarro et al. 1999, Taylor et al., 2001), but not in others (Ramer et al., 2004b; Riddell et al., 2004). It has also been suggested that Schwann cells were of more benefit in some types of injuries such as

following contusion of the spinal cord (Takami et al., 2002), whereas OECs were of more benefit following a hemitransection than Schwann cells (Ramon-Cueto et al., 1998). Both OECs and Schwann cells have been used successfully to remyelinate demyelination models (Blakemore and Crang, 1985; Honmouu et al., 1996; Imaizumi et al., 1998; Barnett et al., 2000), however, it has been reported that Schwann cells were able to remyelinate under conditions where OECs failed (Plant et al., 2002). Taken together, these studies demonstrate that there may be a different potential for OECs and Schwann cells to repair the CNS depending upon the injury type and severity. It may be that different cells are suited to different injuries and further research is required to determine which therapy would best suit certain clinical conditions.

In addition, despite the observation of functional recovery in several transplantation models, as demonstrated by behavioural testing (Li et al., 1997, 2003; Ramon-Cueto et al., 2000; Lu et al., 2002; Nash et al., 2002), little anatomical evidence exists that transected fibres are actually able to regrow across the injury site and form functional synapses (Barnett and Riddell, 2004; Riddell et al., 2004). In contrast, behavioural recovery may instead be resulting from intraspinal sprouting of intact fibres which were spared during injury. Thus, transplants may be functioning by mechanisms other than promoting long distance regeneration following injury. For example, transplantation of OECs has been shown to promote sparing of the intact tissue, and prevent cavitation from occurring (Plant et al., 2003; Ramer et al., 2004a). In order to definitively measure which fibres are responsible for the behavioural recovery recorded, electophysical methods may need to be more routinely employed. Knowledge of which mechanism is the most beneficial may allow therapies to be optimised towards this.

Despite the possibility that the promotion of plasticity and sparing of intact fibres are more achievable targets than long distance regeneration, it may also lead to complications. It has been reported that the distressing condition of autonomic dysreflexia may result from sprouting and uncontrolled synapse formation (Wong et al., 2000). For this reason, only precise and correct synapses would be desirable, otherwise inappropriate firing of neurons may result. To achieve this end, more research into how the correct connections are made during embryogenesis may be useful.

An alternative strategy to promote regeneration following SCI, is to combine several different therapies. This is particularly important due to the various complex aspects of SCI. Since these treatments often target different aspects of the injury, combining these would allow us to take advantages of several improvement strategies at the same time. For example, OECs have been successfully modified using viral vectors to express exogenous genes, such as those encoding neurotrophins (Ruitenberg et al., 2001). Secretion of glial-derived neurotrophic factor (GDNF) by transplanted OECs significantly improved recovery after SCI (Cao et al., 2004), as did transplantation of OECs expressing neurotrophin-3 (NT-3) or brain-derived neurotrophic factor (BDNF; Ruitenberg et al., 2003). Schwann cells have been used in combination with matrix grafts composed of, for example, matrigel (Rodriguez et al., 2000), and collagen IV (Plant et al., 1998). Both were capable of promoting axonal outgrowth, and were suggested to improve the survival of the Schwann cells as well as providing a scaffold for regenerating fibres. In addition, an increased level of sparing, axonal regeneration and also functional recovery, were seen when Schwann cell transplantation was used in conjunction with methods to raise cAMP signalling in axons (Pearse et al., 2004). This allowed the axons to overcome inhibition caused by myelin debris in the lesion.

In conclusion, transplantation therapies are beginning to offer hope that successful repair of the CNS may not be too far in the future, although further research is still needed in order to determine the best strategy or combined approach. Both Schwann cells and OECs, despite their various differences, lend themselves to being a part of this potential treatment, and further understanding of how they interact with the host following transplantation will allow us to maximise their potential and limit the level of reactivity induced. In this thesis, I have demonstrated a role for both N-cadherin and Schwann cell-secreted factors in determining some of these responses. It remains to be seen whether modulation of these factors can result in a better integration between graft and host, and how this can be applied to the clinical setting.

REFERENCES

Alexander CL, Fitzgerald UF, Barnett SC (2002) Identification of growth factors that promote long-term proliferation of olfactory ensheathing cells and modulate their antigenic phenotype. Glia 37:349-364

Alonso G, Privat A (1993) Reactive astrocytes involved in the formation of lesional scars and differ in the mediobasal hypothalamus and in other forebrain regions. J Neurosci Res 34:523-538

Araujo DM, Cotman CW (1992) Basic FGF in astroglial, microglial, and neuronal cultures: characterization of binding sites and modulation of release by lymphokines and trophic factors. J Neurosci 12:1668-1678

Arregui C, Pathre P, Lilien J, Balsamo (2000) The nonreceptor tyrosine kinase fer mediates cross-talk between N-cadherin and β1-integrins. J Cell Biol 149:1263-1273

Asher RA, Morgenstern DA, Shearer MC, Adcock KH, Pesheva P, Fawcett JW (2002) Versican is upregulated in CNS injury and is a product of oligodendrocyte lineage cells. J Neurosci 22:2225-2236

Astic L, Pellier-Monnin V, Saucier D, Charrier C, Mehlen P (2002) Expression of netrin-1 and netrin-1 receptor, DCC, in the rat olfactory nerve pathway during development and axonal regeneration. Neuroscience 109:643-656

Au E, Roskams AJ (2003) Olfactory ensheathing cells of the lamina propria in vivo and in vitro. Glia 41:224-236

Au WW, Treloar HB, Greer CA (2002) Sublaminar organisation of the mouse olfactory bulb nerve layer. J Comp Neurol 446:68-80

Avellino AM, Hart D, Dailey AT, MacKinnon M, Ellegala D, Kliot M (1995) Differential macrophage responses in the peripheral and central nervous system during wallerian degeneration of axons. Exp Neurol 136:183-198

Aviezienyte E, Fincham VJ, Brunton VG, Frame MC (2004) Src SH3/2 domain-mediated peripheral accumulation of src and phospho-myosin is linked to deregulation of E-cadherin and the epithelial-mesenchymal transition. Mol Biol Cell 15:2794-803

Baichwal RR, Bigbee JW, DeVries GH (1988) Macrophage-mediated myelin-related mitogenic factor for cultured Schwann cells. Proc Natl Acad Sci USA 85:1701-5

Balsamo J, Leung T, Ernst H, Zanin MK, Hoffman S, Lilien J (1996) Regulated binding of PTP1B-like phosphatase to N-cadherin: control of cadherin-mediated adhesion by dephosphorylation of beta-catenin. J Cell Biol 134:801-813

Bandtlow C, Zachleder T, Schwab ME (1990) Oligodendrocytes arrest neurite outgrowth by contact inhibition. J Neurosci 10:3837-3848

Bansal R, Magge S, Winkler S (2003) Specific inhibitor of FGF receptor signalling: FGF-2-mediated effects on proliferations, differentiation, and MAPK activation are inhibited by PD173074 in oligodendrocyte-lineage cells. J Neurosci Res 15:486-493

Barber PC, Dahl D (1987) Glial fibrillary acidic protein (GFAP)-like immunoreactivity in normal and transected rat olfactory nerve. Exp Brain Res 65:681-685

Barnett SC, Hutchins AM, Noble M (1993) Purification of olfactory nerve ensheathing cells from the olfactory bulb. Dev Biol 155:337-350

Barnett SC, Alexander CL, Iwashita Y, Gilson JM, Crowther J, Clark L, Dunn LT, Papanastassiou V, Kennedy PG, Franklin RJ (2000) Identification of a human olfactory ensheathing cell that can effect transplant-mediated remyelination of demyelinated CNS axons. Brain 123:1581-1588

Barnett SC, Riddell JS (2004) Olfactory ensheathing cells (OECs) and the treatment of CNS injury; advantages and possible caveats. J Anatomy 24:57-67

Baron-van Evercooren A, Gansmuller A, Gumpel M, Baumann N, Kleitman HK (1986) Schwann cell differentiation in vitro: extracellular matrix deposition and interaction. Dev Neurosci 8:182-196

Baron-van Evercooren A, Duhamel-Clerin E, Boutry JM, Hauw JJ, Gumpel M (1993) Pathways of migration of transplanted Schwann cell in the demyelinated mouse spinal cord. J Neurosci Res 35:428-438

Baron-van Evercooren A, Avellana-Adalid V, Ben Younes-Chennoufi A, Gansmüller A, Nait-Oumesmar B, Vignais L (1996) Cell-cell interactions during the migration of myelin-forming cells transplanted in the demyelinated spinal cord. Glia 16:147-164

Bartsch U, Bandtlow CE, Schnell L, Bartsch S, Spillmann AA, Rubin BP, Hillenbrand R, Montag D, Schwab ME, Schachner M (1995) Lack of evidence that myelin-associated glycoprotein is a major inhibitor of axonal regeneration in the CNS. Neuron 15:1375-1381

Beckerle MC, Burridge K, DeMartino GN, Croall DE (1987) Colocalisation of calcium-dependent protease II and one of its substrates at sites of cell adhesion. Cell 51:569-577

Benfrey and Aguayo (1982) Extensive elongation of axons from rat brain into peripeheral nerve grafts. Nature 11:150-152

Beningo KA, Dembo M, Kaverina I, Small JV, Wang YL (2001) Nascent focal adhesions are responsible for the generation of strong propulsive forces in migrating fibroblasts. J Cell Biol 153:881-8

Behrens J, von Kries JP, Kuhl M, Bruhn L, Wedlich D, Grosschedl R, Birchmeier W (1996) Functional interaction of beta-catenin with the transcription factor LEF-1. Nature 382:638-642

Bergsteinsdottir K, Kingston A, Mirsky R, Jesson KR (1991) Rat Schwann cells produce interleukin-1. J Neuroimmunol 34:15-23

Berry M (1982) Post-injury myelin-breakdown products inhibit axonal growth: an hypothesis to explain the failure of axonal regeneration in the mammalian central nervous system. Bibl Anat 23:1-11.

Beuche W and Friede RL (1986) Myelin phagocytosis in Wallerian degeneration of peripheral nerves depends on silica-sensitive, bg/bg-negative and Fc-positive monocytes. Brain Res 378:97-106

Bhatt A, Kaverina I, Otey C, Huttenlocher A (2002) Regulation of focal complex composition and disassembly by the calcium-dependent protease calpain. J Cell Sci 115:3415-3425

Bignami A, Raju T, Dahl D (1982) Localisation of vimentin, the non-specific intermediate filament protein, in embryonal glia and in early differentiating neurons. Dev Biol 172:126-138

Bignami A, Dahl D (1989) Vimentin-GFAP transition in primary dissociated cultures of rat embryo spinal cord. Int J Dev Neurosci 7:343-357

Bitgood MJ, McMahon AP (1995) Hedgehog and Bmp genes are coexpressed at many diverse sites of cell-cell interaction in the mouse embryo. Dev Biol 172:126-138

Bixby JL, Lilien J, Reichardt LF (1988) Identification of the major proteins that promote neuronal process outgrowth on Schwann cells in vitro. J Cell Biol 107:353-362

Bixby JL, Zhang R (1990) Purified N-cadherin is a potent substrate for the rapid induction of neurite outgrowth. J Cell Biol 110:1253-1260

Blakemore WF (1977) Remyelination of CNS axons by Schwann cells transplanted from the sciatic nerve. Nature 266:68-69

Blakemore WF, Eames RA, Smith KJ, McDonald WI (1977) Remyelination in the spinal cord of the cat following intraspinal injections of lysolecithin. J Neurol Sci 33:31-43

Blakemore WF, Crang AJ (1985) The use of cultured autologous Schwann cells to remyelinate areas of persistant demyelination in the central nervous system. J Neurol Sci 70:207-2023

Blanchard AD, Sinanan A, Parmantier E, Zwart R, Broosl L, Meijer D, Meier C, Jessen KR, Mirsky R (1996) Oct-6 (SCIP/Tst-1) is expressed in Schwann cell precursors, embryonic Schwann cells, and post-natal myelinating Schwann cells: comparison with Oct-1, Krox-20, and Pax-3. J Neurosci Res 46:630-40

Blesch A, Grill RJ, Tuszynski MH (1998) Neurotrophin gene therapy in CNS models of trauma and degeneration. Prog Brain Res 117:473-484

Bomze HM, Bulsara KR, Iskander BJ, Caroni P, Skene JH (2001) Spinal axon regeneration evoked by replacing two growth cone proteins in adult neurons. Nat Neurosci 4:38-43

Boruch AV, Conners JJ, Pipitone M, Deadwyler G, Storer PD, Devries GH, Jones KJ (2001) Neurotrophic and migratory properties of an olfactory ensheathing cell line. Glia 33:225-229

Boucher MJ, Laprise P, Rivard N (2005) Cyclic AMP-dependent protein kinas A negatively modulates adherens junctions integrity and differentiation of intestinal epithelial cells. J Cell Physiol 202:178-190

Bradbury EJ, Moon LDF, Popat RJ, King VR, Bennett GS, Patel PN, Fawcett JW, McMahon SB (2002) Chondroitinase ABC promotes functional recovery after spinal cord injury. Nature 416:636-640

Bregmann BS, McAtee M, Dai HN, Kuhn PL (1997) Neurotrophic factors increase axonal growth after spinal cord injury and transplantation into the adult rat. Exp Neurol 148:475-494

Brierley CM, Crang AJ, Iwashita Y, Gilson JM, Scolding NJ, Compston DA, Blakemore WF (2001) Remyelination of demyelinated CNS axons by transplanted human Schwann cells: the deleterious effect of contaminating fibroblasts. Cell Transplant 10:305-315

Briggs MW, Sacks DB (2003) IQGAP1 as signal integrator: Ca2+, calmodulin, Cdc42 and the cytoskeleton. FEBS Letters 542:7-11

Brittis PA, Canning DR, Silver J (1992) Chondroitin sulfate as a regulator of neuronal patterning in the retina. Science 255:733-736

Brook GA, Lawrence JM, Raisman G (1993) Morphology and migration of cultured Schwann cells transplanted into the fimbria and hippocampus in adult rats. Glia 9:292-304

Brook GA, Lawrence JM, Shah B, Raisman G (1994) Extrusion transplantation of Schwann cells into the adult rat thalamus induces directional host axon growth. Exp Neurol 126:31-43

Brook GA, Lawrence JM, Raisman G (2001) Columns of Schwann cells extruded into the CNS induce in-growth of astrocytes to form organised new glial pathways. Glia 33:118-130

Brose K, Tessier-Lavigne M (2000) Slit proteins: key regulators of axon guidance, axonal branching, and cell migration. Curr Opin Neurobiol 10:95-102

Bruce JH, Norenberg MD, Kraydieh S, Puckett W, Marcillo A, Dietrich D (2000) Schwannosis: role of gliosis and proteogylcan in human spinal cord injury. J Neurotrauma 17:781-788

Buck L, Axel R (1991) A novel multigene family may encode odorant receptors: a molecular basis for odor recognition. Cell 65:175-187

Buck LB (1992) The olfactory multigene family. Curr Opin Neurobiol 2:282-288

Bundesen LQ, Scheel TA, Bregman BS, Kromer LF (2003) Ephrin-B2 and EphB2 regulation of astrocyte-meningeal fibroblast interactions in response to spinal cord lesions in adult rats. J Neurosci 23:7789-7800

Bunge RP, Bunge MB, Eldridge CF (1986) Linkage between axonal ensheathment and basal lamina production by Schwann cells. Annu Rev Neurosci 9:305-328

Burden-Gulley SM, Brady-Kalnay SM (1999) PTPmu regulates N-cadherin-dependent neurite outgrowth. J Cell Biol 144:1323-1236

Burnett MC, Zager EL (2004) Pathophysiology of peripheral nerve injury: a brief review. Neurosurg Focus 16:1-7

Bush TG, Puvanachandra N, Horner CH, Polito A, Ostenfeld T, Svendsen CN, Mucke L, Johnson HM, Sofroniew MV (1998) Leukocyte infiltration, neuronal degradation, and neurite outgrowth after ablation of scar-forming, reactive astrocytes in adult transgenic mice. Neuron 23:297-308

Buss A, Schwab ME (2003) Sequential loss of myelin proteins during Wallerian degeneration in the rat spinal cord. Glia 42:424-432

Cai D, Qiu J, Cao Z, McAtee M, Bregman BS, Filbin MT (2001) Neuronal cyclic AMP controls the developmental loss in ability of axons to regenerate. J Neurosci 21:4731-4739

Camurri L, Mambetisaeva E, Sundaresan V (2004) Rig-1 a new member of Robo family genes exhibits distinct pattern of expression during mouse development. Gene Expr Patterns 4:99-103

Cao L, Liu L, Chen ZY, Wang LM, Ye JL, Qiu HY, Lu CL, He C (2004) Olfactory ensheathing cells genetically modified to secrete GDNF to promote spinal cord repair. Brain 127:535-549

Carey DJ, Eldridge CF, Cornbrooks CJ, Timpl R, Bunge RP (1983) Biosynthesis of type IV collagen by cultured rat Schwann cells. J Cell Biol 97:473-479

Carlstedt T (1988) Reinnervation of the mammalian spinal cord after neonatal dorsal root crush. J Neurocytol 17:335-350

Carragher NO, Fincham VJ, Riley D, Frame MC (2001) Cleavage of focal adhesion kinase by different proteases during src-regulated transformation and apoptosis. Distinct roles for calpain and caspases. J Biol Chem 276:4270-4275

Carragher NO, Frame MC (2002) Calpain: a role in cell transformation and migration. Int J Biochem Cell Biol 34 1539-1543

Carroll WM, Jennings AR (1994) Early recruitment of oligodendrocyte precursors in CNS demyelination. Brain 117:563-578

Cary LA, Chang JF, Guan JL (1996) Stimulation of cell migration by overexpression of focal adhesion kinase and its association with Src and Fyn. J Cell Sci 109:1787-1794

Christofori G, Semb H (1999) The role of the cell-adhesion molecule E-cadherin as a tumour-suppressor gene. Trends Biochem Sci 24:73-76

Chuah MI, Au C (1991) Olfactory Schwann cells are derived from precursor cells in the olfactory epithelium J Neurosci Res 29:172-180

Chuah MI, Au C (1994) Olfactory cell cultures on ensheathing cell monolayers. Chem Senses 19:25-34

Chuah MI, Cossins J, Woodhall E, Tennent R, Nash G, West AK (2000) Glial growth factor 2 induces proliferation and structural changes in ensheathing cells. Brain Res 857:165-174

Clarke SR, Shetty AK, Bradley JL, Turner DA (1994) Reactive astrocytes express the embryonic intermediate neurofilament nestin. Neuroreport 5:1885-1888

Clement AM, Nadanaka S, Masayama K, Mandl C, Sugahara K, Faissner A (1998) The DSD-1 carbohydrate epitope depends on sulfation, correlates with chondroitin sulfate D motifs, and is sufficient to promote neurite outgrowth. J Biol Chem 273:28444-28453

Clemente CD (1964) Regeneration in the vertebrate central nervous system. Int Rev Neurobiol 6:257-301

Cohen J, Burne JF, McKinlay C, Winter J (1987) The role of laminin and laminin/fibronectin complex in the outgrowth of retinal ganglion cell axons. Dev Biol 122:407-418

Cooray P, Yuan Y, Schoenwaelder SM, Mitchell CA, Salem HH, Jackson SP (1996) Focal adhesion kinase (pp125FAK) cleavage and regulation by calpain. Biochem J 318:41-47

Cournams JV, Lin TT, Dai HN, MacARthur L, McAtee M, Nash C, Bregman BS (2001) Axonal regeneration and functional recovery after complete spinal cord transection in rats by delayed treatment with transplants and neurotrophins. J Neurosci 21:934-9344

Covault J, Liu QJ, el-Deeb S (1991) Calcium-activated proteolysis of intracellular domains in the cell adhesion molecules NCAM and N-cadherin. Brain Res Mol Brain Res 11:11-16

Curtis R, Stewart HJ, Hall SM, Wilkin GP, Mirsky R, Jessen KR (1992) GAP-43 is expressed by nonmyelin-forming Schwann cells of the peripheral nervous system. J Cell Biol 116:1455-1464

da Cunha A, Jefferson JJ, Tyor WR, Glass JD, Jannotta FS, Vitkovic L (1993) Control of astrocytosis by interleukin-1 and transforming growth factor-beta 1 in human brain. Brain Res 631:39-45

Dahl D, Bignami A, Weber K, Osborn M (1981a) Filament proteins in rat optic nerves undergoing Wallerian degeneration: localization of vimentin, the fibroblastic 100-A filament protein, in normal and reactive astrocytes. Exp Neurol 73:496-506

Dahl D, Rueger DC, Bignami A, Weber K, Osborn M (1981b) Vimentin, the 57,000 molecular weight protein of fibroblast filaments, is the major cytoskeletal component in immature glia. Eur J Cell Biol 24:191-196

Dahlstrand J, Lardelli M, Lendahl U (1995) Nestin mRNA expression correlates with the central nervous system progenitor cell state in many, but not all, regions of developing central nervous system. Brain Res Dev Brain Res 84:109-129

David S, Aguayo AJ (1981) Axonal elongation into peripheral nervous system bridges after CNS injury in adult rats. Science 214:931-933

Davies SJA, Fitch MT, Memberg SP, Hall AK, Rasiman G, Silver J (1997) Regeneration of adult axons in white matter tracts of the central nervous system. Nature 390:680-684

Delaney CL, Brenner M, Messing A (1996) Conditional ablation of cerebellar astrocytes in postnatal transgenic mice. J neurosci 16: 6908-6918

Devon R, Doucette R (1992) Olfactory ensheathing cells myelinate dorsal root ganglion neurites. Brain Res 389:175-179

Dickson BJ (2001) Rho GTPases in growth cone guidance. Curr Opin Neurobiol 11:103-110

Doetsch F, Caille I, Lim DA, Garcia-Verdugo JM, Alvarez-Buylla A (1999) Subventricular zone astrocytes are neural stem cells in the adult mammalian brain. Cell 97:1-20

Doherty P, Rowett LH, Moore SE, Mann DA, Walsh FS (1991) Neurite outgrowth in response to transfected N-CAM and N-cadherin reveals fundamental differences in neuronal responsiveness to CAMS. Neuron 6:247-258

Dong Z, Brennan A, Liu N, Yarden Y, Lefkowitz G, Mirsky R, Jessen KR (1995) Neu differentiation factor is a neuron-glia signal and regulates survival, proliferation and maturation of rat Schwann cell precursors. Neuron 15:585-596

Dong Z, Sinanan A, Parkinson D, Parmantier E, Mirsky R, Jessen KR (1999) Schwann cell development in embryonic mouse nerve. J Neurosci Res 56:334-348

Dou CL, Levine JM (1994) Inhibition of neurite growth by the NG2 chondriotin sulphate proteoglycan. J Neurosci 14:7616-7628

Doucette JR (1984) The glial cells in the nerve fiber layer of the rat olfactory bulb. Anat Rec 210:385-391

Doucette R (1989) Development of the nerve fiber layer in the olfactory bulb of mouse embryos. J Comp Neurol 285:514-527

Doucette R (1990) Glial influences on axonal growth in the primary olfactory system. Glia 3:433-449

Doucette R (1991) PNS-CNS transitional zone of the first cranial nerve. J Comp Neuro 312:451-466.

Doucette R (1993) Glial progenitor cells of the nerve fiber layer of the olfactory bulb: effect of astrocyte growth media. J Neurosci Res 35:274-287

Doucette R (1996) Immunohistochemical localization of laminin, fibronectin and collagen type IV in the nerve fiber layer of the olfactory bulb. Int J Dev Neurosci 14:945-959

Du X, Saido TC, Tsubuki S, Indig FE, Williams MJ, Ginsberg MH (1995) Calpain cleavage of the cytoplasmic domain of the integrin beta 3 subunit. J Biol Chem 270:26146-26151

Duchossoy Y, Kassar-Duchossoy L, Orsal D, Stettler O, Horvat JC (2001) Reinnervation of the biceps brachii muscle following cotransplantation of fetal spinal cord and autologous peripheral nerve into the injured cervical spinal cord of the adult rat. Exp Neurol 167:329-340

Dusart I, Schwab ME (1994) Secondary cell death and the inflammatory reaction after dorsal hemisection of the rat spinal cord. Eur J Neurosci 6:712-724

Eddleston M, Mucke L (1993) Molecular profile of reactive astrocytes – implications for their role in neurologic disease. Neurosci 54:15-36

Elbashir SM, Harborth J, Lendeckel W, Yalcin A, Weber K, Tuschl T (2001a) Duplexes of 21-nucleotide RNAs mediate RNA interference in cultured mammalian cells. Nature 411:494-498

Elbashir SM, Lendeckel W, Tuschl T (2001b) RNA interference is mediated by 21- and 22-nucleotide RNAs. Genes Dev 15:188-200

Emerson MM, Vactor DV (2002) Robo is Abl to block N-cadherin function. Nature Cell Biol 4:E227-E230

Ernfors P, Henschen A, Olson L, Persson H (1989) Expression of nerve growth factor receptor mRNA is developmentally regulated and increased after axotomy in rat spinal cord motoneurons. Neuron 2:1605-1613

Ernfors P, Persson H (1991) Developmentally regulated expression of HDNF/NT-3 mRNA in rat spinal cord motor neurons and expression of BDNF mRNA in embryonic dorsal root ganglion. Eur J Neurosci 3:953-961

Faissner A, Clement A, Lochater A, Streit A, Mandl C, Schachner M (1994) Isolation of a neural chondroitin sulfate proteoglycan with neurite outgrowth promoting properties. J Cell Biol 126:783-799

Faulkner JR, Herrmann JE, Woo MJ, Tansey KE, Doan NB, Sofroniew MV (2004) Reactive astrocytes protect tissue and preserve function after spinal cord injury. J Neurosci 24:2143-2155

Fawcett JW, Keynes RJ (1990) Peripheral nerve regeneration. Annu Rev Neurosci 13:43-60

Fawcett JW, Asher RA (1999) The glial scar and central nervous system repair. Brain Res Bull 49:377-391

Felts PA, Smith KJ (1992) Conduction properties of central nerve fibers remyelinated by Schwann cell. Brain Res 574:178-192

Ferretti P, Zhang F, O'Neill P (2003) Changes in spinal cord regenerative ability through phylogenesis and development: Lessons to be learnt. Dev Dynamics 226:245-256

Fidler PS, Schuette K, Asher RA, Dobbertin A, Thornton SR, Calle-Patino Y, Muir E, Levine JM, Geller HM, Rogers JH, Faissner A, Fawcett JW (1999) Comparing astrocytic cell lines that are inhibitory or permissive for aconl growth: The major axon-inhibitory proteoglycan is NG2. J Neurosci 19:8778-8788

Fincham VJ, Wyke JA, Frame MC (1995) v-src-induced degradation of focal adhesion kinase during morphological transformation of chicken embryo fibroblasts. Oncogene 10:2247-2252

Fincham VJ, Frame MC (1998) The catalytic activity of Src is dispensable for translocation to focal adhesions but controls the turnover of these structures during cell motility. EMBO 17:81-81

Fitch MT, Silver J (1997a) Glial cell extracellular matrix: Boundaries for axon growth in development and regeneration. Cell Tissue Res 290:379-384

Fitch MT, Silver J (1997b) Activated macrophages and the blood-brain barrier: Inflammation after CNS injury leads to increases in putative inhibitory molecules. Exp Neurol 148:587-603

Fitch MT, Doller C, Combs CK, Landreth GE, Silver J (1999) Cellular and molecular mechanisms of glial scarring and progressive cavitation: in vivo and in vitro analysis of inflammation-induced secondary injury after CNS trauma. J Neurosci 19:8182-8198

Flachenecker P, Rieckmann P (2003) Early intervention in multiple sclerosis: better outcomes for patients and society? Drugs 63:1525-1533

Fournier AE, GrandPre T, Strittmatter SM (2001) Identification of a receptor mediating Nogo-66 inhibition of axonal regeneration. Nature 409:341-346

Fournier AE, Gould GC, Liu BP, Strittmatter SM (2002) Truncated soluble Nogo receptor binds Nogo-66 and blocks inhibition of axon growth by myelin. J Neurosci 22:8876-8883

Franceschini IA, Barnett SC (1996) Low-affinity NGF-receptor and E-N-CAM expression define two types of olfactory nerve ensheathing cells that share a common lineage. Dev Biol 173:327-343

Franklin RJM, Blakemore WF (1993) Requirements for Schwann cell migration within CNS environments: a viewpoint. Int J Dev Neurosci 11:641-649

Franklin RJ, Gilson JM, Franceschini IA, Barnett SC (1996) Schwann cell-like myelination following transplantation of an olfactory bulb-ensheathing cell line into areas of demyelination in the adult CNS. Glia 17:217-224

Franklin RJ, Barnett SC (1997) Do olfactory glia have advantages over Schwann cells for CNS repair? J Neurosci Res 50:665-672

Franklin RJM (2002a) Why does remyelination fail in multiple sclerosis? Nat Rev Neurosci 3:705-714

Franklin RJM (2002b) Remyelination of the demyelinated CNS: The case for and against transplantation of central, peripheral and olfactory glia. Brain Res Bull 57:827-832

Friedlander DR, Milev P, Karthikeyan L, Margolis RK, Margolis RU, Grumet JM (1994) The neuronal chondroitin sulfate proteoglycan neurocan binds to the neural cell adhesion molecules Ng-CAM/L1/NILE and N-CAM, and inhibits neuronal adhesion and neurite outgrowth. J Cell Biol 125:669-680

Frisen J, Johansson CB, Torok C, Risling M, Lendahl U (1995) Rapid, widespread, and longlasting induction of nestin contributes to the generation of glial scar tissue after CNS injury. J Cell Biol 131:453-464

Fu SY, Gordon T (1997) The cellular and molecular basis of peripheral nerve regeneration. Mol Neurobiol 14:67-116

FultonBP, Burne JF, Raff MC (1992) Visualisation of O-2A progenitor cells in developing and adult rat oprtic nerve by quisqualate-stimulated cobalt uptake. J Neurosci 12:4816-4833

Fujisawa H (2004) Discovery of semaphorin receptors, neuropilin and plexin, and their functions in neural development. J Neurobiol 59:24-33

Gale NW, Holland SJ, Valenzuela DM, Flenniken A, Pan L, Ryan TE, Henkemeyer M, Strebhardt K, Hirai H, Wilkinson DG, Pawson T, Davis S, Yancopoulos GD (1996) Eph receptors and ligands comprise two major specificity subclasses, and are reciprocally compartmentalised during embryogenesis. Neuron 17:9-19

Garratt AN, Voiculescu O, Topilko P, Charnay P, Birchmeier C (2000) A dual role of erbB2 in myelination and in expansion of the schwann cell precursor pool. J Cell Biol 148:1035-1046

Geiger B, Bershadsky A, Pankov R, Yamada KM (2001) Transmembrane extracellular matrix-cytoskeleton crosstalk. Nature Rev Mol Cell Biol 2:793-805

Gensert JM, Goldman JE (1997) Endogenous progenitors remyelinate demyelinated axons in the adult CNS. Neuron 19:197-203

Ghirniker RS, Eng LF (1994) Astrocyte-Schwann cell interactions in culture. Glia 11:367-377

Ghose A, Vactor DV (2002) GAPS in slit-robo signalling. Bioessays 24:401-404

Gilmore SA, Duncan D (1968) On the presence of peripheral-like nervous and connective tissue with irradiated spinal cord. Anat Rec 160:675-690

Gimond C, Van der Flier A, van Delft S, Brakebusch C, Kuikman I, Collard JG, Faessler R, Sonnenberg A (1999) Induction of cell scattering by expression of β1 integrins in beta1-deficient epithelial cells requires activation of members of the Rho family of GTPases and downregulation of cadherin and catenin function. J Cell Biol 147:1325-1340

Giuliani F, Yong VW (2003) Immune-mediated neurodegeneration and neuroprotection in MS. Int MS J 10:122-130

Goddard DR, Berry M, Kirvell SL, Butt AM (2002) Fibroblast growth factor-2 induces astroglial and microglial reactivity in vivo. J Anat 200:57-67

Golding J, Cohen J (1997) Border controls at the mammalian spinal cord: Late-surviving neural crest boundary cap cells at dorsal root entry sites may regulate sensory afferent ingrowth and entry zone morphogenesis. Mol Cell Neurosci 9:381-396

Golding J, Shewan D, Cohen J (1997) Maturation of the mammalian dorsal root entry zone – from entry to no entry. Trends Neurosci 20:303-308

Goldstein GW (1988) Endothelial cell-astrocyte interactions. A cellular model of the blood-brain barrier. Ann N Y Acad Sci 529:31-39

Goodman CS, Kolodkin AL, Luo Y, Puschel AW, Raper JA (1999) Unified nomenclature for the semaphorins collapsins. Cell 97:551-552

Goodman MN, Silver J, Jacobberger JW (1993) Establishment and neurite outgrowth properties of neonatal and adult rat olfactory bulb glial cell lines. Brain Res 619:199-213

Grazeidei PP, Grazeidei GA (1979) Neurogenesis and neuron regeneration in the olfactory system of mammals: I, morphological aspects of differentiation and structural organisation of the olfactory sensory neurons. J Neurocytol 8:1-18

Grill R, Murai K, Blesch A, Gage FH, Tuszynski MH (1997) Cellular delivery of neurotrophin-3 promotes corticospinal axonal growth and partial functional recovery after spinal cord injury. J Neurosci 17:5560-5572

Grinspan JB, Marchionni MA, Reeves M, Coulaloglou M, Scherer SS (1996) Axonal interactions regulate Schwann cell apoptosis in developing peripheral nerve: neuregulin receptors and the role of neuregulins. J Neurosci 16:6107-6118

GrandPre T, Nakamura F, Vartanian T, Strittmatter SM (2000) Identification of the Nogo inhibitor of axon regeneration as a Reticulon protein. Nature 403:439-444

GrandPre T Li S, Strittmatter SM (2002) Nogo-66 receptor antagonist peptide promotes axonal regeneration. Nature 417:547-551

Gudino-Cabrera G, Pastor AM, de la Cruz RR, Delgado-Garcia JM, Nieto-Sampedro M (2000) Limits to the capacity of transplants of olfactory glia to promote axonal regrowth in the CNS. Neuroreport 11:467-471

Hall A, Nobes CD (2000) Rho GTPases: molecular switches that control the organization and dynamics of the actin cytoskeleton. Philos Trans R Soc Lond B Biol Sci 355:965-970

Hazan RB, Phillips GR, Qiao RF, Norton L, Aaronson SA (2000) Exogenous expression of N-cadherin in breast cancer cells induces cell migration, invasion and metastasis. J Cell Biol 148:779-790

Herx LM, Yong VW (2001) Interleukin-1 beta is required for the early evolution of reactive astrogliosis following CNS lesion. J Neuropathol Exp Neurol 60:961-971

Hinks Gl, Franklin RJ (1999) Distinctive patterns of PDGF-A, FGF-2, IGF-1, and TGF-beta1 gene expression during remyelination of experimentally-induced spinal cord demyelination. Mol Cell Neurosci 114:153-168

Hong K, Hinck L, Nishiyama M, Poo M, Tessier-Lavigne M, Stein E (1999) A ligand-gated association between cytoplasmic domains of UNC5 and DCC family receptors converts netrin-induced growth cone attraction to repulsion. Cell 97:927-941

Honmou O, Felts PA, Waxman SG, Kocsis JD (1996) Restoration of normal conduction properties in demyelinated spinal cord axons in the adult rat by transplantation of exogenous Schwann cell. J Neurosci 36:3199-3208

Houweling DA, van Asseldonk JT, Lankhorst AJ, Hamers FP, Martin D, Bar PR, Joosten EA (1998) Local application of collagen containing brain-derived neurotrophic factor

decreases the loss of funcion after spinal cord injury in the adult rat. Neurosci Lett 251:193-196

Hudgins SN, Levison SW (1998) Ciliary neurotrophic factor stimulates astroglial hypertrophy in vivo and in vitro. Exp Neurol 150 171-182

Humphries MJ, Akiyma SK, Komoriya A, Olden K, Yamada KM (1988) Neurite extension of chicken peripheral nervous system neurons on fibronectin: relative importance of specific adhesion sites in the central cell-binding domain and the alternatively spliced type III connecting segment. J Cell Biol 106:1289-1297

Huttonlocher A, Palecek SP, Lu Q, Zhang W, Mellgren RL, Lauffenburger DA, Ginsberg MH, Horwitz AF (1997) Regulation of cell migration by the calcium-dependent protease calpain. J Biol Chem 272:32719-32722

Imaizumi T, Lankford KL, Waxman SG, Greer CA, Kocsis JD (1998) Transplanted olfactory ensheathing cells remyelinate and enhance axonal conduction in the demyelinated dorsal columns of the rat spinal cord. J Neurosci 18:6176-6185

Imaizuimi T, Lankford KL, Kocsis JD (2000) Tranplantation of olfactory ensheathing cells or Schwann cells restores rapid and secure conduction across the transected spinal cord. Brain Res 854:70-78

Inoue A, Sanes JR (1997) Lamina-specific connectivity in the brain: regulation by N-cadherin, neurotrophins, and glycoconjugates. Science 276:1428-1431

Itoh K, Krupnik VE, Sokol SY (1998) Axis determination in Xenopus involves biochemical interactions of axin, glycogen synthase kinase 3 and beta-catenin. Curr Biol 8:591-4

Iwashita Y, Fawcett JW, Crang AJ, Franklin RJM, Blakemore WF (2000) Schwann cells transplanted into normal and x-irradiated adult white matter do not migrate extensively and show poor long-term survival. Exp Neurol 164:292-302

Jessen KR, Brennan A, Morgan L, Mirsky R, Kent A, Hashimoto Y, Gavrilovi J. (1994) The Schwann cell precursor and its fate: a study of cell death and differentiation during gliogenesis in rat embryonic nerves. Neuron 12:509-527

Jessen KR, Mirsky R (1983) Astrocyte-like glia in the peripheral nervous system: an immunohistochemical study of enteric glia. J Neurosci 3:2206-2218

Jessen KR, Mirsky R (1991) Schwann cell precursors and their development. Glia 4:185-194

Jessen KR, Mirsky R (1992) Schwann cells: early lineage, regulation of proliferation and control of myelin formation. Curr Opin Neurobiol 2:575-581

Jessen KR, Morgan L, Stewart HJ, Mirsky, R (1990) Three markers of adult non-myelin-forming Schwann cells, 217c(Ran-1), A5E3 and GFAP: development and regulation by neuron-Schwann cell interactions. Development 109:91-103

Jin Z, Strittmatter SM (1997) Rac1 mediates collapsin-1-induced growth cone collapse. J Neurosci 17:6256-6263

Jones LL, Yamaguchi Y, Stallcup WB, Tuszynski MH (2002) NG2 is a major chondroitin sulfate proteoglycan produced after spinal cord injury and is expressed by macrophages and oligodendrocyte progenitors. J Neurosci 22:2792-2803

Kato T, Honmou O, Uede T, Hashi K, Kocsis JD (2000) Transplantation of human olfactory ensheathing cells elicits remyelination of demyelinated rat spinal cord. Glia 30:209-218

Kaverina I, Krylyshkina D, Small JV (2002) Regulation of substrate adhesion dynamics during cell motility. Int J Biochem Cell Biol 34:746-761

Keirstead HS, Blakemore WF (1999) The role of oligodendrocytes and oligodendrocyte progenitors in CNS remyelination. Adv Exp Med Biol. 468:183-197

Key B, Treloar HB, Wangerek L, Ford MD, Nurcombe V (1996) Expression and localisation of FGF-1 in the developing rat olfactory system. J Comp Neurol 366:197-206

Kim JE, Liu BP, Park JH, Strittmatter SM (2004) Nogo-66 receptor prevents raphespinal and rubrospinal axon regeneration and limits functional recovery from spinal cord injury. Neuron 28:439-451

King VR, Henseler M, Brown RA, Priestly JV (2002) Mats made from fibronectin support orientated growth of axons in the damaged spinal cord of the adult rat. Exp Neurol 182:383-398

Kintner C (1992) Regulation of embryonic cell adhesion by the cadherin cytoplasmic domain. Cell 69:225-236

Kirschmann DA, Seftor EA, Nieva DR, Mariano EA, Hendrix MJ (1999) Differentially expressed genes associated with the metastatic phenotype in breast cancer. Breast Cancer Res Treat 55:127-136

Klemke RL, Cai S, Giannini AL, Gallagher PJ, de Lanerolle P, Cheresh DA (1997) Regulation of cell motility by mitogen-activated protein kinase. J Cell Biol 137:481-492

Koch M, Murrell JR, Hunter DD, Olson PF, Jin W, Keene DR, Brunken WJ, Burgeson RE (2000) A novel member of the netrin family, beta-netrin, shares homology with the beta chain of laminin: identification, expression, and functional characterisation. J Cell Biol 151:221-234

Kojima S, Vignjevic D, Borisy GG (2004) Improved silencing vector co-expressing GFP and small hairpin RNA. Biotechiques 36:74-79

Kott JN, Westrum LE, Raines EW, Sasahara M, Ross R (1994) Olfactory ensheathing glia and platelet-derived growth factor B-chain reactivity in the transplanted rat olfactory bulb. Int J Dev Neurosci 12:315-323

Kozlov IG, Yemelyanov AY, Davidova NV, Gorlina NK, Cheredeev AN (1999) Low-molecular collagen peptides have different effects on peritoneal macrophages and neutrophils. Russ J Immunol 4:113-122

Kraftiz KW, Greer CA (1997) The role of laminin in axonal extension from olfactory receptor cells. J Neurobiol 32:298-310

Kraftiz KW, Greer CA (1998) The influence of ensheathing cells on olfactory receptor cell neurite outgrowth in vitro. Ann NY Acad Sci 855:266-269

Kraftiz KW, Greer CA (1999) Olfactory ensheathing cells promote neurite extension from embryonic olfactory receptor cells in vitro. Glia 25:99-110

Krasnoselsky A, Massay MJ, DeFrances MC, Michalopoulos G, Zarnegar R, Ratner N (1994) Hepatocyte growth factor is a mitogen for Schwann cells and is present in neurofibromas. J Neurosci 14:7284-7290

Kreutzberg GW (1996) Microglia: A sensor for pathological events in the CNS. Trends Neurosci 19:312-318

Krohn K, Rozovsky I, Wals P, Teter B, Anderson CP, Finch CE (1999) Glial fibrillary acidic protein transcription responses to transforming growth factor-beta1 and interleukin-1beta are mediated by a nuclear factor-1-like site in the near-upstream promoter. J Neurochem 72:1353-61

Kruger S, Sievers J, Hansen C, Sadler M, Berry M (1986) Three morphologically distinct types of interface develop between adult host and fetal brain transplants: implications for scar formation in the adult central nervous system. J Comp Neurol 249:103-116

Kuhlmann T, Bitsch A, Stadelmann C, Siebert H, Bruck W (2001) Macrophages are eliminated from the injured peripheral nerve via local apoptosis and circulation to regional lymph nodes and the spleen. J Neurosci 21:3401-3408

Lakatos A, Franklin RJ, Barnett SC (2000) Olfactory ensheathing cells and Schwann cells differ in their in vitro interactions with astrocytes. Glia 32:214-225

Lakatos A, Barnett SC, Franklin RJM (2003a) Olfactory ensheathing cells induce less host astrocyte response and chondroitin sulphate proteoglycan expression than Schwann cells following transplantation into adult CNS white matter. Exp Neurol 184:237-246

Lakatos A, Smith PM, Barnett SC, Franklin RJ (2003b) Meningeal cells enhance limited CNS remyelination by transplanted olfactory ensheathing cells. Brain 126:598-609

Laping NJ, Morgan TE, Nichols NR, Rozovsky I, Young-Chan CS, Zarow C, Finch CE (1994) Transforming growth factor-beta 1 induces neuronal and astrocyte genes: tubulin alpha 1, glial fibrillary acidic protein and clusterin. Neuroscience 58:563-572

Le Dourain N, Dulac C, Dupin E, Cameron-Curry P (1991) Glial cell lineages in the neural crest. Glia 4:175-184

Lee IH, Butte JW, Schweinhardt P, Douglas T, Trifunovski A, Hofsletter C, Olsen L, Spencer C (2004) In vivo magnetic resonance tracking of olfactory ensheathing glia grafted into the rat spinal cord. Exp Neurol 187:509-516

Lee SC, Dickson DW, Brosnan CF (1995) Interleukin-1, nitric oxide and reactive astrocytes. Brain Behav Immun 9:45-54

Lehmann M, Fournier A, Selles-Navarro I, Dergham P, Sebok A, Leclerc N, Tigyi G, McKerracher L (1999) Inactivation of Rho signaling pathway promotes CNS axon regeneration. J Neurosci 19:7537-7547

Lendahl U, Zimmerman LB, McKay RD (1990) CNS stem cells express a new class of intermediate filament protein. Cell 60:585-595

Levi ADO, Bunge RP, Lofgren JA, Meima L, Hefti F, Nikolics K, Sliwkowski MX (1995) The influence of heregulins on human Schwann cell proliferation. J Neurosci 15:1329-1340

Levison SW, Goldman JW (1993) Both oligodendrocytes and astrocytes develop from progenitors in the subventricular zone of postnatal rat forebrain. Neuron 10:201-212

Li G, Satyamoorthy K, Herlyn M (2001) N-cadherin-mediated intercellular interactions promote survival and migration of melanoma cells. Cancer Res 61:3819-3825

Li H, Leung TC, Hoffman S, Balsamo J, Lilien J (2000) Coordinate regulation of cadherin and integrin function by the chondroitin sulfate proteoglycan neurocan. J Cell Biology 149:1275-1288

Li M, Shibata A, Li C, Braun PE, McKerracher L, Roder J, Kater SB, David S (1996) Myelin-associated glycoprotein inhibits neurite/axon growth and causes growth cone collapse. J Neurosci Res 46:404-414

Li, Y, Raisman G (1994) Schwann cells induce sprouting in motor and sensory axons in the adult rat spinal cord. J Neurosci 14:4050-4063

Li Y, Field PM, Raisman G (1997) Repair of adult rat corticospinal tract by transplants of olfactory ensheathing cells. Science 277:2000-2002

Li Y, Field PM, Raisman G (1998) Regeneration of adult rat corticospinal axons induced by transplanted olfactory ensheathing cells. J Neurosci 18:10514-10524

Li Y, Decherchi P, Raisman G (2003) Transplantation of olfactory ensheathing cells into spinal cord lesions restores breathing and climbing. J Neurosci 23:727-731

Lieberman AR (1971) The axon reaction. A review of principle features of perikaryal responses to axon injury. Int Rev Neurobiol 14:49-124

Liesi P (1985) Laminin-immunoreactive glia distinguish regenerative adult CNS systems from non-regenerative ones. EMBO J 4:2505-2511

Lilien J, Arregui C, Li H, Balsamo J (1999) The juxtamembrane domain of cadherin regulates integrin-mediated adhesion and neurite outgrowth. J Neurosci Res 58:727-735

Liu S, Qu Y, Stewart TJ, Howard MJ, Chakrabortty S, Holekamp TF, McDonald JW (2000) Embryonic stem cells differentiate into oligodendrocytes and myelinate in culture and after spinal cord transplantation. Proc Natl Acad Sci USA 97:6126-6131

Liu Y, Kim D, Himes BT, Chow SY, Schallert T, Murray M, Tessler A, Fischer I (1999) Transplants of fibroblasts genetically modified to express BDNF promote regeneration of adult rat rubrospinal axons and recovery of forelimb function. J Neurosci 19:4370-4387

Liuzzi FJ, Lasek RJ (1987) Astrocytes block axonal regeneration in mammals by activating the physiological stop pathway. Science 237:642-645

Logan A, Green J, Hunter A, Jackson R, Berry M (1999) Inhibition of glial scarring in the injured rat brain by a recombinant human monoclonal antibody to transforming growth factor-beta2. Eur J Neurosci 11:2367-2374

Lokuta MA, Nuzzi PA, Huttenlocher A (2003) Calpain regulates neutrophil chemotaxis. PNAS 100:4006-4011

Lu J, Feron F, Mackay-Sim A, Waite PM (2002) Olfactory ensheathing cells promote locomotor recovery after delayed transplantation into transited spinal cord. Brain 125:14-21

Lunn ER, Scourfield J, Keynes RJ, Stern CD (1987) The neural tube origin of ventral root sheath cells in the chick embryo. Development 101:221-229

Luo L, Jan LY, Jan YN (1997) Rho family GTP-binding proteins in growth cone signalling. Curr Opin Neurobiol 7:81-86

MacKay-Sim A, Kittel PW (1990) On the life span of olfactory receptor neurons. Eur J Neurosci 3:209-215

McCall MA, Gregg RG, Behringer RR, Brenner M, Delaney SL, Galbreath EJ, Zhang CL, Pearce RA, Chiu SY, Messing A (1996) Targeted deletion in astrocyte intermediate filament (Gfap) alters neuronal physiology. Proc Natl Acad Sci USA 93:6361-6366

McDonald JW, Liu XZ, Qu Y, Liu S, Mackey SK, Turetsky D, Gottlieb DI, Choi DW (1999) Transplanted enbyonic stem cells survive, differentiate and promote recovery in injured rat spinal cord. Nat Med 5:1410-1412

McKeon RJ, Jurynec MJ, Buck CR (1999) The chondroitin sulfate proteoglycan neurocan and phosphocan are expressed by reactive astrocytes in the chronic CNS glial scar. J Neurosci 19:10778-10788

McKerracher L, David S, Jackson DL, Kottis V, Dunn RJ, Braun PE (1994) Identification of myelin associated glycoporteins as a major myelin-derived inhibitor of neurite growth. Neuron 13:805-811

Macklin WB, Weill CL (1985) Appearance of myelin proteins during development in the chick central nervous system. Dev Neurosci 7:170-178

Malnic B, Hirono J, Sato T, Buck LB (1999) Combinatorial receptor codes for odors. Cell 96:713-723

Manitt C, Colicos MA, Thompson KM, Rousselle E, Peterson AC, Kennedy TE (2001) Widespread expression of netrin-1 by neurons and oligodendrocytes in the adult mammalian spinal cord. J Neurosci 21:3911-3922

Marillat V, Cases O, Nguyen-Ba-Charvet KT, Tessier-Lavigne M, Sotelo C, Chedotal A (2002) Spatiotemporal expression patterns of slit and robo genes in the rat brain. J Comp Neurol 442:130-155

Maro GS, Vermeren M, Voiculescu O, Melton L, Cohen J, Charnay P, Topilko P (2004) Neural crest boundary cap cells constitute a source of neuronal and glial cells of the PNS. Nat Neurosci 7:930-938

Martini R, Xin Y, Schachner M (1994) Restricted localisation of L1 and N-CAM at sites of contact between Schwann cells and neurites in culture. Glia 10:70-74

Matafora V, Paris S, Dariozzi S, de Curtis I (2001) Molecular mechanisms regulating the subcellular localization of p95-APP1 between the endosomal recycling compartment and sites of actin organization at the cell surface. J Cell Sci 114:4509-4520

Matulionis DH (1975) Ultrastructure of the mouse olfactory epithelium following destruction by ZnSO4 and its subsequent regeneration. Am J Anat 142:67-89

Meier C, Parmantier E, Brennan A, Mersky R, Jessen KR (1991) Developing Schwann cells acquire the ability to survive without axons by establishing an autocrine circuit involving insulin-like growth factor, neurotrophin 3, and platelet-derived growth factor BB. J Neurosci 19:3847-3859

Meisinger C, Zeschnigk C, Grothe C (1996) In vivo and in vitro effect of glucocorticoids on fibroblast growth factor (FGF)-2 and FGF receptor 1 expression. J Biol Chem 271:16520-16525

Menet V, Gimenez YR, Sandillon F, Privat A (2000) GFAP null astrocytes are a favourable substrate for neuronal survival and neurite outgrowth. Glia 31:267-272

Menon VK, Landerholm TE (1994) Intralesion injection of basic fibroblast growth factor alters glial reactivity to neural trauma. Exp Neurol 129:142-154

Michailov GV, Sereda MW, Brinkmann BG, Fischer TM, Haug B, Birchmeier C, Role L, Lai C, Schwab MH, Nave KA (2004) Axonal neuregulin-1 regulates myelin sheath thickness. Science 304:700-703

Milev P, Friedlander DR, Sakurai T, Karthikeyan L, Flad M, Margolis RK, Grumet M, Margolis RU (1994) Interactions of the chondroitin sulfate proteoglycan phosphacan, the extracellular domain of a receptor-type protein-tyrosine-phosphatase, with neurons, glia, and neural cell-adhesion molecules. J Cell Biol 127:1703-1715

Milev P, Maurel P, Haring M, Margolis RK, Margolis RU (1996) TAG-1/axonin is a high-affinity ligand of neurocan, phosphacan/protein-tyrosine phosphatase-zeta/beta, and N-CAM. J Biol Chem 271:15716-15723

Milev P, Fischer D, Haring M, Schulthess T, Margolis RK, Chiquet ER, Margolis RU (1997) The fibrinogen-like globe of tenascin-C mediates its interactions with neurocan and phosphacan/protein-tyrosine phosphatase-zeta/beta. J Biol Chem 272:15501-15509

Milner R, Anderson HJ, Rippon RF, McKay JS, Franklin RJM, Marchionni MA, Reynolds R, ffrench-Constant C (1997) Contrasting effects of mitogenic growth factors on oligodendrocyte precursor cell migration. Glia 19:85-90

Mikol DD, Stefansson K (1988) A phosphatidylinositol-linked peanut agglutinin-binding glycoprotein in central nervous system myelin and on oligodendrocytes. J Cell Biol 106:1273-1279

Mikol DD, Gulcher JR, Stefansson K (1990) The oligodendrocyte-myelin glycoprotein belongs to a distinct family of proteins and contains the HNK-1 carbohydrate. J Cell Biol 110:471-479

Miragall F, Kadmon G, Husmann M, Schachner M (1988) Expression of cell adhesion molecules in the olfactory system of the adult mouse: presence of the embryonic form of N-CAM. Dev Biol 129:516-531

Miranda JD, White LA, Marcillo AE, Willson CA, Jagid J, Whittemore SR (1999) Induction of EphB3 after spinal cord injury. Exp Neurol 156:218-222

Mirsky R, Jessen KR, Schachner M, Goridis C (1986) Distribution of the adhesion molecules N-CAM and L1 on peripheral neurons and glia in adult rats. J Neurocytol 15:799-815

Mirsky R, Dubois C, Morgan L, Jessen KR (1990) 04 and A007-sulfatide antibodies bind to embryonic Schwann cells prior to the appearance of galactocerebroside; regulation of the antigen by axon-Schwann cell signals and cyclic AMP. Dev 109:105-116

Mirsky and Jessen (1996) Schwann cell development, differentiation and myelination. Curr Opin Neurobiol 6:89-96

Mirsky R, Jessen KR (1999) The neurobiology of Schwann cells. Brain Pathol 9:293-311

Mirsky R, Jessen KR (2001) Embryonic and early postnatal development of Schwann cell. In Glial cell development (Ed Jessen and Richardson; Oxford University Press, Oxford) 1-20

Miyamoto S, Akivama SK, Yamada KM (1995) Synergistic roles for receptor occupancy and aggregation in integrin transmembrane function. Science 267:883-885

Molenaar M, van de Wetering M, Oosterwegel M, Peterson-Maduro J, Godsave S, Korinek V, Roose J, Destree O, Clevers H (1996) XTcf-3 transciption factor mediates beta-catenin-induced axis formation in Xenopus embryos. Cell 86:391-399

Monier-Gavelle F, Duband J (1997) Cross talk between adhesion molecules: Control of N-cadherin activity by intracellular signals elicited by β1 and β3 integrins in migrating neural crest cells. J Cell Biol 137:1663-1681

Moon LD, Brecknell JE, Franklin RJ, Dunnett SB, Fawcett JW (2000) Robust regeneration of CNS axons through a track depleted of CNS glia. Exp Neurol 161:49-66

Moon LD, Asher RA, Rhodes KE, Fawcett JW (2001) Regeneration of CNS axons back to their target following treatment of adult rat brain with chondroitinase ABC. Nat Neurosci 4:465-466

Morgan L, Jessen KR, Mirsky R (1991) The effects of cAMP on differentiation of cultured Schwann cells: Progression from an early phenotype (O4+) to a myelin phenotype (P0+, GFAP-, N-CAM-, NGF-receptor-) depends on growth inhibition. J Cell Biol 112:457-467

Mucke L, Oldstone MBA, Morris JC, Nerenberg MI (1991) Rapid activation of astrocyte expression of GFAP-lacZ transgene by focal injury. New Biol 3:465-474

Murray RC, Calof AL (1999) Neuronal Regeneration: Lessons from the olfactory system. Cell Dev Biol 10:421-431

Murwani R, Hodgkinson S, Armati P (1996) Tumor necrosis factor alpha and interleukin-6 mRNA expression in neonatal Lewis rat Schwann cells and a neonatal rat Schwann cell line following interferon gamma stimulation. J Neuroimmunol 71:65-71

Nagar B, Overduin M, Ikura M, Rini JM (1996) Structural basis of calcium-induced E-cadherin rigidification and dimerization. Nature 380:360-364

Nakagawa S, Takeichi M (1998) Neural crest emigration from the neural tube depends on regulated cadherin expression. Development 125:2963-2971

Nakashiba T, Ikeda T, Nishimura S, Tashiro K, Honjo T, Culotti JG, Itohara S (2000) Netrin-G1: a novel glycosyl phosphatidylinositol-linked mammalian netrin that is functionally divergent from classical netrins. J Neurosci 20:6540-6550

Nash HH, Borke RC, Anders JJ (2002) Ensheathing cells and methylprednisolone promote axonal regeneration and functional recovery in the lesioned adult rat spinal cord. J Neurosci 22:7111-7120

Navarro X, Valero A, Gudino G, Fores J, Rodriguez FJ, Verdu E, Passcual R, Chuadras J, Nieto-Sampedro M (1999) Ensheathing glia transplants promote dorsal root regeneration and spinal reflex restitution after multiple rhizotomy. Ann Neurol 45:207-215

Neumann S, Woolf C (1999) Regeneration of dorsal column fibres into and beyond the lesion site following adult spinal cord injury. Neuron:23 83-91

Neumann S, Bradke F, Tessier-Lavigne M, Basbaum AI (2002) Regeneration of sensory axons within the injured spinal cord induced by intraganglionic cAMP elevation. Neuron 34:885-893

Newman EA (2003) New roles for astrocytes: Regulation of synaptic transmission. Trends Neurosci 26:536-542

Niederländer C, Lumsden A (1996) Late emigrating neural crest cells migrate specifically to the exit points of cranial branchiomotor nerves. Development 122:2367-2374

Nobes CD, Hall A (1995) Rho, rac and cdc42 GTPases regulate the assembly of multimolecular focal complexes associated with actin stress fibers, lamellipodia and filopodia. Cell 81:53-62

Norenberg MD (1994) Astrocyte reponses to CNS injury. J Nuropathol Exp Neurol 53:213-220

Nomura T, Yabe T, Rosenthal ES, Krzan M, Schwartz JP (2000) PSA-NCAM distinguishes reactive astrocytes in 6-OHDA-lesioned substuntia nigra from those in the striatal terminal fields. J Neurosci Res 61:588-596

Qiu J, Cai D, Dai H, McAtee M, Hoffman PN, Bregman BS, Filbin MT (2002) Spinal axon regeneration induced by elevation of cyclic AMP. Neuron 34:895-903

Papadopulos CM, Tsai SY, Alsbiei T, O'Brien TE, Schwab ME, Kartje GL (2002) Functional recovery and neuroanatomical plasticity following middle cerebral artery occlusion and IN-1 antibody treatment in the adult rat. Ann Neurol 51:433-441

Parmantier E, Lynn B, Lawson D, Turmaine M, Namini SS, Chakrabarti L, McMahon AP, Jessen KR, Mirsky R (1999) Schwann cell-derived desert hedgehog controls the development of peripheral nerve sheaths. Neuron 23:713-724

Parsons JT (2003) Focal adhesion kinase: the first ten years. J Cell Sci 116:1409-1416

Pearse DD, Pereira FC, Marcillo AE, Bates ML, Berrocal YA, Filbin MT, Bunge MB (2004) cAMP and Schwann cells promote axonal growth and functional recovery after spinal cord injury. Nat Med 10:610-616

Peles E, Nativ M, Campbell PL, Sakurai T, Martinez R, Lev S, Clary DO, Schilling J, Barnea G, Plowman GD, Grumet M, Schlessinger J (1995) The carbonic-anhydrase domain of receptor tyrosine phosphatase-beta is a functional ligand for the axonal cell recognition molecule contactin. Cell 82:251-160

Perea G, Araque A (2002) Communication between astrocytes and neurons: a complex language. J Physiol 96:199-207

Peshev P, Speiss E, Schachner M (1989) J1-160 and J1-180 are oligodendrocyte-secreted nonpermissive substrates for cell adhesion. J Cell Biol 109:1765-1778

Perl AK, Wilgenbus P, Dahl U, Semb H, Chrisofori G (1998) A causal role for E-cadherin in the transition from adenoma to carcinoma. Nature 392:190-193

Plant GW, Bates ML, Bunge MB (2001) Inhibitory proteoglycan immunoreactivity is higher at the caudal than the rostral Schwann cell graft-transected spinal cord interface. Mol Cell Neurosci 17:471-487

Plant GW, Currier PF, Cuervo EP, Bates ML, Pressman Y, Bunge MB, Wood PM (2002) Purified adult ensheathing glia fail to myelinate axons under culture conditions that enable Schwann cells to form myelin. J Neuroci 22:6083-6091

Plant GW, Christensen CL, Oudega M, Bunge MB (2003) Delayed transplantation of olfactory ensheathing glia promotes sparing/regeneration of supraspinal axons in the contused adult rat spinal cord. J Neurotrauma 20:1-16

Pollock GS, Franceschini IA, Graham G, Marchionni MA, Barnett SC (1999) Neuregulin is a mitogen and survival factor for olfactory bulb ensheathing cells and an isoform is produced by astrocytes. Eur J Neurosci 11:769-780

Popovich PG, Guan Z, Wei P, Huitinga I, van Rooijen N, Stokes BT (1999) Depletion of hematogenous macrophages promotes partial hindlimb recovery and neuroanatomical repair after experimental spinal cord injury. Exp Neurol 158:351-365

Prayoonwiwat N, Rodriguez M (1993) The potential for oligodendrocyte proliferation during demyelinating disease. J Neuropathol Exp Neurol 52:55-63

Price LS, Hajdo-Milasinovic A, Zhao J, Zwartkruis FJT, Collard JG, Bos JL (2004) Rap1 regulates E-cadherin-mediated cell-cell adhesion. J Biol Chem 279:35127-35132

Prinjha R, Moore SE, Vinson M, Blake S, Morrow R, Christie G, Michalovich D, Simmons DL, Walsh FS (2000) Inhibitor of neurite outgrowth in humans. Nature 403:383-384

Probstmeier R, Braunewell KH, Pesheva P (2000) Involvement of chondroitin sulfates on brain-derived tenascin-R in carbohydrate-dependent interactions with fibronectin and tenascin-C. Brain Res 863:42-51

Prydz K, Dalen KT (2000) Synthesis and sorting of proteoglycans. J Cell Sci 113:193-205

Raabe TD, Clive DR, Neuberger TJ, Wen D, DeVries GH (1996) Cultured neonatal Schwann cells contain and secrete neuregulins. J Neurosci Res 46:263-270

Raff MC, Miller RH, Noble M (1983) A glial progenitor cell that develops in vitro into an astrocyte or an oligodendrocyte depending on culture medium. Nature 303:390-396

Raghavan S, Vaezi A, Fuchs E (2003) A role for αβ1 integrins in focal adhesion function and polarized cytoskeletal dynamics. Dev Cell 5:415-427

Raisman G, Lawrence JM, Brook GA (1993) Schwann cells transplanted into the CNS. Int J Dev Neurosci 11:651-669

Raisman G (2001) Olfactory ensheathing cells – another miracle cure for spinal cord injury? Nature Rev Neurosci 2:369-374

Ramer LM, Au E, Richter MW, Liu J, Tetzlaff W, Roskams AJ (2004a) Peripheral olfactory ensheathing cells reduce scar and cavity formation and promote regeneration after spinal cord injury. J Corp Neurol 473:1-15

Ramer LM, Richter MW, Roskams AJ, Tetzlaff W, Ramer MS (2004b) Peripherally-derived olfactory ensheathing cells do not promote primary afferent regeneration following dorsal root injury. Glia 47:189-206

Ramer MS, Priestley JV, McMahon SB (2000) Functional regeneration of sensory axons into the adult spinal cord. Nature 403:312-316

Ramirez JJ, Caldwell JL, Majure M, Wessner DR, Klein RL, Meyer EM, King MA (2003) Adeno-associated virus vector expressing nerve growth factor enhances cholinergic axonal sprouting after cortical injury in rats. J Neurosci 23:2797-2803

Ramon y Cajal (1928) Degeneration and Regeneration of the Nervous System. Oxford University Press, Oxford. – cited in Fry EJ (2001) Central Nervous System Regeneration: Mission Impossible? Clin Exp Pharmacol Physiol 28:253-258

Ramon-Cueto A, Nieto-Sampedro M (1994) Regeneration into the spinal cord of transected dorsal root axons is promoted by ensheathing glia transplants. Exp Neurol 127:232-244

Ramon-Cueto A, Valverde F (1995) Olfactory bulb ensheathing glia: A unique cell type with axonal growth-promoting properties. Glia 14:163-173

Ramon-Cueto A, Avila J (1998) Olfactory ensheathing glia: Properties and function. Brain Res Bull 46:175-187

Ramon-Cueto A, Plant GW, Avila J, Bunge MB (1998) Long-distance axonal regeneration in the transected adult rat spinal cord is promoted by olfactory ensheathing glia transplants. J Neurosci 18:3803-3815

Ramon-Cueto A, Cordero MI, Santos-Benito FF, Avila J (2000) Functional recovery of paraplegic rats and motor axon regeneration in their spinal cords by olfactory ensheathing glia. Neuron 25:425-435

Ranscht B, Clapshaw PA, Price J, Noble M, Seifert W (1982) Development of oligodendrocytes and Schwann cells studied with a monoclonal body against galactocerebroside. Proc Natl Acad Sci USA 79:2709-2713

Ransom B, Behar T, Nedergaard M (2003) New roles for astrocytes (Stars at last). Trends Neurosci 26:520-522

Redies C (1997) Cadherins and the formation of neural circuitry in the vertebrate CNS. Cell Tiss Res 290:405-413

Reier P, Houle JD (1988) The glial scar: Its bearing on axonal elongation and transplantation approaches to CNS repair. Adv Neurol 47:87-138

Reilly JF, Maher PA, Kumari VG (1998) Regulation of astrocyte GFAP expression by TGF-beta1 and FGF-2. Glia 22:202-210

Rhee J, Mahfooz NS, Arregui C, Lilien J, Balsamo J, VanBerkum MFA (2002) Activation of the repulsive receptor Roundabout inhibits N-cadherin-mediated cell adhesion. Nature Cell Biol 4:798-805

Richardson A, Malik RK, Hildebrand JD, Parsons JT (1997) Inhibition of cell spreading by expression of the C-terminal domain of focal adhesion kinase (FAK) is rescued by coexpression of src or catalytically inactive FAK: a role for paxillin tyrosine phosphorylation. Mol Cell Biol 17:6906-6914

Richardson PM, McGuiness UM, Aguayo AJ (1980) Axons from CNS neurons regenerate into PNS gafts. Nature 284:264-265

Riddell JS, Enriquez-Denton M, Toft A, Fairless R, Barnett SC (2004) Olfactory ensheathing cell grafts have minimal influence on regeneration at the dorsal root entry zone following rhizotomy. Glia 47:150-167

Rios-Doria J, Day KC, Kuefer R, Rashid MG, Chinnaigan AM, Rubin MA, Day ML (2003) The role of calpain in the proteolytic cleavage of E-cadherin in prostrate and mammary epithelial cells. J Biol Chem 278:1372-1379

Rottner K, Hall A, Small JV (1999) Interplay between Rac and Rho in the control of substrate contact dynamics. Curr Biol 9:640-648

Rudge JS, Morrissey D, Lindsay RM, Pasnikowski EM (1994) Regulation of ciliary neurotrophic factor in cultured rat hippocampal astrocytes. Eur J Neurosci 6:218-229

Ruitenberg MJ, Plant GW, Christensen CL, Blits B, Niclou SP, Harvey AR, Boer GJ, Verhaagen J (2002) Viral vector-mediated gene expression in olfactory ensheathing cell implants in the lesioned rat spinal cord. Gene Ther 9:135-146

Ruitenberg MJ, Plant GW, Hamers FPT, Wortel J, Blits B, Dijkhuizen PA, Gispen WH, Boer GJ, Verhaagen J (2003) Ex vivo adenoviral vector-mediated neurotrophic gene transfer to olfactory ensheathing glia: Effects on rubrospinal tract regeneration, lesion size and functional recovery after implantation in the injured rat spinal cord. J Neurosci 23:7045-7058

Ruitenberg MJ, Blits B, Dijkhuizen PA, te Beek ET, Bakker A, van Heerikhuize JJ, Pool CW, Hermens WTJ, Boer GJ, Verhaagen J (2004) Adeno-associated viral vector-mediated gene transfer of brain-derived neurotrophic factor reverses atrophy of rubrospinal neurons following both acute and chronic spinal cord injury. Neurobiol Disease 15:394-406

Rutka JT, Apodaca G, Stern R, Rosenblum M (1988) The extracellular matrix of the central and peripheral nervous systems: structure and function. J Neurosurg 69:155-170

Rutkowski JL, Kirk CJ, Lerner MA, Tennekoon GI (1995) Purification and expansion of human Schwann cells in vitro. Nat Med 1:80-3

Rutkowski JL, Tuite GF, Lincoln PM, Boyer PJ, Tennekoon GI, Kunkel SL (1999) Signals for proinflammatory cytokine secretion by human Schwann cells. J Neuroimmunol 101:47-60

Sakurai T, Lustig M, Nativ M, Hemperly JJ, Schlessinger J, Peles E, Grumet M (1997) Induction of neurite outgrowth through contactin and Nr-CAM by extracellular regions of glial receptor tyrosine phosphatase β. J Biol Chem 136:907-918

Salzer JL, Bunge RP (1980) Studies of Schwann cell proliferation. 1. An analysis in tissue culture of proliferation during development, Wallerian degeneration and direct injury. J Cell Biol 84:739-51

Salzer JL, Williams AK, Glaser L, Bunge RP (1980) Studies of Schwann cell proliferation. 2. Characterisation of the stimulation and specificity of the response to a neurite membrane fraction. J Cell Biol 84: 753-66

Schachner M, Bartsch U (2000) Multiple functions of the myelin-associated glycoprotein MAG (siglec-4a) in formation and maintenance of myelin. Glia 29:154-165

Schearer MC, Fawcett JW (2001) The astrocyte/meningeal cell interface – a barrier to successful nerve regeneration? Cell Tissue Res 305:267-273

Scherer SS, Xu YT, Roling D, Wrabetz L, Feltri ML, Kamholz J (1994) Expression of growth-associated protein-43 kD in Schwann cells is regulated by axon-Schwann cell interactions and cAMP. J Neurosci Res 38:575-589

Scherer SS (1997) The biology and pathobiology of Schwann cells. Curr Opin Neurol 10:386-397

Schlaepfer DD, Mitra SK (2004) Multiple connections link FAK to cell motility and invasion. Curr Opin Gen Dev 14:92-101

Schmechel DE, Rakic P (1979) A Golgi study of radial glial cells in developing monkey telencephalon: morphogenesis and transformation into astrocytes. Anat Embryol 156:115-152

Schnaedelbach O, Ozen Illknur, Blaschuk OW, Gour BJ, Meyer RL, Fawcett JW (2001) N-cadherin is involved in axon-oligodendrocyte contact and myelination. Mol Cell Neurosci 17:1084-1093

Schnaelfedt M, Bandtlow CE, Dours-Zimmermann MT, Winterhalter KW, Zimmermann DR (2000) Brain derived versican V2 is a potent inhibitor of axonal growth. J Cell Sci 113:807-816

Schousboe A, Westergaard N, Sonnewalk U, Petersen SB, Yu AC, Hertz L (1992) Regulatory role of astrocytes for neuronal biosynthesis and homeostasis of glutamate and GABA. Prog Brain Res 94:199-211

Schwab ME, Bartholdi D (1996) Degeneration and regeneration of axons in the lesioned spinal cord. Physiol Rev 76:319-370

Sisci D, Aquila S, Middea E, Gentile M, Maggiolini M, Mastroianni F, Montanaro D, Ando S (2004) Fibronectin and type IV collagen activate ERalpha AF-1 by c-Src pathway: effect on breast cancer cell motility. Oncogene – e-published ahead of print

Seiki T, Arai Y (1993) Distribution and possible roles of the highly polysialylated neural cell adhesion molecule (NCAM-H) in the developing and adult central nervous system. Neurosci Res. 17:265-290

Shapiro L, Fannon, Kwong PD, Thompson A, Lehmann MS, Grubel G, Legrand JF, Als-Nielsen J, Colman DR, Hendrickson WA (1995) Structural basis of cell-cell adhesion by cadherins. Nature 374:327-337

Sharma K, Korade Z, Frank E (1995) Late-migrating neuroepithelial cells from the spinal cord differentiate into sensory ganglion cells and melanocytes. Neuron 14:143-152

Shields SA, Blakemore WF, Franklin RJM (2000) Schwann cell remyelination is restricted to astrocyte-deficient areas after transplantation into demyelinated adult rat brain. J Neurosci res 60: 571-578

Shinoda H, Marini AM, Cosi C, Schwartz JP (1989) Science 245:415-417

Sims TJ, Gilmore SA (1994) Regrowth of dorsal root axons into a radiation-induced glial-deficient environment in the spinal cord. Brain Res 634:113-126

Skapa SD, Facci L, Williams G, Williams EJ, Walsh FS, Doherty P (2004) A dimeric version of the short N-cadherin binding motif HAVDI promotes neuronal cell survival by

activating an N-cadherin/fibroblast growth factor receptor signalling cascade. Mol Cell Neurosci 26:17-23

Skundric DS, Bealmear B, Lisak RP (1997) Induced upregulation of IL-1, IL-1RA and IL-1R type I gene expression by Schwann cells. J Neuroimmunol 74:9-18

Slezak M, Pfriegar FW (2003) New roles for astrocytes: Regulation of CNS synaptogenesis. Trends Neurosci 26:531-535

Smale KA, Doucette R, Kawaja MD (1996) Implantation of olfactory ensheathing cells in the adult rat brain following fimbria-fornix transection. Exp Neurol 137:225-233

Smith GM, Rutishauser U, Silver J, Miller RH (1990) Maturation of astrocytes in vitro alters the extent and molecular basis of neurite outgrowth. Dev Biol 138:377-390

Smith KJ, Hall SM (1980) Nerve conduction during peripheral demyelination and remyelination. J Neurol Sci 48:201-219

Smith PM, Sim J, Barnett SC, Franklin RJM (2001) SCIP/Oct-6, Krox-20, and desert hedgehog mRNA expression during CNS remyelination by transplanted olfactory ensheathing cells. Glia 36:342-353

Smith-Thomas LC, Stevens J, Fok-Seang J, Faissner A, Rogers JH, Fawcett JW (1995) Increased axon regeneration in astrocytes grown in the presence of proteoglycan synthesis inhibitors. J Cell Sci 108:1307-1315

Sommer I, Schachner M (1981) Monoclonal antibodies (O1 to O4) to oligodendrocyte cell surfaces: an immunocytological study in the central nervous system. Dev Biol 83:311-327

Song H, Ming G, He Z, Lehmann M, McKerracher L, Tessier-Lavigne M, Poo M (1998) Conversion of neuronal growth cone responses from repulsion to attraction by cyclic nucleotides. Science 281:1515-1518

Song H, Ming G, Poo M (1997) cAMP-induced switching in turning direction of nerve growth cones. Nature 388:275-279

Steinberg MS, McNutt PM (1999) Cadherins and their connections: adhesion functions have broader functions. Curr Opin Mol Biol 11:554-560

Stoll G, Griffin JW, Li CY, Trapp BD (1989) Wallerian degeneration in the peripheral nervous system: participation of both Schwann cells and macrophages in myelin degradation. J Neurocytol 18:671-683

Suarez I, Raff MC (1989) Subpial and perivascular astrocytes associate with nodes of Ranvier in the rat optic nerve. J Neurocytol 18:577-582

Suyama K, Shapiro I, Guttman M, Hazan RB (2002) A signalling pathway leading to mestastasis is controlled by N-cadherin and the FGF receptor. Cancer Cell 2:301-314

Sykova E, Svoboda J, Simonova Z, Jendelova P (1992) Role of astrocytes in ionic and volume homeostasis in spinal cord during development and injury. Prog Brain Res 94:47-56

Tai MH, Cheng H, Wu JP, Liu YL, Lin PR, Kuo JS, Tseng CJ, Tzeng SF (2003) Gene transfer of glial cell line-derived neurotrophic factor promotes functional recovery following spinal cord contusion. Exp Neurol 183:508-515

Takami T, Oudega M, Bates ML, Wood PM, Kleitman N, Bunge MB (2002) Schwann cell but not olfactory ensheathing glia transplants improve hindlimb locomotor performance in the moderately contused adult rat thoracic spinal cord. J Neurosci 22:6670-6681

Tamamaki N, Nakamura K, Okamoto K, Kaneko T (2001) Radial glia is a progenitor of neocortical neurons in the developing cerebral cortex. Neurosci Res 41:51-60

Tanaka H, Shan Wm Phillips GR, Arndt K, Bozdagi O, Shapiro L, Huntley GW, Benson DL, Colman DR (2000) Molecular modification of N-cadherin in response to synaptic activity. Neuron 25:93-107

Tang S, Woodhall RW, Shen YJ, deBellard ME, Saffell JL, Doherty P, Walsh FS, Filbin MT (1997) Soluble myelin-associated glycoprotein (MAG) found in vivo inhibits axonal regeneration. Mol Cell Neurosci 9:333-346

Targett MP, Sussman J, Scolding N, O'Leary MT, Compston DA, Blakemore WF (1996) Failure to achieve remyelination of demyelinated rat axons following transplantation of glial cells obtained from the adult human brain. Neuopathol Appl Neurobiol 22:199-206

Taylor JS, Muneton-Gomez VC, Eguia-Recuero R, Nieto-Sampedro M (2001) Transplants of olfactory bulb ensheathing cells promote functional repair of multiple dorsal rhizotomy. Prog Brain Res 132:641-654

Teng YD, Lavik EB, Qu X, Park KI, Ourednik J, Zurakowski D, Langer R, Smyder EY (2000) Functional recovery following traumatic spinal cord injury mediated by a unique polymer scaffold seeded with neural stem cells. Proc Nat Acad USA 99:3024-3029

Thallmair M, Metz GA, Z'Graggen WJ, Raineteau O, Kartje GL, Schwab ME (1998) Neurite growth inhibitors restrict plasticity and functional recovery following corticospinal tract lesions. Nat Neurosci 1:124-131

Thompson RJ, Roberts B, Alexander CL, Willians SK, Barnett SC (2000) Comparison of neuregulin-1 expression in olfactory ensheathing cells, Schwann cells and astrocytes. J Neurosci Res 61:172-185

Tomita K, van Bokhoven A, van Leenders GJ, Ruijter ET, Jansen CF, Bussemakers MJ, Schalken JA (2000) Cadherin switching in human prostrate cancer progression. Cancer Res 60:3650-3654

Torigoe K, Tanaka HF, Takahashi A, Awaya A, Hashimoto K (1996) Basic behaviour of migratory Schwann cells in peripheral nerve regeneration. Exp Neurol 137:301-308

Trachtenberg JT, Thompson WJ (1996) Schwann cell apoptosis at developing neuromuscular junctions is regulated by glial growth factor. Nature 379:174-177

Tramontin AD, Garcia-Verdugo JM, Alvarez-Buylla A (2002) The origin of adult neural stem cells. Soc Neurosci Abstr 525.2

Tran NL, Nagle RB, Cress AE, Heimark RL (1999) N-cadherin expression in human prostrate carcinoma cell lines. An epithelial-mesenchymal transformation mediating adhesion with stromal cell. Am J Pathol 155:787-798

Treloar HB, Purcell AL, Greer CA (1999) Glomerular formation in the developing rat olfactory bulb. J Comp Neurol 413:289-304

Ubink R, Halasz N, Zhang X, Dagerlind A, Hokfelt T (1994) Neuropeptide tyrosine is expressed in ensheathing cells around the olfactory nerves in the rat olfactory bulb. Neuroscience 60:709-726

Utton MA, Eickholt B, Howell FV, Wallis J, Doherty P (2001) Soluble N-cadherin stimulates fibroblast growth factor receptor dependent neurite outgrowth and N-cadherin and the fibroblast growth factor receptor co-cluster in cells. J Neurochemistry 76:1421-1430

Valverde F, Santacana M, Heredia M (1992) Formation of an olfactory glomerulus: morphological aspects of development and organisation. Neuroscience 49:255-275

van der Laan LJ, De Groot CJ, Elices MJ, Dijkstra CD (1997) Extracellular matrix proteins expressed by human adult astrocytes in vivo and in vitro: an astrocyte surface protein containing the CS1 domain contributes to binding of lymphoblasts. J Neurosci Res 50:539-548

van den Pol AN, Santarelli JG (2003) Olfactory ensheathing cells: Time lapse imaging of cellular interactions, axonal support, rapid morphologic shifts, and mitosis. J Comp Neurol 458:175-194

Vaudano E, Campbell G, Anderson PN, Davies Ap, Woolhead C, Schreyer DJ, Lieberman AR (1995) The effects of a lesion or a peripheral nerve graft on GAP-43 upregulation in

the adult rat brain: an in situ hybridisation and immunocytochemical study. J Neurosci 15:3594-3611

Verdu E, Garcia-Alias G, Fores J, Gudino-Cabrera G, Muneton VC, Nieto-Sampedro M, Navarro X (2001) Effects of ensheathing cells transplanted into photochemically damaged spinal cord. Neuroreport 12:2303-2309

Vidal-Sanz M, Bray GM, Villegas-Perez MP, Thanos S, Aguayo AJ (1987) Axonal regeneration and synapse formation in the superior colliculus by retinal ganglion cells in the adult rat. J Neurosci 7:2894-2909

Vincent AJ, West AK, Chuah MI (2003) Morpholigcal plasticity of olfactory ensheathing cells is regulated by cAMP and endothelin-1. Glia 41:393-403

Voigt T (1989) Development of glial cells in the cerebral wall of ferrets: direct tracing of their transformation from radial glia into astrocytes. J Comp Neurol 289:74-88

Wang KC, Kim AJ, Sivasankaran R, Segal R, He Z (2002a) p75 interacts with the Nogo receptor as a co-receptor for Nogo, MAG and Omgp. Nature 420:74-78

Wang KC, Koprivica V, Kim JA, Sivasankaran R, Guo Y, Neve RL, He Z (2002b) Oligodendrocyte-myelin glycoprotein is a Nogo receptor ligand that inhibits neurite outgrowth. Nature 417:941-944

Wanner IB, Wood PM (2002) N-cadherin mediates axon-aligned process growth and cell-cell interaction in rat Schwann cells. J Neurosci 22:4066-4079

Wagner R, Myers RR (1996) Schwann cells produce tumor necrosis factor alpha: expression in injured and non-injured nerves. Neurosci 73:625-629

Webb DJ, Parsons JT, Horwitz AF (2002) Adhesion assembly, disassembly and turnover in migrating cells – over and over and over again. Nat Cell Biol 4:E97-E100

Wehrle-Haller B, Imhof B (2002) Actin, microtubules and focal adhesion dynamics during cell migration. Int J Biochem Cell Biol 35:39-50

Weinstein DE, Shelanski ML, Liem RK (1991) Suppression by antisense mRNA demonstates a requirement for the glial fibriallry acidic protein in the formation of stable astrocytic processes in response to neurons J Cell Biol 112:1205-1213

Wendt A, Thompson VF, Goll DE (2004) Interation of calpastatin with calpain: a review. Biol Chem 385:465-472

Wewetzer K, Verdu E, Angelov DN, Navarro X (2002) Olfactory ensheathing glia and Schwann cells: two of a kind? Cell Tissue Res 309:337-345

Wilby MJ, Muir EM, Fok-Seang J, Gour BJ, Blaschuk OW, Fawcett JW (1999) N-Cadherin inhibits Schwann cell migration on astrocytes. Mol Cell Neurosci 14:66-84

Williams EJ, Mittal B, Walsh FS, Doherty P (1995) FGF inhibits neurite outgrowth over monolayers of astrocytes and fibroblasts expressing transfected cell adhesion molecules. J Cell Sci 108:3523-3530

Williams EJ, Furness J, Walsh FS, Doherty P (1994) Characterisation of the second messenger pathway underlying neutrite outgrowth stimulated by FGF. Development 120:1685-1693

Williams E, Williams G, Gour BJ, Blaschuk OW, Doherty P (2000) A novel family of cyclic peptide antagonists suggests that N-cadherin specificity is determined by amino acids that flank the HAV motif. J Biol Chem 275:4007-4012

Williams G, Williams EJ, Doherty P (2002) Dimeric versions of two short N-cadherin binding motifs (HAVDI and INPISG) function as N-cadherin agonists. J Biol Chem 277 6:4361-4367

Williams SK, Franklin RJM, Barnett SC (2004) The response of olfactory ensheathing cells to the degeneration and regeneration of the peripheral olfactory system and the involvement of the neuregulins. J Comp Neurol 470:50-62

Willson CA, Irizarry-Ramirez M, Gaskins HE, Cruz-Orengo L, Figueroa JD, Whittemore SR, Miranda JD (2002) Upregulation of EphA receptor expression in the injured adult rat spinal cord. Cell Transplant 11:229-239

Wilkin GP, Marriott DR, Cholewinski AJ (1990) Astrocyte heterogeneity. Trends Neurosci 13:43-46

Wilkinson DG (2001) Multiple roles of Eph receptors and ephrins in neural development. Nature Rev Neurosci 2:155-164

Wong K, Ren KR, Huang YZ, Xie Y, Liu G, Saito H, Tang H, Wen L, Brady-Kalnay SM, Mei L, Wu JY, Xiong WC, Rao Y (2001) Signal transduction in neuronal migration: roles of GTPase activating proteins and the small GTPase cdc42 in the slit-robo pathway. Cell 107:209-221

Wong ST, Atkinson BA, Weaver LC (2000) Confocal microscopic analysis reveals sprouting of primary afferent fibres in rat dorsal horn after spinal cord injury. Neurosci Letts 296:65-68

Wong ST, Henley JR, Kanning KC, Huang J, Bothwell M, Poo M (2002) A p75NTR and Nogo receptor complex mediates repulsive signalling by myelin-associated glycoprotein. Nature Neurosci 5:1303-1308

Woodhall E, West AK, Chuah MI (2001) Cultured olfactory ensheathing cell express nerve growth factor, brain-derived neurotrophic factor, glia cell line-derived neurotrophic factor and their receptors. Mol Brain Res 88:203-213

Woodruff RH, Franklin RJM (1999) Demyelination and remyelination of the caudal cerebellar peduncle of adult rats following stereotaxic injections of lysolecithin, ethidium bromide, and complement/anti-galactocerebroside: a comparative study. Glia 25:216-228

Woolf CJ, Bloechlinger S (2002) It takes more than two to Nogo. Science 297:1132-1134

Wu VW, Nishmiyama N, Schwartz JP (1998) A culture model of reactive astrocytes: increased nerve growth factor synthesis and reexpression of cytokine responsiveness. J Neurochem 71:749-756

Xu XM, Guenard V, Kleitman N, Aebischer P, Bunge MB (1995a) A combination of BDNF and NT-3 promotes supraspinal axonal regeneration into Schwann cell grafts in adult rat thoracic spinal cord. Exp Neurol 134:261-271

Xu XM, Guenard V, Kletiman N, Bunge MB (1995b) Axonal regeneration into Schwann cell-seeded guidance channels grafted into transected adult rat spinal cord. J Comp Neurol 351:145-166

Xu XM, Zhang SX, Li H, Aebischer P, Bunge MB (1999) Regrowth of axons into the distal spinal cord through a Schwann cell-seeded mini-channl implanted into hemisected adult rat spinal cord. Eur J Neurosci 11:1723-1740

Yamada H, Fredette B, Shitara K, Haghihara K, Miura R, Ranscht B, Stallcup WB, Yamguchi Y (1997) The brain chondroitin sulfate brevican associates with astrocytes ensheathing cerebellar glomeruli and inhibits neurite outgrowth from granule neurons. J Neurosci 17:7784-7795

Yamada KM, Miyamoto S (1995) Integrin transmembrane signalling and cytoskeletal control. Curr Opin Cell Biol 7 681-689

Yamaguchi R, Maki M, Hatanaka M, Sabe H (1994) Unphosphorylated and tyrosine-phosphorylated orms of a focal adhesion protein, paxillin, are substrates for calpain II in vitro: implications for the possible involvement of calpain II in mitosis-specific degradation of paxillin. FEBS Lett 356:114-116

Yamamoto M, Sobue G, Li M, Arakawa Y, Mitsuma T, Kimata K (1993) Nerve growth factor (NGF), brain-derived neutrophin factor (BDNF) and low-affinity nerve growth

factor receptor (LNGFR) mRNA levels in cultured rat Schwann cells; differential time- and does-dependent regulation by cAMP. Neurosci Lett 152:37-40

Yan H, Nie X, Kocsis JD (2001) Hepatocyte growth factor is a mitogen for olfactory ensheathing cells. J Neurosci Res 66:698-704

Yan Q, Johnson EM (1987) A quantitative study of the developmental expression of nerve growth factor (NGF) receptor in rats. Dev Biol 121:139-148

Yano H, Mazaki Y, Kurokawa K, Hanks SK, Matsuda M, Sabe H (2004) Roles played by a subset of integrin signalling molecules in cadherin-based cell-cell adhesion. J Cell Biol 166:283-295

Yeh HJ, Ruit KG, Wang YW, Parks WC, Snider WD, Deuel TF (1991) PDGF-A chain gene during development and in maturity. Cell 64:209-216

Yin Y, Sanes JR, Miner JH (2000) Identification and expression of mouse netrin-4. Mech Dev 96:115-109

Yoon SY, Choi JE, Hwang O, Hong HN, Lee H, Kim YK, Choo SW, Kim H, Kim DH (2004) Construction of a vector generating both siRNA and a fluorescent reporter: a siRNA study in cultured neurons. Mol Cells 18:127-130

Yu TW, Bargmann CI (2001) Dynamic regulation of axon guidance. Nat Neurosci 4:1169-1175

Zamvil SS, Steinman L (2003) Diverse targets for intervention during inflammatory and neurodegenerative phases of multiple sclerosis. Neuron 38:685-688

Zhang BT, Hikawa N, Horie H, Takenaka T (1995) Mitogen induced prolieration of isolated adult mouse Schwann cells. J Neurosci Res 41:648-654

Zheng B, Atwal J, Hol C, Case L, He XL, Garcia KC, Steward O, Tessier-Lavigne M (2005) Genetic deletion of the Nogo receptor does not reduce neurite inhibition in vitro or promote corticospinal tract regeneration in vivo. Proc Natl Acad Sci USA 102:1205-1210

APPENDIX

1 Equipment

Axioplan 2 fluorescent microscope	Zeiss, Herts, UK
Axioshop fluorescent microscope	Zeiss, Herts, UK
Axiovert S100 time-lapse microscope	Zeiss, Herts, UK
Beckman DU 650 Spectrophotometer	Beckman, Bucks, UK
Biorad power pack 3000	Biorad, Hemel Hempstead, UK
Camera controller (time-lapse)	Hamamatsu Photonics Ltd, Middlesex, UK
Clifton unstirred water bath	Bennett Scientific, Devnon, UK
Dry blotter – AE-6675	ATTO, Tokyo, Japan
Electronic heat sealer	Hulme Martin, Woking, UK
Ettan IPGphor isoelectric focussing system	Amersham Pharmacia Biotech ltd., Bucks, UK
FACSVantage SE sorter	Becton Dickinson, Oxford, UK
Fine Pix S1 pro digital camera	Fuji Photo Film, London, UK
Halogen hot plate/stirrer	Bibby Sterilin, Stone, UK
Heraeus 6000 incubator	Kendro, Hertfordshire, UK
Kodak 480 RA X-ray processor	Kodak, Hemel Hempstead, UK
Leica SP2 confocal microscope	Leica, Milton Keynes, UK

Microcentaur desk top centrifuge	MSE Ltd, Kent, UK
Microplate reader	Dynatech Laboratories, UK
Olympus CK2 phase microscope (in T/C)	Olympus, London, UK
R100/TW rotator shaker	Luckham Ltd, Sussex, UK
Sigma 4K15 centrifuge (tissue culture)	Sigma, Osterode am Harz, Germany
Soniprep 150 sonicator	MSE, Ltd, Kent, UK
Sorvall RC3C centrifuge	Du Pont, Hertfordshire, UK
Tissue culture hoods	Medical Air Technology, Oldham, UK
Typhoon 9400 transilluminator	Amersham Pharmacia Biotech ltd., Bucks, UK
X-Cell II mini cell gel tank	Novex, Frankfurt, Germany

2 General plastic ware

Bijous – 5 ml	Bibby-Sterilin, Stone, UK
Centricon Plus-20	Millipore, Watford, UK
Cell scrapers	Corning Inc, NY, UK
Cell strainer – 70 μl	Becton Dickinson, Oxford, UK
Coverslips	BDH, Poole, UK
Eppendorfs – 0.5 ml, 1.5 ml	Eppendorf, Cambridge, UK

Falcon tubes – 15 ml, 30 ml	Becton Dickinson, Oxford, UK
Filters with receiver – 250 ml	Nalge Nunc Int., Rochester, NY, USA
Flasks – T25, T75, T125	Bibby-Sterilin, Stone, UK
Haemocytometer	Weber Scientific Int. ltd., Middlesex, UK
Microscope slides	BDH, Poole, UK
Microcentrifuge tubes	Elkay Lab products, Basingstoke, UK
Needles – 21G, 23G	Becton Dickenson, Oxford, UK
Pastettes	Elkay Lab products, Basingstoke, UK
Petri dishes	Bibby-Sterilin, Stone, UK
Pippette tips	Elkay Lab products, Basingstoke, UK
Plates – 96-well, 24-well, 6-well	Bibby-Sterilin, Stone, UK
Polystyrene round bottom tubes – 5 ml (for FACS)	Becton Dickinson, Oxford, UK
Scalpels	Swann-Morton Ltd, Sheffield, UK
Syringes – 5 ml,10 ml	Benton Dickenson, Oxford UK
Syringe filters – 0.2 μm	PALL Life Sciences, NY, USA
Universals – 30 ml	Bibby-Sterilin, Stone, UK

3 Immunoblotting and autoradiography equipment

3MM filter paper	Whatman Int., Maidestone, UK
0.45mm pore size nitrocellulose membrane	Millipore, Watford, UK
ECL kit	Amersham Pharmacia Biotech Ltd., Bucks, UK
X-ray film	Fuji Photo Film, London, UK
4-12% Bis-Tris Gels – IPG well, 10-well, 15-well	Invitrogen, Paisley, UK

4 Chemicals and reagents

Absolute Alcohol	James Burrough Ltd., Essex, UK
Amphotericin-B	Gibco Life Sciences, Paisley, Scotland
Antioxidant	Invitrogen, Paisley, UK
Aprotinin	Sigma Aldrich, Dorset, UK
Apo-transferrin (human)	Sigma Aldrich, Dorset, UK
Bovine Pituitary Extract	Gibco Life Sciences, Paisley, Scotland
Bromophenol Blue	Fisher Scientific, Leicestershire, UK
BSA – fraction A	Sigma Aldrich, Dorset, UK
BSA – for standard curves	Sigma Aldrich, Dorset, UK
BSA path-o-cyte 4	Sigma Aldrich, Dorset, UK

Bicinchironic acid	Sigma Aldrich, Dorset, UK
Bovine pancreas DNAse	Sigma Aldrich, Dorset, UK
CHAPS	BDH Chemicals, Dagenham, UK
Collagenase	Sigma Aldrich, Dorset, UK
$CuSO_4$	Sigma Aldrich, Dorset, UK
Cytosine Arabinoside	Sigma Aldrich, Dorset, UK
DAPI	Sigma Aldrich, Dorset, UK
DMEM – 1885, 1966	Invitrogen, Paisley, UK
DCS	Sigma Aldrich, Dorset, UK
DTT	Sigma Aldrich, Dorset, UK
EDTA	Fisher Scientific, Leicestershire, UK
EGF	Peprotech, London, UK
EGTA	Sigma Aldrich, Dorset, UK
FBS	Autogen Bioclear, Caine, UK
Fibronectin	Sigma Aldrich, Dorset, UK
FGF	Peprotech, London, UK
Formaldehyde	Fisher Scientific, Leicestershire, UK
Forskolin	Sigma Aldrich, Dorset, UK

FuGENE	Roche Diagnostics, West Sussex, UK
β-glycerophosphate	Sigma Aldrich, Dorset, UK
Glycerol	Fisher Scientific, Leicestershire, UK
Gentamycin	Sigma Aldrich, Dorset, UK
L-glutamine	Sigma Aldrich, Dorset, UK
Hanks balanced salts (without sodium bicarbonate)	Imperial Labs, Andover, UK
Heregulin	R&D Systems, Abingdon, UK
HEPES buffer	Gibco Life Sciences, Paisley, Scotland
Hydrochloric acid	Fisher Scientific, Leicestershire, UK
Hydrocortisone	Sigma Aldrich, Dorset, UK
Insulin (bovine pancreas)	Sigma Aldrich, Dorset, UK
Iodoacetamide	Sigma Aldrich, Dorset, UK
IPG buffer pH 3-10	Amersham Pharmacia Biotech ltd., Bucks, UK
L15	Gibco Life Sciences, Paisley, Scotland
Laminin	Sigma Aldrich, Dorset, UK
Leupeptin	Sigma Aldrich, Dorset, UK
Modified MCDB 153 medium	Clonetics, San Diego, CA, USA
Milk powder	Marvel, Premier Brands, Lincs, UK

Methanol	Fisher Scientific, Leicestershire, UK
β-mercaptoethanol	Sigma Aldrich, Dorset, UK
MOPS running buffer	Invitrogen, Paisley, UK
NaOH	Fisher Scientific, Leicestershire, UK
NaCl	Fisher Scientific, Leicestershire, UK
Na_3VO_4	Sigma Aldrich, Dorset, UK
Oligofectamine	Invitrogen, Paisley, UK
Optimem	Invitrogen, Paisley, UK
Paraformaldehyde	BDH, Poole, UK
Penicillin/streptomycin	Invitrogen, Paisley, UK
PLL	Sigma Aldrich, Dorset, UK
PMSF	Sigma Aldrich, Dorset, UK
Progesterone	Sigma Aldrich, Dorset, UK
Putrescine	Sigma Aldrich, Dorset, UK
Rabbit complement	Harlan Olac Ltd
Re-blot plus strong	Chemicon International
4x Sample buffer	Invitrogen, Paisley, UK
SDS	Fisher Scientific, Leicestershire, UK

SeeBlue Plus2 pre-stained standards	Invitrogen, Paisley, UK
Selenium	Sigma Aldrich, Dorset, UK
siRNA	Dharmacon Research
Sodium azide	BDH/Merck Biosciences, Nottingham, UK
Sodium deoxycholate	Sigma Aldrich, Dorset, UK
Sodium fluoride	Sigma Aldrich, Dorset, UK
Sodium pyrophosphate	Sigma Aldrich, Dorset, UK
Soybean trypsin inhibitor	Sigma Aldrich, Dorset, UK
SYPRO Orange protein gel stain	Molecular Probes, Leiden, Netherlands
Thyroxine	Sigma Aldrich, Dorset, UK
Tris	Melford Labs, Suffolk, UK
Tween 20	Sigma Aldrich, Dorset, UK
Tri-iodo-thyonine	Sigma Aldrich, Dorset, UK
Triton X-100	Sigma Aldrich, Dorset, UK
Trypsin	Invitrogen, Paisley, UK
Trypsin – bound to beads	Sigma Aldrich, Dorset, UK
Ultra high purity water	Braun, Sheffield, UK
Urea	Sigma Aldrich, Dorset, UK

Vectashield mounting medium	Vector Laboratories, Burlingame, USA
Vybrant cell tracer kit	Molecular Probes, Leiden, Netherlands
IgG beads (sepharose and agarose)	Amersham Pharmacia Biotech ltd, Bucks, UK

5 Inhibitors

See Table 2.1 (Materials and Methods) for list of inhibitors used

N-cadherin inhibitory peptide (10 mg/ml)	Prof. P. Doherty, King's College, London
N-cadherin agonist peptide (20 mg/ml)	Prof. P. Doherty, King's College, London

6 Buffers, solutions and media

all solutions made in dH_20 unless otherwise noted

6.1 General reagents

Phosphate Buffered Saline (PBS), pH 7.4

140 mM NaCl

2.7 mM KCl

10 mM Na_2HPO_4

1.8 mM KH_2PO_4

6.2 Tissue culture reagents

i) **Bottenstein-Sato's serum free media (DMEM-BS)**

25 μg/ml Gentamycin

5 ng/ml Insulin

50 ng/ml Transferrin

0.011% SATO mix (see below)

100 mM Glutamine

in DMEM – 1885

ii) **Bottenstein-Sato's serum free media in DMEM-1966 (DMEM-BS-1966)**

25 μg/ml Gentamycin

5 ng/ml Insulin

50 ng/ml Transferrin

0.011% SATO mix (see below)

100 mM Glutamine

in DMEM – 1966

iii) **Collagenase**

1.33% Collagenase (155 U/mg or 6.6 mg/ml)

in L15

iv) **Dubco's Modified Eagle Medium with 10% FBS (DMEM-10%)**

10% FBS

25 μg/ml Gentamycin

100 mM Glutamine

in DMEM 1885

v) **Dubco's Modified Eagle Medium with 1% FBS (DMEM-1%)**

1% FBS

25 μg/ml Gentamycin

100 mM Glutamine

in DMEM 1885

vi) **Dubco's Modified Eagle Medium with 10% FBS from DMEM-1966 (DMEM-10%-1966)**

10% FBS

25 μg/ml Gentamycin

100 mM Glutamine

in DMEM 1966

vii) **OEC mitogen media (OMM)**

75% SATO

5% FBS

500 ng/ml FGF2

50 ng/ml Heregulin

$5x10^{-7}$M Forskolin

20% ACM (astrocyte conditioned medium)

viii) SATO mix

0.01288% BSA path-o-cyte 4

72.5 μg/ml Putrescine

180.2 μg/ml Thyroxine

151.8 μg/ml Tri-iodo-thyonine

28.1 μg/ml Progesterone

17.4 μg/ml Selenium

ix) Soybean trypsin inhibitor-DNase (SD)

0.52 mg/ml Soybean trypsin inhibitor

0.04 mg/ml Bovine pancrease DNAse

3.0 mg/ml Bovine serum albumin, fraction A

in L15

x) Keratinocyte Growth Medium

0.4% Bovine pituitary extract

10 ng/ml EGF

0.5 μg/ml Hydrocortisone

5 mg/ml Insulin

50 ng/ml Amphotericin-B

50 μg/ml Gentamycin

in modified MCDB 153 medium

6.3 Immunocytochemistry reagents

i) Hanks staining solution

10% Hanks balanced salt solution (HBSS) 10x

5% DCS

0.1 M HEPES buffer

0.25% Sodium azide

ii) Solution A

1 mM $MgCl_2$

0.1 mM CaCl2

in PBS

6.4 Immuno-blotting reagents

i) Blocking solution

5% Marvel

in PBS-Tween

ii) Chondroitinase activating buffer, pH 8.0

50 mM Tris

60 mM Sodium acetate

0.02% BSA

iii) Coomassie blue

0.5% Coomassie blue

30% MeOH

10% Acetic acid

iv) Destain

7% Acetic acid

5% MeOH

v) Dry blot buffer

10% 10x Dry blot buffer stock

20% MEOH

vi) Dry blot buffer stock (10x)

50 mM Tris

40 mM Glycine

1.3 mM SDS

20% MeOH

vii) **Lysis buffer, pH 7.5**

500 mM HEPES

150 mM NaCl

1 mM EDTA

2.5 mM EGTA

1 mM DTT

0.1% Tween 20

10% Glycerol

1 mM Sodium fluoride

10 μg/ml Leupeptin

2 μg/ml Aprotinin

10 mM Glycerophosphate

100 μM Na_3VO_4

100 μM PMSF

viii) **PBS-Tween**

0.2% Tween 20

in PBS, pH 7.4

ix) RIPA

50 mM Tris

150 mM NaCl

1% Triton X-100

0.5% Sodium deoxycholate

0.1% SDS

2 mM EDTA

10 mM Sodium pyrophosphate

2 μg/ml Apoprotin

100 μM PMSF

100 μM Na_3VO_4

6.5 Two-Dimensional electrophoresis reagents

i) 2D gel sample buffer 1

2 M Thiourea

6 M Urea

4% CHAPS

bromophenol blue

0.5% IPG buffer (3-10)

0.5-1% DTT

ii) 2D gel sample buffer 2

200 µl sample buffer (4X Nupage)

300 µl glycerol

500 µl urea

0.5% DTT

iii) 2D gel sample buffer 3

200 µl sample buffer (4X Nupage)

300 µl glycerol

500 µl urea

0.5% DTT

1% iodacetamide

7 Antibodies

The class and source of antibodies used are shown in Table 2.2 (Materials and Methods)

8 Hybridoma cells

O4 (Somner and Schachner 1981 – IgM)

Gal C	(Ranscht et al 1982 – 1gG3)	
$P75^{NTR}$	(Yan and Johnson, 1987)	
Thy 1.1 (cell line T11D7)	ECACC,	Wiltshire,UK